THE EFFECTS OF HIV-1-PROTEINS AND ANTIRETROVIRAL THERAPY ON AORTIC ENDOTHELIAL CELLS (AECS) – A MECHANISTIC *IN VITRO* APPROACH

by

Maria Elizabeth Clara Marincowitz

Thesis presented in fulfilment of the requirements for the degree of Master of Science in the Faculty of Medicine and Health Sciences at Stellenbosch University

Supervisor: Dr Amanda Genis

Co-supervisor: Prof Hans Strijdom

April 2019

DECLARATION

By submitting this thesis electronically, I declare that the entirety of the work contained therein is my own, original work, that I am the sole author thereof (save to the extent explicitly otherwise stated), that reproduction and publication thereof by Stellenbosch University will not infringe any third party rights and that I have not previously in its entirety or in part submitted it for obtaining any qualification.

April 2019

ABSTRACT

Introduction: Endothelial dysfunction is an early precursor of cardiovascular disease characterized by decreased nitric oxide (NO) levels following the development of oxidative stress. Oxidative stress has been shown to result not only in the inactivation of NO itself, but also of endothelial NO synthase (eNOS), the enzyme responsible for NO synthesis. This contributes to creating a pro-inflammatory environment in the vasculature, which can lead to atherosclerosis and cardiovascular disease. Increased endothelial dysfunction and cardiovascular risk have been observed in both HIV-1 infection and antiretroviral therapy (ART).

Objectives: To establish a simulated model of *in vitro* HIV-1-infection and determine the effects of non/nucleoside reverse transcriptase inhibitors (NRTI/NNRTIs) and protease inhibitors (PIs) on markers of endothelial function and the expression/activation of important vascular signalling proteins within this HIV-1-model.

Methods: A simulated HIV-1-model was established by adding recombinant HIV-1 proteins (100 ng/ml each of Nef, Tat and Gp160) to the growth medium of cultured rat aortic endothelial cells (AECs). Subsequently, the effects of NRTI/NNRTIs (efavirenz, emtricitabine and tenofovir) and PIs (lopinavir and ritonavir) on these HIV-1 exposed AECs were determined using fluorescent probes to assess cell viability, NO-production and oxidative stress via reactive nitrogen species (RNS) production. The expression/activation of important vascular signalling proteins, including eNOS and IκBα (an inhibitor of the inflammatory NFκB signalling pathway), was also evaluated by western blotting.

Results: Exposure to 100 ng/ml of HIV-1 Nef, Tat and Gp160 for 24 hours led to a significant decrease in NO production in AECs (DAF-2/DA fluorescence intensity: 72.05±8.37% *vs.* 100±1.55%). NRTI/NNRTI treatment within an HIV-1-protein medium environment for 24 hours had no effect on NO production, possibly abrogating the reduced levels observed with HIV-1-protein treatment on its own. Furthermore, a decrease in RNS was observed (DHR-123 fluorescence intensity: 83.19±3.5% *vs.* 100±0.22%). PI treatment within an HIV-1-protein medium environment for 24 hours resulted in a reduction in NO production in a concentration-dependent manner (DAF-2/DA fluorescence intensity: 92.74±1.4% *vs.* 100±0.67% and 85±1.81% *vs.* 100±0.56%), probably due to decreased eNOS expression (0.28±0.04 *vs.* 1±0.21). Interestingly, neither HIV-1 protein exposure on its own, nor PI treatment in isolation had any effects on eNOS. The same was observed for IκBα, where combined HIV-1-protein and PI exposure reduced levels (0.37±0.03 *vs.* 1±0.15) and neither of these treatments in isolation had any effects.

Conclusion: HIV-1 Nef, Tat and Gp160 attenuated NO production in AECs, while NRTI/NNRTI treatment within this HIV-1 protein environment showed minimal adverse effects, and could possibly even be beneficial, potentially reversing the detrimental consequences of HIV-1 proteins on NO production. PI treatment, on the other hand, seemed to demonstrate a harmful interaction with HIV-1 proteins, resulting

in a downregulation of the eNOS-NO biosynthesis pathway. The PI-HIV-1 protein combination was also associated with up-regulation of the pro-inflammatory NFκB signalling pathway, which may provide an explanation for the decreased eNOS expression.

OPSOMMING

Inleiding: Endoteeldisfunksie is ’n voorloper van kardiovaskulêre siektes wat gepaard gaan met verlaagde stikstofoksied (NO) vlakke as gevolg van oksidatiewe stres. Studies het getoon dat oksidatiewe stres nie net NO inaktiveer nie, maar ook endoteel NO sintase (eNOS), die ensiem verantwoordelik vir NO sintese. Hierdie dra by tot die ontwikkeling van ’n pro-inflammatoriese toestand in die vaskulêre omgewing, wat kan lei tot aterosklerose en kardiovaskulêre siektes. Verhoogde endoteeldisfunksie en kardiovaskulêre risiko is al in beide HIV-1-infeksie en antiretrovirale terapie gemerk.

Doelstellings: Om ’n gesimuleerde model van *in vitro* HIV-1-infeksie te ontwikkel en vas te stel wat die gevolge van behandeling met nie-/nukleosied tru-transkriptase inhibeerders (NRTI/NNRTIs) en protease inhibeerders (PIs) op merkers van endoteeldisfunksie en die uitdrukking/aktivering van belangrike vaskulêre seinproteïne in hierdie HIV-1-model is.

Metodes: ’n Gesimuleerde HIV-1-model is ontwikkel deur rekombinante HIV-1 proteïne (100 ng/ml elk van Nef, Tat en Gp160) by die groei media van gekweekte rot aorta endoteelselle (AESe) te voeg. Hierna is die uitwerking van NRTI/NNRTIs (efavirenz, emtricitabine en tenofovir) en PIs (lopinavir en ritonavir) op die HIV-1 blootgestelde AESe vasgestel met die gebruik van fluoressensie ondersoeke om sel lewensvatbaarheid, NO-produksie en oksidatiewe stres via die produksie van reaktiewe stikstof spesies (RSS) te assesseer. Die uitdrukking/aktivering van belangrike vaskulêre seinproteïne, insluitend eNOS en IκBα (’n onderdrukker van die inflammatoriese NFκB seinpaaie), is geëvalueer deur middel van western blot analises.

Resultate: Blootstelling aan 100 ng/ml elk van HIV-1 Nef, Tat en Gp160 vir 24 uur het gelei tot ’n beduidende vermindering in NO produksie in AESe (DAF-2/DA fluoressensie intensiteit: 72.05±8.37% *vs.* 100±1.55%). NRTI/NNRTI behandeling in ’n HIV-1-protein medium omgewing vir 24 uur het geen uitwerking op NO produksie gehad nie en het moontlik die verminderde vlakke weens HIV-1-protein behandeling op sy eie verbeter. Bowendien, is ’n afname in RSS gemerk (DHR-123 fluoressensie intensiteit: 83.19±3.5% *vs.* 100±0.22%). PI behandeling in ’n HIV-1-protein media omgewing vir 24 uur het verminderde NO produksie tot gevolg gehad in ’n dosis-afhanklike wyse (DAF-2/DA fluoressensie intensiteit: 92.74±1.4% *vs.* 100±0.67% en 85±1.81% *vs.* 100±0.56%), waarskynlik as gevolg van verminderde eNOS uitdrukking (0.28±0.04 *vs.* 1±0.21). Interessant genoeg, het nóg HIV-1 proteïne, nóg PI behandeling op hul eie enige uitwerking op eNOS gehad nie. Dieselfde is waargeneem vir IκBα, waar blootstelling aan gekombineerde HIV-1-protein en PI behandeling IκBα vlakke verlaag het (0.37±0.03 *vs*. 1±0.15), terwyl die HIV-1 en PI behandelings op hul eie geen uitwerking gehad het nie.

Gevolgtrekking: HIV-1 Nef, Tat en Gp160 het NO produksie in AESe verminder, terwyl NRTI/NNRTI behandeling binne hierdie HIV-1 proteïen omgewing minimale negatiewe gevolge getoon het en moontlik selfs voordelig was, deur potensieel die negatiewe uitwerkings van HIV-1 proteïne op NO produksie te

herstel. PI behandeling, aan die ander kant, het geblyk om ’n skadelike interaksie met die HIV-1 proteïne te toon, wat gelei het tot ’n afname in eNOS-NO biosintese. Die PI-HIV-1 proteïen kombinasie was ook geassosieer met ’n opregulering van die pro-inflammatoriese NFκB seinpaaie, wat moontlik ’n verklaring is vir die verminderde eNOS uitdrukking.

ACKNOWLEDGEMENTS

- Firstly, I would like to thank my supervisors, Dr Amanda Genis and Prof Hans Strijdom for their continued guidance and support. During the two years of my MSc, I learned so much from them and for that I am exceedingly grateful.
- I would like to thank the Division of Medical Physiology for the warm and supportive environment in which I had the privilege to work. I can honestly say it is the most welcoming department I have ever come across.
- A special thank you to all my colleagues at the Division of Medical Physiology, but especially Mignon van Vuuren, Victoria Patten and Jordyn Rawstorne for their assistance with laboratory techniques that were new to me.
- I would like to acknowledge the Harry Crossley Foundation (Stellenbosch University), Early Research Career Funding (Stellenbosch University), the National Research Foundation of South Africa and the Department of Science and Technology for providing the necessary funding without which this work would not have been possible.
- Lastly, I would like to thank all my friends and family for their continued support and encouragement throughout my studies.

TABLE OF CONTENTS

LIST OF FIGURES

Chapter 1

Chapter 2

Chapter 3

Chapter 4

LIST OF TABLES

Chapter 4

LIST OF ABBREVIATIONS

3TC	Lamivudine
ADMA	Asymmetric dimethylarginine
AEC	Aortic Endothelial Cell
AGE	Advanced Glycation End-product
AIDS	Acquired Immunodeficiency Syndrome
AMPK	AMP-activated Kinase
ANOVA	Analysis of variance
ART	Antiretroviral Therapy
ATP	Adenosine triphosphate
AZT	Zidovudine
Ca^{2+}	Calcium
CAD	Coronary Artery Disease
CaMKII	Calmodulin-dependent Kinase II
cAMP	Cyclic adenosine monophosphate
CCR5	Co-receptor C-C Chemokine Receptor 5
CD28	Cluster of Differentiation 28
CD4	Cluster of Differentiation 4
CD40	Cluster of Differentiation 40
cGMP	Cyclic guanosine monophosphate
CHD	Coronary Heart Disease
CVC	Combined Vehicle Control

CVD	Cardiovascular Disease
CXCR4	C-X-C Chemokine Receptor 4
DAF-2/DA	4,5-Diaminofluorescein diacetate
DEA/NO	Diethylamine NONOate diethylammonium
dH_2O	Distilled water
DHR-123	Dihydrorhodamine-1,2,3
DMSO	Dimethyl sulfoxide
DNA	Deoxyribonucleic Acid
ECL	Clarity™ Enhanced Chemiluminescence
EDRF	Endothelium-derived Relaxing Factor
EDTA	Ethylenediaminetetraacetic acid
EFV	Efavirenz
EGTA	Ethylene Glycol Tereaacetic Acid
eNOS	Endothelial Nitric Oxide Synthase
ER	Endoplasmic Reticulum
ESS	Endothelial Shear Stress
FBS	Fetal Bovine Serum
FDC	Fixed Dose Combination
FTC	Emtricitabine
H_2O_2	Hydrogen peroxide
HAART	Highly Active Antiretroviral Therapy
HCl	Hydrochloric acid
HDL	High-density Lipoprotein

Hg	Mercury
HIV	Human Immunodeficiency Virus
HKP	House Keeping Protein
HO·	Hydroxyl radical
HPAEC	Human Pulmonary Artery Endothelial Cell
HRP	Horseradish peroxidase
ICAM-1	Intercellular Adhesion Molecule 1
IL-6	Interleukin 6
IL-8	Interleukin 8
iNOS	Inducible Nitric Oxide Synthase
IκBα	Nuclear factor kappa-B inhibitor alpha
JAM-1	Junctional Adhesion Molecule 1
JNK	c-Jun N-terminal Kinase
LDL	Low-density Lipoprotein
LPV	Lopinavir
LPV/r	Lopinavir boosted with Ritonavir
M	Molar
MAPK	Mitogen-Activated Protein Kinase
MCP-1	Monocyte Chemoattractant Protein-1
MeOH	Methanol
mg	Milligram
MHCI	Major Histocompatibility Complex class I
MHCII	Major Histocompatibility Complex class II

ml	Millilitre
mM	Milli molar
mm	Millimetre
MRI	Magnetic Resonance Imaging
Na_3VO_4	Sodium orthovanadate
NaCl	Sodium Chloride
NADPH	Reduced Nicotinamide-Adenine-Dinucleotide Phosphate
NaF	Sodium Fluoride
NaOH	Sodium hydroxide
Nef	Negative regulator factor
NFκB	Nuclear Factor kappa-light-chain-enhancer of activated B cells
ng	Nanogram
nM	Nano molar
nNOS	Neuronal Nitric Oxide Synthase
NNRTI	Non-nucleoside Reverse Transcriptase Inhibitor
NO	Nitric Oxide
NPC	Nuclear Pore Complex
NRTI	Nucleoside-analogue Reverse Transcriptase Inhibitor
O_2	Oxygen
O_2^-	Superoxide anion
$ONOO^-$	Peroxynitrite
PARP	Poly (ADP-ribose) Polymerase
PBS	Phosphate Buffered Saline

PI	Protease Inhibitor
PIC	Pre-integration Complex
PKA	Protein Kinase A
PKB/Akt	Protein Kinase B
PKG	Protein Kinase G
PLWHA	People Living with HIV/AIDS
PMSF	Phenylmethylsulphonyl fluoride
Prop. I	Propidium Iodide
R3-IGF-1	Long-chain human insulin-like growth factor
Rev	Regulator of expression of the virion
rhEGF	Recombinant human epidermal growth factor
rhFGF-B	Recombinant human fibroblastic growth factor B
RNA	Ribonucleic Acid
RNS	Reactive Nitrogen Species
ROS	Reactive Oxygen Species
Rpm	Revolutions per minute
RTC	Reverse-transcription Complex
RTV	Ritonavir
SDS	Soudium Dodecyl Sulphate
SEM	Standard Error of the Mean
SIV	Simian Immunodeficiency Virus
Tat	Transactivator of transcription
TBS	Tris-buffered saline

TDF	Tenofovir
TNF-α	Tumour Necrosis Factor alpha
TPN	Total Protein Normalisation
VC	Vehicle Control
VCAM-1	Vascular Cell Adhesion Molecule 1
VEGF	Vascular Endothelial Growth Factor
Vif	Virus infectivity factor
Vpr	Viral protein R
Vpu	Viral protein U
WHO	World Health Organisation
ZO-1	Zonula Occludens-1
µg	Microgram
µl	Microlitre
µM	Micro molar

CHAPTER 1: LITERATURE REVIEW

1.1. CARDIOVASCULAR DISEASE (CVD)

1.1.1 Epidemiology

Cardiovascular disease (CVD) is the leading cause of mortality worldwide. In 2015, an estimated 17.7 million deaths were attributed to CVD, which represented 31% of the global total, and of these deaths, more than 70% occurred in low- and middle-income countries (WHO, 2017). The bulk of cardiovascular deaths are attributed to two conditions, namely, ischaemic heart disease and cerebrovascular disease (predominantly ischaemic stroke). Globally, these are the number one and two causes of years of life lost, respectively (Wang *et al.*, 2016). Underpinning both these conditions is a chronic inflammatory state of the arteries: atherosclerosis (Nabel and Braunwald, 2012; Barquera *et al.*, 2015).

1.1.2 Atherosclerosis

Atherosclerosis occurs at vulnerable sites in large and medium sized arteries, where it results in the development of atherosclerotic plaques. It is a chronic inflammatory process which develops in response to the biologic effects of cardiovascular risk factors. Joseph *et al.* (2017) showed that short-term changes in arterial inflammation could predict long-term atherosclerosis progression. Participants with increased carotid inflammation over a six-month period, showed MRI evidence of increased carotid mean wall thickness and mean wall area at two years. Conversely, in participants without increased arterial inflammation, no significant long-term atherosclerosis progression was observed. Exposure to cardiovascular risk factors activates the vascular endothelial cells, resulting in changes in their permeability, which promotes the entry of low-density lipoprotein (LDL) particles into the sub-endothelial space of the intima layer of the blood vessel. Once in the intima, these LDL particles are modified, which includes being oxidised by reactive oxygen species (ROS), and this perpetuates the activation process. Consequently, these endothelial cells release chemokines into the bloodstream which attract circulating leukocytes, especially monocytes. These monocytes then adhere to the activated endothelium and enter the sub-endothelial space, where they differentiate into macrophages which ingest the various LDL particles and eventually transform into lipid filled foam cells **(Figure 1.1)** (Mestas and Ley, 2008; Insull, 2009; Moore and Tabas, 2011; Nabel and Braunwald, 2012), a process in which oxidative stress plays a crucial role (Förstermann, Xia and Li, 2017).

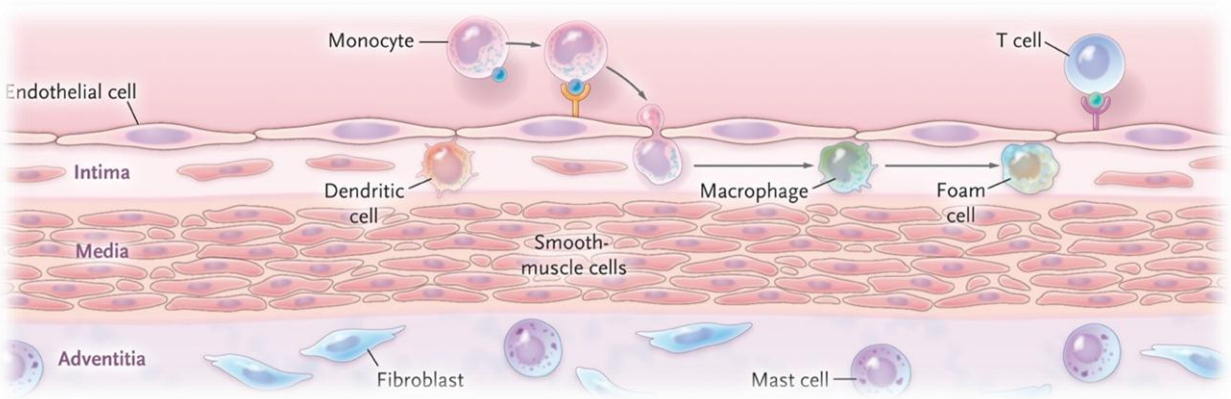

Figure 1.1: Foam cell formation. Adapted from Nabel and Braunwald (2012).

Elevated levels of LDL cholesterol in the blood plasma aggravates the atherosclerotic process, since, in this scenario, levels of LDL-influx into the sub-endothelial space exceeds the eliminating capacity. Arterial wall LDL accumulation is either the result of increased lipoprotein influx caused by enhanced endothelial permeability and subsequent LDL deposition or a decreased lipoprotein efflux. At areas of disturbed flow in the vasculature, LDL influx from the circulation is even higher due to flow stagnation and longer contact between the blood and vascular endothelial cells. Should serum LDL-levels remain high, a self-perpetuating process develops, where the accumulation of excess extracellular LDL triggers a continuous inflammatory recruitment of monocytes and the subsequent build-up of macrophage foam cells **(Figure 1.2)** (Moore and Tabas, 2011; Förstermann, Xia and Li, 2017). Oxidised LDL particles cause endoplasmic reticulum (ER) stress within the macrophages and should this stress continue, it can lead to macrophage apoptosis (Sanson *et al.*, 2009). Initially, these apoptotic macrophage foam cells can be removed by phagocytes, but if the process is perpetuated and the lesion progresses, the clearance of apoptotic foam cells becomes ineffective and a necrotic core develops within the atherosclerotic plaque (Moore and Tabas, 2011). Under the vascular endothelium, fibrous tissue then accumulates to form a cap over this lipid-rich necrotic core (Insull, 2009).

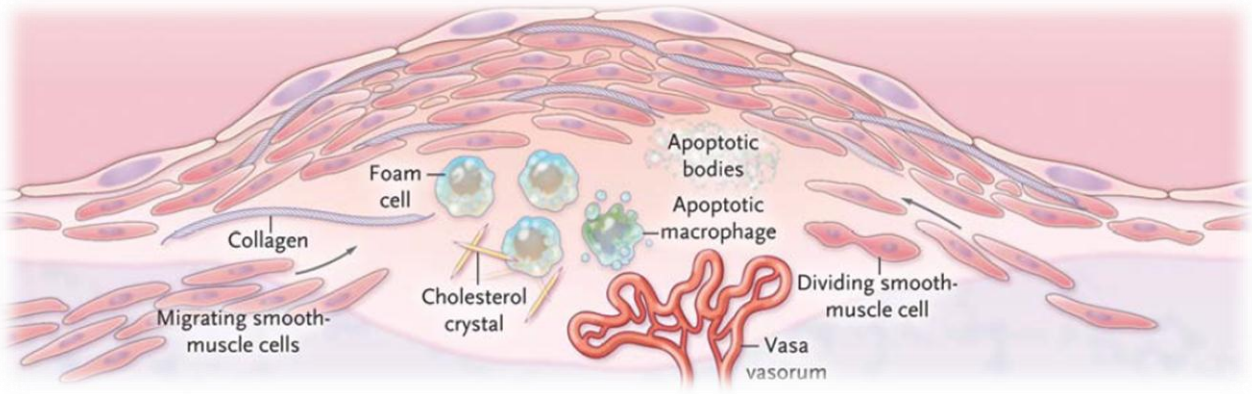

Figure 1.2: Atherosclerotic plaque formation. Adapted from Nabel and Braunwald (2012).

1.1.3 Traditional Risk Factors

The underlying causes of atherosclerosis and consequent cardiovascular disease are multiple and complex, however, the INTERHEART study (Yusuf *et al.*, 2004), a large case-control study, has identified nine potentially modifiable factors that seem to be associated with more than 90% of the risk for an acute myocardial infarction: Smoking, abnormal lipids, adverse psychosocial factors, abdominal obesity, diabetes, and hypertension were associated with increased myocardial infarction risk, while a daily vegetable and fruit intake, physical exercise and the moderate consumption of alcohol were considered protective.

Smoking

Exposure to cigarette smoke results in endothelial cell activation, dysfunction, injury and death, leading to lipid accumulation and the recruitment of leukocytes (Morris et al., 2015). In people aged 60 years and older, smoking strongly correlates with acute coronary events, stroke, and cardiovascular deaths. In this cohort, being a smoker advanced the risk of dying from CVD by 5.5 years compared to non-smokers. Among smokers, the excess risk also increased with greater cigarette consumption and in former smokers the risk decreased with time after quitting in a dose-response manner (Mons et al., 2015). A meta-analysis by Hackshaw et al. (2018) found that a major proportion of the risk of coronary heart disease and stroke came from smoking only a few cigarettes.

Abnormal lipids

LDL cholesterol is a primary causal agent in the development of atherosclerosis and high serum levels are an essential determinant of cardiovascular risk. LDL cholesterol reduction with statin therapy has consistently been shown to be a safe and highly effective method to reduce cardiovascular risk (Ridker, 2014). Cholesterol lowering with a low dose of rosuvastatin therapy was associated with a significant

reduction in cardiovascular events even in individuals who did not suffer from CVD and who were only at intermediate risk (Yusuf et al., 2016). In contrast with LDL cholesterol, high-density lipoprotein (HDL) cholesterol protects against atherosclerosis and is inversely associated with coronary heart disease risk. HDL cholesterol alleviates endothelial dysfunction, aids in the removal of excess cholesterol from macrophages and has antioxidant, anti-inflammatory and antiapoptotic properties. However, under certain circumstances, HDL can become dysfunctional and loose its atheroprotective properties (Rader and Hovingh, 2014; Rosenson et al., 2016). Triglycerides, or more specifically triglyceride-rich lipoproteins, are considered another causal risk factor for CVD. However, triglycerides can be degraded by most cells, whereas cholesterol cannot and thus it is more likely that it is the cholesterol content of these triglyceride-rich lipoproteins that plays this causal part in CVD development. Plasma triglyceride levels can therefore more accurately be described as a marker of remnant cholesterol, which is the cholesterol content of triglyceride-rich lipoproteins (Nordestgaard and Varbo, 2014).

Abdominal obesity

An association between body weight and CVD has long been established. In the 1980s, The Framingham study demonstrated that degree of obesity was an important long-term predictor of CVD incidence, particularly in younger participants (Hubert HB, Feinleib M, McNamara PM, 1983). Overweight and obesity are risk factors for a number of conditions, including type II diabetes, cancer and CVD (Guh et al., 2009). In a large longitudinal community- and population-based cohort, greater accumulation of abdominal fat volume, including abdominal subcutaneous adipose tissue and visceral adipose tissue, was associated with an increased incidence of CVD and adverse changes in cardiovascular risk factors above and beyond the risk associated with general- and central adiposity (Lee et al., 2016).

Diabetes mellitus

Hyperglycaemia negatively impacts the vasculature in several ways. High glucose concentrations can activate nuclear factor kappa-light-chain-enhancer of activated B cells (NFκB) in endothelial cells, monocyte-derived macrophages and vascular smooth muscle cells which affects the transcription of multiple genes. Advanced glycation end-products (AGEs) are formed when proteins and lipids are exposed to high concentrations of glucose and this can increase reactive oxygen species (ROS) production. In this way high glucose levels lead to oxidative stress. High glucose concentrations can also contribute to the modification of lipoproteins which likely promotes atherosclerosis. These lipoprotein changes result in reduced cholesterol efflux from macrophages and promote proinflammatory phenotypes. Altered lipoprotein particles also activate endothelial cells, increasing adhesion molecule expression and the consequent inflammatory response (Mazzone, Chait and Plutzky, 2008).

Hypertension

The link between CVD and hypertension is well established. In a meta-analysis by Ettehad et al. (2016), blood pressure lowering medication significantly reduced the risk of CVD and CVD mortality in multiple populations of patients. A 10 mm Hg reduction in systolic blood pressure decreased the risk of major CVD

events by 20%, coronary heart disease by 17%, stroke by 27%, heart failure by 28%, and all-cause mortality by 13%.

Diet

The link between diet and CVD has lately become a contentious topic. Traditionally, low-fat diets were prescribed for reducing weight and cardiovascular risk, however, recently this view has been disputed. Both low-fat and low-carbohydrate diets have been shown to be effective for weight-loss yet, low-carbohydrate diets seem to offer more favourable changes in terms of cardiovascular risk reduction (Foster et al., 2010; Bazzano et al., 2014). However, De Souza et al. (2015) found no clear association between a higher intake of saturated fats and all-cause mortality, coronary heart disease (CHD), CHD mortality, ischemic stroke or type II diabetes in healthy adults. Conversely, the consumption of trans-unsaturated fatty acids was associated with a 34% increase in all-cause mortality, a 28% increase in the risk of CHD mortality and an increased risk of 21% for CHD.

Physical exercise

Physical activity has been described as one of the most fundamental factors necessary for maintaining health and dispelling cardiovascular risk (Schuler, Adams and Goto, 2013). In 7744 men initially free of CVD, being physically active was associated with a reduction in the risk of CVD death, while sedentary activities including time spent riding in a car and watching television were predictors of CVD mortality. Interestingly, high levels of physical activity were related to reduced CVD mortality even in individuals who also spent large amounts of time participating in sedentary activities (Warren et al., 2010).

1.1.4 Emerging Cardiovascular Risk Factors: HIV and Antiretroviral Therapy

Since the advent of antiretroviral therapy (ART), human immunodeficiency virus (HIV) has increasingly become regarded as a chronic and manageable disease and subsequently new challenges have arisen. Comorbidities with non-communicable conditions such as CVD pose additional obstacles for persons infected with this virus. Moreover, increased cardiovascular risk has been associated with HIV-infection itself as well as with ART. A meta-analysis by Islam *et al.* (2012) showed that the relative risk of developing CVD in HIV-positive persons was 61% higher than that of their HIV-negative counterparts. Additionally, the investigators found the cardiovascular risk in people living with HIV receiving highly active antiretroviral therapy (HAART) to be double that of treatment-naïve HIV-positive individuals. These findings are also echoed by a recent systematic review, meta-analysis and burden assessment, which showed the risk of CVD in people living with HIV to be twice that of the uninfected population. Furthermore, the authors of this paper purport that the incidence of CVD associated with HIV is comparable to that of other high cardiovascular risk groups, including diabetes mellitus. Worryingly, they also found sub-Saharan Africa to carry a large proportion of this burden (Shah *et al.*, 2018). Hsue and Waters (2018) argue that the time has come to regard HIV infection as a major cardiovascular risk factor, together with conditions such as diabetes mellitus, hypertension and hyperlipidaemia. The novel

cardiovascular risk factors of HIV and ART will thus be the focus of this thesis, with more detail to follow later in the text.

1.1.5 Progression

As described above, atherosclerosis begins with the pathophysiological activation of endothelial cells, leading to permeability changes and the entry of monocytes and cholesterol containing LDL particles into the artery intima. What follows is the development of the atherosclerotic plaque. These plaques are responsible for the clinical symptoms associated with CVD. Plaques in the arteries of the heart can cause flow-limiting stenosis and this results in stable angina, or they can provoke the formation of a thrombus that interrupts blood flow either temporarily, resulting in unstable angina, or a permanently, causing a myocardial infarction. The rupture of atherosclerotic plaques exposes procoagulant material within the core of the plaque which can initiate the coagulation cascade, prompting thrombosis and also potentially resulting in a myocardial infarction **(Figure 1.3)** (Nabel and Braunwald, 2012). While the process of atherogenesis is irreversible, its precursors, endothelial activation and dysfunction fortunately are not. In this regard, endothelial dysfunction is thought to be an early predictor of atherosclerosis and subsequent CVD (Mudau *et al.*, 2012).

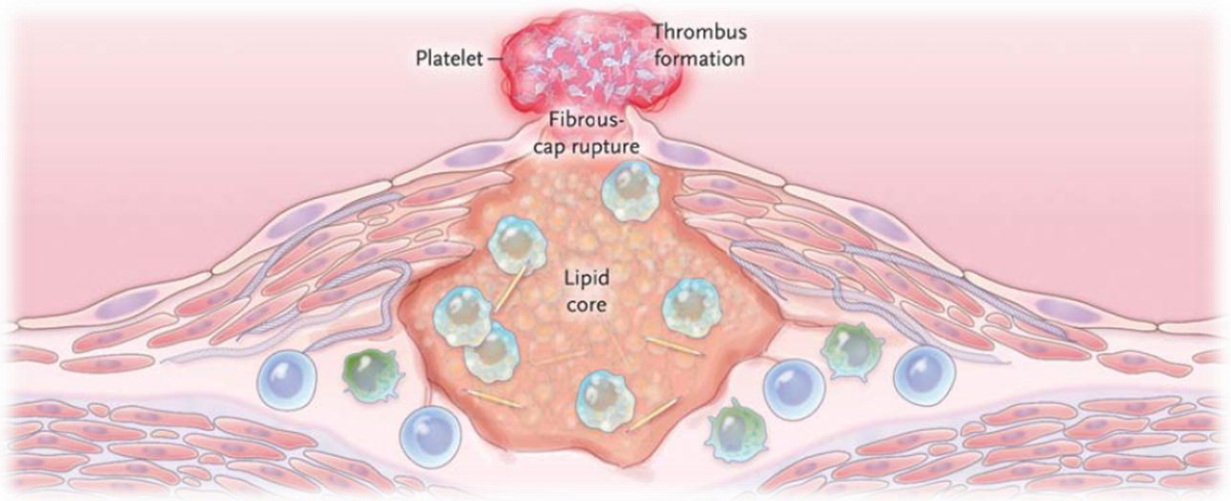

Figure 1.3: Thrombus formation. Adapted from Nabel and Braunwald (2012).

1.2. ENDOTHELIAL DYSFUNCTION

1.2.1 The Vascular Endothelium

The vascular endothelium, a monolayer of selectively permeable endothelial cells, plays an essential role in regulating vascular homeostasis. It responds to various physical and chemical signals by producing a broad spectrum of factors that regulate vascular tone, cell adhesion, coagulation, smooth muscle cell proliferation and inflammation (Deanfield, Halcox and Rabelink, 2007). One of the vascular endothelium's primary functions is to maintain the balance between vasodilation and vasoconstriction and nitric oxide (NO), a gaseous free radical synthesized by the enzyme endothelial NO synthase (eNOS), is a crucial agent in this regard (Davignon and Ganz, 2004; Mudau *et al.*, 2012).

Endothelial Nitric Oxide Synthase (eNOS)

In mammals, nitric oxide synthase (NOS) exists in three different isoforms, namely, neuronal NOS (nNOS), inducible NOS (iNOS) and endothelial NOS (eNOS). nNOS is expressed in specific neurons of the central and peripheral nervous systems. In the central nervous system it plays a role in synaptic plasticity and central blood pressure regulation, while in the peripheral nervous system it is involved in atypical neurotransmission and penile erection. iNOS plays a role in inflammation and the immune response and its transcription is induced by cytokines. eNOS is primarily expressed in endothelial cells (Knowles and Moncada, 1994; Luiking, Engelen and Deutz, 2010; Förstermann and Sessa, 2012). In its functional form, eNOS exists as a dimer and is regulated by intracellular calcium (Ca^{2+}) levels and phosphorylation. Phosphorylation of the serine 1177 residue increases enzyme activity, while the threonine 495 residue is a negative regulatory site and its phosphorylation results in decreased enzyme activity. NOS converts the amino acid L-arginine into NO and L-citrulline, utilising oxygen and reduced nicotinamide-adenine-dinucleotide phosphate (NADPH) as co-substrates **(Figure 1.4)** (Davignon and Ganz, 2004; Förstermann and Sessa, 2012).

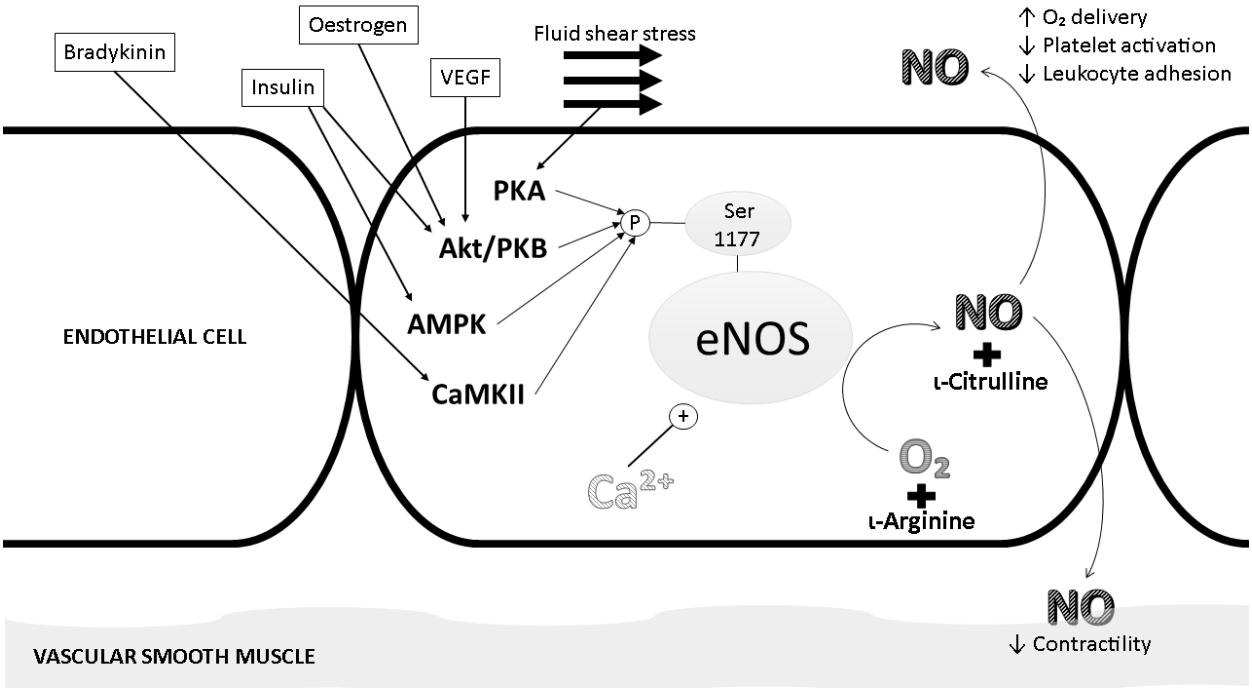

Figure 1.4: NO synthesis in an endothelial cell. eNOS activity is regulated by intracellular Ca^{2+} and phosphorylation. Protein kinase A (PKA), Protein kinase B (PKB/Akt), AMP-activated kinase (AMPK) and calmodulin-dependent kinase II (CaMKII) can all phosphorylate eNOS at Ser1177, thus enhancing the enzyme's activity. eNOS converts oxygen and L-arginine into nitric oxide and L-citrulline. NO decreases leukocyte adhesion and in platelets it decreases activation, adhesion and aggregation. It results in the relaxation of vascular smooth muscle and reacts with the haemoglobin in red blood cells, increasing oxygen delivery to tissues. Figure designed by the author of this thesis, based on content from Förstermann and Sessa, (2012) and Gimbrone and García-Cardeña (2016).

Nitric Oxide (NO)

NO is a powerful vasodilator and functions to maintain the vascular wall in a homeostatic state by inhibiting inflammation, cellular proliferation and thrombosis (Deanfield, Halcox and Rabelink, 2007). This molecule also protects against atherosclerosis (Förstermann and Sessa, 2012). Its actions were once thought to be the doing of a mystery substance termed endothelium-derived relaxing factor (EDRF) until it was discovered that NO and EDRF were in fact one and the very same (Palmer, Ferrige and Moncada, 1987). NO is constitutively synthesized in endothelial cells by eNOS in response to various stimuli. The NO then diffuses to adjacent vascular smooth muscle cells where it initiates cell signalling cascades resulting in vasorelaxation **(Figure 1.5)** (Förstermann and Sessa, 2012).

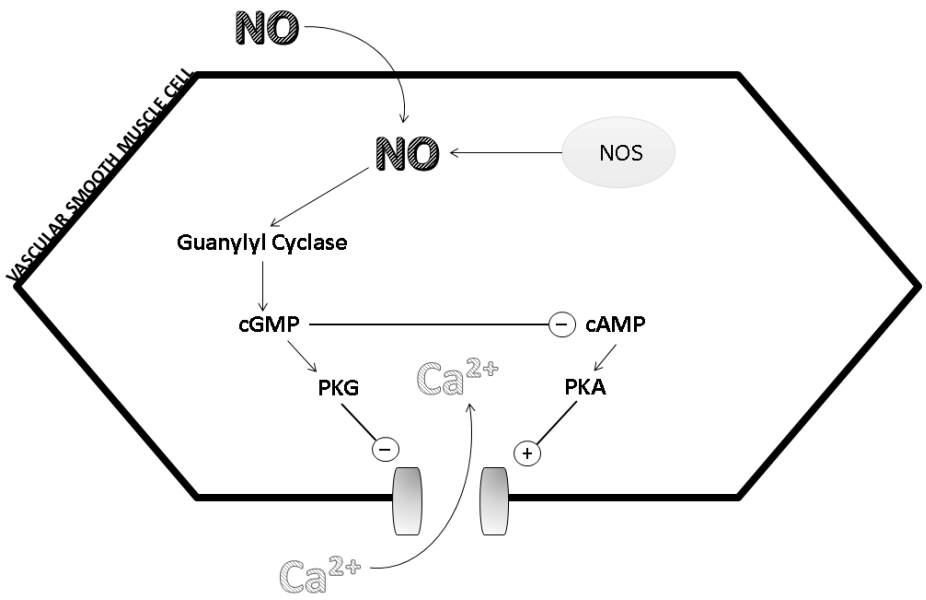

Figure 1.5: NO signalling in a vascular smooth muscle cell. NO leads to the downstream phosphorylation of protein kinase G (PKG). PKG then causes L-type calcium channels in the muscle cell to close, preventing the influx of calcium ions. This inhibits muscle cell contraction and results in vasorelaxation. Figure designed by the author of this thesis, based on content from Maron and Michel (2012) and Mudau *et al.* (2012).

1.2.2 Endothelial Dysfunction

When the vascular endothelium can no longer maintain homeostasis, endothelial dysfunction ensues. This pathophysiological state is characterised by a loss of the balance between vasodilation and vasoconstriction, with vasoconstriction becoming dominant, and, as mentioned before, it is regarded as an early precursor to the development of atherosclerosis and subsequent CVD. Central to endothelial dysfunction is reduced NO bioavailability, which can be accounted for by a number of mechanisms including reduced eNOS protein levels, decreased substrate and cofactor availability, changes in eNOS phosphorylation and furthermore, ROS can inactivate eNOS and scavenge NO itself. Oxidative stress is believed to be the putative pathophysiological process responsible for reduced NO bioavailability as it results in the modification of both NO and eNOS (Davignon and Ganz, 2004; Liu and Huang, 2008; Mudau *et al.*, 2012).

Oxidative Stress

When reactive oxygen species (ROS) such as the superoxide anion ($O_2^{\cdot-}$), hydrogen peroxide (H_2O_2) or hydroxyl radical (HO·) overcome cellular antioxidant defences, it results in oxidative stress and whilst NO

protects against atherosclerosis, vascular oxidative stress is pro-atherogenic (Förstermann, Xia and Li, 2017). ROS are generated endogenously, for example via mitochondrial oxidative phosphorylation, and/or originate from exogenous sources. Under physiological conditions cells are well equipped to deal with ROS **(Table 1.1)**, however, when levels rise beyond the neutralisation capabilities of the cell or when there is a decrease in cellular antioxidant capacity, oxidative stress occurs (Ray, Huang and Tsuji, 2012). In the context of endothelial dysfunction, oxidative stress has two primary consequences. Firstly, it is responsible for the inactivation of NO itself by its reaction with O_2^-, turning it into peroxynitrite ($ONOO^-$), a potent reactive nitrogen species (RNS) (Förstermann and Sessa, 2012; Mudau *et al.*, 2012). This can lead to nitrosative stress, a damaging state, detectible via the nitration of the amino acid tyrosine, resulting in nitrotyrosine formation (Duncan, 2003). Secondly, oxidative stress can result in the uncoupling of eNOS, converting it from a dimer to a monomer that acts as a O_2^- generating enzyme further exacerbating the level of oxidative stress (Förstermann and Sessa, 2012; Mudau *et al.*, 2012). A number of factors can contribute to the cellular antioxidant defences being overwhelmed and the development of oxidative stress, including irregular blood flow and cardiovascular risk factors (Li, Horke and Förstermann, 2013; Hsieh *et al.*, 2014).

Table 1.1: Summary of reactive oxygen species (ROS) producing systems in the vascular wall and antioxidant defences. Content from Förstermann, Xia and Li (2017).

ROS-producing systems		Antioxidant enzymes	
NADPH Oxidases	Two membrane-bound subunits: p22phox and a Nox homologue.	**Superoxide Dismutase**	Catalyzes the dismutation of superoxide into oxygen and hydrogen peroxide.
	Several cytosolic regulatory subunits.		
	Produces superoxide.		
Xanthine Oxidase	Produces superoxide and hydrogen peroxide	**Catalase**	Located in peroxisomes
			Catalyses the reduction of hydrogen peroxide to oxygen and water.
Mitochondria	Produce excess ROS under pathological conditions, including superoxide.	**Glutathione Peroxidases**	The major antioxidant enzyme within many cells
			Reduces hydrogen peroxide to water
			Reduces lipid hydroperoxides

Uncoupled eNOS	Produces superoxide	**Paraoxonases**	Family of three proteins
			Reduce oxidative stress
			Decreases lipid peroxidation.

Blood Flow

Endothelial shear stress (ESS) is the parallel frictional drag force acting along the vascular endothelium due to blood flow and it plays an integral part in the development of atherosclerosis – especially with regards to where atherosclerotic plaques tend to develop. Atherosclerotic plaques do not develop randomly, but rather, at susceptible sites in arteries where blood flow is irregular and characterised by low and oscillatory endothelial shear stress (ESS) (Cunningham and Gotlieb, 2005; Hsieh *et al.*, 2014). Low and oscillatory ESS occur at curved, branched and diverged regions in arteries. Where arteries are straight, and the blood flow is laminar, ESS tends to be moderate or physiological. This is termed regular flow and atherosclerotic plaques generally do not develop in regions characterised by regular flow (Wentzel *et al.*, 2012; Hsieh *et al.*, 2014).

Regular flow and the resultant moderate or physiological ESS leads to the activation of protein kinase A (PKA) which in turn phosphorylates eNOS at Ser1177, increasing the enzyme's sensitivity to intracellular Ca^{2+}, resulting in the synthesis of NO and subsequent vasodilation **(Figure 1.4)** (Förstermann and Sessa, 2012). Furthermore, besides the immediate vasodilatory effect, moderate or physiological ESS also facilitates more long-term changes through vascular remodelling. Regular flow stimulates NO production and attenuates ROS production leading to the generation of an anti-oxidant state and the activation of transcription factors that promote an anti-atherogenic vascular wall environment. Contrary to this, irregular flow reduces NO production and promotes ROS formation which leads to a state of oxidative stress and the activation of inflammatory transcription factors such as NFκB (Hsieh *et al.*, 2014). Multiple pathways can lead to the activation of NFκB. The canonical NFκB activation pathway results in the proteolysis of IκBα (an inhibitory protein that prevents the translocation of NFκB to the nucleus) and the phosphorylation of the RelA/p65 subunit of NFκB on serine 276 (Brasier, 2010). NFκB and other inflammatory transcription factors favour the creation of a pro-atherogenic environment resulting in the proliferation of vascular endothelial and smooth muscle cells, as well as increased leukocyte adhesion (Qi *et al.*, 2011; Liao, 2013).

As multiple cardiovascular risk factors have been implicated in the development of oxidative stress, the consequences for these already susceptible sites are cumulative. Hypertension, hypercholesterolemia, diabetes mellitus and smoking all induce oxidative stress in the vascular wall with a subsequent decrease in NO bioavailability and ensuing endothelial dysfunction (Li, Horke and Förstermann, 2013). Additionally,

NO normally has an inhibitory effect on NFκB, however, decreased NO bioavailability caused by exposure to cardiovascular risk factors, further enhances the activation of NFκB in areas of irregular flow (Liao, 2013).

Cardiovascular Risk Factors

Multiple cardiovascular risk factors have been implicated in the development of oxidative stress and endothelial dysfunction (Mudau *et al.*, 2012). Risk factors stimulate the production of ROS via multiple sources including NADPH oxidases, xanthine oxidase, mitochondria and uncoupled eNOS, consequently decreasing NO bioavailability (Förstermann, Xia and Li, 2017). This leads to endothelial dysfunction and endothelial cell activation with subsequent atherosclerosis (Mudau *et al.*, 2012). Both native LDL cholesterol and minimally oxidised LDL cholesterol have been linked to vascular endothelial O_2^-generation (Stepp *et al.*, 2002). In mice and human subjects, fat accumulation was shown to correlate with systemic oxidative stress. In the adipose tissue of obese mice ROS production was augmented and the expression of antioxidant enzymes decreased. Elevated levels of fatty acids in cultured adipocytes increased oxidative stress and this was linked to the dysregulation of adipocytokines (Furukawa *et al.*, 2004). Hypertension has also been linked to oxidative stress (Montezano *et al.*, 2015) as well as type II diabetes. The "Coronary Artery Risk Development In young Adults" (CARDIA) study showed that biomarkers of oxidative stress positively correlated with type II diabetes. Additionally higher levels of E-selectin, a cell-surface adhesion molecule and plasma biomarker of endothelial dysfunction activated by proinflammatory cytokines like TNF-α and IL-6 (Liao, 2013), was also strongly associated with type II diabetes (Odegaard *et al.*, 2016). The isolated aortic rings of cigarette smoke-exposed mice showed in a significant impairment of endothelium-dependent vasorelaxation, indicative of endothelial dysfunction (Talukder *et al.*, 2011). Furthermore, both HIV and ART have been linked to oxidative stress and endothelial dysfunction (Lambert *et al.*, 2016).

1.3. Human Immunodeficiency Virus (HIV)

1.3.1 Epidemiology

Human Immunodeficiency Virus Type 1 (HIV-1) and Type 2 (HIV-2) belong to a group of pathogens termed lentiviruses, which can infect various mammalian species. The prefix, "lenti" is derived from the Latin word, *lento*, meaning "slow," as most diseases associated with this group of viruses have a slow onset and result in chronic infections (Campbell and Robinson, 1998). Genetically, HIV-1 and HIV-2 are only distantly related, but clinically they cause similar symptoms. HIV-2 is largely restricted to West Africa and its prevalence is declining. It is not very aggressive and most infected individuals do not progress to Acquired Immunodeficiency Syndrome (AIDS) (Sharp and Hahn, 2011), the end-stage disease of HIV-infection, a consequence of the activation and eventual destruction of the host immune system (Weiss,

1993). HIV-1 is responsible for the global pandemic. It is not a single virus, but four distinct lineages: groups M, N, O and P, of which group M is the most virulent. Both HIV-1 and HIV-2 evolved following zoonotic transfers of lentiviruses infecting primates in West Central Africa, possibly a consequence of bushmeat hunting. Four independent cross-species transmission events of Simian Immunodeficiency Viruses (SIVs) are believed to be responsible for the human infection by the SIV precursors of each of the four HIV-1 lineage groups. Subsequent viral adaptations, aided by the fact that Immunodeficiency Viruses evolve rapidly, had to occur to enable these precursors to replicate in their new species host. Of the four groups, M was most successful, making it unsurprising that it is this group that drives the global HIV pandemic (Sharp and Hahn, 2011). Furthermore, HIV-1 group M consists of a number of subtypes, varying in occurrence from region to region across the globe, with the greatest diversity found in Central Africa (Hemelaar *et al.*, 2011). In Southern Africa subtype C dominates (Sharp and Hahn, 2011). Additionally, since HIV-1 is such a variable pathogen, subtypes do not exist homogenously within infected individuals, but as clusters of closely related, yet non-identical viral genomes (McCutchan, 2006).

In 2015 17.0 million people were living with HIV and receiving antiretroviral therapy worldwide. In 2010 1.5 million AIDS related deaths were recorded, a figure that decreased to 1.1 million in 2015 (UNAIDS, 2016). While HIV prevalence is dropping globally, declines are only evident where prevention strategies have been broadly implemented and embraced by the target population. Despite intervention, Sub-Saharan Africa remains the epicentre for the HIV pandemic (Vermund, 2014). A global decline noted in annual new infections among adults has, however, plateaued in recent years and, in 2015, remained nearly static at about 1.9 million. Notwithstanding, this figure encompasses many disparities, with some populations still at a disadvantage (UNAIDS, 2016).

Young women aged 15-24 years are a group exceedingly at risk for HIV infection, globally this group accounted for 20% of new HIV infections among adults in 2015. Other populations at increased risk of HIV infection include sex workers, people who inject drugs, transgender people, prisoners and men who have sex with men (UNAIDS, 2016). Sex workers face an exceedingly large burden of HIV and access to prevention as well as treatment lags behind the general population (Shannon *et al.*, 2015). In countries of all incomes, HIV epidemics in men who have sex with men are increasing (Beyrer *et al.*, 2012). Furthermore, geographic differences in HIV prevalence exist and, in many countries, HIV incidence tends to be higher in urban areas (UNAIDS, 2016).

HIV-1 is an extremely adept pathogen able to successfully commandeer host cellular processes for its own ends, whilst simultaneously neutralising anti-viral defences (Sorin and Kalpana, 2006), all of which is achieved utilising only fourteen viral proteins (Turner and Summers, 1999).

1.3.2 Structure

The HIV-1 genome contains 9 main genes: *gag, pol, env, tat, rev, vpu, vpr, vif* and *nef.* *Gag* encodes for three structural proteins, which include matrix proteins, capsid proteins and nucleocapsid proteins. *Pol* encodes for three enzymes that are essential for the synthesis of the viral proteins. They include reverse transcriptase, which allows the transcription of single-stranded viral RNA into double-stranded provisional DNA that can be integrated into the host cell genome by the enzyme integrase. The third viral enzyme, protease, cleaves translated viral precursor proteins produced by hijacked host cell machinery into mature proteins. *Env* encodes for the envelope protein Gp160, comprising two proteins, Gp120 and Gp41. The remaining viral genes encode for proteins that perform various accessory and regulatory functions. *Tat* and *rev* encode for the regulatory proteins, transactivator of transcription (Tat) and regulator of expression of the virion (Rev), while *vpu, vpr, vif* and *nef* encode for the accessory proteins viral protein U (Vpu), viral protein R (Vpr), virus infectivity factor (Vif) and negative regulator factor (Nef) (Götte, Li and Wainberg, 1999; Turner and Summers, 1999; Kline and Sutliff, 2008; Freed, 2015).

The virus envelope is comprised of phospholipids originating from the host cell plasma membrane and the envelope proteins are embedded in this membrane. The matrix is located between the envelope and the capsid, a cone-shaped structure at the centre of the mature virion. The capsid contains viral RNA, enzymes and nucleocapsid proteins **(Figure 1.6)** (Turner and Summers, 1999). The auxiliary viral proteins are expressed at various locations during the virus life cycle, depending on their function (Li *et al.*, 2005).

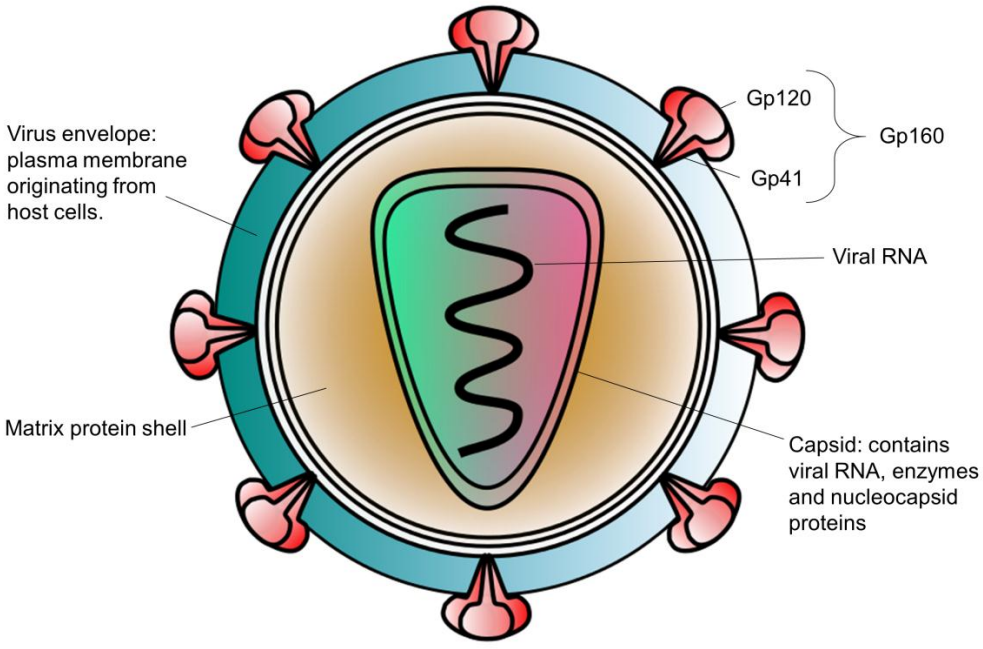

Figure 1.6: A representation of the HIV-1 virus. (Marincowitz *et al.,* 2018)

1.3.3 Transmission

HIV-1 transmission can occur via two routes: exposure to the virus at mucosal surfaces and percutaneous inoculation. Transmission probability is dependent on various factors, including coital act (Table 2). Early- and late-stage infection, higher viral loads, the presence of other sexually transmitted infections, especially ulcerating types, and younger age of the infected partner are all factors significantly associated with higher rates of transmission (Wawer *et al.*, 2005; Shaw and Hunter, 2012). Antiretroviral therapy has been invaluable in halting HIV transmission, as a reduced viral load protects others from infection (Vermund, 2014). A review by Weller and Davis-Beaty indicates that consistent heterosexual use of condoms results in an 80% reduction in HIV transmission, however, the studies included did not report on the correctness of condom use and quality of the condoms (Weller and Davis-Beaty, 2002). Male circumcision is another factor that reduces the chances of contracting HIV – for the circumcised individual. Furthermore, socioeconomic variables can influence HIV-1 transmission indirectly.

Globally, heterosexual transmission is responsible for almost 70% of all HIV-1 infections, while men who have sex with men, maternal-infant transmission, and injection drug use accounts for most of the remaining transmissions (Shaw and Hunter, 2012). High per-act transmission probability, especially receptive anal sex, and casual partnerships are factors that put men who have sex with men at a high risk of contracting HIV-1 (Beyrer *et al.*, 2012). Wawer *et al.* (2005) showed the rate of HIV transmission per coital act to be highest during early-stage infection, a time when newly infected individuals undergo seroconversion and thus do not know their HIV status or receive ART. Although the rate of transmission was also found to be high during late-stage infection, the authors mention that during this stage of the disease, individuals report less sexual intercourse and have fewer partners and thus its overall contribution to the HIV epidemic is unlikely to be extensive.

Table 1.2: HIV-1 Transmission Probability. Adapted from Shaw and Hunter (2012).

HIV INVASION SITE	TRANSMISSION MEDIUM	TRANSMISSION PROBABILITY PER EXPOSURE EVENT
Female genital tract	Semen; blood	0.05% – 0.5%
Male genital tract	Cervicovaginal and rectal secretions; blood	0.03% – 0.14%
Rectum	Semen; blood	0.33% – 5%
Upper GI tract	Semen; blood	0.04%
	Maternal blood and genital secretions (intrapartum)	10% – 20%
	Breast milk	10% – 20%
Placenta	Maternal blood (intrauterine)	5% – 10%
Bloodstream	Blood products, sharps	0.67% – 95%

1.3.4 Life Cycle and Pathogenesis

Activated CD4 T-lymphocytes are the preferred targets of HIV-1, although other cells bearing CD4 surface proteins can also be infected and CD4-independent infection of cells is possible. The virus commandeers the target cell and either utilises its machinery for pro-viral functions, or suppresses cellular processes to abate their anti-viral functions. After infection by the founder virus, an exponential increase in HIV replication occurs. This is followed by host inflammatory- and immune responses until the viral load decreases to a set-point. With time, host CD4 T-cells eventually become depleted and this is the hallmark of HIV-infection (Sorin and Kalpana, 2006; Maartens, Celum and Lewin, 2014).

The HIV-1 life cycle can be divided into two phases. The early phase constitutes all events occurring from the moment the HIV-1 virus binds to the surface of the host cell up until the point where the viral DNA is integrated into the host cell genome. This is the reason the disease can persist in patients even when they are receiving antiretroviral therapy: in the absence of virus production, resting memory T-cells remain latently infected as the viral genome is integrated into their DNA. The late phase includes all the processes that occur after integration up to the release and maturation of new virions (Freed, 2015).

Early Phase

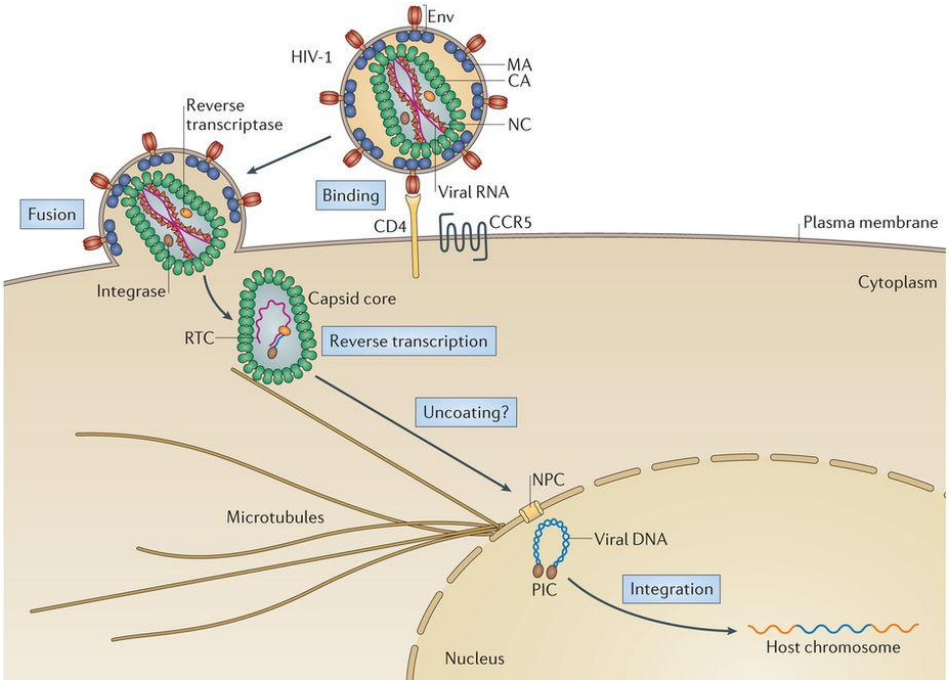

Figure 1.7: Early phase of the HIV-1 life cycle (Campbell and Hope, 2015)

Binding and entry: HIV-1 enters the host cell via interactions between the virus envelope glycoprotein, Gp160, with CD4 receptors and co-receptor C-C chemokine receptor 5 (CCR5) or C-X-C chemokine receptor 4 (CXCR4) on the surface of the host cell. Gp160 is comprised of two associated envelope proteins, namely, Gp120 and Gp41 **(Figure 1.6)**. The Gp120 component is a glycoprotein expressed on the surface of HIV virions and infected host cells, while the Gp41 component is a transmembrane protein. Gp120 dissociates from Gp41 and a Gp41 fusion peptide is inserted into the host cell membrane. The virus and host membranes subsequently fuse and the capsid and its contents are released into the cytoplasm of the host cell **(Figure 1.7)** (Nisole and Saïb, 2004; Sorin and Kalpana, 2006; Maartens, Celum and Lewin, 2014; Campbell and Hope, 2015).

Reverse transcription, trafficking and uncoating: After the release of the capsid into the cytoplasm of the host cell, reverse transcription occurs, where the viral enzyme, reverse transcriptase, converts the single stranded viral RNA into double stranded DNA (Campbell and Hope, 2015). The accessory protein, Vif, is involved in the stimulation of reverse transcription (Li *et al.*, 2005). While the viral RNA is being reverse-transcribed, the capsid is trafficked towards the nucleus, commandeering the host cell cytoskeleton and making use of its microtubules, microfilaments and molecular motors (Gaudin *et al.*, 2013). At this point, the capsid is thought to serve two main purposes: firstly, to maintain reverse

transcriptase and viral RNA in a closed environment and secondly, to protect the viral genome from host cell defences (Campbell and Hope, 2015). The viral capsid eventually disassembles, a process termed uncoating, which results in the formation of sub-viral particles named reverse-transcription complexes (RTCs) while reverse transcription is ongoing and subsequently pre-integration complexes (PICs) **(Figure 1.7)**. HIV PICs are high molecular weight nucleoprotein complexes that comprise the double-stranded reverse-transcribed viral DNA associated with several known and unknown cellular and viral proteins including viral matrix proteins and the enzymes reverse transcriptase and integrase as well as Vpr, which plays a role in the eventual nuclear import of the PIC (Nisole and Saïb, 2004; Li *et al.*, 2005; Sorin and Kalpana, 2006; Campbell and Hope, 2015). HIV-1 Nef and Vif and the cellular protein cyclophilin A are associated with the incoming capsid and seem to affect reverse-transcription and/or uncoating (Nisole and Saïb, 2004). Additionally, Vif has been shown to bind to APOBEC3G, a cytidine deaminase nucleic acid-editing enzyme which forms part of an antiviral pathway in human T lymphocytes, and targets it for degradation by the proteasome (Marin *et al.*, 2003). Nef also seems to have modulating effects on host anti-HIV immune responses by downregulating certain cellular receptors, including CD4, MHCI, MHCII and CD28. The downregulation of MHC I is believed to protect HIV-infected cells from the host cell's cytotoxic T cell response, while CD4 down-regulation probably limits the adhesion of HIV-infected T cells to antigen-presenting cells, preserving the movement of these infected cells into the circulation and consequently the spread of the virus. An additional explanation for CD4 down-regulation is that it guarantees no interaction between CD4 receptors of the already infected cell and the Gp160 proteins of new virions budding from it. In this way, CD4 downregulation contributes to Nef's role in enhancing viral infectivity (Li *et al.*, 2005). The uncoating process is not yet fully understood and three possible mechanisms have been proposed by which it might occur. The immediate uncoating theory maintains that capsid uncoating takes place very soon after the HIV-1 virion fuses with the host cell plasma membrane. Cytoplasmic uncoating theory postulates that capsid disassembly happens in the cytoplasm and that a reasonable amount of viral capsid proteins remains associated with the RTC. The nuclear pore complex (NPC) uncoating theory describes the capsid as remaining intact until it arrives at the NPC of the host cell. NPCs are supramolecular protein structures that traverse the nuclear membrane, protruding from the cytoplasm into the nucleoplasm. The NPC uncoating theory allows for the capsid to protect the replicating viral genome all the way from the cell membrane up to the nuclear membrane (Campbell and Hope, 2015).

Nuclear import and integration: When the PIC, which now contains the double stranded viral genome, arrives at the nuclear membrane, it is translocated into the nucleus via NPCs (Nisole and Saïb, 2004). This trafficking process is largely dependent on the viral capsid protein (Campbell and Hope, 2015). Viral Protein R is also involved and it is known to interfere with host cell cycle progression and can induce apoptosis (Li *et al.*, 2005). The PIC then integrates its double stranded genome into the host cell DNA utilising a reaction catalysed by the viral enzyme integrase (Sorin and Kalpana, 2006; Gaudin *et al.*, 2013).

Late Phase

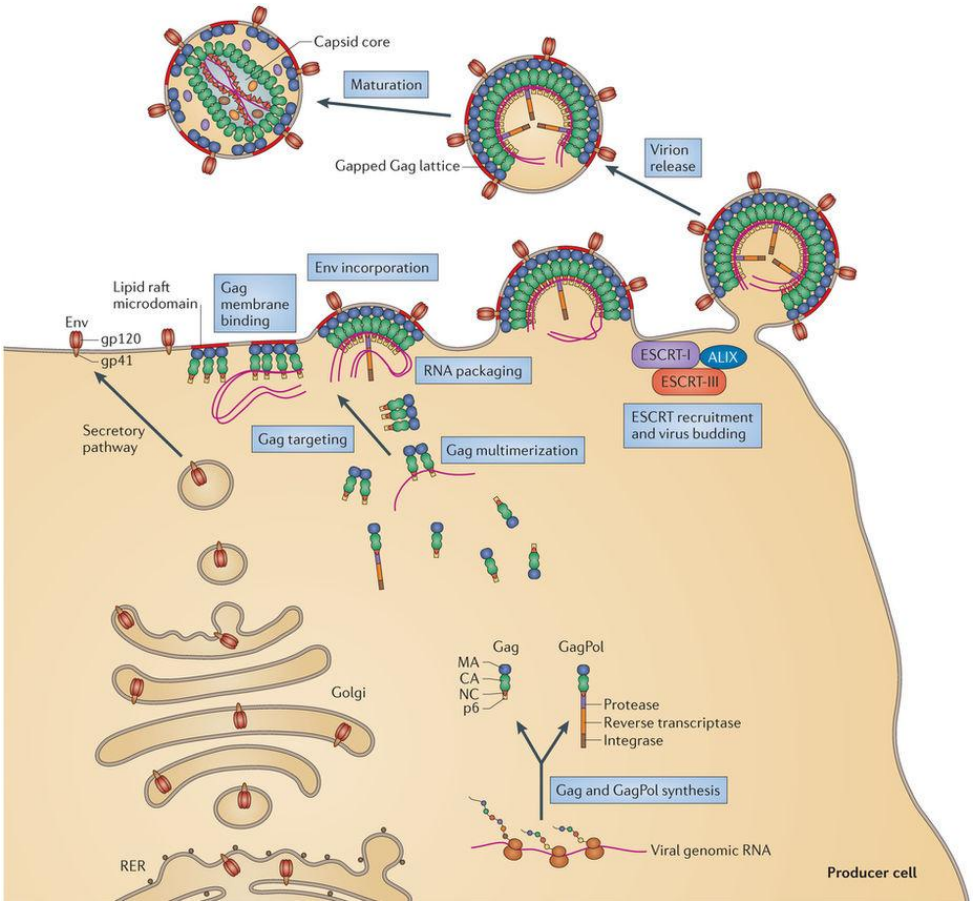

Figure 1.8: Late phase of the HIV-1 life cycle (Freed, 2015)

Transcription, export and translation: Once the viral genome has been integrated into the host cell DNA, it is transcriptionally activated by the viral regulatory protein Tat. In conjunction with host cellular transcription factors, Tat enhances the transcription and replication of the integrated proviral DNA to enable maximal transcription of the viral genes into RNA (Sorin and Kalpana, 2006; Debaisieux *et al.*, 2012). Once the new viral RNA molecules have then been formed within the nucleus, they are exported to the cytoplasm where they are translated to produce Gag polyprotein precursors, GagPol polyprotein precursors, viral envelope glycoproteins, as well as the regulatory and accessory viral proteins. The Gag polyprotein precursor contains matrix, capsid and nucleocapsid domains, while the GagPol polyprotein precursor additionally includes the viral enzyme domains **(Figure 1.8)**. The viral proteins necessary for the construction of the new virion are encoded for by spliced viral RNA molecules, while un-spliced viral RNA gets packaged into the new capsid (Sorin and Kalpana, 2006; Freed, 2015). The regulatory viral protein Rev is involved in the nuclear export of un-spliced viral RNA (Li *et al.*, 2005).

Trafficking and assembly: The assembly of the new virus particle takes place at the host cell plasma membrane and its various components, including newly synthesized viral RNAs and precursor proteins, are transported here by the host cell microtubule network and associated motors (Gaudin *et al.*, 2013). Gp160 envelope glycoproteins (Env) travel via the secretory pathway: from the nucleus, through the endoplasmic reticulum, to the golgi apparatus and then in vesicles to the plasma membrane **(Figure 1.8)** (Freed, 2015). The new virion assembly process constitutes Gag multimerization, the binding of these Gag multimers to viral genomic RNA and the formation of complexes, including the Gag-Gag/Pol complex as well as larger subsequent complexes containing the viral proteins and various host cell proteins required for assembly and budding (Sorin and Kalpana, 2006). The viral structural protein domains perform various functions in this regard. Matrix protein domains target Gag to the plasma membrane and promote the incorporation of Env glycoproteins into the forming virions, while capsid domains drive the Gag multimerization and nucleocapsid domains recruit viral RNA for the new virion's genome (Freed, 2015).

Budding and maturation: Finally, the assembled virus particle must undergo a membrane fission event and bud off from the producer cell, incorporating the host plasma membrane as its viral envelope while doing so (Sorin and Kalpana, 2006; Freed, 2015). The viral accessory protein Vpu is involved in enhancing the release of the progeny virions from infected cells. It is a membrane protein that, similar to Nef, aids in the degradation of the CD4 receptor in HIV-infected lymphocytes. Additionally, it has the ability to form ion channels in cell membranes. These mechanisms enable Vpu to counteract host cell factors that hamper the release of progeny virions from infected cells (Li *et al.*, 2005; Guatelli, 2009). Vpu also acts as an antagonist to the host innate immune response. In lymphocytic cell lines, it has been shown that the increased expression of intercellular adhesion molecule 1 (ICAM-1) mRNA observed in these cells upon HIV-1 infection is counteracted by Vpu. Vpu causes a downregulation of ICAM-1 and subsequently a decrease in the formation of conjugates between infected CD4-positive T cells and NK cells resulting in a reduction in the NK cell-mediated killing of HIV-infected T cells (Sugden, Pham and Cohen, 2017). The viral enzyme, protease, eventually cleaves the Gag polyprotein allowing virion maturation to occur. Once the individual Gag domains are liberated, the capsid proteins assemble to form the conical capsid core and the other structural proteins to form the mature virion (Sorin and Kalpana, 2006; Freed, 2015) **(Figure 1.8)**.

1.4. ANTIRETROVIRAL THERAPY (ART)

Current antiretroviral therapy cannot cure HIV-1 – a consequence of the pool of latently infected CD4 T cells created during early infection – and lifelong chronic and continuous ART is the gold standard of HIV-management. Antiretroviral drugs do however limit HIV-associated morbidity and mortality as well as reduce transmission-rates. Sustained ART-mediated suppression of plasma viral loads conserves and restores immune system function, prevents the development of drug-resistance, and may additionally contribute to lessening the virus-associated immune activation and inflammation thought to augment the progression to AIDS. (Cihlar and Fordyce, 2016). ART counteracts the HIV-1 virus by blocking its replication at multiple stages in the virus life-cycle and these drugs are divided into five classes according to where they act (Maartens, Celum and Lewin, 2014) **(Table 1.3)**.

Table 1.3: An overview of current antiretroviral drugs and their actions. Content from Arts and Hazuda (2012).

Antiretroviral Drugs and their Actions		
Class	**Action**	**Drugs**
Nucleoside-analogue Reverse Transcriptase Inhibitors (NRTIs)	NRTIs are analogues of nucleoside substrates which interfere with the reverse transcription of single-stranded viral RNA into double-stranded viral DNA by arresting the assembly of the viral DNA chain.	Abacavir Didanosine Emtricitabine Lamivudine Stavudine Zidovudine Tenofovir (a nucleotide RT inhibitor)
Non-nucleoside Reverse Transcriptase Inhibitors (NNRTIs)	NNRTIs bind to a noncatalytic allosteric pocked on the viral enzyme, reverse transcriptase, altering its activity which inhibits the generation of double-stranded viral DNA from single-stranded viral RNA.	Etravirine Delavirdine Efavirenz Nevirapine
Integrase Inhibitors	Inhibit the integration of viral DNA into the host cellular DNA.	Raltegravir

Protease Inhibitors (PIs)		PIs inhibit the cleavage of *Gag* and *Gag-Pol* precursor proteins by the viral enzyme protease into mature proteins.	Amprenavir Atazanavir Darunavir Fosamprenavir Indinavir Lopinavir Nelfinavir Ritonavir Saquinavir Tipranavir
Entry Inhibitors	Fusion Inhibitors	Entry Inhibitors disrupt various steps in the process of virion fusion with the host cell and the subsequent release of the virus core into the host cytoplasm.	Enfuvirtide
	Coreceptor Antagonists		Maraviroc

1.4.1 Highly Active Antiretroviral Therapy (HAART)

HAART (also referred to as combination ART) is a combination of three or more antiretroviral drugs (Carr and Cooper, 2000) and initial therapy usually consists of two Nucleoside-analogue Reverse Transcriptase Inhibitors (NRTIs) combined with a third drug, often a non-nucleoside reverse transcriptase inhibitor (NNRTI), or an integrase inhibitor or protease inhibitor (PI). Originally, patient HAART regimens were initiated based on decreasing CD4 cell counts or clinical indications of AIDS. However, recently therapy is often commenced immediately after a positive HIV-diagnosis (Cihlar and Fordyce, 2016). Current World Health Organisation (WHO) guidelines strongly recommend that ART should be initiated in all adults living with HIV regardless of their clinical stage and CD4 cell count (World Health Organization, 2016).

1.4.2 Adverse Events

Unstructured ART interruptions have been associated with an increased risk of mortality, opportunistic infections, virologic failure, treatment resistance and limited immunological recovery. Unfortunately treatment interruptions are common and result in poorer patient outcomes (Kranzer and Ford, 2011). Drug-related adverse events often contribute to treatment interruption. A meta-analysis by Al-Dakkak *et*

al., (2013) found that ART-related adverse events decreased treatment adherence and that the effect and magnitude thereof varied between the specific adverse events. These authors purport that managing adverse events can improve medication adherence, and therefore, decrease viral resistance to therapy, patient progression to AIDS and mortality.

Short Term Adverse Events

Short term ART-associated adverse events include gastrointestinal toxicities, drug hypersensitivity reactions, central nervous system toxicity and lactic acidosis. Gastrointestinal toxicity is one of the primary treatment limiting adverse events for PIs and it can manifest as nausea, vomiting and diarrhoea. Hypersensitivity reactions to some antiretroviral drugs do occur and can potentially be fatal: should a patient be re-exposed to the offending drug anaphylaxis can ensue. Central nervous system toxicity is frequently associated with the NNRTI, Efavirenz and this can include vivid dreams, balance problems, drowsiness as well as dizziness (Hawkins, 2010). One of the most serious short term adverse events of ART is lactic acidosis, which has been linked to mitochondrial toxicity (Carr and Cooper, 2000). Other common short-term side-effects include fatigue, dizziness and dyspepsia as well as rash. Anaemia and jaundice can also occur (Hawkins, 2010).

Long Term Adverse Events

The long-term use of some ARTs has been associated with hepatotoxicity as well as renal adverse events. The drug Tenofovir, especially, has been linked to renal dysfunction (Hawkins, 2010). Distal sensory peripheral neuropathy which subjectively manifests as numbness and/or pain in the extremities has also been described following long-term exposure to certain ARTs and could be the result of mitochondrial toxicity and impaired ATP synthesis (Hawkins, 2010). An important long-term complication of ART use is an increased risk for CVD, which has especially been reported in the context of lipodystrophy, another long-term adverse event associated predominantly with the use of certain NRTIs and PIs (Flint *et al.*, 2009; Hawkins, 2010). The primary clinical features of lipodystrophy are peripheral fat loss and central and dorsocervical fat accumulation. Metabolic features of this adverse event include hypertriglyceridaemia, hypercholesterolaemia, insulin resistance and type II diabetes mellitus. These metabolic abnormalities are also more prevalent in individuals receiving PI treatment (Flint *et al.*, 2009; Villarroya, Domingo and Giralt, 2010).

1.4.3 Fixed Dose Combination (FDC)

Recently, the use of once-daily fixed-dose combination drugs (FDC) has become popular due to a decrease in regimen complexity consequent to smaller pill burdens and less frequent dosing. This, together with the enhanced drug tolerability of modern regimens, has allowed for improved initial ART regimen durability (Willig *et al.*, 2008). Presently, the WHO strongly recommends that FDC and once-daily regimens are used as the preferred mode of antiretroviral treatment. First-line FDC for adults should

consist of two NRTIs plus an NNRTI or an integrase inhibitor. The preferred option to initiate ART is tenofovir (TDF) with lamivudine (3TC) or emtricitabine (FTC) and efavirenz (EFV) as a fixed-dose. Second-line ART in adults should consist of an NRTI backbone together with a ritonavir-boosted protease inhibitor. The favoured FDC NRTI backbone approach is the use of zidovudine (AZT) and 3TC (World Health Organization, 2016).

1.5. HIV, ART AND CVD

The scope of the cardiovascular risk associated with HIV/ART has reached a point where there is controversy regarding what offers the bigger cardiovascular threat – living with HIV or being on ART (Wang *et al.*, 2015). In the "Data Collection on Adverse Events of Anti-HIV Drugs (DAD)" study, a large, on-going cohort study of HIV-infected patients on treatment, a significant association was observed between the period of ART exposure and the risk of myocardial infarction. The study findings also suggest that this risk varies according to the ART drug class, with a significant increase in myocardial infarction risk being attributed to PIs. However, this might have partly been a consequence of the adverse effects of these drugs on serum lipids (Reiss *et al.*, 2007). PIs have also been connected to higher IL-6 levels, compared to efavirenz (Borges *et al.*, 2015) (For more information on the involvement of inflammatory cytokines in HIV and ART, view my review paper in Appendix A). Furthermore, HIV-infection *per se* is characterised by continuous immune activation, which is maintained even upon receiving ART, and inflammation is considered a pivotal mechanism responsible for the high levels of CVD in the HIV-infected population (Hunt, 2012). The sustained immune activation observed in HIV-infection has been attributed to ongoing viral replication; coinfections (especially chronic viral infections); the translocation of microbial by-products across a dysfunctional gut mucosa; decreases in immunoregulatory cells and immune structure damage (Deeks, 2011; Younas *et al.*, 2016). Moreover, HIV-infected persons receiving ART are at a greater risk for certain age-linked diseases, such as CVD, and some scholars even consider HIV to be associated with premature ageing, which has been attributed, in part, to the immune dysfunction observed in this infection (Deeks, 2011). Additionally, dyslipidaemia and impaired cholesterol metabolism, which are both involved in the atherosclerotic process, are possibly enhanced by HIV and ART (Mu *et al.*, 2007; Crowe *et al.*, 2010).

Given the many cardiovascular and other adverse effects of ART, the "Strategies for Management of AntiRetroviral Therapy (SMART)" trial investigated whether a CD4-positive T-cell count-guided use of antiretrovirals, would be more beneficial compared to lifelong continuous use, yet, contrary to expectations, they noted an increase in the rate of adverse cardiovascular events associated with the interruption of ART (Phillips *et al.*, 2008). The accumulating evidence for an interplay between HIV, ART and CVD **(Figure 1.9)** makes the fact that in 2015 17.0 million people worldwide were living with HIV and

receiving treatment (UNAIDS, 2016) disconcerting, as this represents a very large population of CVD-vulnerable individuals. Consequently, this warrants zooming-in on the mechanisms involved in this double-burden of disease, in order to devise customised treatment strategies for HIV-positive individuals with increased cardiovascular risk.

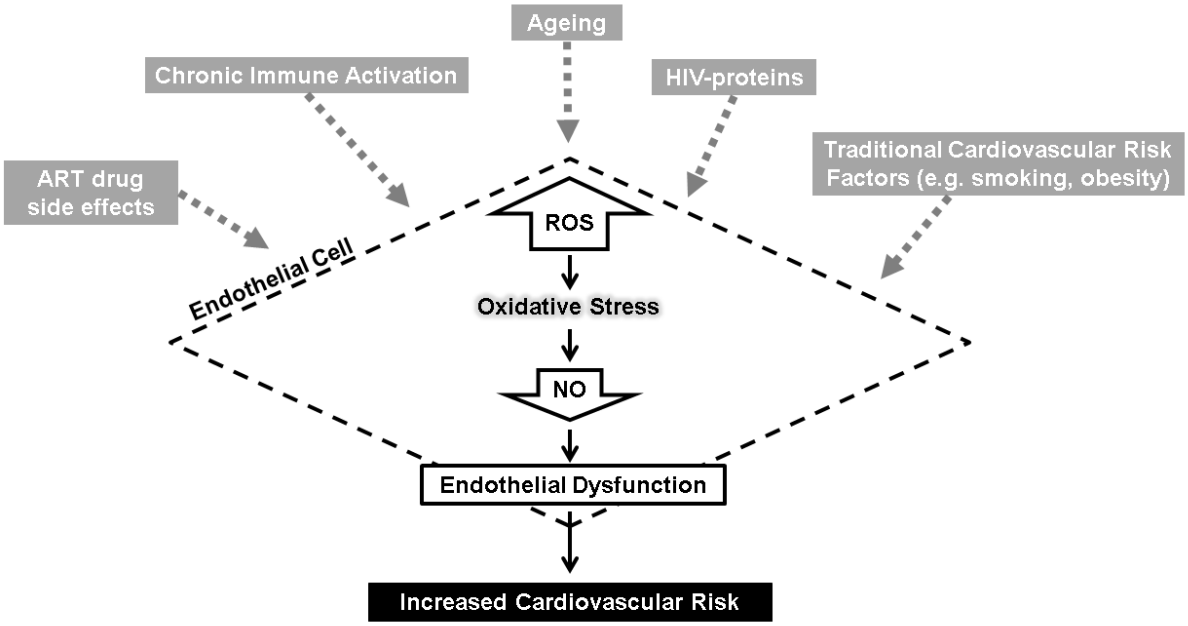

Figure 1.9: Schematic diagram of the interplay between HIV, ART and CVD. Via multiple and complex pathways, all cardiovascular risk factors seem to influence endothelial cell functioning and oxidative stress appears to act as the central causal mechanism. Increased reactive oxygen species (ROS) lead to oxidative stress, which reduces nitric oxide (NO) bioavailability. This results in endothelial dysfunction and increased cardiovascular risk. Figure designed by the author of this thesis.

1.5.1 HIV, ART and Endothelial Dysfunction

As the pathophysiological process believed to be at the heart of CVD, it makes it unsurprising that endothelial dysfunction has been linked to HIV/AIDS and ART as well. Perinatally infected HIV-positive adolescents were shown to have higher levels of endothelial dysfunction compared to their behaviourally-infected peers, possibly due to a longer cumulative duration of HIV/ART exposure (Dirajlal-Fargo *et al.*, 2017). Asymmetric dimethylarginine (ADMA), a marker of endothelial dysfunction, levels were raised in HIV-infected individuals compared with HIV-negative controls. Levels were also higher in HIV-positive individuals receiving ART compared with untreated HIV-positive persons. In untreated HIV-infection, viral replication was independently associated with endothelial dysfunction (Haissman *et al.*, 2016). Pronounced coronary endothelial dysfunction was present in HIV-positive patients without significant

coronary artery disease (CAD) – as severe as that observed in HIV-negative clinical CAD patients (Iantorno *et al.*, 2017).

However, whether or not HIV directly infects vascular endothelial cells *in vivo* has been described as controversial (Kline and Sutliff, 2008), with some reviewers arguing that this is indeed the case (Lambert *et al.*, 2016), whilst others have been more cautious (Maartens, Celum and Lewin, 2014). Currently, the accepted explanation with regards to HIV/AIDS-associated endothelial dysfunction is that both HIV-proteins and components of ART act as causal agents. The vascular endothelium of an HIV-infected individual is continuously exposed to these stimuli via the bloodstream which interfere with endothelial cell signalling pathways. A primary consequence of this seems to be a decrease in NO bioavailability, possibly due to increased ROS generation and oxidative stress, propelling the vascular endothelium into a dysfunctional state (Kline and Sutliff, 2008; Lambert *et al.*, 2016).

1.5.2 HIV-1-Proteins and Endothelial Dysfunction

Tat

HIV-1 Tat has the ability to enter the host cell's nucleus and, additionally, it can be actively secreted by infected cells and imported by various other cells, including endothelial cells (Debaisieux *et al.*, 2012). Tat has been associated with many of the features of endothelial dysfunction, including increased ROS production, enhanced endothelial cell permeability and adhesion molecule expression.

Contact with Tat in rat brain endothelial cells, triggered a significant increase in oxidative stress (Price *et al.*, 2005). In human pulmonary artery endothelial cells, Tat's ability to induce ROS production seemed to be linked to the activation of NFκB. In these cells, Tat exposure induced the expression of vascular cell adhesion molecule 1 (VCAM-1), which might have been mediated by ROS production, p38 mitogen-activated protein kinase (MAPK) activation and the nuclear translocation of NFκB (Liu *et al.*, 2005). Tat treatment of human umbilical vein endothelial cells resulted in monocyte adhesion via increased ICAM-1 expression. This also occurred via activation of the MAPK pathways and eventual NFκB nuclear translocation (Duan *et al.*, 2013).

Tat has been shown to alter tight junction proteins in brain endothelial cells, increasing their permeability. In these cells in culture, Tat decreased the expression of claudin-1, claudin-5 and zonula occludens-2 (ZO-2) (Andras *et al.*, 2003) as well as occludin mRNA and protein levels, firstly by inhibiting its expression and secondly by cleaving it via matrix metalloproteinase-9 (Xu *et al.*, 2012). Together, Tat and pro-atherogenic shear stress synergistically increased the endothelial cell expression of cathepsin K, a protease which has been associated with coronary artery disease (Cheng *et al.*, 2013), in cultured human aortic endothelial cells and HIV-transgenic mice (Parker *et al.*, 2014). Moreover, in primary human lung microvascular endothelial cells, Tat was found to cause apoptosis following the activation of caspase-3 by a pathway distinct from the established Fas-ligand or TNF extrinsic pro-apoptotic pathways (Park *et al.*,

2001). Caspase-3 is the most important executioner caspase and the two main apoptotic pathways (extrinsic and intrinsic) as well as the perforin/grandzyme pathway all culminate in its activation via cleavage by various initiator caspases (Elmore, 2007).

Gp160

Like Tat, Gp160, especially its Gp120 component, has been linked to endothelial dysfunction. It has been shown to reduce eNOS levels and increase oxidative stress as well as endothelial barrier permeability (Price *et al.*, 2005; Kanmogne *et al.*, 2007; Yang *et al.*, 2009; Jiang *et al.*, 2010). In porcine coronary artery rings pre-treated with the inflammatory cytokine, TNF-α, exposure to Gp120 significantly decreased endothelium-dependent vasorelaxation compared to untreated controls. eNOS mRNA levels and protein expression were also significantly reduced in these porcine coronary rings as well as in cultured human coronary artery endothelial cells (Jiang *et al.*, 2010). Exposure to Gp120 was shown to cause a significant increase in oxidative stress in rat brain endothelial cells (Price *et al.*, 2005). In human brain microvascular endothelial cells, Gp120 up-regulated interleukin-6 (IL-6) and interleukin-8 (IL-8) expression, which resulted in the adhesion and migration of monocytes across *in vitro* blood brain barrier models (Yang *et al.*, 2009). Gp120 was also shown to activate protein kinase C, which resulted in increased intracellular calcium release. This led to cytoskeletal changes, including the disruption of tight junctions, and ultimately decreased blood brain barrier tightness, causing increased monocyte migration across the barrier (Kanmogne *et al.*, 2007).

Nef

Nef interferes with host cell signal transduction as well as the regulation of cholesterol trafficking (Li *et al.*, 2005). Additionally, it has the ability to enter endothelial cells and while the mechanism by which it achieves this remains to be elucidated, it has been associated with nocuous consequences, such as atherosclerotic chemokine release, ROS formation, mitochondrial dysfunction and apoptosis (Duffy *et al.*, 2009; Wang *et al.*, 2014). In Jurkat T cell- and THP1 monocyte cell lines, Wang *et. al.* (2014) showed that Nef could independently induce its own transfer from these cells to cultured human coronary artery endothelial cells utilising a mechanism that involved direct cell to cell contact. Furthermore, once in these cells, Nef induced endothelial activation, dysfunction and apoptosis via an NADPH oxidase and ROS-dependent mechanism. Nef-exposure also induced the release of monocyte chemoattractant protein-1 (MCP-1) in an NFκB dependent manner.

After being incubated in solutions supplemented with various concentrations of Nef for 24 hours, endothelium-dependent vasorelaxation in porcine pulmonary artery rings was significantly reduced. Furthermore, Nef exposure caused a significant increase in superoxide production in cultured human pulmonary artery endothelial cells (HPAECs) as well as porcine pulmonary arteries, resulting in oxidative stress. In cultured porcine pulmonary artery endothelial cells and HPAECs, Nef was also shown to reduce eNOS expression (Duffy *et al.*, 2009). In two mouse models of atherosclerosis, injecting the animals with

recombinant Nef led to dyslipidaemia as well as the accumulation of cholesterol in macrophages in their vessel walls (Cui *et al.*, 2014). Given the above, Nef undoubtedly contributes to the development of endothelial dysfunction, and by extension atherosclerosis.

Vpu and Vpr

The endothelial effects of Vpu and Vpr have not been widely researched and currently much remains to be elucidated. In an *in vitro* experiment, where cultured human umbilical vein endothelial cells were infected with recombinant adenoviruses expressing individual HIV-proteins, cultured B-lymphocyte cells solely adhered to Vpu-expressing endothelial cells. This was ascribed to Vpu's ability to upregulate endothelial CD40, which led to the efficient expression of VCAM-1 (Henderson *et al.*, 2004). In primary human brain microvascular endothelial cells, Vpr treatment induced apoptosis, an effect that was synergistically enhanced by ethanol co-treatment (Acheampong *et al.*, 2002).

1.5.3 Common Antiretroviral Drugs and Endothelial Dysfunction

Common First-line FDC Drugs

First-line therapy is treatment considered optimal for the initial treatment of a condition or disease (AIDS info, 2018). In South Africa government roll-out first-line FDC consists of two NRTIs, Tenofovir (TDF) and Emtricitabine (FTC), and one NNRTI, Efavirenz (EFV). EFV is the NNRTI that has most widely been researched in terms of its endothelial effects and an association with endothelial dysfunction has been established (Gupta *et al.*, 2012; Faltz *et al.*, 2017). EFV significantly augmented monolayer permeability in an *in vitro* study of human coronary artery endothelial cells, which was associated with decreased tight junction protein expression, including ZO-1, claudin-1, occludin and JAM-1. These effects were mediated by an increase in ROS generation and the activation of JNK and NFκB (Jamaluddin *et al.*, 2010). In human cerebral microvascular endothelial cells as well as in mice, EFV was shown to affect endothelial cell integrity. Exposure to the drug decreased levels of the tight junction protein, claudin-5, and increased endothelial permeability (Bertrand, Dygert and Toborek, 2016). Treating human umbilical vein endothelial cells with EFV resulted in an increase in ROS and this was associated with the induction of heat-shock proteins, endoplasmic reticulum stress as well as autophagy (Weiß *et al.*, 2016). Autophagy controls cellular protein and organelle degradation. It is a highly conserved cellular pathway involved in survival, development and homeostasis (Yang and Klionsky, 2010). Endothelial cells in the brain microvessels of HIV transgenic mice on continuous EFV treatment showed endoplasmic reticulum (ER) stress associated with decreased autophagy. The same correlation was observed in human blood brain barrier cells, including cultured cerebral microvascular endothelial cells, which was somewhat unexpected as ER stress is generally associated with increased autophagic activity (Bertrand and Toborek, 2015). Considering its effects on blood brain barrier cells, it may thus be unsurprising that, in a retrospective cohort study of 445 HIV-positive participants, long-term EFV use was associated with poorer neurocognitive outcomes in comparison with Lopinavir boosted with Ritonavir (LPV/r) (Ma *et al.*, 2016).

The EFV component of Atripla®, a FDC antiretroviral drug comprising TDF, FTC and EFV, and not TDF or FTC, was associated with increased oxidative stress and PARP activity (PARP is involved in DNA repair and apoptosis; once cleaved by executioner caspases such as caspase-3, PARP is involved in some of the changes noted in apoptotic cells (Elmore, 2007)), as well as increased apoptosis and necrosis in cultured endothelial cells. EFV also caused impaired endothelial function in rat aortic rings (Faltz *et al.*, 2017).

Although TDF and FTC are not as well researched as EFV, current evidence suggests that these first-line FDC components are not associated with endothelial dysfunction. De Pablo *et al.* (2012) observed no changes in leukocyte-endothelial cell interactions when human umbilical vein endothelial cells and leukocytes were treated with TDF and FTC *in vitro*, both in combination and separately. Additionally, in human coronary artery endothelial cells Kim *et. al.* (2011) found no evidence of any direct effects by TDF on the transcription and expression of pro-oxidative stress, proinflammatory or pro-apoptotic genes.

Common Second-line Antiretroviral Drugs

Second-line therapy is commenced only when a patient on first-line therapy has experienced virological failure despite good adherence or has experienced severe adverse events (National Department of Health of South Africa, 2015). Of the common protease inhibitor-components of second-line ART, Ritonavir has been most directly associated with endothelial dysfunction. Chai *et al.* (2005) investigated the effects of several HIV protease inhibitors on porcine coronary arteries and significant vasomotor dysfunction was observed, as well as decreased eNOS expression and increased superoxide anion production, with Ritonavir (RTV) accounting for the more potent effects. In porcine pulmonary arteries and human pulmonary artery endothelial cells, RTV seemed to cause impaired endothelial function via an increment in oxidative stress and reduced eNOS expression. In the porcine pulmonary artery rings, contraction and endothelium-dependent relaxation was significantly reduced by RTV in a concentration-dependent manner. Additionally, subsequent to the RTV treatment, a significant decrease in eNOS mRNA and protein levels was shown in cultured human pulmonary artery endothelial cells (Wang *et al.*, 2009). Ritonavir-boosted protease inhibitors have been shown to augment ROS production, inflammation and cell senescence to varying degrees in human coronary artery endothelial cells, as well as causing vascular endothelial dysfunction, with the strongest effects detected in cells treated with LPV/r. Both eNOS expression and NO production were hampered by LPV/r, while the expression of endothelin-1 (an endothelium-derived vasoconstrictor) was increased. The secretion of soluble ICAM or soluble VCAM, which is indicative of altered cell integrity, was increased 2-3 times by LPV/r (Auclair *et al.*, 2014). Contrary to the aforementioned *in vitro* studies, however, a study exploring the effects of LPV/r in healthy, non-obese human subjects, showed no evidence of endothelial dysfunction (Dubé *et al.*, 2008). Besides the direct endothelial effects of RTV, the drug can possibly also contribute to endothelial dysfunction in a more indirect way, since it has additionally been linked to serum lipid changes, a known contributor to endothelial dysfunction. In a cohort of HIV-negative participants, 100 mg of Ritonavir taken two times a

day significantly increased total cholesterol, LDL cholesterol, total cholesterol/HDL cholesterol ratio and triglycerides and reduced HDL cholesterol (Shafran, Mashinter and Roberts, 2005). Human subjects from a study conducted in Ethiopia exhibited elevated cholesterol, total cholesterol/HDL cholesterol ratio and triglycerides as well as elevated markers of inflammation leading the researchers to suggest that current EFV and LPV/r ART regimens might play a role in the development of HIV-associated preclinical atherosclerosis (Gleason *et al.*, 2015).

1.6. A South African Perspective

South Africa presents a unique challenge to healthcare providers. HIV prevalence is disproportionally high, and the incidence of CVD is on the rise. In 2010 38.9% of age-standardised death rates in South Africa were due to non-communicable diseases and of these 287/100000 were accounted for by CVDs (Nojilana *et al.*, 2016). In fact, non-communicable diseases including CVDs, type II diabetes mellitus and cancer have been growing in the whole Sub-Saharan region (Dalal *et al.*, 2011). Statistics South Africa reports that of the total deaths in 2014, cerebrovascular disease ranked second as the leading underlying cause of death after tuberculosis, followed by diabetes mellitus. HIV and other forms of heart disease ranked fifth and sixth respectively (Statistics South Africa, 2015). According to the WHO, Sub-Saharan Africa is the region most affected by HIV, where 25.6 million people were living with the virus in 2015, and it accounts for two-thirds of the global total of new infections as well (WHO, 2018). In South Africa in 2012, “The National HIV Prevalence, Incidence and Behaviour Survey” found the overall HIV-prevalence to be 12.2%, with women being more affected than men at 14.4% *versus* 9.9%. The highest prevalence-group was adults aged 25 – 49 years at a shocking 25.2% (Zuma *et al.*, 2016).

The abovementioned statistics make the HIV/AIDS-CVD intersection an area of mounting concern. A systematic literature review by Hyle *et al.* (2017) found that data on people living with HIV/AIDS (PLWHA) in Sub-Saharan Africa suggested an increased risk of early atherosclerosis and stroke. Furthermore, they noted that traditional cardiovascular risk factors were also prevalent in the general population, which could indicate that PLWHA may additionally have multiple cardiovascular risk factors, increasing their overall risk of CVD. An ecological study found that Sub-Saharan countries with higher HIV incidence had a higher prevalence of hypertension when adjusted for age, sex, year of study, markers of socioeconomic development and ART coverage (Angkurawaranon *et al.*, 2016). Worryingly, however, Rabkin *et al.* (2015) report that although patients were adherent with chronic HIV treatment, screening for and management of cardiovascular risk factors were suboptimal at a Free State Community Health Centre in South Africa. Furthermore, whilst South Africa has managed to scale-up ART coverage, there have been perturbing increases in many HIV-related risk behaviours (Zuma *et al.*, 2016) **(Table 1.4)**.

Table 1.4: Key findings from "The National HIV Prevalence, Incidence and Behaviour Survey, 2012". Data obtained from Zuma *et al.* (2016).

	2008	2012	
HIV prevalence	10.6%	12.2%	↑
ART exposure	16.6%	31.2%	↑
Multiple sexual partners in the previous 12 months	11.5%	18.3%	↑
Condom use	45.1%	36.2%	↓
Knowledge about HIV transmission and prevention	31.5%	26.8%	↓

1.7. Concluding Remarks

The increased cardiovascular risk observed in HIV/AIDS creates a unique double-burden of disease and given the exceedingly high HIV-prevalence in South Africa, this is an area that warrants the attention of government, clinicians and researchers alike. Investigating the cellular mechanisms involved in the HIV-ART-CVD interplay is thus of utmost importance, especially in a manner customized for the South African setting. Antiretroviral drugs commonly used in government roll-out programmes and their effects on the vascular endothelium in the context of HIV provide a key area of research in the quest to elucidate the underlying causes of this burgeoning double epidemic.

1.8. Problem Identification and Study Aims

1.8.1 Problem Identification

The association between HIV, ART and CVD, has been well established (Phillips *et al.*, 2008; Islam *et al.*, 2012; Hyle *et al.*, 2017) and numerous studies point to endothelial dysfunction as the possible underlying cause (Francisci *et al.*, 2009; Ross *et al.*, 2009; Baker *et al.*, 2012; Gupta *et al.*, 2012; Pirro *et al.*, 2016; Dirajlal-Fargo *et al.*, 2017). However, the mechanisms involved appear to be multiple and complex, with many of the endothelial cell signalling pathways affected remaining to be elucidated.

Sub-Saharan Africa is the region most affected by the global HIV-pandemic (WHO, 2018), making it imperative that research into the cellular mechanisms involved in the interplay between HIV, ART and ED

is tailored for this region, especially with regards to the specific antiretroviral drugs used in government roll-out programmes. In South Africa first-line FDC government roll-out antiretroviral drugs include TDF, FTC and EFV, and of these EFV has been shown to negatively impact endothelial functioning (Gupta *et al.*, 2012; Faltz *et al.*, 2017). Second-line treatment usually includes the protease inhibitors Lopinavir (LPV) and RTV of which RTV has been associated with endothelial dysfunction (Chai *et al.*, 2005; Wang *et al.*, 2009). These associations with endothelial dysfunction need further investigation to elucidate the mechanisms involved. An understanding of how these drugs contribute to endothelial dysfunction within the context of HIV will aid clinicians in tailoring treatment regimens for patients who present with increased cardiovascular risk. Therefore, the pathophysiological mechanisms associated with these antiretroviral drugs commonly used in South African government roll-out programmes were investigated in endothelial cells within an *in vitro* simulated HIV-microenvironment.

1.8.2 Main Study Aim

To investigate the effects of first line antiretroviral drug components (a combination of the NRTI/NNRTIs efavirenz, emtricitibine and tenofivir, commonly found in FDC in South Africa), and second -line antiretroviral drug components (the PIs lopinavir and ritonavir) on aortic endothelial cell (AEC) function – a mechanistic *in vitro* approach.

Objective 1

To develop an *in vitro* HIV-1-model by supplementing endothelial growth medium with HIV-proteins. This objective encompassed determining the optimal HIV-protein concentrations and exposure time of AECs to this HIV-protein-medium (time- and concentration-response investigations) needed for maximal observed differences compared to untreated controls, with regards to cell viability, NO production and nitrosative stress.

Objective 2

To determine the AEC effects of NRTI/NNRTI treatment within an HIV-protein-medium environment (as optimised in objective 1) on cell viability, nitric oxide production and nitrosative stress. This objective encompassed determining the optimal NRTI/NNRTI treatment concentrations (concentration-response investigations) needed for maximal observed differences compared to untreated controls.

Objective 3

To determine the AEC effects of PI treatment within an HIV-protein-medium environment (as optimised in objective 1) on cell viability, nitric oxide production and nitrosative stress. This objective encompassed determining the optimal PI treatment concentrations (concentration-response investigations) needed for maximal observed differences compared to untreated controls.

Objective 4

To determine the effects of HIV-protein-medium (as optimised in objective 1) as well as NRTI/NNRTI treatment (as optimised in objective 2) and PI treatment (as optimised in objective 3) within HIV-protein-medium and normal endothelial growth medium on the expression and phosphorylation of important vascular signal transduction proteins in cultured AECs, including eNOS, PKB/Akt (an upstream activator of eNOS), IκBα (an inhibitor of the pro-inflammatory transcription factor, NFκB), p22phox (a subunit of the ROS-producing enzyme, NADPH-oxidase), nitrotyrosine (indicative of peroxynitrite and nitrosative stress), cleaved caspase-3 (the activated form of this important executioner caspase involved in apoptosis) and cleaved PARP (involved in apoptosis and cleaved by executioner caspases such as caspase-3).

CHAPTER 2: METHODS

2.1. AORTIC ENDOTHELIAL CELL CULTURE

A rat aortic endothelial commercial cell line was selected to investigate the endothelial effects of various common South African government roll-out first- and second-line antiretroviral drugs within an *in vitro* HIV-1-model.

2.1.1 Materials

- Adult rat Aortic Endothelial Cells (AECs): Supplied by *VEC Technologies* (University at Albany Foundation, 1 University Pl, Rensselaer, NY 12144, USA).
- Endothelial cell growth medium (EGM-2): Supplied by *Lonza Ltd* (Clonetics, Cambrex Bio Science, Walkersville, USA) and distributed locally by *Whitehead Scientific*. This was supplemented with 2% FBS, heparin, long-chain human insulin-like growth factor (R3-IGF-1), recombinant human epidermal growth factor (rhEGF), antibiotic GA 1000 (containing gentamicin and amphotericin), vascular endothelial growth factor (VEGF), ascorbic acid, recombinant human fibroblastic growth factor B (rhFGF-B) and hydrocortisone from the bullet kit in accordance with the manufacturer's instructions. The FBS content was further increased to 10% as is the standard practice for *in vitro* research and has additionally been found by our laboratory to provide the optimum conditions for culturing AECs. This medium was initially used for culturing AECs for the various plate-reader assays.
- Rat endothelial cell growth medium: Supplied by *Cell Applications Inc.* (5820 Oberlin Dr Suite 101, San Diego, CA 92121, USA) and distributed locally by *Sigma-Aldrich*. This medium was used for culturing AECs for western blotting due to problems with the supplier of the previously mentioned medium.
- All salts used to prepare Phosphate Buffered Saline (PBS) were supplied by *Merck,* Darmstadt, Germany.
- Attachment factor: Supplied by *Gibco*® by *Life Technologies, Cascade Biologics*™*,* now owned by *ThermoFisher,* Waltham, Massachusetts, USA.
- Trypsin (0.25%): Supplied by *Gibco*® by *Life Technologies;* (now owned by *ThermoFisher,* Waltham, Massachusetts, USA) purchased as a 2.5% solution and diluted with PBS.
- Foetal bovine serum (FBS): Supplied by *Biocom-Biotech,* Centurion, South Africa.
- Dimethyl sulfoxide (DMSO): Supplied by *Sigma-Aldrich,* St. Louis, Missouri, USA.

2.1.2 Methods

AECs were received from the supplier in culture in 75 mm² flasks and, upon arrival, the medium was removed and replaced with fresh EGM-2 endothelial growth medium. Thereafter, flasks were placed in an incubator (Forma Series II, Thermo Electron Corporation, Waltham, MA, USA) at 37°C with a 5% CO_2 atmosphere and 40 – 60 % humidity and left to grow until confluent. The cells received fresh growth medium every second day. Once confluent, AECs were passaged in a 1:2 ratio to yield three generations of sub-cultures for future use, named P1 (Parent 1), P2 and P3 **(Figure 2.1)**, which were frozen away in a freezing medium (90 % FBS, 5 % growth medium and 5 % DMSO or 900 µl FBS, 5 ml growth medium and 5 ml DMSO for 1ml of freezing medium) suspension and stored in liquid nitrogen.

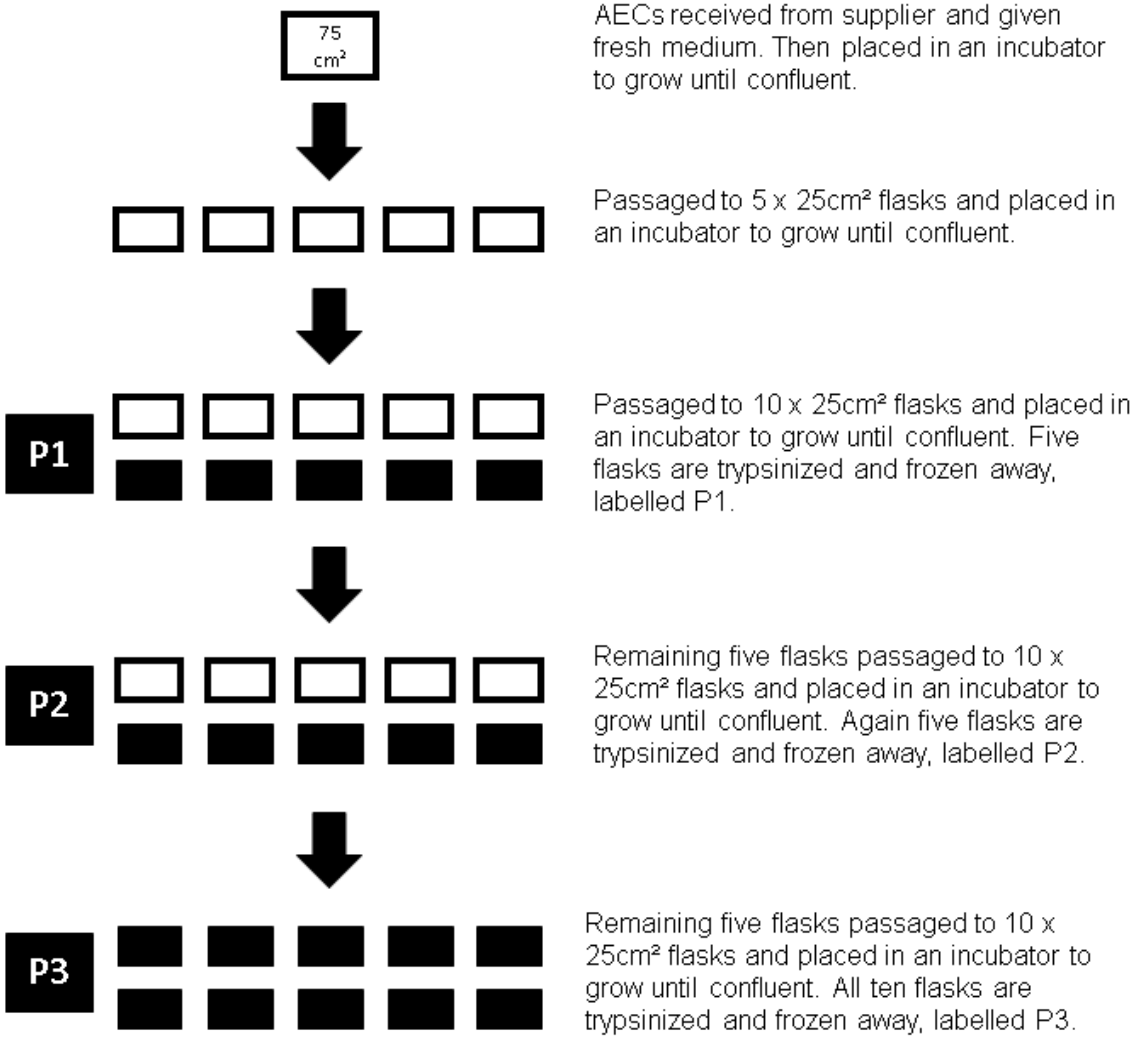

Figure 2.1: Passaging of AECs received from supplier

For experimental purposes, a Parent crytotube would be removed from the liquid nitrogen storage, allowed to thaw, given fresh medium and seeded in two gelatine-containing attachment factor coated 35 mm petri dishes. As soon as the cells reached confluency, they were passaged in a 1:2 ratio **(Figure 2.2)**. Note that, depending on the parent generation used (P1, P2 or P3), AECs can only be passaged a limited number of times before the cell yield starts diminishing. In this study, a P1 cell line was passaged a maximum of seven times, a P2 cell line six times and a P3 cell line five times. The passaging process commenced with the cells being washed with PBS and incubated in 0.25% trypsin for approximately 3 minutes until detached from the attachment factor layer at the bottom of the petri dish. They were then transferred to a 15 ml conical tube containing fresh growth medium, as the FBS in the medium deactivates trypsin, thus protecting the cells from its protease activity. The cells were then centrifuged for 3 minutes at 1000 revolutions per minute (rpm) at 4°C. Finally, the supernatant was aspirated, removing any remaining trypsin, and the pellet re-suspended in fresh growth medium. This cell-containing medium was equally divided amongst new 35 mm petri dishes pre-incubated (for at least 1 hour) with attachment factor.

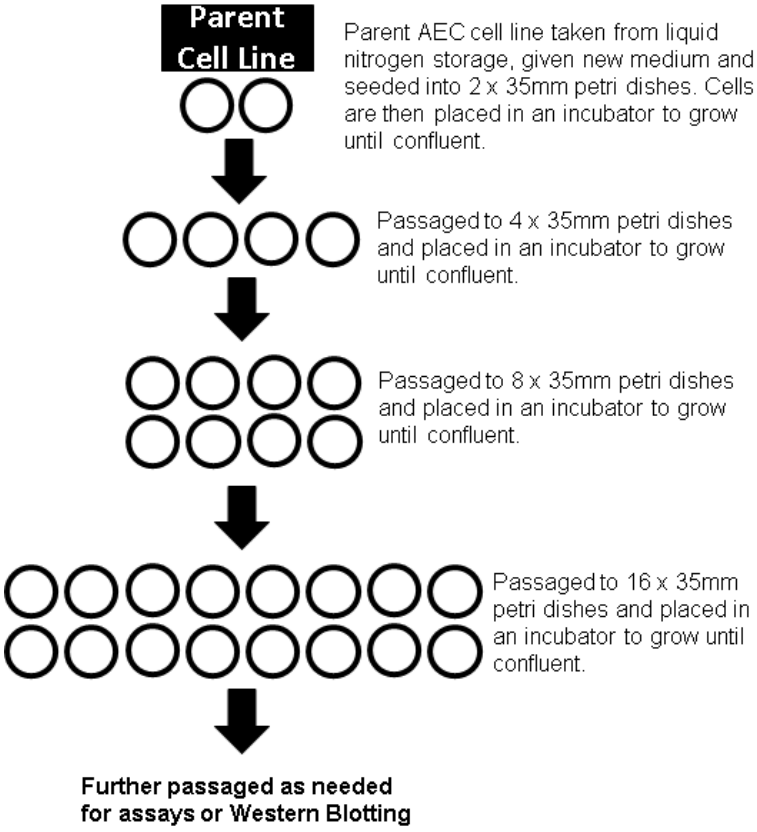

Figure 2.2: Passaging of parent AEC cell lines

2.2. HIV-1-Protein Medium

Creating an *in vitro* HIV-1-model optimised for AECs encompassed the development of an HIV-1-protein medium which was subject to time- and concentration-response investigations. Three different concentrations of three HIV-proteins that have previously been shown to impact vascular endothelial cells – Tat, Gp160 and Nef (Kline and Sutliff, 2008) – at two different durations (24-hours and 48-hours) were incorporated into the development of the optimal model.

2.2.1 Materials

- Recombinant HIV1 Tat protein (ab83353): Supplied by *Abcam* (Cambridge, UK) and distributed locally by *Whitehead Scientific*.
- Recombinant HIV1 Gp120 + Gp41 (ab68127) (Gp 160): Supplied by *Abcam* (Cambridge, UK) and distributed locally by *Whitehead Scientific*.
- Recombinant HIV1 Nef protein (ab58914): Supplied by *Abcam* (Cambridge, UK) and distributed locally by *Whitehead Scientific*.

2.2.2 Methods

All HIV-1-proteins were diluted in PBS to create concentrated stock-solutions of each (25 µg/ml, 50 µg/ml or 100 µg/ml), which were aliquoted and frozen away at temperatures according to the manufacturer's guidelines. For experimental purposes, these concentrated HIV-1-protein stock solutions were thawed and added to endothelial cell growth medium to create three different final concentrations of HIV-1-proteins in correspondence with what has previously been reported in the literature (Kline and Sutliff, 2008). HIV-medium 1 contained 25 ng/ml of each of the three proteins, HIV-medium 2 contained 50 ng/ml of each of the three proteins and HIV-medium 3 contained 100ng/ml of each of the three proteins. Since the proteins were initially diluted in a PBS vehicle, vehicle control cocktails were created to control for any possible cellular effects of the PBS. Each of the three HIV-media were thus matched with a corresponding vehicle control cocktail containing endothelial growth medium and PBS – the same concentration of PBS as present in its HIV-medium counterpart. For a more detailed description of the HIV-1-protein medium and vehicle control cocktail dilutions and their preparation, view Appendix B.

2.3. Antiretroviral Drug Treatment

Antiretroviral treatment experiments consisted of two groups: a nucleoside-analogue reverse transcriptase inhibitor/non-nucleoside reverse transcriptase inhibitor (NRTI/NNRTI) treatment group and a protease inhibitor (PI) treatment group. The NRTI/NNRTI group contained components used in the

current SA Government first-line fixed dose roll out treatment regimen, namely, efavirenz (EFV), tenofovir (TDF) and emtricitabine (FTC), and the PI group contained components commonly found in second-line regimens, namely, lopinavir (LPV) and ritonavir (RTV). After the HIV-1-model was optimised for AECs, the antiretroviral treatment was subject to concentration-response investigations within this HIV-1 environment.

2.3.1 Materials

- Efavirenz (EFV): Supplied by *SantaCruz Biotechnology,* Dallas, Texas, USA.
- Tenofovir (TDF): Supplied by *SantaCruz Biotechnology,* Dallas, Texas, USA.
- Emtricitabine (FTC): Supplied by *SantaCruz Biotechnology,* Dallas, Texas, USA.
- Lopinavir (LPV): Supplied by *SantaCruz Biotechnology,* Dallas, Texas, USA.
- Ritonavir (RTV): Supplied by *SantaCruz Biotechnology,* Dallas, Texas, USA.
- Dimethyl sulfoxide (DMSO), supplied by *Sigma-Aldrich*, St. Louis, Missouri, USA.
- Methanol (MeOH), supplied by *Merck*, Darmstadt, Germany.
- Distilled water (dH_2O), supplied by *Merck,* Darmstadt, Germany.

2.3.2 Methods

NRTI/NNRTI Treatment: Efavirenz (EFV), Tenofovir (TDF) and Emtricitabine (FTC)

Drugs were received in powder form. Upon arrival, EFV was dissolved in methanol (MeOH) and TDF and FTC in distilled water (dH_2O) to create concentrated stock solutions (21 mM EFV, 10 mM FTC and 393 µM TDF). The stocks were aliquoted and frozen away at -20°C for future use. For experimental purposes, the drug stocks were further diluted in PBS and then added to the optimised HIV-1-protein medium to obtain the desired final dosages in correspondence with what has been used in previous studies (Feng *et al.*, 2009; Grigsby *et al.*, 2010). NRTI/NNRTI treatment comprised 5.6 nM EFV, 500 nM TDF and 1.3 µM FTC. These dosages were furthermore halved and doubled, allowing for three different NRTI/NNRTI drug concentrations to be tested. To control for the vehicles used when dissolving the drugs (the MeOH and dH_2O), as well as for the additional PBS vehicle used to dilute the HIV-1-proteins, vehicle control cocktails were prepared. Three vehicle control cocktails in total, each controlling for the concentrations of vehicle present in the three different NRTI/NNRTI drug dosages, as well as in the HIV-1-protein stock solutions were prepared and added to endothelial growth medium. For a more detailed description of NRTI/NNRTI treatment and vehicle control cocktail dilutions and their preparation, view Appendix C.

PI Treatment: Lopinavir (LPV) and Ritonavir (RTV)

The PI drugs arrived in powdered form and were diluted in DMSO, aliquoted and stored as concentrated stock solutions (10 mM LPV and 2 mM RTV) at 4°C for future use. For experimental purposes, the stocks were added to the HIV-1-protein medium to obtain a final single-dose concentration of 10 µM Lopinavir

and 2 µM Ritonavir. The concentrations were based on what was used previously by Noor *et al.* (2006) and, as with the NRTI/NNRTI treatment, concentration responses for half- single- and double doses were investigated. To control for the DMSO vehicle used to initially dissolve the drugs, as well as the PBS vehicle present in the HIV-1-protein medium, vehicle control cocktails were created by adding DMSO and PBS to endothelial cell growth medium ensuring the same final concentrations of DMSO and PBS as present in the three different PI treatment concentrations. For a more detailed description of PI treatment and vehicle control cocktail dilutions and preparation, view Appendix C.

2.4. Plate Reader Analyses

A plate reader (FLUOstar Omega, serial no: 415-1364, BMG Labtech, Ortenberg, Germany) was utilised to measure fluorescence intensity of the respective probes (see below) in the abovementioned time- and concentration-response investigations. This commenced with the creation of the HIV-1-model, in other words, determining the ideal AEC exposure-time to HIV-1-proteins, as well as determining which of the three HIV-1-protein mediums (25ng/ml, 50ng/ml or 100ng/ml) resulted in an optimal HIV-1-environment. Once the HIV-1-model was created, the ART concentration-response investigations were performed within the optimised HIV-1-microenvironment.

2.4.1 Materials

- Clear base, black-frame 24-well Vision Plates™: Supplied by *4titude,* Surrey, UK and supplied locally by *Separations*.
- Serum free endothelial cell growth medium (EGM-2): Supplemented as described in 1.1, but without FBS.
- Propidium iodide solution (1.0 mg/ml in water): Supplied by *Sigma-Aldrich,* St. Louis, Missouri, USA.
- 4,5-Diaminofluorescein diacetate (DAF-2 DA) (1mg): Supplied by *Calbiochem®, EMD Millipore Corp.,* Billerica, MA, USA and distributed locally by *Merck*.
- Diethylamine NONOate diethylammonium salt (DEA/NO) (D5431-50MG): Supplied by *Sigma-Aldrich,* St. Louis, Missouri, USA.
- Dihydrorhodamine-1, 2, 3 (DHR-123): Supplied by *Sigma-Aldrich* (St Louis, Mo, USA).
- Peroxynitrite (Cat# 516620): Supplied by *Calbiochem®, EMD Chemicals, Inc.* San Diego, CA 92121, and distributed locally by *Merck*.

2.4.2 Methods

Cell Culture

Aortic endothelial cells were cultured as described in 1 above and finally passaged to 24-well plates. A P1 parent cell line yielded nine 24-well plates in total, a P2 parent cell line eight 24-well plates and a P3 parent cell line five 24-well plates. View Appendix D for a visual representation.

HIV-1-protein medium time- and concentration-response investigation protocol

Once the cells in the 24-well plates reached ±80% semi-confluence, usually on day two after seeding the wells, they were serum starved for 24 hours. The 80% semi-confluence cut-off point was used in the case of the 24-well plates as a precaution against over-confluence at the time of analysis. Over-confluence can result in cell death and, due to the diminutive size of the wells (diameter: 14.5 mm) together with the 48 hour period between serum starvation and analysis, this was a possibility that had to be avoided. Serum starvation was employed to induce cell cycle synchronization, enhancing the otherwise healthy cells' responses to the various treatments (Gerber *et al.*, 1998; Russell and Hamilton, 2014). This entailed aspirating the FBS containing endothelial cell growth medium (EGM-2) and replacing it with serum free EGM-2, containing no FBS. After 24 hours, the serum free medium was aspirated and replaced with the various treatment and control mediums. Each 24-well plate was assigned three positive control wells, twelve treatment wells and nine vehicle control wells. The treatment wells were divided into three groups of four wells each, each for a different treatment concentration. Similarly, the vehicle control wells were divided into three groups of three wells each, each group to control for one of the three different treatment concentrations. The positive control wells were included to test the effectiveness of the various fluorescent probes and were given the normal EGM-2 **(Figure 2.3)**. After 24 hours, the various media were aspirated and the plate reader assays conducted. The 48 hour treatment investigations entailed replacing the various media after 24 hours and exposing the AECs to these media for another 24 hours equalling a total of 48 hours before the various plate reader assays were conducted **(Figure 2.4)**.

Figure 2.3: Well assignment for HIV-1-protein medium time- and concentration-response investigations. +: positive control; HIV1: HIV-medium 1 (25 ng/ml); HIV2: HIV-medium 2 (50 ng/ml); HIV3: HIV-medium 3 (100 ng/ml); VC1: vehicle control for HIV-medium 1; VC2: vehicle control for HIV-medium 2; VC3: vehicle control for HIV-medium 3.

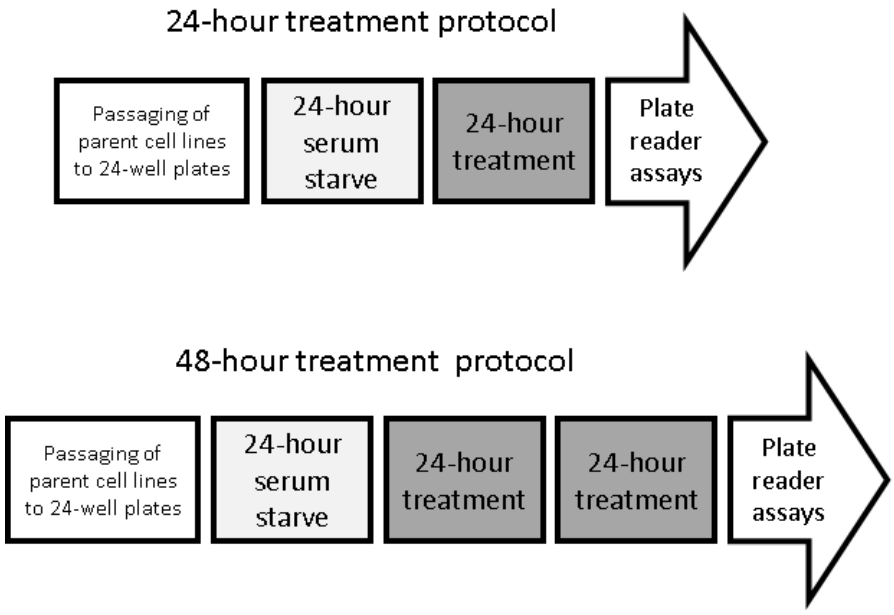

Figure 2.4: Treatment Protocols

Antiretroviral drug treatment concentration-response investigation protocol

After the development of the HIV-1-model, which stipulated that AECs be incubated in HIV-medium 3 (100ng/ml) for 24 hours, the antiretroviral drug treatment concentration-response investigations were carried out. As with the HIV-1-protein medium time- and concentration-response investigations, AECs were serum starved for 24 hours upon reaching ±80% semi-confluence. Thereafter, as described above, the serum free medium was aspirated and replaced with the various treatment and control media as well as normal endothelial cell growth medium for the positive control wells **(Figure 2.5)**. The cells were left to incubate for 24 hours, after which the plate reader assays were carried out **(Figure 2.4)**. This process was repeated for the NRTI/NNRTI treatment and for the PI treatment. The antiretroviral drug media were only subjected to concentration-response investigations, as the findings from the HIV-1-model time-response investigations suggested that a 24 hour treatment period was optimal.

Figure 2.5: Well assignment for antiretroviral drug treatment (NRTI/NNRTI and PI) concentration-response investigations. +: positive control; ART1: half-dose NRTI/NNRTI or PI treatment in HIV-medium 3; ART2: single-dose NRTI/NNRTI or PI treatment in HIV-medium 3; ART3: double-dose NRTI/NNRTI or PI treatment in HIV-medium 3; VC1: vehicle control for vehicles used in half-dose ART treatment and HIV-medium 3; VC2: vehicle control for vehicles used in single-dose ART treatment and HIV-medium 3; VC3: vehicle control for vehicles used in double-dose ART treatment and HIV-medium 3.

Propidium Iodide Cell Viability Assay

After the 24 or 48 hour treatment period the various treatment, control and positive control media were aspirated and the cells washed with PBS. Hereafter, the cells were treated with a Propidium Iodide (Prop. I) probe at a concentration of 5 µM. Prop. I is a large molecule that acts as a DNA stain, which, due to its size, is only able to enter cells once their membrane integrity has been compromised – as is the case with

necrosis (Riccardi and Nicoletti, 2006). Prop. I fluorescence is thus used as a measure for cell viability. For all the wells except the three positive control wells, the Prop. I was diluted in PBS, for the three positive control wells it was diluted in distilled water. PBS is isotonic to the cytosol, while distilled water is not. When distilled water is added to the cells, it results in water molecules diffusing across the semi-permeable cell membrane from an area of high osmotic potential (the distilled water) to an area of low osmotic potential (the cytosol) eventually causing the cells to burst, thus exposing the DNA to the Prop. I for staining and resulting in a strong fluorescent signal. After adding the probe, the cells were incubated for 15 minutes and then taken to the plate reader for analysis **(Figure 2.6)**. An excitation wavelength of 544 nm was used and 640 nm for emission. For a more detailed description of the protocol view Appendix E.

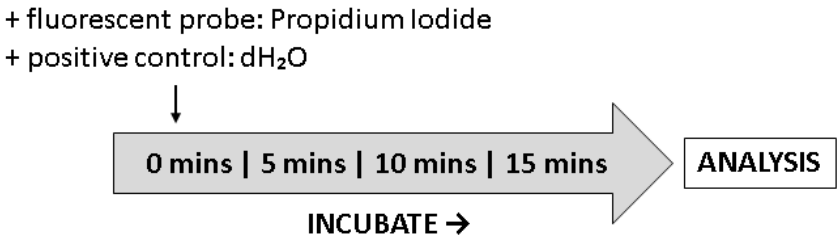

Figure 2.6: Propidium Iodide Cell Viability Assay.

DAF-2/DA Nitric Oxide Detection Assay

As described above, the various treatment media were removed and the cells washed with PBS, after which they were treated with the DAF-2/DA fluorescent probe diluted in PBS for a final concentration of 10 µM. DAF-2/DA measures intracellular nitric oxide production. This molecule is able to pass through the plasma membrane and enter the cell, where it is hydrolysed to form DAF-2. DAF-2 cannot cross the plasma membrane and thus remains inside the cell where it reacts with NO to form fluorescent DAF-2 T (Kojima *et al.*, 1998). Cells were incubated with DAF-2/DA for 90 minutes before 100 µM of the positive control, DEA/NO, which acts as a nitric oxide donor, was added to each of the three positive control wells. The cells were incubated for another 30 minutes where after the probe was aspirated and replaced with PBS and the cells were taken to the plate reader for analysis **(Figure 2.7)**. The excitation wavelength used was 485 nm and emission 520 nm. For a more detailed description of the protocol view Appendix E.

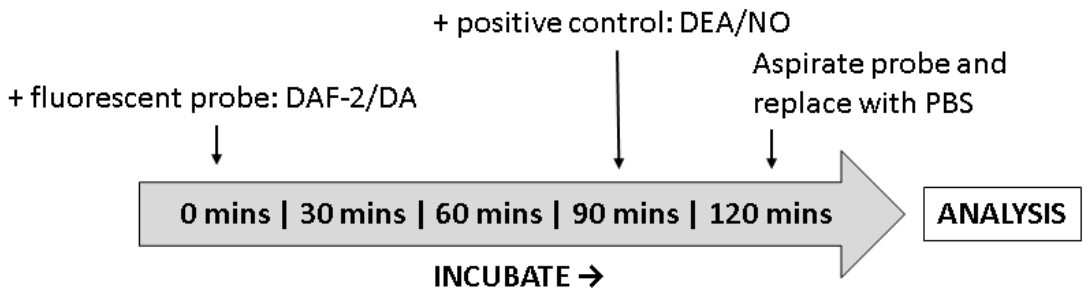

Figure 2.7: DAF-2/DA NO Detection Assay.

DHR-123 Nitrosative Stress Assay

As with the previous assay protocols, treatment and control media were aspirated and the cells washed with PBS. Subsequently they were treated with DHR-123 diluted in PBS with a final concentration of 2 µM. DHR-123 is an indicator of reactive nitrogen species (RNS), including peroxynitrite. It is able to penetrate the cell and once it reacts with peroxynitrite, DHR-123 is oxidised to rhodamine-123 which is highly fluorescent (Tarpey and Fridovich, 2001). Cells were incubated with DHR-123 for one hour, after which 100 µM of peroxynitrite was added to each of the three positive control wells. Cells were incubated for an additional 2 hours before being taken to the plate reader for analysis **(Figure 2.8)**. The excitation wavelength used for the DHR-123 assay was 485 nm and the emission wavelength 520 nm. Refer to Appendix E for a more detailed description of the protocol.

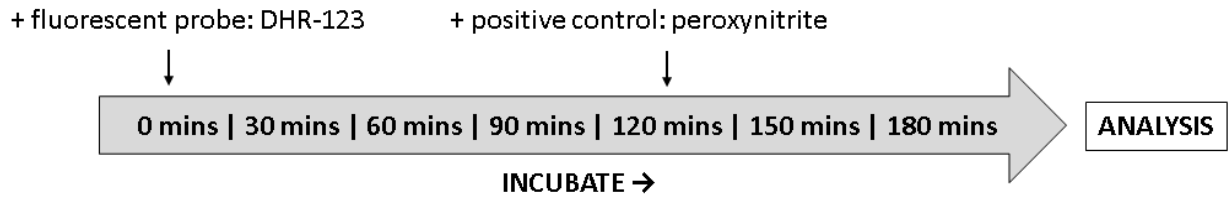

Figure 2.8: DHR-123 Nitrosative Stress Assay.

2.5. Western Blot Analyses

2.5.1 Materials

- Criterion™ TGX Stain-Free™ (4-20%) 26-well Precast Gels: Supplied by *Bio-Rad Laboratories, Inc.* (Hercules, CA, USA).

- PageRuler™ Prestained Protein Ladder: Supplied by *Thermo Scientific* (Lithuania, EU)
- Immobilon®-P Transfer Membrane (filter type: PVDF; pore size: 0.45µm): Supplied by *Merck* Millipore Ltd. (Tullagreen, Carrigtwohill, Co. Cork, Ireland).
- Primary antibodies supplied by *Cell Signaling Technologies* (Beverly, MA, USA) and distributed locally by *Anatech:*
    - Total eNOS Rabbit (9572S; Lot 3)
    - Phospho eNOS (S1177) Rabbit (9571S; Lot 14)
    - Total PKB (Akt) Rabbit (9272S; Lot 27)
    - Phospho PKB (Akt) (S473) (D9E) XP(R) Rabbit (4060S; Lot 23)
    - IκBα Rabbit (9242S; Lot 10)
    - Cleaved PARP (D214) (Rat Specific) Rabbit (9545S; Lot 2)
    - Cleaved Caspase-3 (D175) Rabbit (9661S; Lot 45)
- Primary antibodies supplied by *Santa Cruz Biotechnologies* (Santa Cruz, CA, USA) and distributed locally by *Whitehead Scientific*:
    - Nitrotyrosine (PNK) Rabbit Polyclonal IgG (sc-55256; Lot #D1112)
    - p22-phox (FL-195) Rabbit Polyclonal IgG (sc-20781; Lot #F1512)
- Primary SingalBoost™ Immunoreaction Enhancer: Supplied by *Millipore* (Billerica, MA, USA) and distributed locally by *Merck*.
- Anti-rabbit immunoglobulin G, HRP-linked secondary antibody: Supplied by *Cell Signaling Technologies* (Beverly, MA, USA) and distributed locally by *Anatech.*
- Clarity™ enhanced chemiluminescence (ECL) detection reagent: Supplied by *Bio-Rad* (Hercules, CA, USA) and distributed locally by *Lasec.*
- All other chemicals and buffer reagents were supplied by *Sigma-Aldrich (St Louis, Mo, USA)* and *Merck* (Darmstadt, Germany).

2.5.2 Methods

Cell Culture

AECs were cultured as described previously and finally passaged to six 100 mm petri dishes **(Figure 2.9)**. A final total of three P1 parent cell lines were used for western blotting purposes, to ensure a final sample size made up of biological replicates derived from three different parent cell lines based on experiments performed on separate occasions.

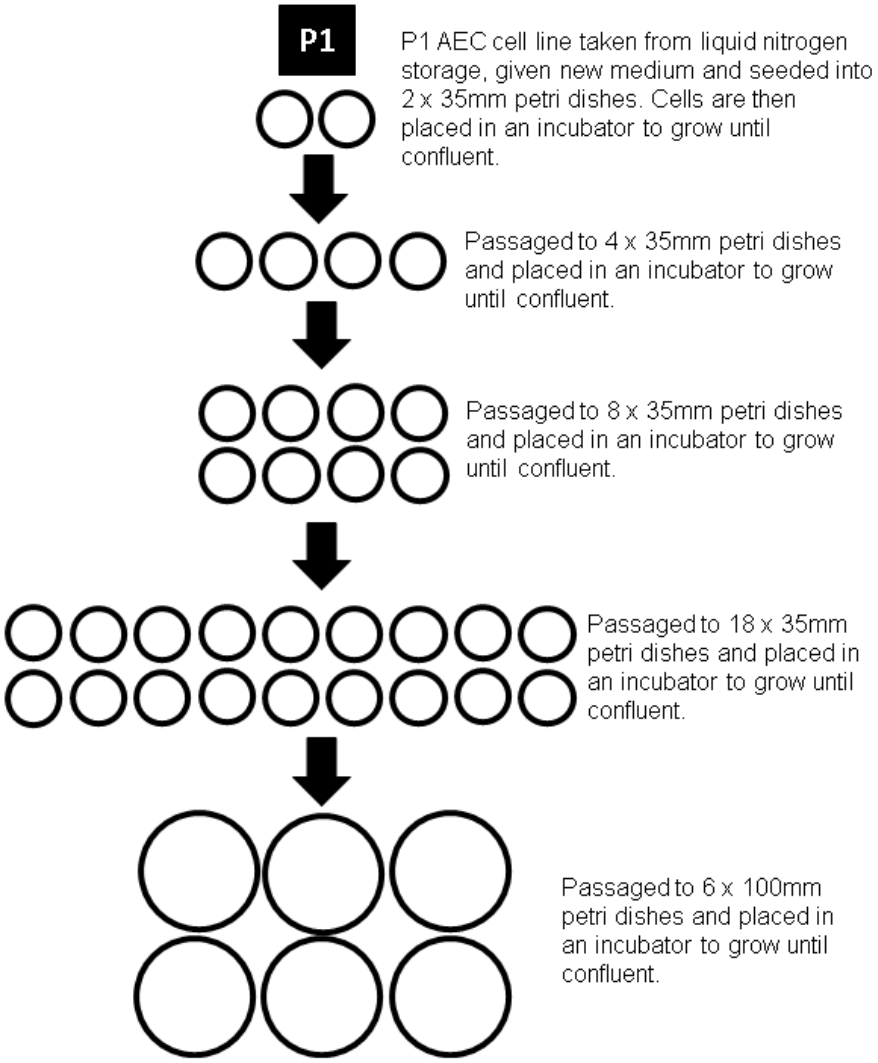

Figure 2.9: Passaging a P1 cell-line to six 100mm petri dishes.

Treatment Protocol

Upon reaching confluence, cells were serum starved following the same procedure as described for the plate reader assays. For western blotting purposes, cells were allowed to grow to full confluence as a high protein yield was essential. One fully confluent 100 mm petri dish yielded sufficient protein for one lysate. Hereafter, cells were treated for 24 hours before being lysed for protein extraction. View the various treatment groups in **Table 2.1**.

Table 2.1: Western Blotting Treatment Groups.

1. Combined Vehicle Control (CVC)	AECs incubated in combined vehicle control medium for 24 hours (see a more detailed description of this medium in the following section).
2. HIV-Protein Treatment Group	AECs incubated in HIV-medium 3 (100 ng/ml of Tat, Gp160 and Nef) for 24 hours.
3. NRTI/NNRTI Treatment Group	AECs incubated in endothelial growth medium containing a single-dose of NRTI/NNRTI treatment (5.6 nM EFV, 500 nM TDF and 1.3 µM FTC) for 24 hours.
4. PI Treatment Group	AECs incubated in endothelial growth medium containing a single-dose of PI treatment (10 µM LPV and 2 µM RTV) for 24 hours.
5. HIV-Protein + NRTI/NNRTI Treatment Group	AECs incubated in HIV-medium 3 (100 ng/ml of Tat, Gp160 and Nef) containing a single dose of NRTI/NNRTI treatment (5.6 nM EFV, 500 nM TDF and 1.3 µM FTC) for 24 hours.
6. HIV-Protein + PI Treatment Group	AECs incubated in HIV-medium 3 (100 ng/ml of Tat, Gp160 and Nef) containing a single dose of PI treatment (10 µM LPV and 2 µM RTV) for 24 hours.

Combined Vehicle Control (CVC)

To avoid having multiple vehicle controls, each controlling for the different vehicles and concentrations in each of the treatment groups, a combined vehicle control medium was created. Prior to use, this combined vehicle control medium was also subject to plate reader analyses (Prop. I and DAF-2/DA) to determine whether this cocktail had any seriously detrimental effects on AECs, and it was ascertained that the combined vehicle control had no effects on these parameters. Furthermore, western blotting for eNOS and PKB/Akt was performed to determine whether the combined vehicle control still allowed for the detection of these proteins, which it did. The combined vehicle control medium contained 1.6 % PBS, controlling for the PBS vehicle used for the HIV-1-proteins and NRTI/NNRTI drugs, and 0.2 % DMSO controlling for the DMSO vehicle of the PI drugs. The additional NRTI/NNRTI drug vehicles of MeOH and dH_2O constituted such insignificant amounts (0.000027 % MeOH and 0.000143 % dH_2O) that they would be impossible to pipette and thus deemed negligible. Moreover, vehicles not present in a certain treatment group had to be added to that group (the same concentration as in the groups containing it) to ensure that that all the vehicles were controlled for in all six groups **(Table 2.2)**.

Table 2.2: Controlling for Vehicles.

	Original vehicle concentration	Concentration of vehicle added	Final vehicle concentration
1. Combined Vehicle Control (CVC)	-	0.2 % DMSO 1.6 % PBS	0.2 % DMSO 1.6 % PBS
2. HIV-Protein Treatment Group	1.3 % PBS	0.2 % DMSO 0.3 % PBS	0.2 % DMSO 1.6 % PBS
3. NRTI/NNRTI Treatment Group	0.3 % PBS	0.2 % DMSO 1.3 % PBS	0.2 % DMSO 1.6 % PBS
4. PI Treatment Group	0.2 % DMSO	1.6 % PBS	0.2 % DMSO 1.6 % PBS
5. HIV-Protein + NRTI/NNRTI Treatment Group	1.6 % PBS	0.2 % DMSO	0.2 % DMSO 1.6 % PBS
6. HIV-Protein + PI Treatment Group	0.2 % DMSO 1.3 % PBS	0.3 % PBS	0.2 % DMSO 1.6 % PBS

Protein Extraction

After the 24 hour treatment period, the treatment and control media were aspirated, the cells washed and 8 ml of PBS added to each petri dish. The cells were removed from the bottom of the petri dish using a rubber cell-scraper. The cell-containing PBS was transferred to marked 15 ml conical tubes and centrifuged for 3 minutes at 1000 rpm at 4°C, where after most of the PBS was aspirated and the pellets transferred to marked Eppendorf Tubes®. The centrifugation was subsequently repeated in order to aspirate any remaining PBS. Zirconium oxide beads (0.5 mm), at an amount roughly the size of the pellet, were added to each Eppendorf Tube® as well as 800 µl of lysis buffer **(Table 2.3)**. The cells were homogenized using a *Bullet Blender*™ (*Next Advance, Inc.,* NY, USA) and the samples left on ice for 20 minutes after which they were centrifuged for 20 minutes at 15000 rpm at 4 °C. Finally, the supernatant was removed and placed in new, marked Eppendorf Tubes®, before being frozen away at -80 °C for future use.

Table 2.3: Lysis Buffer

Reagent	Final concentration in buffer	Amount of 10X stock for 10ml	Action
Tris-HCl (pH 7.5)	20.0 mM	1.0 ml	Buffer
EGTA [ethylene glycol tetraacetic acid]	1.0 mM		Chelating agent
EDTA [ethylenediaminetetraacetic acid]	1.0 mM	0.1 ml	Chelating agent (metalloprotease inhibitor)
NaCl	150 mM	1.5 ml	Salt
B-glycerophosphate	1.0 mM	0.002 g	Serine/Threonine phosphatase inhibitor
Tetra-sodium pyrophosphate	2.5 mM	0.01 g	Serine/Threonine phosphatase inhibitor
Sodium dodecyl sulphate (SDS)	0.1 %	0.1 ml	Detergent
Na_3VO_4 (0.18g/10ml dH_2O)	1.0 mM	0.1 ml	Tyrosine and alkaline phosphatase inhibitor
Triton-X100 (10%)	1.0 %	1 ml	Detergent
Protease Inhibitor Cocktail 1) AEBSF [4-(2-Aminoethyl) benzenesulfonyl fluoride hydrochloride] 2) Aprotinin 3) Bestatin hydrochloride 4) E-64 [N-(trans-Epoxysuccinyl)-L-leucine 4-guanidinobutylamide] 5) Leupeptin hemisulfate salt 6) Pepstatin A	1.0 %	0.01 ml	 Serine protease inhibitor Serine protease inhibitor Aminopeptidase inhibitor cysteine protease inhibitor Serine and cysteine protease inhibitor acid protease inhibitor
NaF	50 nM	0.0213 g	Serine/Threonine and acidic phosphatase inhibitor
PMSF [Phenylmethylsulfonyl fluoride]	50 µg/ml	0.03 ml	Serine protease inhibitor
Fill up to 10 ml with distilled water (add 6.16 ml)			

Lysate Preparation

Once the supernatants of all the western blot P1 parent cell lines had been collected, they were removed from -80 °C storage, thawed and subjected to the Bradford assay (Bradford, 1976) for protein content determination. Lysates were prepared accordingly, containing 2X Laemmli buffer **(Table 2.4)**, lysis buffer

and supernatant ensuring a final protein content of 8 µg per 18 µl of lysate for all samples. Lysates were boiled for 5 minutes and frozen away at -80 °C for later use. View Appendix F for more details on the Bradford assay calculations.

Table 2.4: 2X Laemmli Buffer (Laemmli, 1970).

Reagent	Concentration
SDS	4 %
Glycerol	20 %
2-Mercaptoethanol	10 %
Bromophenol blue	0.004 %
Tris HCl	0.125 M

Separation and Transfer of Proteins

Lysates were from -80°C storage, thawed, boiled for 3 minutes and centrifuged for 5 minutes at 15000 rpm before being loaded in 26-well Criterion™ TGX Stain-Free™ gels. A PageRuler™ ladder was loaded into the first and last well of each gel and 18 µl of lysate was loaded per sample **(Figure 2.10)**. Proteins were separated at 200 V and 200 mA for 50 minutes to separate the proteins according to size. Once the running process was completed, the gels were activated using the Chemidoc™ MP Imager System with Image Lab™- 5 software (*Bio-Rad*, CA, USA), to ascertain whether protein loading for the different samples was equal. Hereafter, the separated proteins on the gels were transferred to Immobilon®-P transfer membranes using the Trans-Blot® Turbo™ Transfer System (*Bio-Rad*, CA, USA). This was done on ice at 200 V and 200 mA for 90 minutes. Subsequently, the membranes were visualised on the Chemidoc™ to ensure that all proteins had transferred correctly, and so images could later be used for normalisation. Proteins on the membranes were fixed by submerging in MeOH for 5 minutes.

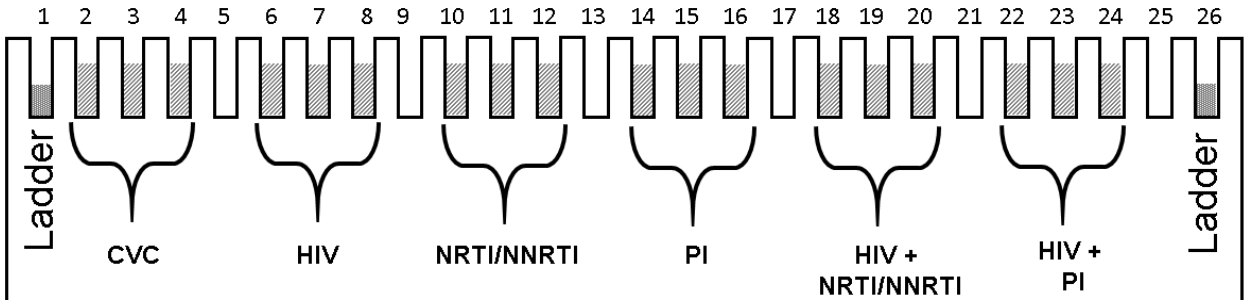

Figure 2.10: Lysate loading. Within each treatment group of three wells each, the first originated from P1 parent cell line 1, the second from P1 parent cell line 2 and the third from P1 parent cell line 3, hence providing three distinct biological replicates.

Immunodetection of Proteins

Membranes were blocked for non-specific binding for 2 hours using a 10 % Tris-buffered saline, 0.1 % Tween solution (TBS-Tween) with 5 % fat-free milk. After blocking, the membranes were washed using TBS-Tween (3 x 5minute cycles), cut and the various sections each incubated overnight at 4 °C in a primary antibody **(Table 2.5)**. Due to the relatively low protein content of the lysates, all primary antibodies were diluted with SignalBoost™. The following morning, the membranes were washed and incubated for 1 hour at room temperature in an anti-rabbit immunoglobulin G, horseradish peroxidase (HRP) conjugated secondary antibody optimised for the various proteins **(Table 2.5)**. Hereafter, membranes were washed and incubated in Clarity™ ECL for 5 minutes before being exposed using the Chemidoc™. Image Lab™- 5 software was used for normalisation, a process which involved correcting for any differences in protein loading evident from the initial membrane visualisation step. The membrane sections were then stripped of their original antibody and re-incubated in a different one. Stripping entailed first washing membranes in dH_2O (2 x 5 minute cycles), followed by a 5 minute wash in 0.2 M NaOH and finally two more dH_2O wash cycles. Hereafter the immunodetection process, commencing with the blocking of the membranes, was repeated.

Table 2.5: Primary and Secondary Antibody Dilutions

<table>
<tr><th>Protein</th><th>Weight</th><th>Function</th><th>Primary Antibody Dilution</th><th>Secondary Antibody Dilution</th></tr>
<tr><td>Total eNOS</td><td rowspan="2">140 kDa</td><td rowspan="2">Nitric Oxide synthesis</td><td rowspan="6">1:1000
(5 µl in 5 ml Primary SignalBoost™)</td><td rowspan="5">1:4000
(5 µl in 20 ml TBS-Tween)</td></tr>
<tr><td>Phospho eNOS</td></tr>
<tr><td>Total PKB (Akt)</td><td rowspan="2">60 kDa</td><td rowspan="2">Upstream activation of eNOS</td></tr>
<tr><td>Phospho PKB (Akt)</td></tr>
<tr><td>IκBα</td><td>39 kDa</td><td>Marker of inflammation</td></tr>
<tr><td>Cleaved-PARP</td><td>89kDa</td><td>Marker of apoptosis</td></tr>
<tr><td>Cleaved Caspase-3</td><td>17/19 kDa</td><td>Marker of apoptosis</td></tr>
<tr><td>Nitrotyrosine</td><td>90 kDa</td><td>Marker of nitrosative stress</td><td rowspan="2">1:200
(25 µl in 5 ml Primary SignalBoost™)</td><td rowspan="2">1:4000 5 % milk
(5 µl in 20 ml TBS-Tween supplemented with 5 % milk)</td></tr>
<tr><td>p22-phox</td><td>22 kDa</td><td>Marker of oxidative stress</td></tr>
</table>

Protein Normalisation

All raw values (pixel counts) were normalised using Image Lab™- 5 software (*Bio-Rad*, CA, USA) to quantify protein expression and account for protein loading. Total protein normalisation (TPN) was employed, where western blot data are analysed using the total protein in samples, thus making the use

of house-keeping proteins (HKP) unnecessary. The TPN technique is faster, more accurate and more reliable than HKP-based normalisation (Gürtler *et al.*, 2013). The best way to measure total protein in a blot or gel is via stain-free technology which relies on a UV-mediated reaction between a trihalo compound present in the stain-free acrylamide gels and tryptophan residues on proteins, which produces fluorescence. This allows for the reliable detection of any tryptophan-containing protein, including the majority of actively researched proteins (MacDonald *et al.*, 2008). To view the images of the Immobilon®-P transfer membranes (with proteins transferred from the Criterion™ TGX Stain-Free™ (4-20%) 26-well Precast Gels) used for this TPN process, refer to Appendix I.

2.6. Statistical Analysis

All data were analysed using GraphPad Prism 7 software (*GraphPad Software,* San Diego, CA, USA). Statistical significance was set at $p < 0.05$.

2.6.1 Plate Reader Assays

One parent cell line was regarded as a single n-value and thus all experiments performed on cells sub-cultured from a single parent cell line were considered to be technical replicates **(Table 2.6)**. All technical replicate values were therefore averaged to obtain a single value (n=1) per treatment group per parent cell line for statistical analysis. A final n=4 was used for all experimental groups in the plate-reader analyses. Furthermore, all raw fluorescence values were converted to and expressed as a percentage of the vehicle control. Student's t-tests were employed when comparing two groups and for more than two groups, one-way analysis of variance (ANOVA) with Tukey's multiple comparisons post hoc tests were utilised.

Table 2.6: Example of technical replicates *versus* n-values (biological replicates). One parent cell line yields multiple technical replicates, but only constitutes n=1 per treatment group. HIV1: HIV-medium 1; HIV2: HIV-medium 2; HIV3: HIV-medium 3.

HIV-1-Protein Medium Treatment									
Parent Cell Line	**Propidium Iodide**			**DAF-2/DA**			**DHR-123**		
P3									
	HIV1	**HIV2**	**HIV3**	**HIV1**	**HIV2**	**HIV3**	**HIV1**	**HIV2**	**HIV3**
	4 tech reps	4 tech reps	4 tech reps	4 tech reps	4 tech reps	4 tech reps	4 tech reps	4 tech reps	4 tech reps

				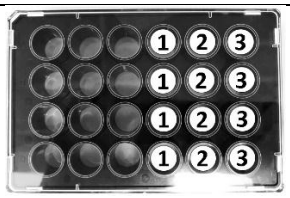			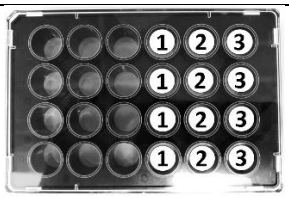		
				HIV1	**HIV2**	**HIV3**	**HIV1**	**HIV2**	**HIV3**
				4 tech reps	4 tech reps	4 tech reps	4 tech reps	4 tech reps	4 tech reps
Sub-Total Technical Repeats	**HIV1**	**HIV2**	**HIV3**	**HIV1**	**HIV2**	**HIV3**	**HIV1**	**HIV2**	**HIV3**
	4	4	4	8	8	8	8	8	8
Sub-Total n-value	1	1	1	1	1	1	1	1	1
P2	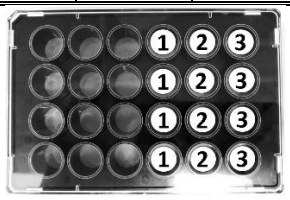			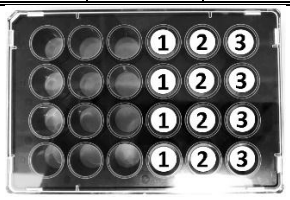			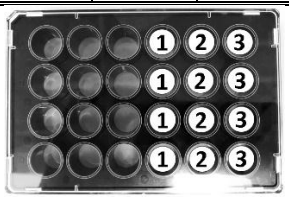		
	HIV1	**HIV2**	**HIV3**	**HIV1**	**HIV2**	**HIV3**	**HIV1**	**HIV2**	**HIV3**
	4 tech reps	4 tech reps	4 tech reps	4 tech reps	4 tech reps	4 tech reps	4 tech reps	4 tech reps	4 tech reps
	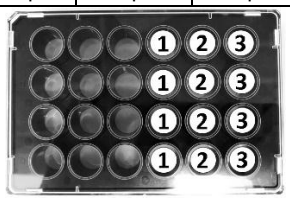			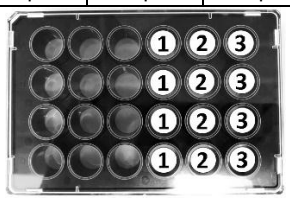					
	HIV1	**HIV2**	**HIV3**	**HIV1**	**HIV2**	**HIV3**			
	4 tech reps	4 tech reps	4 tech reps	4 tech reps	4 tech reps	4 tech reps			
	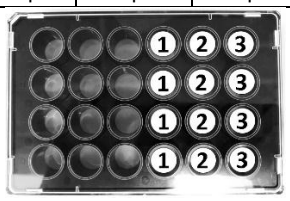			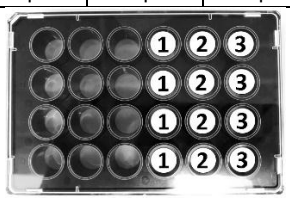			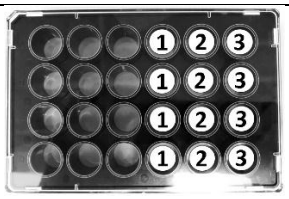		
	HIV1	**HIV2**	**HIV3**	**HIV1**	**HIV2**	**HIV3**	**HIV1**	**HIV2**	**HIV3**
	4 tech reps	4 tech reps	4 tech reps	4 tech reps	4 tech reps	4 tech reps	4 tech reps	4 tech reps	4 tech reps
Sub-Total Technical Repeats	**HIV1**	**HIV2**	**HIV3**	**HIV1**	**HIV2**	**HIV3**	**HIV1**	**HIV2**	**HIV3**
	12	12	12	12	12	12	8	8	8
Sub-Total n-value	1	1	1	1	1	1	1	1	1
Total Technical Repeats	**HIV1**	**HIV2**	**HIV3**	**HIV1**	**HIV2**	**HIV3**	**HIV1**	**HIV2**	**HIV3**
	16	16	16	20	20	20	16	16	16
Total n-value	2	2	2	2	2	2	2	2	2

2.6.2 Western Blot Analyses

Initially, the intention was to have a sample size of n=4 /group for the western blot measurements – as with the plate reader assays. Knowing that AECs often do not yield sufficient protein, five P1 cell lines were cultured for western blotting purposes. However, only three of these P1 parent cell lines yielded a sufficient amount of protein. This resulted in a final n=3 per treatment group. Normalised raw values were converted to fractions of the combined vehicle control. Ordinary one-way ANOVAs with Tukey's multiple comparisons post hoc tests were employed.

CHAPTER 3: RESULTS

The results are presented chronologically, commencing with the plate reader analyses utilised in the development of the HIV-1-protein model (time- and concentration-response investigations) (Section 3.1), followed by the antiretroviral drug concentration-response investigations within this optimised HIV-1-protein environment (Section 3.2). Finally, the western blot protein expression and phosphorylation data are described in Section 3.4. All data are presented graphically. For the exact mean ± SEM values of all the experiments, please view **Tables 3.2 – 3.26** in Appendix G.

3.1. HIV-1-PROTEIN MEDIUM TIME- AND CONCENTRATION-RESPONSE INVESTIGATIONS

After exposure to serum starvation for 24 hours, AECs were treated with three different concentrations (25 ng/ml, 50 ng/ml and 100 ng/ml) of a HIV-protein cocktail consisting of Tat, Nef and Gp160 for a duration of either 24 or 48 hours. This was compared with vehicle controls containing matching concentrations of the PBS vehicle used to dissolve the HIV-1-proteins. Subsequently the effects on cell viability, nitric oxide production and nitrosative stress were assessed using a plate reader. For all groups n=4. Results regarding the functionality of the various fluorescent probes can be viewed in Appendix H. For a more detailed description of the methods involved, refer to Chapter 2.

3.1.1 24-hour Exposure

Propidium Iodide Cell Viability Assay

No significant effects on cell viability were detected following the treatment of AECs with three different concentrations of HIV-1 proteins for 24 hours. An ordinary one-way ANOVA with Tukey's multiple comparisons test was performed.

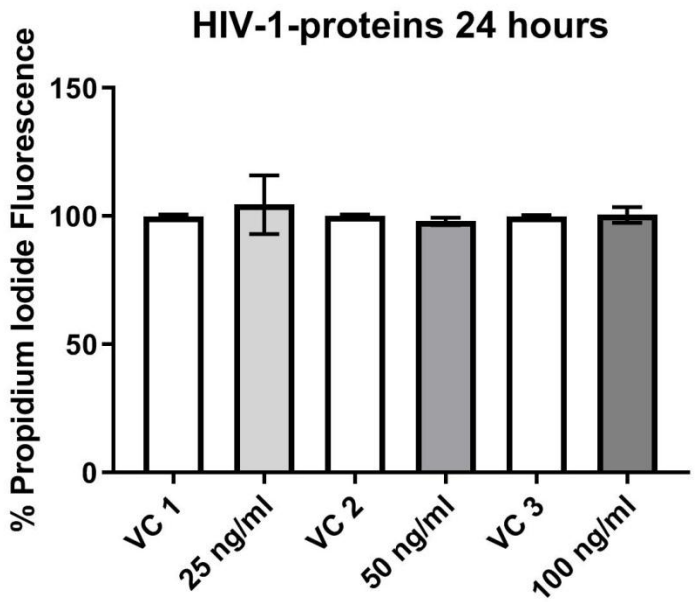

Figure 3.1: Cell viability after 24 hours of HIV-1-protien exposure. VC 1: vehicle control for 25 ng/ml HIV-protein cocktail; VC 2: vehicle control for 50 ng/ml HIV-protein cocktail; VC 3: vehicle control for 100 ng/ml HIV-protein cocktail. n=4/group. Note that all raw fluorescence values were converted to and expressed as a percentage of the vehicle controls, thus 100% fluorescence does not indicate 100% non-viable cells for a treatment group, but merely the proportion of non-viable cells in that treatment group compared to the vehicle control.

DAF-2/DA Nitric Oxide Production Assay

Treatment of AECs with 100 ng/ml of HIV-1 proteins for 24 hours resulted in a significant reduction in Nitric Oxide (NO) production compared to 25 ng/ml of HIV-proteins (72.05 ± 8.37% vs. 100.8 ± 5.25%; p=0.02) and Vehicle Control 3 (72.05 ± 8.37% vs. 100 ± 1.55%; p=0.02). An ordinary one-way ANOVA with Tukey's multiple comparisons test was performed.

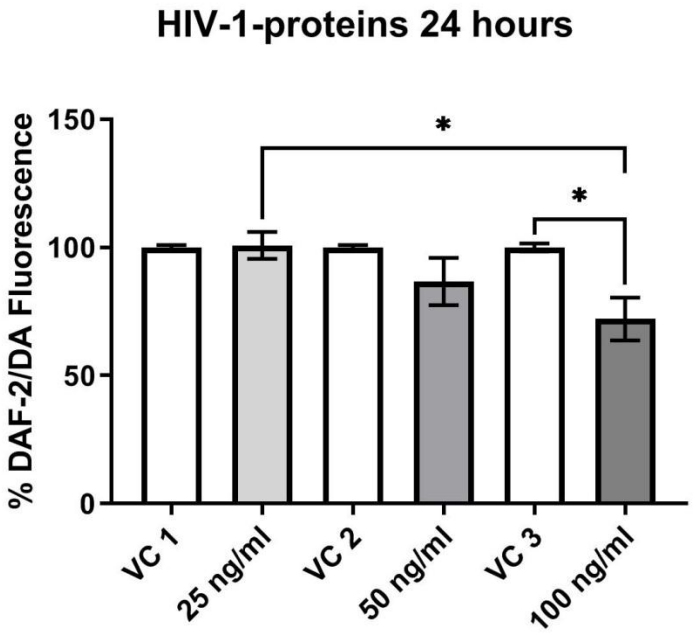

Figure 3.2: NO production after 24 hours of HIV-1-protein exposure. VC 1: vehicle control for 25 ng/ml HIV-protein cocktail, VC 2: vehicle control for 50 ng/ml HIV-protein cocktail; VC 3: vehicle control for 100 ng/ml HIV-protein cocktail. *: $p<0.05$. n=4/group. Note that all raw fluorescence values were converted to and expressed as a percentage of the vehicle controls.

DHR-123 Nitrosative Stress Assay

No significant effects on nitrosative stress were detected following the treatment of AECs with three different concentrations of HIV-1 proteins for 24 hours. An ordinary one-way ANOVA with Tukey's multiple comparisons test was performed.

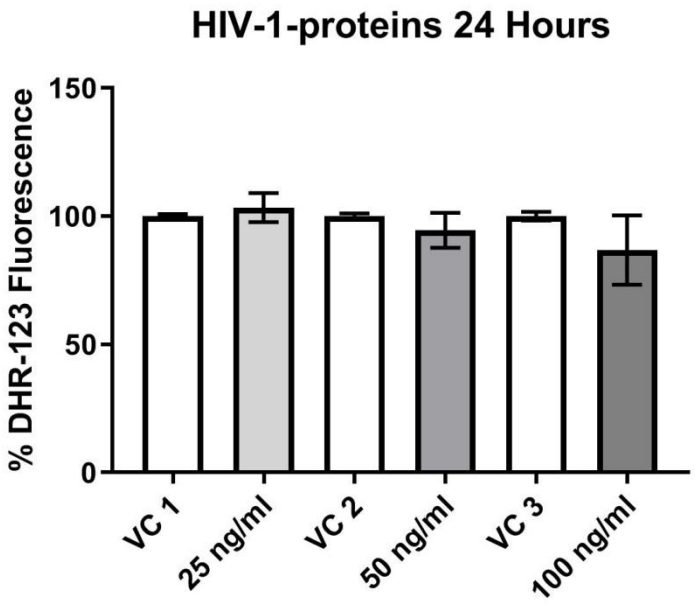

Figure 3.3: Nitrosative stress after 24 hours of HIV-1-protein exposure. VC 1: vehicle control for 25 ng/ml HIV-protein cocktail, VC 2: vehicle control for 50 ng/ml HIV-protein cocktail; VC 3: vehicle control for 100 ng/ml HIV-protein cocktail. n=4/group. Note that all raw fluorescence values were converted to and expressed as a percentage of the vehicle controls.

3.1.2 48-hour Exposure

Propidium Iodide Cell Viability Assay

Treatment of AECs with 100 ng/ml of HIV-1 proteins for 48 hours resulted in a significant increase in non-viable cells compared to the 25 ng/ml group (118.2 ± 7.69% vs. 98.37 ± 4.61%; p=0.04), however, there was no significance compared to the vehicle control. An ordinary one-way ANOVA with Tukey's multiple comparisons test was performed.

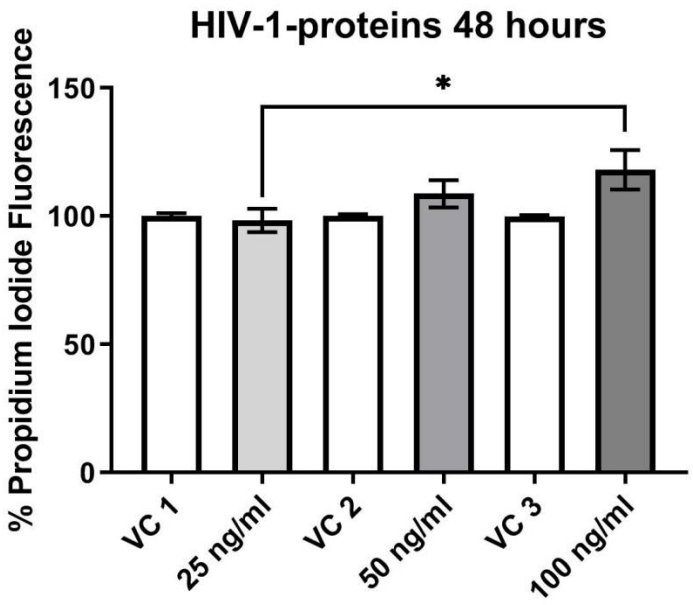

Figure 3.4: Cell viability after 48 hours of HIV-1-protien exposure. VC 1: vehicle control for 25 ng/ml HIV-protein cocktail, VC 2: vehicle control for 50 ng/ml HIV-protein cocktail; VC 3: vehicle control for 100 ng/ml HIV-protein cocktail. *: $p<0.05$. n=4/group. Note that all raw fluorescence values were converted to and expressed as a percentage of the vehicle controls, thus 100% fluorescence does not indicate 100% non-viable cells for a treatment group, but merely the proportion of non-viable cells in that treatment group compared to the vehicle control.

DAF-2/DA Nitric Oxide Production Assay

No significant differences in NO production were detected following the treatment of AECs with three different concentrations of HIV-1 proteins for 48 hours. An ordinary one-way ANOVA with Tukey's multiple comparisons test was performed.

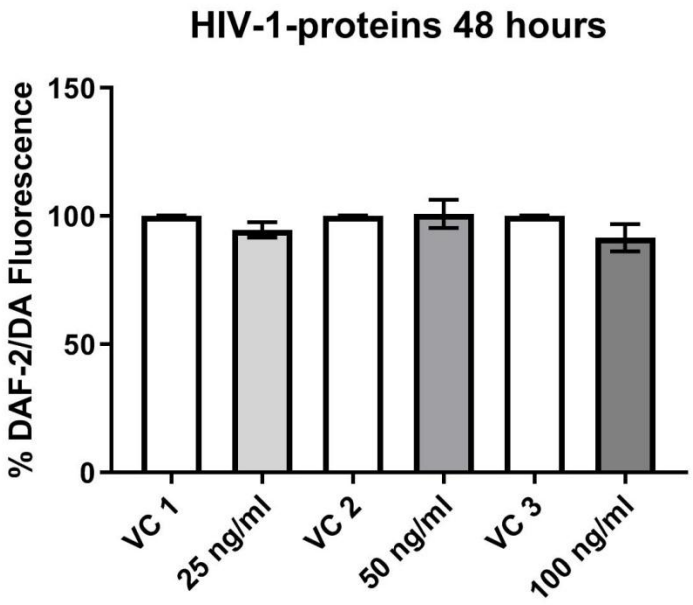

Figure 3.5: NO production after 48 hours of HIV-1-protein exposure. VC 1: vehicle control for 25 ng/ml HIV-protein cocktail; VC 2: vehicle control for 50 ng/ml HIV-protein cocktail; VC 3: vehicle control for 100 ng/ml HIV-protein cocktail. n=4/group. Note that all raw fluorescence values were converted to and expressed as a percentage of the vehicle controls.

DHR-123 Nitrosative Stress Assay

No significant effects on nitrosative stress were detected following the treatment of AECs with three different concentrations of HIV-1 proteins for 48 hours. An ordinary one-way ANOVA with Tukey's multiple comparisons test was performed.

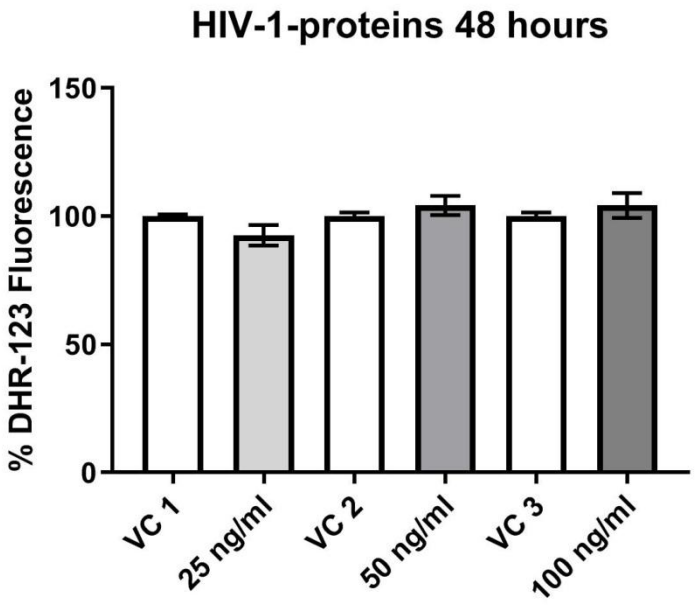

Figure 3.6: Nitrosative stress after 48 hours of HIV-1-protein exposure. VC 1: vehicle control for 25 ng/ml HIV-protein cocktail; VC 2: vehicle control for 50 ng/ml HIV-protein cocktail; VC 3: vehicle control for 100 ng/ml HIV-protein cocktail. n=4/group. Note that all raw fluorescence values were converted to and expressed as a percentage of the vehicle controls.

3.1.3 HIV-1-Model

Based on the above results, an HIV-1-model was decided upon for use in the next set of investigations. Exposing AECs to 100 ng/ml of HIV-1-proteins for 24 hours elicited a cellular response (decreased NO production – a marker of impaired endothelial cell function) without causing a significant increase in non-viable cells. Thus, the HIV-1-model constituted treating serum starved AECs with 100 ng/ml of a Tat, Nef and Gp160 cocktail or 24 hours.

3.2. Antiretroviral Drug Treatment Concentration-Response Investigations

After the HIV-1-model was developed, the antiretroviral drug treatment was subject to concentration-response investigations within the previously established HIV-1 environment (financial constraints and the limited space of the 24-well plates meant that the drugs could not be tested individually). The effects of NRTI/NNRTIs and PIs with HIV-1-proteins on cell viability, NO production and nitrosative stress were determined using a plate reader. After exposure to serum starvation for 24 hours, AECs were treated with three different concentrations of antiretroviral drugs plus 100 ng/ml of Tat, Nef and Gp160 for 24 hours. For all groups n=4. Results regarding the functionality of the various fluorescent probes can be viewed in Appendix H. For a more detailed description of the methods involved, refer to Chapter 2.

3.2.1 NRTI/NNRTI Treatment

The three different concentrations of NRTI/NNRTI treatment included single dose treatment (5.6 nM EFV, 500 nM TDF, 1.3 µM FTC), half dose treatment (2.8 nM EFV, 250 nM TDF, 0.65 µM FTC) and double dose treatment (11.2 nM EFV, 1 µM TDF, 2.6 µM FTC). These drugs were all administered in conjunction with the 100 ng/ml HIV-1-protein cocktail. This was compared with vehicle controls containing matching concentrations of the vehicles used to dissolve the HIV-1-proteins (PBS) as well as the NRTI/NNRTI drugs (PBS, MeOH, dH_2O). The vehicle controls did not contain HIV-1- proteins.

Propidium Iodide Cell Viability Assay

Treatment with double dose NRTI/NNRTI resulted in a significant increase in non-viable cells compared to half dose (104.7 ± 2.7% vs. 95.56 ± 0.63; p=0.02) and single dose (104.7 ± 2.7 vs. 96.17 ± 3.4; p=0.04) treatment, however, not compared to the vehicle control. An ordinary one-way ANOVA with Tukey's multiple comparisons test was performed.

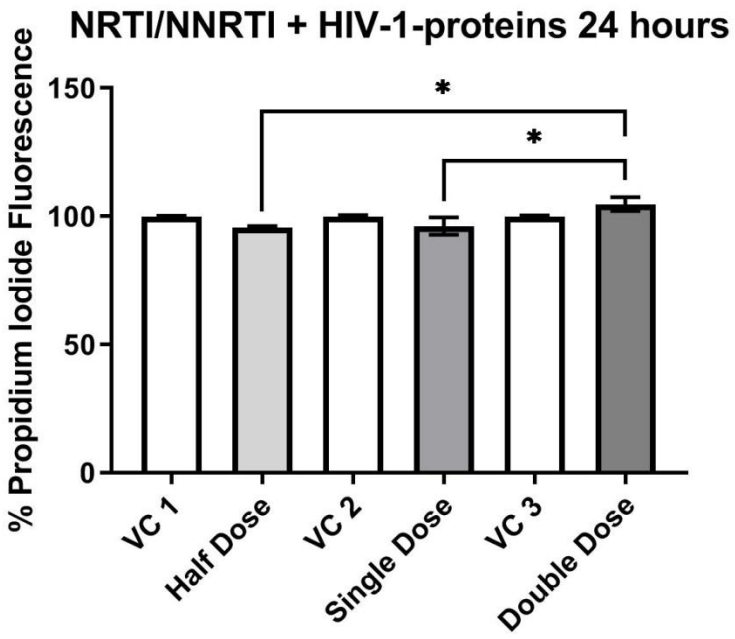

Figure 3.7: Cell viability after 24 hours of NRTI/NNRTI treatment within an HIV-1 environment. VC 1: vehicle control for half dose NRTI/NNRTI treatment, VC 2: vehicle control for single dose NRTI/NNRTI treatment; VC 3: vehicle control for double dose NRTI/NNRTI treatment. *: $p<0.05$. n=4/group. Note that all raw fluorescence values were converted to and expressed as a percentage of the vehicle controls, thus 100% fluorescence does not indicate 100% non-viable cells for a treatment group, but merely the proportion of non-viable cells in that treatment group compared to the vehicle control.

DAF-2/DA Nitric Oxide Production Assay

No significant effects on NO production were detected following the treatment of AECs with NRTI/NNRTIs. An ordinary one-way ANOVA with Tukey's multiple comparisons test was performed.

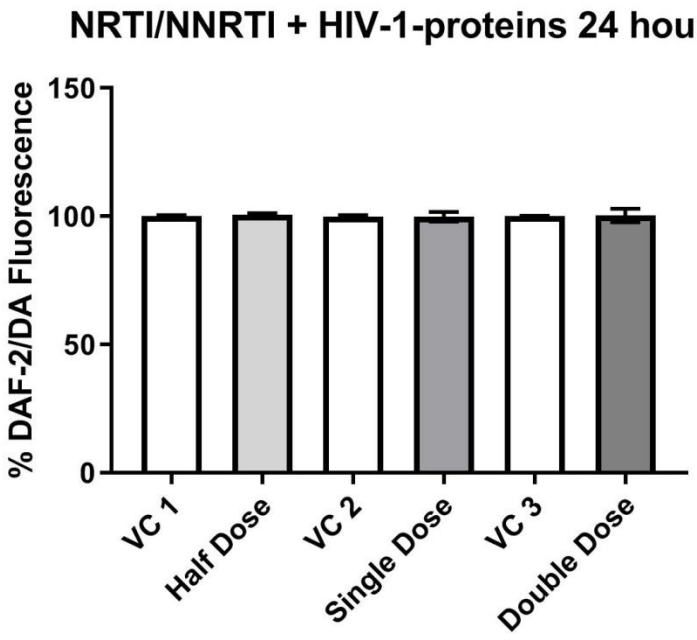

Figure 3.8: NO levels after 24 hours of NRTI/NNRTI treatment within an HIV-1 environment VC 1: vehicle control for half dose NRTI/NNRTI treatment, VC 2: vehicle control for single dose NRTI/NNRTI treatment; VC 3: vehicle control for double dose NRTI/NNRTI treatment. n=4/group. Note that all raw fluorescence values were converted to and expressed as a percentage of the vehicle controls.

DHR-123 Nitrosative Stress Assay

All three NRTI/NNRTI dosages resulted in significant reductions in nitrosative stress in AECs [Half Dose *vs.* Vehicle Control 1 (86.57 ± 3.52% vs. 100 ± 0.28% p=0.01); Single Dose *vs.* Vehicle Control 2 (83.19% ± 3.5 vs. 100 ± 0.22%; p=0.002); Double Dose *vs.* Vehicle Control 3 (86.14 ± 3.29% vs. 100 ± 0.48%; p=0.009)]. An ordinary one-way ANOVA with Tukey's multiple comparisons test was performed.

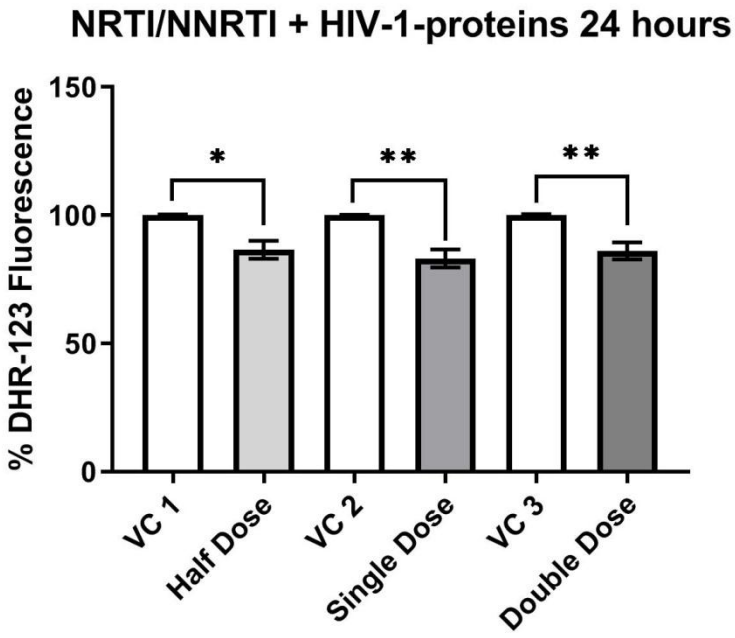

Figure 3.9: Nitrosative stress after 24 hours of NRTI/NNRTI treatment within an HIV-1 environment. VC 1: vehicle control for half dose NRTI/NNRTI treatment, VC 2: vehicle control for single dose NRTI/NNRTI treatment; VC 3: vehicle control for double dose NRTI/NNRTI treatment. *: $p<0.05$; **: $p<0.01$. n=4/group. Note that all raw fluorescence values were converted to and expressed as a percentage of the vehicle controls.

3.2.2 PI Treatment

The three different concentrations of PI treatment included a single dose (10 µM LPV, 2 µM RTV), half dose (5 µM LPV, 1 µM RTV) and double dose of PI drugs (20 µM LPV, 4 µM RTV). As with the NRTI/NNRTI groups, these drugs were administered in conjunction with 100 ng/ml of the HIV-1-protein cocktail. This was compared with vehicle controls containing matching concentrations of the vehicles used to dissolve the HIV-1-proteins (PBS) as well as the PI drugs (DMSO). The vehicle controls did not contain HIV-1-proteins.

Propidium Iodide Cell Viability Assay

Double dose PI treatment resulted in a significant increase in the non-viable cells compared to half dose (106.7 ± 6.14% vs. 94.26 ± 0.89%; p=0.03) and single dose (106.7 ± 6.14% vs. 94.33 ± 0.79; p=0.03) treatment, but not compared to the vehicle control. An ordinary one-way ANOVA with Tukey's multiple comparisons test was performed.

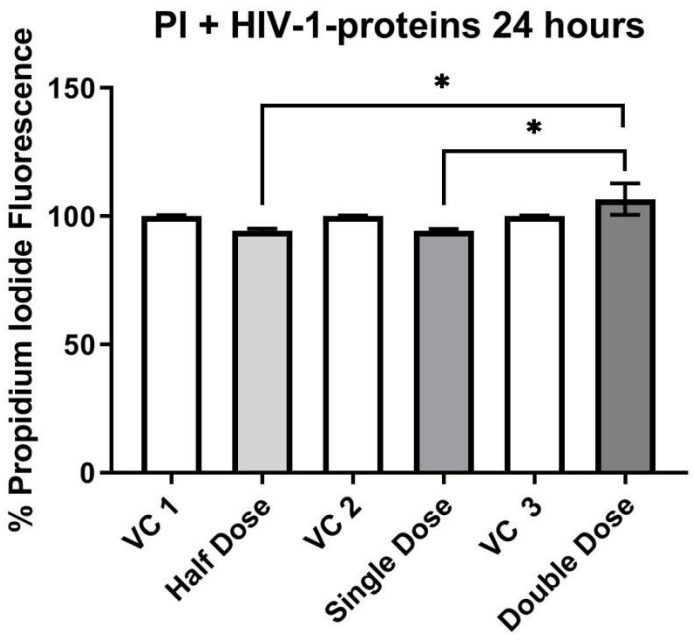

Figure 3.10: Cell viability after 24 hours of PI treatment within an HIV-1 environment. VC 1: vehicle control for half dose PI treatment, VC 2: vehicle control for single dose PI treatment; VC 3: vehicle control for double dose PI treatment. *: p<0.05. n=4/group. Note that all raw fluorescence values were converted to and expressed as a percentage of the vehicle controls, thus 100% fluorescence does not indicate 100% non-viable cells for a treatment group, but merely the proportion of non-viable cells in that treatment group compared to the vehicle control.

DAF-2/DA Nitric Oxide Production Assay

Treatment with both single dose and double dose PI resulted in significant reductions in NO production [Single Dose *vs*. Half Dose (92.74 ± 1.4% vs. 100.2 ± 1.85% p=0.006); Double Dose *vs*. Half Dose (85 ± 1.81% vs. 100.2 ± 1.85% p<0.001); Single Dose *vs*. Vehicle Control 2 (92.74 ± 1.4% vs. 100 ± 0.67%; p=0.008); Double Dose *vs*. Single Dose (85 ± 1.81% vs. 92.74 ± 1.4%; p=0.004); Double Dose *vs.* Vehicle Control 3 (85 ± 1.81% vs. 100 ± 0.56%; p<0.001)]. An ordinary one-way ANOVA with Tukey's multiple comparisons test was performed.

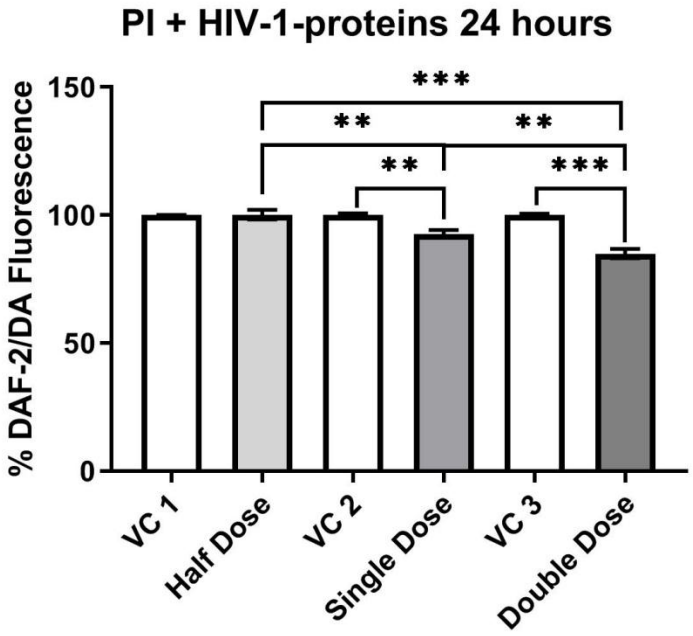

Figure 3.11: NO levels after 24 hours of PI treatment within an HIV-1 environment. VC 1: vehicle control for half dose PI treatment, VC 2: vehicle control for single dose PI treatment; VC 3: vehicle control for double dose PI treatment. *: p<0.05; **: p<0.01; ***: p<0.001. n=4/group. Note that all raw fluorescence values were converted to and expressed as a percentage of the vehicle controls.

DHR-123 Nitrosative Stress Assay

PI treatment had no significant effect on nitrosative stress levels for any of the treatment concentrations. An ordinary one-way ANOVA with Tukey's multiple comparisons test was performed.

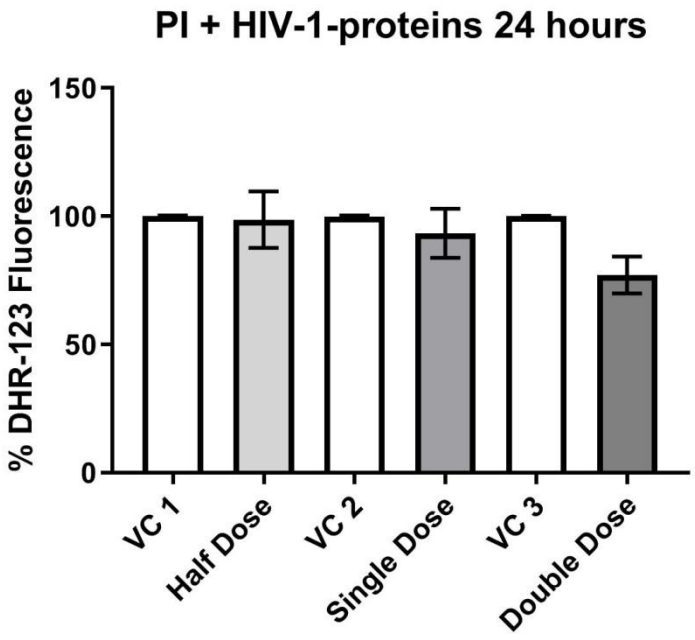

Figure 3.12: Nitrosative stress after 24 hours of PI treatment within an HIV-1 environment. VC 1: vehicle control for half dose PI treatment, VC 2: vehicle control for single dose PI treatment; VC 3: vehicle control for double dose PI treatment. n=4/group. Note that all raw fluorescence values were converted to and expressed as a percentage of the vehicle controls.

3.3. Combined Vehicle Control

To avoid having multiple vehicle controls for western blotting, a combined vehicle control was created. This entailed combining all the vehicles used in the HIV-1-protein, NRTI/NNTRI and PI treatments which included PBS and DMSO. Before using this combined vehicle control cocktail, its effects on cell viability and NO production were assessed using a plate reader. Western blot analysis was used to probe for PKB/Akt.and eNOS to ensure that these key vascular signalling proteins could still be detected. After being serum starved for 24 hours, AECs either received normal growth medium (Control) or they were treated with the combined vehicle control (CVC) cocktail for 24 hours. A single cell line was used due to time and financial constraints; the n-values described below are thus only technical repeats. Results regarding the functionality of the various fluorescent probes can be viewed in Appendix H. For a more detailed description of the methods involved, refer to Chapter 2.

3.3.1 Plate-reader Assays

Propidium Iodide Cell Viability Assay

The combined vehicle control had no effect on cell viability compared to the normal growth medium control. A Student's t-test was performed.

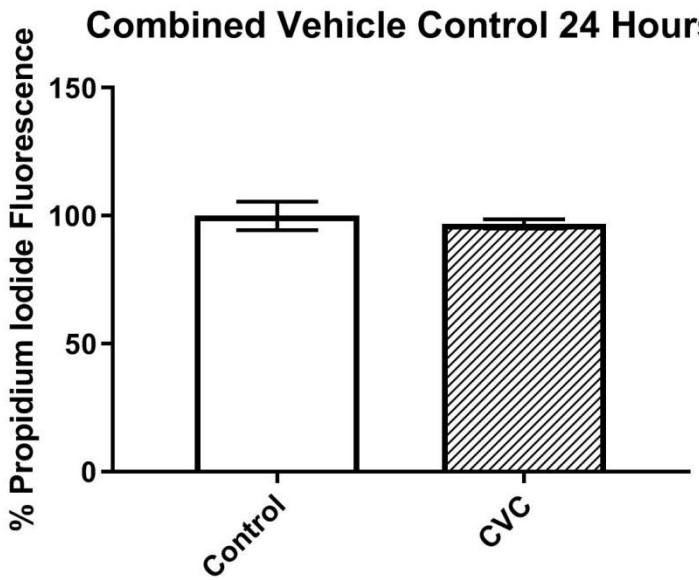

Figure 3.13: Cell viability after 24 hours of CVC exposure. CVC: combined vehicle control. For Control n=3 and for CVC n=6. Note that all raw fluorescence values were converted to and expressed as a percentage of the control.

DAF-2/DA Nitric Oxide Production Assay

The combined vehicle control had no effect on NO production compared to the normal growth medium control. A Student's t-test was performed.

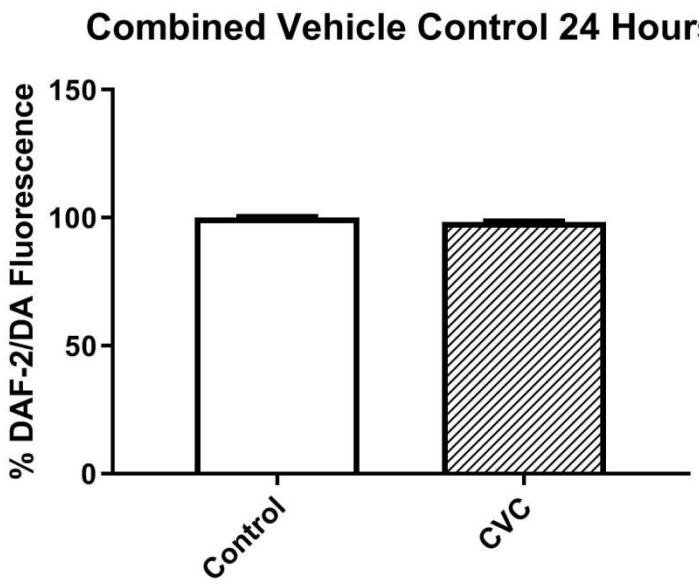

Figure 3.14: NO levels after 24 hours of CVC exposure. CVC: combined vehicle control. For Control n=3 and for CVC n=6. Note that all raw fluorescence values were converted to and expressed as a percentage of the control.

3.3.2 Western Blotting

Total eNOS

Exposure to the CVC did not affect the expression of total eNOS in the AECs.

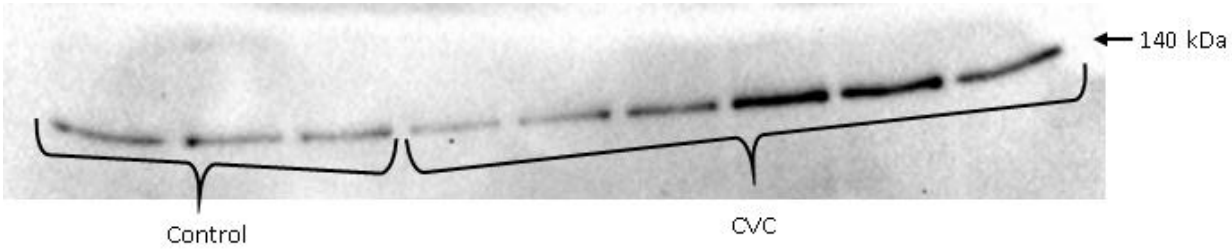

Figure 3.15: eNOS expression after 24 hours of CVC exposure. For Control n=1 and for CVC n=2.CVC: Combined Vehicle Control.

Total PKB/Akt

Total PKB/Akt was expressed in the AECs of both the control and CVC.

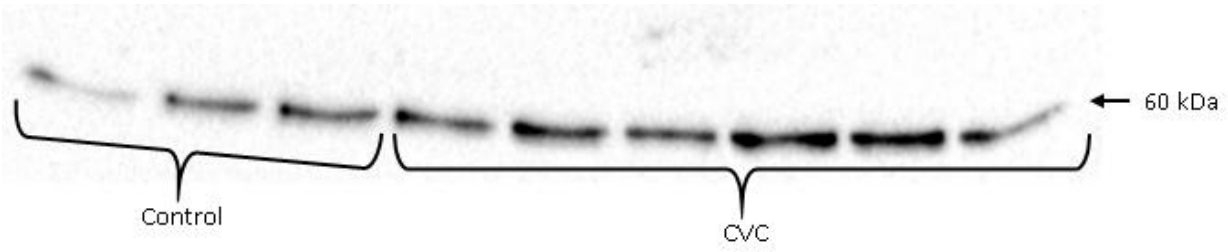

Figure 3.16: PKB/Akt expression after 24 hours of CVC exposure. For Control n=1 and for CVC n=2. CVC: Combined Vehicle Control.

3.4. Vascular Signalling Proteins

After the time- and concentration-response investigations were concluded, western blot analyses were performed to determine the expression and activation of various important vascular signalling proteins. View the various treatment groups in **Table 3.1** below. For all groups an n=3 was performed, unless otherwise specified. For a more detailed description of the methods involved, refer to Chapter 2.

Table 3.1: Western blotting treatment groups

Name	Treatment	Controlling for Vehicles
1. Combined Vehicle Control	-	0.2% DMSO and 1.6% PBS
2. HIV	100 ng/ml of Tat, Gp160 and Nef	0.2% DMSO and 0.3% PBS
3. NRTI/NNRTI	5.6 nM EFV, 500 nM TDF and 1.3 µM FTC	0.2% DMSO and 1.3% PBS
4. PI	10 µM LPV and 2 µM RTV	1.6% PBS
5. HIV + NRTI/NNRTI	100 ng/ml of Tat, Gp160 and Nef + 5.6 nM EFV, 500 nM TDF and 1.3 µM FTC	0.2% DMSO
6. HIV + PI	100 ng/ml of Tat, Gp160 and Nef +10 µM LPV and 2 µM RTV	0.3% PBS

3.4.1 Nitric Oxide Synthesis

eNOS

Combined HIV-protein and PI treatment resulted in a significant reduction in eNOS expression in AECs compared to the combined vehicle control (0.28 ± 0.04 vs. 1 ± 0.21; p=0.01), HIV-protein only group (0.28 ± 0.04 vs. 1.17 ± 0.16; p=0.003) and PI group (0.28 ± 0.04 vs. 0.93 ± 0.1; p=0.03). None of the interventions had any effects on phosphorylated eNOS levels. Analyses included phosphorylated eNOS as well as phosphorylated / total eNOS ratios. Ordinary one-way ANOVAs with Tukey's multiple comparisons tests were performed.

A

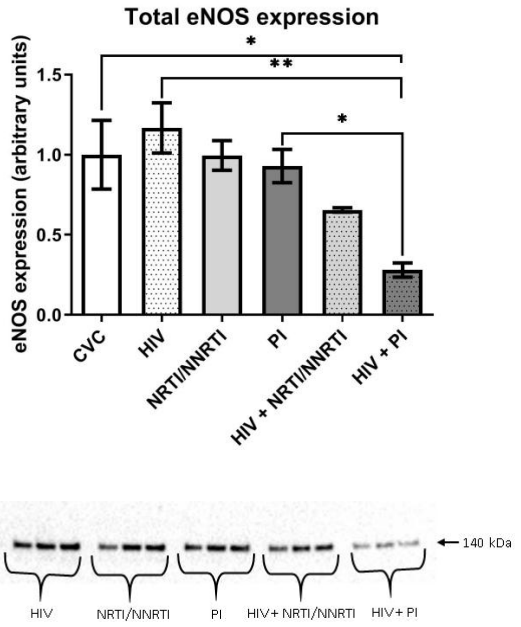

B

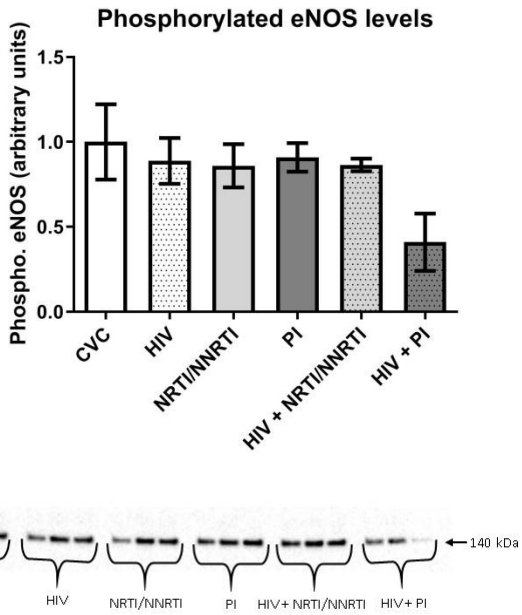

C

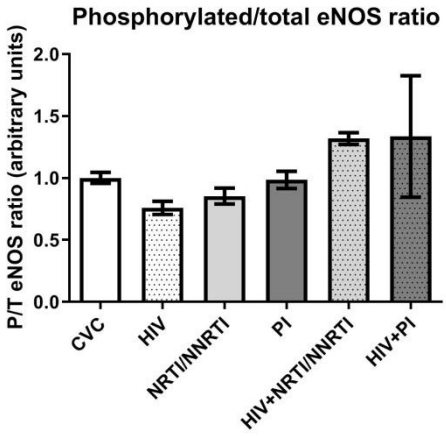

Figure 3.17: eNOS expression and phosphorylation after 24 hours. CVC: Combined vehicle control; HIV: HIV-protein cocktail; NRTI/NNRTI: nucleoside analogue reverse transcriptase inhibitors/non-nucleoside reverse transcriptase inhibitors; PI: protease inhibitors. *: p<0.05; **: p<0.01. Arbitrary units: pixel counts depicted here as ratios relative to the CVC, which was expressed as 1. n=3/group.

PKB/Akt

Significant reductions in PKB/Akt expression were observed in most treatment groups [HIV *vs.* CVC (0.84 ± 0.3 vs. 1 ± 0.03; p= 0.04); NRTI/NNRTI *vs.* CVC (0.79 ± 0.04 vs. 1 ± 0.03; p=0.008); PI *vs.* CVC (0.79 ± 0.01 vs. 1 ± 0.03; p=0.008); HIV + NRTI/NNRTI vs. CVC (0.83 ± 0.05 vs. 1 ± 0.03; p=0.03); HIV + PI *vs*. CVC (0.68 ± 0.02 vs. 1 ± 0.03; p<0.001); HIV + PI *vs.* HIV (0.68 ± 0.02 vs. 0.84 ± 0.03; p=0.04)]. None of the interventions had any effects on phosphorylated PKB/Akt levels. Analyses included phosphorylated PKB as well as phosphorylated / total PKB/Akt ratios. Ordinary one-way ANOVAs with Tukey's multiple comparisons tests were performed.

A

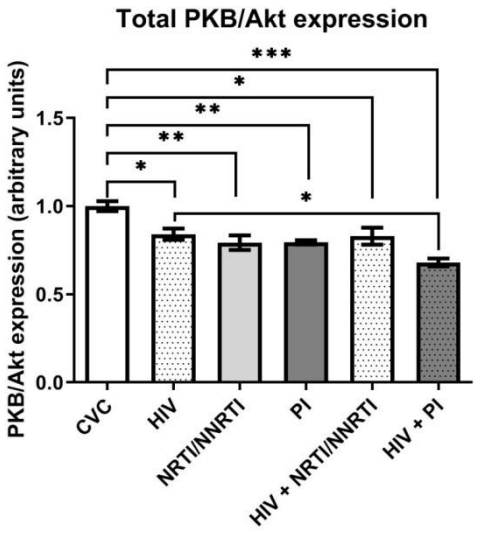

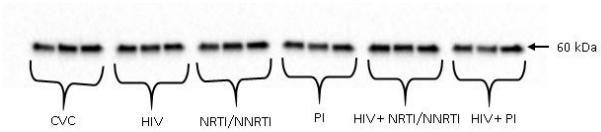

B

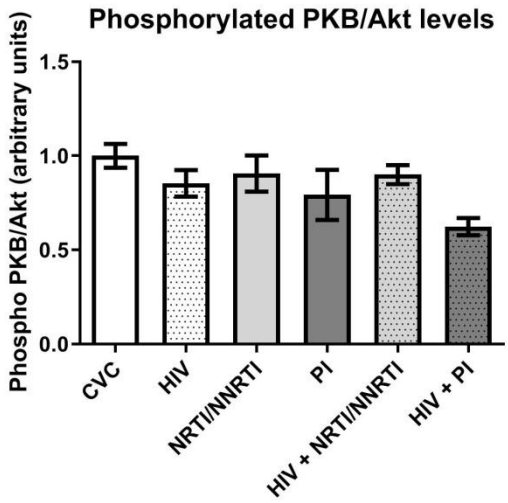

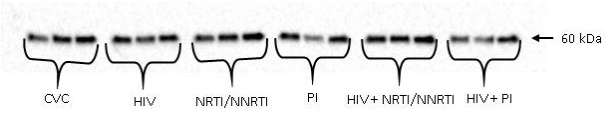

C

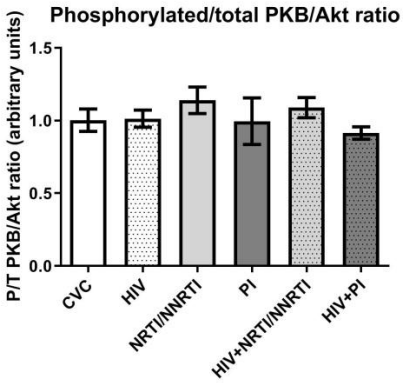

Figure 3.18: PKB/Akt expression and phosphorylation after 24 hours. CVC: Combined vehicle control; HIV: HIV-protein cocktail; NRTI/NNRTI: nucleoside analogue reverse transcriptase inhibitors/non-nucleoside reverse transcriptase inhibitors; PI: protease inhibitors. *: p<0.05; **: p<0.01; ***: p<0.001. Arbitrary units: pixel counts depicted here as ratios relative to the CVC, which was expressed as 1. n=3/group.

3.4.2 Inflammation

IκBα

Combined HIV-protein and PI treatment resulted in a significant reduction in IκBα expression in AECs compared to the combined vehicle control (0.37 ± 0.03 vs. 1 ± 0.15; p<0.001), the HIV only treatment group (0.37 ± 0.03 vs. 0.93 ± 0.019; p=0.002) and the combined HIV and NRTI/NNRTI treatment group (0.37 ± 0.03 vs. 0.79 ± 0.05; p=0.02). An ordinary one-way ANOVA with Tukey's multiple comparisons test was performed.

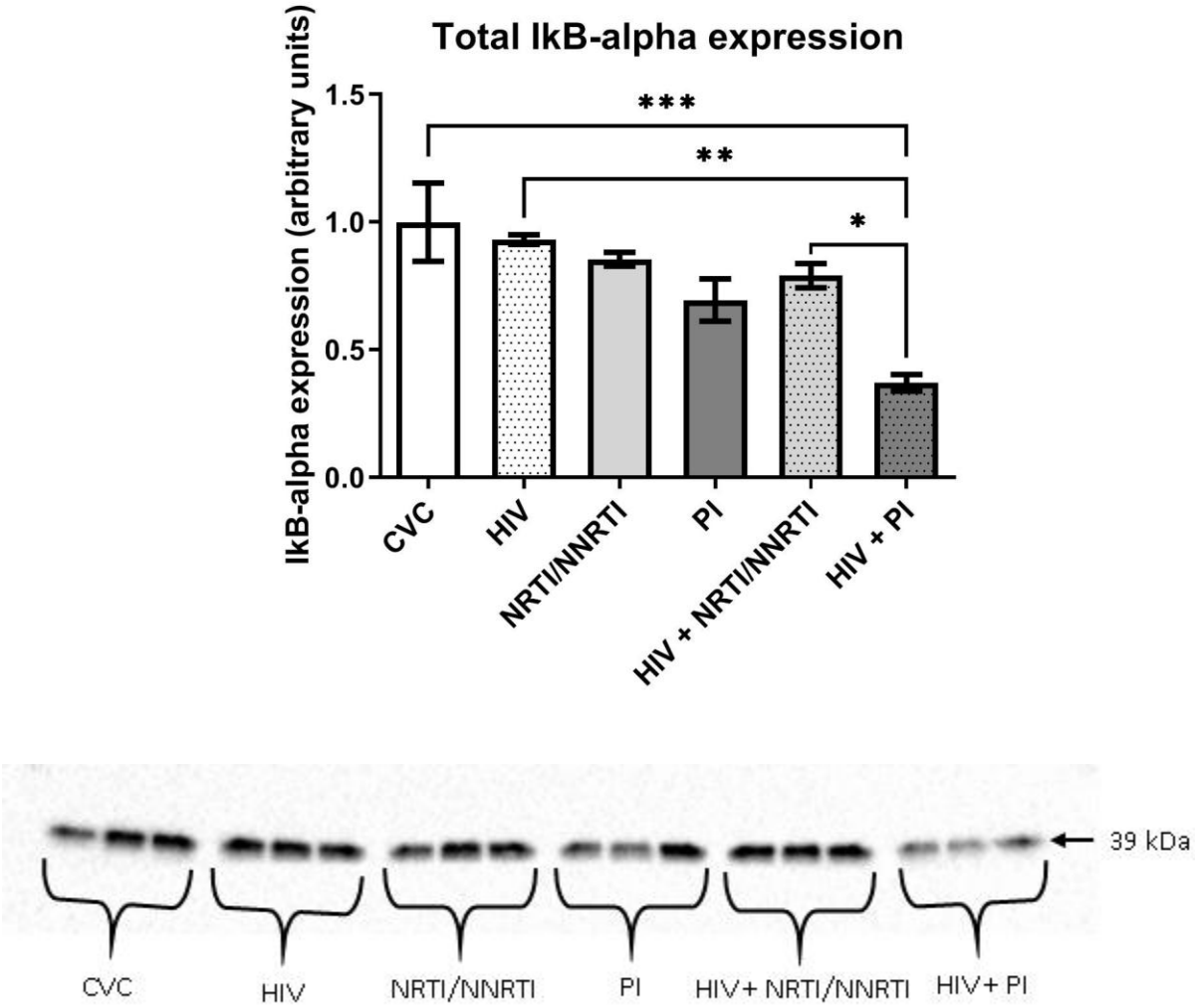

Figure 3.19: IκBα expression after 24 hours. CVC: Combined vehicle control; HIV: HIV-protein cocktail; NRTI/NNRTI: nucleoside analogue reverse transcriptase inhibitors/non-nucleoside reverse transcriptase inhibitors; PI: protease inhibitors. *: p<0.05; **: p<0.01; ***: p<0.001. Arbitrary units: pixel counts depicted here as ratios relative to the CVC, which was expressed as 1. n=3/group.

3.4.3 Apoptosis

Cleaved PARP

Significant reductions in cleaved PARP levels were observed in AECs in the NRTI/NNRTI treatment group (0.74 ± 0.05 vs. 1 ± 0.03; p=0.03) and in the HIV + PI treatment group (0.64 ± 0.05 vs. 1 ± 0.03; p=0.002) compared to the combined vehicle control. An ordinary one-way ANOVA with Tukey's multiple comparisons tests was performed.

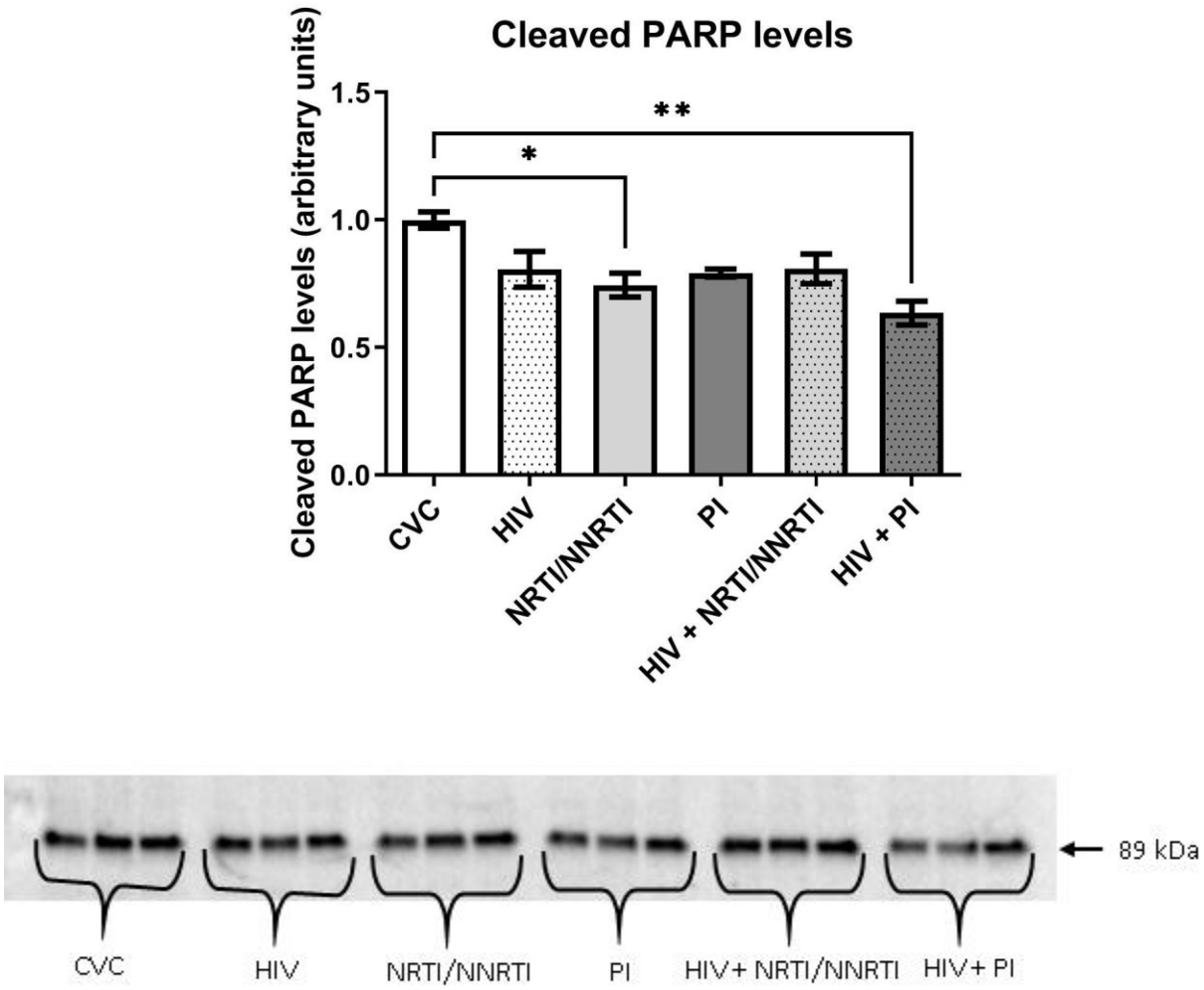

Figure 3.20: Cleaved PARP after 24 hours. CVC: Combined vehicle control; HIV: HIV-protein cocktail; NRTI/NNRTI: nucleoside analogue reverse transcriptase inhibitors/non-nucleoside reverse transcriptase inhibitors; PI: protease inhibitors. *: p<0.05; **: p<0.01. Arbitrary units: pixel counts depicted here as ratios relative to the CVC, which was expressed as 1. n=3/group.

Cleaved Caspase-3

None of the interventions had any effects on cleaved caspase-3 levels. An ordinary one-way ANOVA with Tukey's multiple comparisons test was performed.

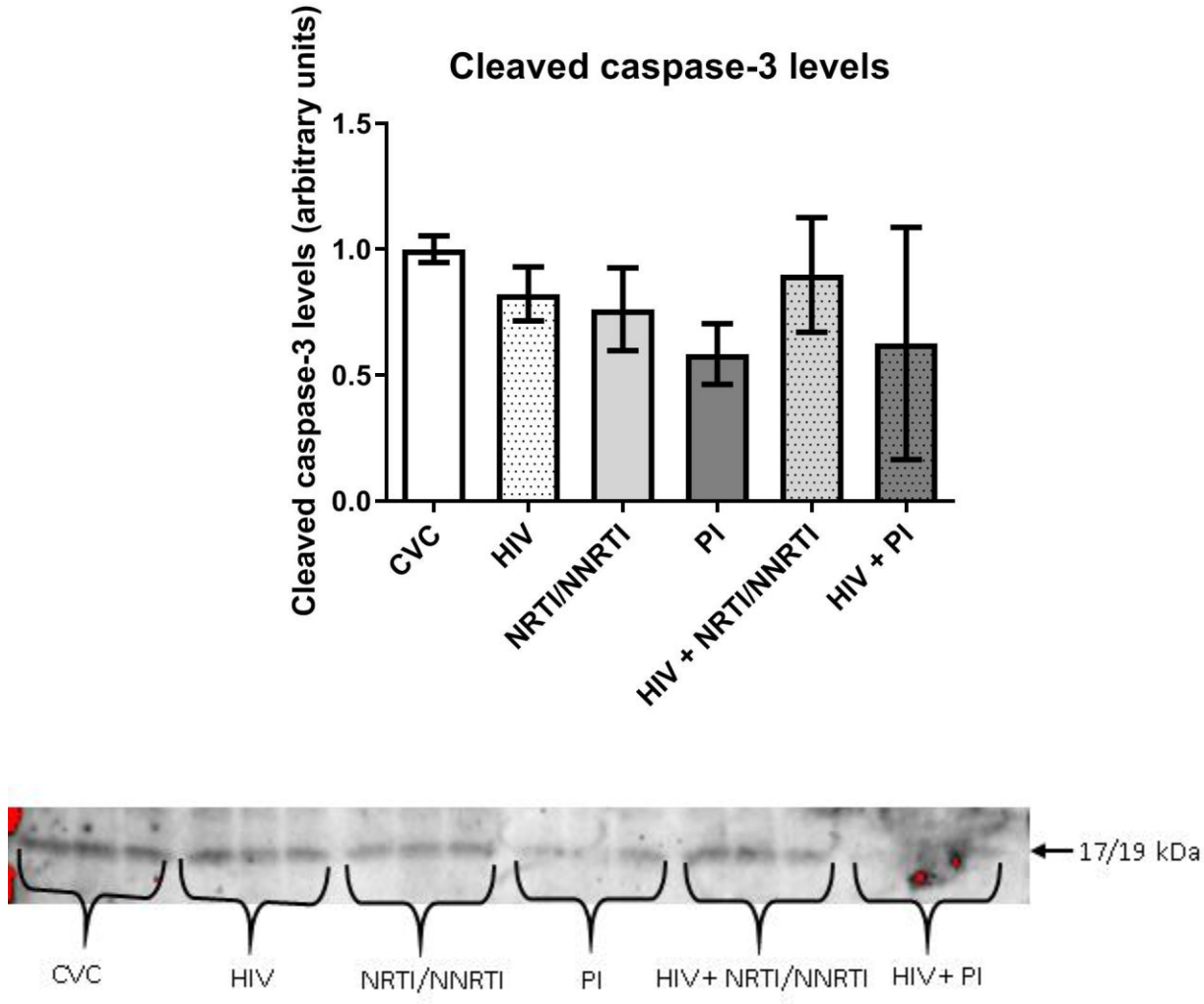

Figure 3.21: Cleaved Caspase-3 after 24 hours. CVC: Combined vehicle control; HIV: HIV-protein cocktail; NRTI/NNRTI: nucleoside analogue reverse transcriptase inhibitors/non-nucleoside reverse transcriptase inhibitors; PI: protease inhibitors. Arbitrary units: pixel counts depicted here as ratios relative to the CVC, which was expressed as 1. n=3/group, except HIV + PI, where n=2.

3.4.4 Nitrosative Stress

Nitrotyrosine

None of the interventions had any effects on nitrotyrosine levels. An ordinary one-way ANOVA with Tukey's multiple comparisons test was performed.

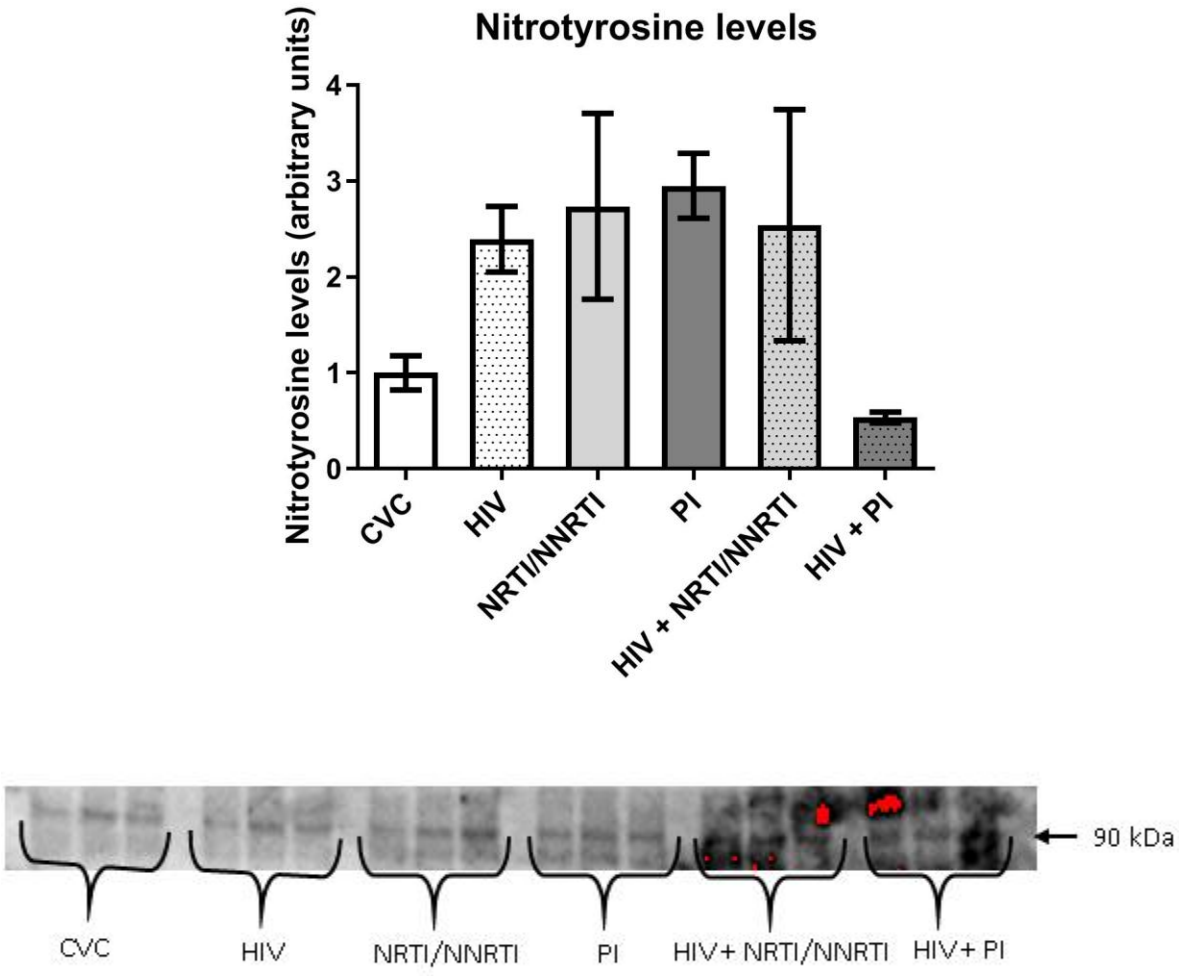

Figure 3.22: Nitrotyrosine levels after 24 hours. CVC: Combined vehicle control; HIV: HIV-protein cocktail; NRTI/NNRTI: nucleoside analogue reverse transcriptase inhibitors/non-nucleoside reverse transcriptase inhibitors; PI: protease inhibitors. Arbitrary units: pixel counts depicted here as ratios relative to the CVC, which was expressed as 1. n=3/group, except HIV + NRTI/NNRTI and HIV + PI, where n=2.

3.4.5 Oxidative Stress

p22phox

None of the interventions had any effects on p22phox levels. An ordinary one-way ANOVA with Tukey's multiple comparisons test was performed.

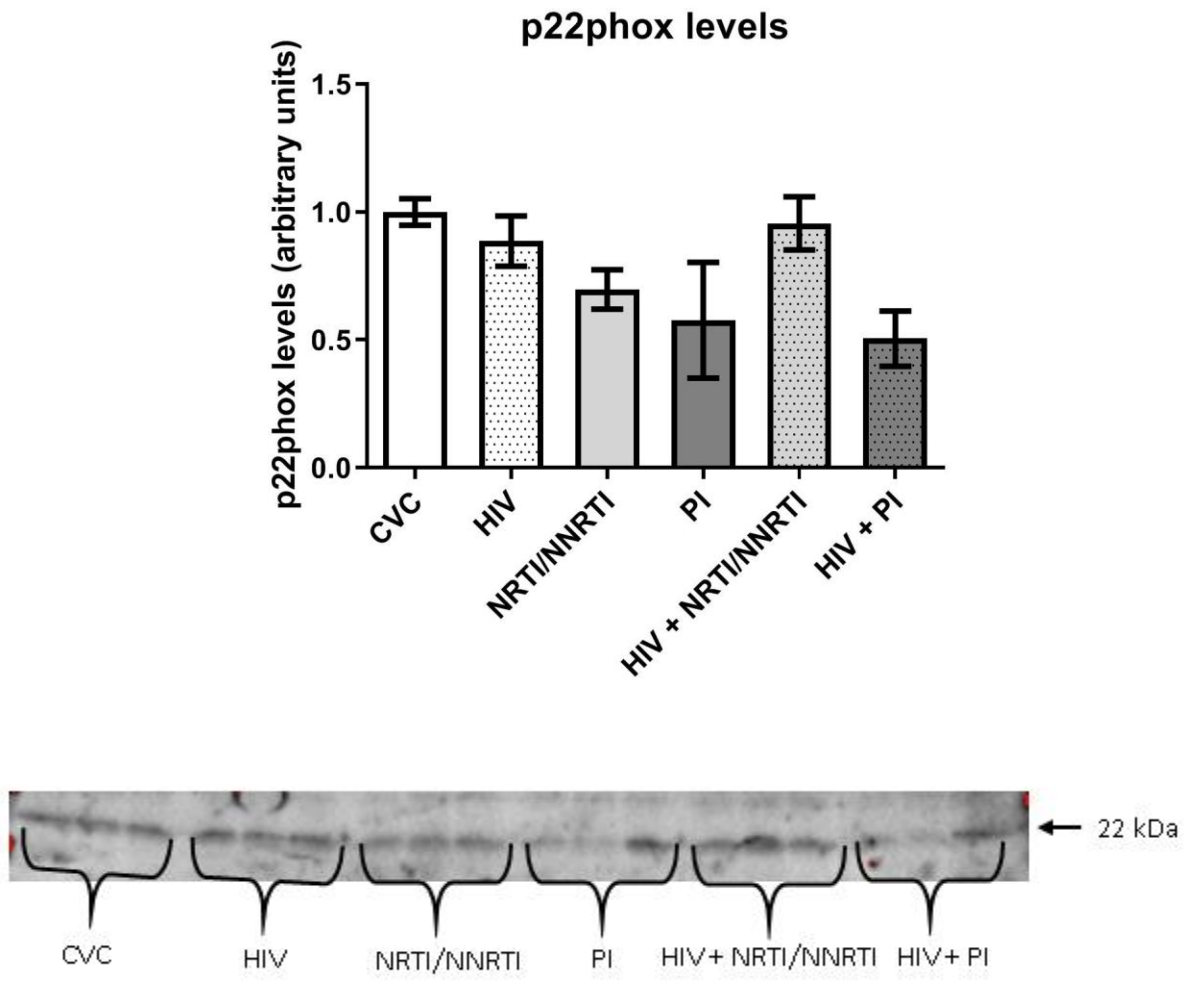

Figure 3.23: p22phox levels after 24 hours. CVC: Combined vehicle control; HIV: HIV-protein cocktail; NRTI/NNRTI: nucleoside analogue reverse transcriptase inhibitors/non-nucleoside reverse transcriptase inhibitors; PI: protease inhibitors. Arbitrary units: pixel counts depicted here as ratios relative to the CVC, which was expressed as 1. n=3/group.

CHAPTER 4: DISCUSSION AND CONCLUSION

What follows is a general discussion of all the results of this study, commencing with the time- and concentration-response investigations and thereafter, the vascular signalling protein analyses. This is succeeded by a summary of the primary findings, integrating the results from the various experimental procedures and finally leading up to the conclusion. It is worth mentioning that literature searches yielded no evidence of previous studies investigating the combined effects of HIV-1-proteins and antiretroviral drugs on endothelial cells in an *in vitro* setting, which, whilst adding novelty to the results, makes contextualisation difficult.

4.1 GENERAL DISCUSSION

4.1.1 Time- and Concentration-Response Investigations

HIV-1-Protein Medium

Table 4.1: Summary of HIV-1-protein medium time- and concentration-response investigation results

	25 ng/ml	50 ng/ml	100 ng/ml
24 hours of HIV-1-protein exposure			
Non-viable cells (Propidium Iodide probe)	-	-	-
NO production (DAF-2/DA probe)	-	-	↓ *vs.* Control
Nitrosative stress (DHR-123 probe)	-	-	-
48 hours of HIV-1-protein exposure			
Non-viable cells (Propidium Iodide probe)	-	-	↑ *vs.* 25 ng/ml
NO production (DAF-2/DA probe)	-	-	-
Nitrosative stress (DHR-123 probe)	-	-	-

25 ng/ml, 50 ng/ml or 100 ng/ml of Tat, Gp160 and Nef were added to endothelial growth medium and the effects on cell viability, NO production and nitrosative stress assessed.

Exposure to 100 ng/ml of HIV-1 Nef, Tat and Gp160 (Gp120 + Gp41) for 24 hours led to a significant decrease in NO production in AECs **(Figure 3.2)**, with no effect on nitrosative stress or cell viability. NO levels seemed to normalise with 48 hours of HIV-1 protein exposure, with no significant differences between treatment and control groups. A slight increase in non-viable cells was observed for 48 hours of

100 ng/ml of HIV-1 protein treatment, however only compared to the 25 ng/ml group and not the control **(Figure 3.4).** The reduction in NO observed after 24 hours of HIV-1 protein exposure is corroborated by other studies of a similar nature. Human coronary artery endothelial cells pre-treated with TNF-α and then exposed to 1 µg/ml of Gp120 for 16 hours showed a significant reduction in NO levels (Jiang *et al.*, 2010). Similarly, in human pulmonary artery endothelial cells treated with 10 ng/ml or 50 ng/ml of Nef, NO production was reduced in a concentration-dependent manner (Duffy *et al.*, 2009). However, neither of the aforementioned studies investigated NO production in endothelial cells exposed to more than 24 hours of HIV-1 proteins, making it difficult to contextualise the 48-hour results. A possible explanation for the normalisation of the NO levels observed in this experimental group is that the initial reduction was transient in nature with cellular adaptive mechanisms coming into play over time; however, more research is needed to substantiate this observation. Most reviewers have attributed reductions in endothelial NO bioavailability to increased oxidative stress (Higashi *et al.*, 2009; Förstermann and Sessa, 2012; Maron and Michel, 2012; Mudau *et al.*, 2012), via the inactivation of NO by its reaction with superoxide (O_2^-), a potent ROS, turning it into peroxynitrite, as well as the uncoupling of eNOS, rendering the enzyme dysfunctional (Förstermann and Sessa, 2012; Mudau *et al.*, 2012). Contrary to expectation, no changes were observed in the levels of nitrosative stress as assessed by DHR-123, which detects increases in peroxynitrite and thus potential increases in O_2^- and by extension oxidative stress. In contrast, most other researchers have noted increases in ROS and oxidative stress associated with HIV-1-proteins. Duffy *et al.* (2009) found that the decreased NO they observed was linked to increased superoxide (O_2^-). In other studies HIV-1-proteins were also linked to oxidative stress. In rat brain endothelial cells, exposure to 1 µg of Tat and 1 µg or 2 µg of Gp120 for 2 hours resulted in an increase in oxidative stress (Price *et al.*, 2005) and in human pulmonary artery endothelial cells exposure to different concentrations of Tat (100, 250 and 500 ng/ml) for 1 hour all resulted in significant increases in ROS (Liu *et al.*, 2005). However, for this thesis O_2^- and other ROS production were not assessed directly. Only nitrosative stress was considered, specifically peroxynitrite detection by DHR-123, and since this product is not produced by cells directly, but via the reaction of NO with O_2^-, one could speculate that cellular antioxidant defences, such as superoxide dismutase, could possibly have counteracted slight increases in O_2^-, causing its detection to be missed. A further possibility with regards to the discrepancy is the differences in the concentrations of HIV-1 proteins utilised. Most researchers exposed cells to a higher concentration of HIV-1 proteins compared to what was used for the present study (Liu *et al.*, 2005; Price *et al.*, 2005; Jiang *et al.*, 2010). Other researchers have reported increases in markers of apoptosis upon the exposure of endothelial cells to HIV-1 proteins for 12 or 24 hours (Park *et al.*, 2001; Wang *et al.*, 2014). For this thesis only a slight increase in non-viable cells was noted after 48 hours of HIV-1 protein exposure. However, Park *et al.* (2001) and Wang *et al.* (2014) looked at specific markers of apoptosis only, including DNA fragmentation, while the propidium iodide probe used here detects loss of cell membrane integrity as found in necrosis, which could explain why decreases in cell viability were only noted at 48 hours, when the HIV-1 proteins could have caused more severe cell damage.

Antiretroviral Drug Treatment

Table 4.2 Summary of ART treatment concentration-response investigation results

	Half Dose (HD)	Single Dose (SD)	Double Dose (DD)
NRTI/NNRTI treatment in HIV-1-protein medium			
Non-viable cells (Propidium Iodide probe)	-	-	↑ *vs.* HD & SD
NO production (DAF-2/DA probe)	-	-	-
Nitrosative stress (DHR-123 probe)	↓ *vs.* Control	↓ *vs.* Control	↓ *vs.* Control
PI treatment in HIV-1-protein medium			
Non-viable cells (Propidium Iodide probe)	-	-	↑ *vs.* HD & SD
NO production (DAF-2/DA probe)	-	↓ *vs.* Control & HD	↓ *vs.* Control, HD & SD
Nitrosative stress (DHR-123 probe)	-	-	-

Different dosages of NRTI/NNRTI (efavirenz, tenofovir and emtricitabine) or PI (lopinavir and ritonavir) antiretroviral drugs were added to HIV-1-protein medium (containing 100 ng/ml each of Tat, Gp160 and Nef) and the effects on cell viability, NO production and nitrosative stress assessed. HD: half dose; SD: single dose; DD: double dose.

NRTI/NNRTI treatment within an HIV-1-protein medium environment for 24 hours had no effect on NO production, possibly abrogating the reduced levels observed with HIV-1-protein treatment on its own, although clear conclusions cannot be drawn from these experiments as an HIV-1-protein group was not included due to technical constraints, making this merely a speculation. Furthermore, combined NRTI/NNRTI and HIV-1-protein treatment led to a reduction in nitrosative stress **(Figure 3.9)** and had minimal effects on cell viability, with only the highest concentration of NRTI/NNRTI treatment showing a slight increase in non-viable cells and this was not compared to the control **(Figure 3.7).** Of the three drugs in the NRTI/NNRTI cocktail, efavirenz has mostly been implicated in having detrimental endothelial consequences. In a transformed human umbilical vein endothelial cell line, 24 hours of efavirenz treatment negatively impacted cell viability in a concentration dependent manner. It also resulted in a concentration-dependent increase in apoptosis and necrosis. In contrast, tenofovir and emtricitabine had no effects (Faltz *et al.*, 2017). In another study utilising the same cell line, efavirenz induced a gradual decrease in cell viability over 72 hours of treatment (Weiß *et al.*, 2016). Efavirenz has also been linked to increased ROS production and oxidative stress in endothelial cells by a number of researchers (Jamaluddin *et al.*, 2010; Weiß *et al.*, 2016; Faltz *et al.*, 2017). In contrast, tenofovir did not increase apoptotic or oxidative stress gene expression in human coronary artery endothelial cells (Kim *et al.*, 2011). Some of the abovementioned results are contradictory to what was found by the present thesis. A possible explanation for this discrepancy is that while most researchers investigated these drugs in isolation, an NRTI/NNRTI cocktail was utilised in this case, making it conceivable that tenofovir and emtricitabine, drugs that have not been linked to negative endothelial consequences, counteracted the

detrimental effects of efavirenz. Furthermore, protocol differences with regards to exposure time and concentrations could also have had an impact. It is additionally worth reiterating that the investigations were conducted within an HIV-1 protein environment, which was not the case in most of the available literature.

PI treatment within an HIV-1-protein medium environment for 24 hours resulted in a reduction in NO production in a concentration-dependent manner **(Figure 3.11)**. Furthermore, the HIV-1 + PI combination treatment had no effect on nitrosative stress and had minimal consequences for cell viability, with only the highest concentration of PI treatment showing a slight increase in non-viable cells, and not compared to the control **(Figure 3.10)**. In human coronary artery endothelial cells exposed to 20 days of clinically relevant concentrations of lopinavir boosted with ritonavir, Auclair *et al.* (2014) showed that NO levels were significantly reduced and that this reduction was linked to oxidative stress. In human pulmonary artery endothelial cells, 24 hours of ritonavir treatment caused a significant increase in O_2^- production (Wang *et al.*, 2009). In the present study, an increase in nitrosative stress was not noted via DHR-123, and as described before, by extension O_2^- production and oxidative stress. However, Wang *et al.* (2009) assessed O_2^- production directly, whereas here it was measured indirectly via peroxynitrite formation and thus, as mentioned before, it is possible that cellular antioxidant defences could have mitigated these effects. Auclair *et al.*, (2014) also assessed oxidative stress more indirectly, but using different markers. Interestingly, none of the papers found investigating the endothelial consequences of lopinavir and/or ritonavir treatment reported on their effects on cell viability.

4.1.2. Vascular signalling proteins

Table 4.3: Summary of vascular signalling protein investigation results

	HIV-protein medium	NRTI/ NNRTI treatment	PI treatment	NRTI/NNRTI treatment in HIV-protein medium	PI treatment in HIV-protein medium
Total eNOS	-	-	-	-	↓ *vs.* Control, PI & HIV
Phospho eNOS	-	-	-	-	-
Total PKB/Akt	↓ *vs.* Control	↓ *vs.* Control	↓ *vs.* Control	↓ *vs.* Control	↓ *vs.* Control & HIV
Phospho PKB/Akt	-	-	-	-	-
IκBα	-	-	-	-	↓ *vs.* Control, HIV & HIV + NRTI/NNRTI
Nitrotyrosine	-	-	-	-	-
p22phox	-	-	-	-	-
Cleaved caspase-3	-	-	-	-	-
Cleaved-PARP	-	↓ *vs.* Control	-	-	↓ *vs.* Control

eNOS and PKB/Akt

Total eNOS expression was significantly reduced in AECs only when exposed to combined HIV-1-protein and PI treatment for 24 hours, with no effects on the phosphorylation of this protein **(Figure 3.17)**. Interestingly the expression of PKB/Akt, an upstream activator of eNOS, was reduced in all groups, but especially in the combined HIV-1-protein and PI treatment group. No effects were observed on PKB/Akt phosphorylation **(Figure 3.18)**. It would appear that no other studies have assessed the effects of NRTI/NNRTIs or PIs on endothelial cells within an HIV-1-protein microenvironment. However, in isolation, both HIV-1-proteins and PI drugs have been shown to reduce eNOS expression (Duffy *et al.*, 2009; Wang *et al.*, 2009; Jiang *et al.*, 2010; Auclair *et al.*, 2014). With regards to NRTI/NNRTI treatment, the results of this thesis do correspond with Weiß *et al.* (2016), where pharmacologically relevant concentrations of efavirenz were shown to have no effect on eNOS expression. Most of the literature focussed on eNOS expression while not reporting on its phosphorylation or on the expression/phosphorylation of PKB/Akt, making it difficult to contextualise findings. When speculating with regards to possible explanations for the observed decreases in PKB/Akt expression with unaffected eNOS phosphorylation for the HIV-1-protein, NRTI/NNRTI, PI and combined HIV-1-protein and NRTI/NNRTI treatment groups, it is worth noting that PKB/Akt is only one of several kinases responsible for the activation of eNOS by its phosphorylation at serine 1177 (Förstermann and Sessa, 2012) and thus reductions in PKB/Akt expression would not necessarily lead observable decreases in eNOS phosphorylation. Another possible explanation as to why changes in the phosphorylation of PKB/Akt and eNOS was not noted, is that phosphorylation usually constitutes an immediate form of protein activation, while changes in the transcription levels of a protein generally take longer. Here, the phosphorylation status of these proteins was only assessed at one time-period (after 24 hours of HIV-1-protien and/ or antiretroviral drug exposure) and thus more immediate changes could have been missed.

IκBα

PI treatment within an HIV-1-protein environment led to a significant reduction in IκBα levels **(Figure 3.19)**. IκBα forms part of the canonical NFκB activation pathway where it acts as an inhibitor of NFκB. The proteolysis of IκBα results in the nuclear translocation of NFκB from the cytosol leading to the transcription of various inflammatory genes (Brasier, 2010). A reduction in cellular IκBα levels would thus be indicative of inflammation. Augmented NFκB signalling in response to HIV-1 proteins as well as PI treatment has been reported in a number of *in vitro* endothelial studies (Liu *et al.*, 2005; Duan *et al.*, 2013; Auclair *et al.*, 2014; Wang *et al.*, 2014). In human coronary artery endothelial cells, lopinavir boosted with ritonavir (LPV/r) markedly increased RelA/p65 (a subunit of NFκB) phosphorylation (Auclair *et al.*, 2014). However, this was on the serine 536 residue, which is thought to act independently of the IκBα canonical pathway (Sasaki *et al.*, 2005; Brasier, 2010). Furthermore, it was observed without HIV-1-protein co-treatment, whereas, in the present study, a significant reduction in IκBα was only noted with combined HIV-1-protein and PI treatment. Furthermore, cells were exposed to LPV/r treatment for a much longer period (20 days) compared to the protocol followed here, possibly accounting for this difference. HIV-1

Tat protein treatment of human umbilical vein endothelial cells was shown to induce the nuclear translocation of NFκB-RelA/p65 in a time-dependent manner (Duan *et al.*, 2013), similarly, in human pulmonary artery endothelial cells, Tat treatment increased NFκB transcriptional activity, and this also appeared to be time-dependent (Liu *et al.*, 2005). However, in the study by Liu *et al.* a much higher concentration of recombinant Tat was used (250 ng/ml) compared to this protocol, possibly accounting for the reason no IκBα effects were detected for the HIV-1-protein treatment in isolation. HIV-1 Nef has been shown to induce the production of the inflammatory mediator, monocyte chemoattractant protein-1 (MCP-1), in an NFκB dependent manner (Wang *et al.*, 2014).

Nitrotyrosine and p22phox

Contrary to expectation no changes in the levels of nitrotyrosine (indicative of peroxynitrite and nitrosative stress) or p22phox (indicative of oxidative stress) were observed. Other researchers however, have reported increases in oxidative stress and ROS in endothelial cells exposed to HIV-1-proteins (Liu *et al.*, 2005; Price *et al.*, 2005) as well as efavirenz (Jamaluddin *et al.*, 2010; Weiß *et al.*, 2016; Faltz *et al.*, 2017) and lopinavir and/or ritonavir (Wang *et al.*, 2009; Auclair *et al.*, 2014). In the present study O_2^{-} and other ROS production were not assessed directly and only one protein marker of oxidative stress, namely p22phox, was measured, creating the possibility that oxidative stress could have been overlooked. Furthermore, none of the abovementioned studies assessed levels of p22phox, making true comparisons impossible. Observations with regards to nitrotyrosine levels correspond with the fluorescence-based assay results, where no increases in nitrosative stress were observed, as assessed by DHR-123 – a probe which detects peroxynitrite, the molecule primarily responsible for the nitration of the amino acid tyrosine and the consequent formation of nitrotyrosine (Duncan, 2003). However, no endothelial cell research within the framework of HIV and ART effects on markers of nitrosative stress was found, making it difficult to contextualise findings.

Cleaved caspase-3 and cleaved-PARP

No changes in the levels of cleaved caspase-3 were noted, while significant decreases in the levels of cleaved-PARP were observed for the NRTI/NNRTI treatment group as well as the combined HIV-1-protein and PI treatment group **(Figure 3.20)**. These results did not corroborate those reported in the literature. Faltz *et al.* (2017) showed that efavirenz time- and concentration- dependently increased PARP activity, while tenofovir and emtricitabine did not. In a study by Weiß *et al.* (2016), efavirenz induced slight PARP cleavage, but only at high drug concentrations. A possible reason for the discrepancy between the results of the present study and those reported in the literature, is that the levels of cleaved PARP were assessed only at one time period (24 hours) and for a single dosage of NTRI/NNRTI drugs. It is also possible, as mentioned before, that the tenofovir and emtricitabine components of the NRTI/NNRTI cocktail used mitigated the effects of efavirenz. While no changes in the levels of cleaved-PARP and cleaved caspase-3 were observed in AECs exposed to HIV-1-proteins here, some researchers did. Park *et al.* (2001) report that the induction of apoptosis by PARP-cleavage followed Tat exposure for 24 hours

and this was mediated by caspase-3. Unfortunately, literature searches yielded no endothelial cell studies investigating these biomarkers of apoptosis subsequent to lopinavir and/or ritonavir treatment within the context of HIV-1-proteins, making it difficult to interpret the results in this regard.

4.2 Primary Findings

HIV-1 Nef, Tat and Gp160 attenuate eNOS-independent NO production in AECs

Exposure to 100 ng/ml of HIV-1 Nef, Tat and Gp160 for 24 hours led to a significant decrease in NO production in AECs. Yet, this was not accompanied by changes in nitrosative stress or peroxynitrite measurements, or oxidative stress markers, and not associated with reduced eNOS expression or phosphorylation. Decreased NO levels in endothelial cells subsequent to HIV-1-protein exposure has been reported by a number of investigations, however, this finding has generally been associated with reduced eNOS expression and increased oxidative stress (Liu *et al.*, 2005; Price *et al.*, 2005; Duffy *et al.*, 2009; Jiang *et al.*, 2010), warranting further investigations into the cause behind this discrepancy with the results of the present study.

Efavirenz, Tenofovir and Emtricitabine treatment of HIV-1 Nef, Tat and Gp160 exposed AECs have minimal adverse effects, and could possibly even be beneficial.

NRTI/NNRTI treatment within an HIV-1-protein medium environment for 24 hours had no effect on NO production, possibly abrogating the reduced levels observed with HIV-1-protein treatment on its own. However, this is merely speculation due to the absence of an HIV-1-protein group for these experiments. eNOS expression was also unaffected. Furthermore, reductions in nitrosative stress was noted and no indications of apoptosis. While efavirenz on its own has been linked to detrimental endothelial cell consequences, mostly in terms of increased ROS/oxidative stress and apoptosis, tenofovir and emtricitabine have not (Jamaluddin *et al.*, 2010; Kim *et al.*, 2011; Weiß *et al.*, 2016; Faltz *et al.*, 2017), creating the possibility that in cocktail form, the adverse effects of efavirenz are counteracted, perhaps explaining why this decrease in nitrosative stress levels was observed and no evidence of apoptosis induction found. Furthermore, combined efavirenz, tenofovir and emtricitabine treatment could possibly be beneficial to endothelial cells exposed to HIV-1-proteins, as the proteins' detrimental effects on NO production were potentially mitigated. However, since no studies have investigated the combined effects of efavirenz, tenofovir and emtricitabine treatment in an HIV-1-protein environment on endothelial cells, further investigation is needed to support this speculation.

The interaction between Lopinavir/Ritonavir treatment and HIV-1 Nef, Tat and Gp160 result in a downregulation of the eNOS-NO biosynthesis pathway in AECs.

PI treatment within an HIV-1-protein medium environment for 24 hours resulted in a reduction in NO production in a concentration-dependent manner, probably due to decreased total eNOS expression.

Interestingly, neither HIV-1 protein exposure on its own, nor PI treatment in isolation had any effects on eNOS, while, in combination, they seemed to interact, causing a significant reduction in the expression of this enzyme. In endothelial cells, decreased NO levels and eNOS expression have been associated with HIV-1-proteins on their own (Duffy *et al.*, 2009; Jiang *et al.*, 2010) as well as with lopinavir/ritonavir treatment in isolation (Wang *et al.*, 2009; Auclair *et al.*, 2014), however, no studies have investigated the endothelial effects of lopinavir/ritonavir treatment in an HIV-1-protein environment, making the findings of the present study novel in this regard. Nevertheless, more research is needed into the mechanisms involved, as increases in oxidative or nitrosative stress were not detected and this is generally accepted to be the pathophysiological process responsible for reduced NO and eNOS in endothelial cells (Higashi *et al.*, 2009; Förstermann and Sessa, 2012; Maron and Michel, 2012; Mudau *et al.*, 2012).

The interaction between Lopinavir/Ritonavir treatment and HIV-1 Nef, Tat and Gp160 result in increased inflammatory NFκB signalling and possibly accounts for the downregulation of eNOS expression in AECs

PI treatment within an HIV-1-protein environment led to a significant reduction in IκBα levels (indicative of increased NFκB signalling and inflammation), while neither HIV-1-protein treatment on its own nor PI treatment in isolation had any significant effects. Increased NFκB signalling in response to HIV-1 proteins as well as PI treatment has been reported in a number of endothelial cell studies (Liu *et al.*, 2005; Duan *et al.*, 2013; Auclair *et al.*, 2014; Wang *et al.*, 2014), yet, these investigations assessed at the effects of either individual HIV-1-proteins or PI drugs in isolation. Furthermore, Lee *et al.* (2014) implicated NFκB in the negative regulation of eNOS expression in human umbilical vein endothelial cells, via microRNA miR-155. MicroRNAs are involved in regulating protein expression by targeting mRNAs for cleavage or translational repression (Bartel, 2004) and the possibility therefore arises that a similar mechanism was responsible for the reduced eNOS expression observed in the HIV-1 + PI group **(Figure 4.1)**. However, more research is needed to substantiate this speculation. Additionally, no endothelial cell studies investigating NFκB signalling within a combined HIV-1-protein and PI treatment setting were found, highlighting the importance of the current work as well as emphasising the need for more research into this particular aspect of the HIV-ART-endothelial dysfunction interplay.

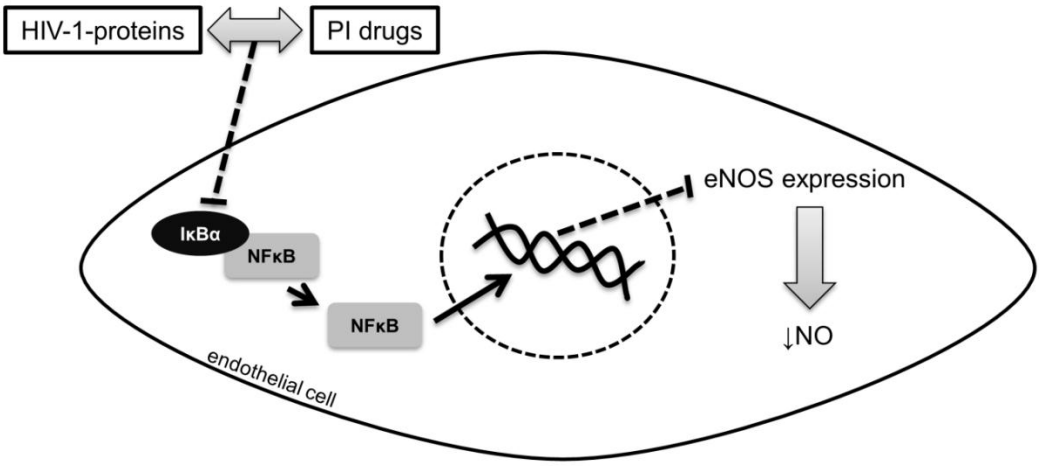

Figure 4.1: Proposed mechanism of eNOS-NO downregulation in response to combined HIV-1-protein and PI drug treatment in endothelial cells. The interaction between the HIV-1-proteins Nef, Tat and Gp160 and PI drugs lopinavir and ritonavir result in decreased IκBα levels. IκBα is an inhibitor of NFκB and its downregulation results in the increased nuclear translocation of NFκB, augmenting pro-inflammatory transcriptional activity. This has been linked to decreased eNOS expression, via post-translational modifications mediated by microRNAs. PI: protease inhibitor; eNOS: endothelial nitric oxide synthase; NO: nitric oxide; NFκB: nuclear factor kappa-B; IκBα: nuclear factor kappa-B inhibitor alpha.

4.3 CONCLUSION

HIV-1 Nef, Tat and Gp160 attenuate NO production in endothelial cells, while efavirenz, tenofovir and emtricitabine treatment within this HIV-1 protein environment have minimal adverse effects. On the other hand, lopinavir and ritonavir treatment seemed to interact with these HIV-1 proteins resulting in a downregulation of the eNOS-NO biosynthesis pathway. This interaction was also observed for the inflammatory NFκB signalling pathway, which appeared to be upregulated, and possibly provides an explanation for the downregulation of eNOS expression detected. There is a paucity in the literature on the endothelial effects of combined HIV-1-protein and antiretroviral drugs, which given the evidence of interaction with regards to PIs, is problematic, especially since it is in this combined context that the endothelium of people living with HIV/AIDS and who are on PI-containing ART, may be affected. This emphasises the novelty of these findings, which may serve as a basis for future investigations into the HIV-1-PI interaction exposed by this thesis and additionally lead to an elucidation of the mechanisms involved and thus potentially aid in tailoring treatment for the growing population of people living with HIV/AIDS and who are also at increased cardiovascular risk.

CHAPTER 5: LIMITATIONS, RESEARCH OUTPUTS AND FUTURE DIRECTIONS

5.1 LIMITATIONS

- Time- and financial constraints meant that experiments could not be repeated to confirm or refute unexpected results, and prevented the inclusion of additional experimental groups investigating the individual drug components separately.
- Technical constraints, due to the size of the 24-well plates used for the plate-reader analyses, meant that an HIV-1-protein group could not be included in the antiretroviral drug concentration response investigations, making it difficult to draw any clear conclusions from these results.
- Low protein content of AECs furthermore meant that certain experimental groups could not be used for western blotting and thus reduced the final n-value of the vascular signalling protein analysis part of our study from five to three.
- Only one time-point was chosen for the signalling protein western blot analyses; if time and finances allowed, more and earlier time-points could have been included to assess whether changes in the phosphorylation of signalling proteins (especially eNOS) were not missed.

5.2 RESEARCH OUTPUTS ASSOCIATED WITH THIS STUDY

Peer-reviewed publication

- **Review article: Marincowitz, C.** *et. al.* (2018) 'Vascular endothelial dysfunction in the wake of HIV and ART', *The FEBS Journal.* doi: 10.1111/febs.14657. *(View in Appendix A).*

Peer-reviewed conference abstracts

- **National conference: Marincowitz, C.**, Strijdom, H., Charania, S. and Genis, A. 'The effects of HIV-1 proteins and antiretroviral therapy on aortic endothelial cells (AECs) – a mechanistic *in vitro* approach'. First Conference of Biomedical and Natural Sciences and Therapeutics (CoBNeST), Spier Estate, Stellenbosch, 7 – 10 October 2018.
- **International conference with published abstract:** Genis, A., Ogundipe, T. P., **Marincowitz, C.**, Strijdom, H. 'Investigating endothelial dysfunction as a pathophysiological consequence of HIV-infection and anti-retroviral treatment'. 2018/4/1. Journal Cardiovascular Research, 114, suppl_1, pages S43.

Other conference proceedings

- **University Research Day: Marincowitz, C.**, Strijdom, H., Charania, S. and Genis, A. 'The effects of HIV-1 proteins and antiretroviral therapy on aortic endothelial cells (AECs) – a mechanistic *in vitro* approach'. Department of Biomedical Sciences Annual Research Day, Stellenbosch University, Tygerberg Campus, 21 November 2018. *(Received first prize for an oral presentation).*

5.3 Future Directions

- To the best of our knowledge, this is the only study investigating the endothelial effects of common antiretroviral drugs within a simulated HIV-1-protein microenvironment. Thus, given the fact that we observed evidence of interaction between HIV-1-proteins and PI antiretroviral drugs (with regards to eNOS expression and inflammatory NFκB signalling), more research is needed to elucidate the mechanisms involved.
- Given differences observed between our research and other similar studies, especially with regards to apoptosis and oxidative stress measures, we would recommend that more research, utilising different markers as well as incorporating additional concentrations and time-periods, be conducted to investigate these discrepancies. Also, the addition of individual drug component experiments will assist in understanding how the combined drug cocktail effects differ from the individual drugs in isolation.
- While previous work in our laboratory indicated that one fully confluent 100 mm petri dish of cultured AECs yielded sufficient protein for one lysate, we found that this was not the case. Thus, for future similar investigations, we would recommend using two 100 mm petri dishes per lysate to ensure higher protein content and better blots.

REFERENCES

Acheampong, E. *et al.* (2002) 'Ethanol strongly potentiates apoptosis induced by HIV-1 proteins in primary human brain microvascular endothelial cells', *Virology*, 304(2), pp. 222–234. doi: 10.1006/viro.2002.1666.

AIDS info (2018) *Glossary of HIV/AIDS-related terms*. 9th Editio. Rockville: AIDS info. Available at: https://aidsinfo.nih.gov/contentfiles/glossaryhivrelatedterms_english.pdf.

Al-Dakkak, I. *et al.* (2013) 'The impact of specific HIV treatment-related adverse events on adherence to antiretroviral therapy: A systematic review and meta-analysis', *AIDS Care - Psychological and Socio-Medical Aspects of AIDS/HIV*, 25(4), pp. 400–414. doi: 10.1080/09540121.2012.712667.

Andras, I. E. *et al.* (2003) 'HIV-1 Tat protein alters tight tunction protein expression and distribution in cultured brain endothelial cells', *Journal of Neuroscience Research*, 74(2), pp. 255–265. doi: 10.1002/jnr.10762.

Angkurawaranon, C. *et al.* (2016) 'Ecological study of HIV infection and hypertension in sub-Saharan Africa: Is there a double burden of disease?', *PLoS ONE*, 11(11), pp. 1–11. doi: 10.1371/journal.pone.0166375.

Arts, E. J. and Hazuda, D. J. (2012) 'HIV-1 antiretroviral drug therapy', *Cold Spring Harbor Perspectives in Medicine*, 2, p. a007161. doi: 10.1101/cshperspect.a007161.

Auclair, M. *et al.* (2014) 'Impact of darunavir, atazanavir and lopinavir boosted with ritonavir on cultured human endothelial cells: Beneficial effect of pravastatin', *Antiviral Therapy*, 19(8), pp. 773–782. doi: 10.3851/IMP2752.

Baker, J. V. *et al.* (2012) 'HIV replication, inflammation, and the effect of starting antiretroviral therapy on plasma asymmetric dimethylarginine, a novel marker of endothelial dysfunction', *Journal of Acquired Immune Deficiency Syndromes*, 60(2), pp. 128–134. doi: 10.1097/QAI.0b013e318252f99f.

Barquera, S. *et al.* (2015) 'Global overview of the epidemiology of atherosclerotic cardiovascular disease', *Archives of Medical Research*, 46(5), pp. 328–338. doi: 10.1016/j.arcmed.2015.06.006.

Bartel, D. P. (2004) 'MicroRNAs: genomics, biogenesis, mechanism, and function', *Cell*, 116(2), pp. 281–297. doi: 10.1016/S0092-8674(04)00045-5.

Bazzano, L. A. *et al.* (2014) 'Effects of low-carbohydrate and low-fat diets: a randomized trial', *Annals of Internal Medicine*, 161(5), pp. 309–318. doi: 10.7326/M14-0180.

Bertrand, L., Dygert, L. and Toborek, M. (2016) 'Antiretroviral treatment with efavirenz disrupts the blood-

brain barrier integrity and increases stroke severity', *Scientific Reports*. Nature Publishing Group, 6(December), p. 39738. doi: 10.1038/srep39738.

Bertrand, L. and Toborek, M. (2015) 'Dysregulation of endoplasmic reticulum stress and autophagic responses by the antiretroviral drug efavirenz', *Molecular Pharmacology*, 88(2), pp. 304–315. doi: 10.1124/mol.115.098590.

Beyrer, C. *et al.* (2012) 'Global epidemiology of HIV infection in men who have sex with men', *The Lancet*. Elsevier Ltd, 380(9839), pp. 367–377. doi: 10.1016/S0140-6736(12)60821-6.

Borges, Á. H. *et al.* (2015) 'Factors associated with plasma IL-6 levels during HIV infection', *Journal of Infectious Diseases*, 212(4), pp. 585–595. doi: 10.1093/infdis/jiv123.

Bradford, M. M. (1976) 'A rapid and sensitive method for the quantitation of microgram quantities of protein utilizing the principle of protein-dye binding', *Analytical Biochemistry*, 72(1–2), pp. 248–254. doi: 10.1016/0003-2697(76)90527-3.

Brasier, A. R. (2010) 'The nuclear factor- kappa B – interleukin-6 signalling pathway mediating vascular inflammation', *Cardiovascular Research*, 86, pp. 211–218. doi: 10.1093/cvr/cvq076.

Campbell, E. M. and Hope, T. J. (2015) 'HIV-1 capsid: The multifaceted key player in HIV-1 infection', *Nature Reviews Microbiology*. Nature Publishing Group, 13(8), pp. 471–483. doi: 10.1038/nrmicro3503.

Campbell, R. S. F. and Robinson, W. F. (1998) 'The comparative pathology of the lentiviruses', *Journal of Comparative Pathology*. W.B. Saunders, pp. 333–395. doi: 10.1016/S0021-9975(98)80033-9.

Carr, A. and Cooper, D. A. (2000) 'Adverse effects of antiretroviral therapy', *The Lancet*, 356(October), pp. 1423–1430. doi: 10.1016/S0140-6736(00)02854-3.

Chai, H. *et al.* (2005) 'Effects of 5 HIV protease inhibitors on vasomotor function and superoxide anion production in porcine coronary arteries', *Journal of Acquired Immune Deficiency Syndromes*, 40(1), pp. 12–19. doi: 10.1097/01.qai.0000172368.05327.7b.

Cheng, X. W. *et al.* (2013) 'Circulating cathepsin K as a potential novel biomarker of coronary artery disease', *Atherosclerosis*. Elsevier Ltd, 228(1), pp. 211–216. doi: 10.1016/j.atherosclerosis.2013.01.004.

Cihlar, T. and Fordyce, M. (2016) 'Current status and prospects of HIV treatment', *Current Opinion in Virology*. Elsevier B.V., 18, pp. 50–56. doi: 10.1016/j.coviro.2016.03.004.

Crowe, S. M. *et al.* (2010) 'The macrophage: the intersection between HIV infection and atherosclerosis', *Journal of Leukocyte Biology*, 87(4), pp. 589–598. doi: 10.1189/jlb.0809580.

Cui, H. L. *et al.* (2014) 'HIV protein Nef causes dyslipidemia and formation of foam cells in mouse models

of atherosclerosis', *FASEB Journal*, 28(7), pp. 2828–2839. doi: 10.1096/fj.13-246876.

Cunningham, K. S. and Gotlieb, A. I. (2005) 'The role of shear stress in the pathogenesis of atherosclerosis', *Laboratory Investigation*. Nature Publishing Group, pp. 9–23. doi: 10.1038/labinvest.3700215.

Dalal, S. *et al.* (2011) 'Non-communicable diseases in sub-Saharan Africa: What we know now', *International Journal of Epidemiology*, 40(4), pp. 885–901. doi: 10.1093/ije/dyr050.

Davignon, J. and Ganz, P. (2004) 'Role of endothelial dysfunction in atherosclerosis', *Circulation*, 109 [suppl, p. III-27-III-32. doi: 10.1161/01.CIR.0000131515.03336.f8.

Deanfield, J. E., Halcox, J. P. and Rabelink, T. J. (2007) 'Endothelial function and dysfunction: Testing and clinical relevance', *Circulation*, 115(10), pp. 1285–1295. doi: 10.1161/CIRCULATIONAHA.106.652859.

Debaisieux, S. *et al.* (2012) 'The ins and outs of HIV-1 Tat', *Traffic*, pp. 355–363. doi: 10.1111/j.1600-0854.2011.01286.x.

Deeks, S. G. (2011) 'HIV infection, inflammation, immunosenescence, and aging', *Annual Review of Medicine*, 62(1), pp. 141–155. doi: 10.1146/annurev-med-042909-093756.

Dirajlal-Fargo, S. *et al.* (2017) 'HIV-positive youth who are perinatally infected have impaired endothelial function', *Aids*, 31(14), pp. 1917–1924. doi: 10.1097/QAD.0000000000001556.

Duan, M. *et al.* (2013) 'HIV Tat induces expression of ICAM-1 in HUVECs: mplications for miR-221/-222 in HIV-associated cardiomyopathy', *PLoS ONE*, 8(3), pp. 1–11. doi: 10.1371/journal.pone.0060170.

Dubé, M. P. *et al.* (2008) 'No impairment of endothelial function or insulin sensitivity with 4 weeks of the HIV protease inhibitors atazanavir or lopinavir-ritonavir in healthy subjects without HIV Infection: a placebo-controlled trial', *Clinical Infectious Diseases*, 47(4), pp. 567–574. doi: 10.1086/590154.

Duffy, P. *et al.* (2009) 'HIV Nef protein causes endothelial dysfunction in porcine pulmonary arteries and human pulmonary artery endothelial cells', *Journal of Surgical Research*. Elsevier Ltd, 156(2), pp. 257–264. doi: 10.1016/j.jss.2009.02.005.

Duncan, M. W. (2003) 'A review of approaches to the analysis of 3-nitrotyrosine', *Amino Acids*, 25, pp. 351–361. doi: 10.1007/s00726-003-0022-z.

Elmore, S. (2007) 'Apoptosis: a review of programmed cell death', *Toxicologic Pathology*, 35, pp. 495–516. doi: 10.1080/01926230701320337.

Ettehad, D. *et al.* (2016) 'Blood pressure lowering for prevention of cardiovascular disease and death: A

systematic review and meta-analysis', *The Lancet*. Elsevier Ltd, 387(10022), pp. 957–967. doi: 10.1016/S0140-6736(15)01225-8.

Faltz, M. *et al.* (2017) 'Effect of the anti-retroviral drugs efavirenz, tenofovir and emtricitabine on endothelial cell function: role of PARP', *Cardiovascular Toxicology*. Springer US, 17(4), pp. 393–404. doi: 10.1007/s12012-016-9397-4.

Feng, J. Y. *et al.* (2009) 'The triple combination of tenofovir, emtricitabine and efavirenz shows synergistic anti-HIV-1 activity in vitro: A mechanism of action study', *Retrovirology*, 6, pp. 1–16. doi: 10.1186/1742-4690-6-44.

Flint, O. P. *et al.* (2009) 'The role of protease inhibitors in the pathogenesis of HIV-associated lipodystrophy: Cellular mechanisms and clinical implications', *Toxicologic Pathology*, 37(1), pp. 65–77. doi: 10.1177/0192623308327119.

Förstermann, U. and Sessa, W. C. (2012) 'Nitric oxide synthases: Regulation and function', *European Heart Journal*. Oxford University Press, pp. 829–837. doi: 10.1093/eurheartj/ehr304.

Förstermann, U., Xia, N. and Li, H. (2017) 'Roles of vascular oxidative stress and nitric oxide in the pathogenesis of atherosclerosis', *Circulation Research*, 120(4), pp. 713–735. doi: 10.1161/CIRCRESAHA.116.309326.

Foster, G. D. *et al.* (2010) 'Weight and metabolic outcomes after 2 years on a low-carbohydrate versus low-fat diet: a randomized trial', *Annals of Internal Medicine*, 153(3), pp. 147–157. doi: 10.1059/0003-4819-153-3-201008030-00005.

Francisci, D. *et al.* (2009) 'HIV type 1 infection, and not short-term HAART, induces endothelial dysfunction', *Aids*, 23(5), pp. 589–596. doi: 10.1097/QAD.0b013e328325a87c.

Freed, E. O. (2015) 'HIV-1 assembly, release and maturation', *Nature Reviews Microbiology*. Nature Publishing Group, 13(8), pp. 484–496. doi: 10.1038/nrmicro3490.

Furukawa, S. *et al.* (2004) 'Increased oxidative stress in obesity and its impact on metabolic syndrome', *The journal of clinical investigation*, 114(12), pp. 1752–1761. doi: 10.1172/JCI200421625.1752.

Gaudin, R. *et al.* (2013) 'HIV trafficking in host cells: Motors wanted!', *Trends in Cell Biology*, 23(12), pp. 652–662. doi: 10.1016/j.tcb.2013.09.004.

Gerber, H. *et al.* (1998) 'Vascular endothelial growth factor regulates endothelial cell survival through the phosphatidylinositol 3 -kinase / Akt signal', *Journal of Biological Chemistry*, 273(46), pp. 30336–30343.

Gimbrone, M. A. and García-Cardeña, G. (2016) 'Endothelial cell dysfunction and the pathobiology of

atherosclerosis', *Circulation Research*, 118(4), pp. 620–636. doi: 10.1161/CIRCRESAHA.115.306301.

Gleason, R. L. *et al.* (2015) 'Current efavirenz (EFV) or ritonavir-boosted lopinavir (LPV/r) use correlates with elevate markers of atherosclerosis in HIV-infected subjects in Addis Ababa, Ethiopia', *PLoS ONE*, 10(4), p. e0117125. doi: 10.1371/journal.pone.0117125.

Götte, M., Li, X. and Wainberg, M. A. (1999) 'HIV-1 reverse transcription: A brief overview focused on structure- function relationships among molecules involved in initiation of the reaction', *Archives of Biochemistry and Biophysics*, 365(2), pp. 199–210. doi: 10.1006/abbi.1999.1209.

Grigsby, I. F. *et al.* (2010) 'Tenofovir treatment of primary osteoblasts alters gene expression profiles: Implications for bone mineral density loss', *Biochemical and Biophysical Research Communications*. Elsevier Inc., 394(1), pp. 48–53. doi: 10.1016/j.bbrc.2010.02.080.

Guatelli, J. C. (2009) 'Interactions of viral protein U (Vpu) with cellular factors', in Spearman, P. and Freed, E. O. (eds) *Current Topics in Microbiology and Immunology: HIV Interactions with Host Cell Proteins*. Berlin Heidelberg: Springer-Verlag, pp. 27–45. doi: 10.1007/978-3-642-02175-6_2.

Guh, D. P. *et al.* (2009) 'The incidence of co-morbidities related to obesity and overweight: A systematic review and meta-analysis', *BMC Public Health*, 9, pp. 1–20. doi: 10.1186/1471-2458-9-88.

Gürtler A., *et al.* (2013) 'Stain-free technology as a normalization tool in western blot analysis', *Analytical Biochemistry,* 433(2), pp.105-11.

Gupta, S. K. *et al.* (2012) 'Worsening endothelial function with efavirenz compared to protease inhibitors: A 12-month prospective study', *PLoS ONE*, 7(9), pp. 5–10. doi: 10.1371/journal.pone.0045716.

Hackshaw, A. *et al.* (2018) 'Low cigarette consumption and risk of coronary heart disease and stroke: meta-analysis of 141 cohort studies in 55 study reports', *BMJ*, 360, p. j5855. doi: 10.1136/bmj.j5855.

Haissman, J. M. *et al.* (2016) 'Marker of endothelial dysfunction asymmetric dimethylarginine is elevated in HIV infection but not associated with subclinical atherosclerosis', *Journal of Acquired Immune Deficiency Syndromes*, 73(5), pp. 507–513. doi: 10.1097/QAI.0000000000001148.

Hawkins, T. (2010) 'Understanding and managing the adverse effects of antiretroviral therapy', *Antiviral Research*, 85(1), pp. 201–209. doi: 10.1016/j.antiviral.2009.10.016.

Hemelaar, J. *et al.* (2011) 'Global trends in molecular epidemiology of HIV-1 during 2000– 2007', *AIDS (London, England)*, 25(5), pp. 679–689. doi: 10.1097/QAD.0b013e328342ff93.Global.

Henderson, W. W. *et al.* (2004) 'Human immunodeficiency virus (HIV) type 1 Vpu induces the expression of CD40 in endothelial cells and regulates HIV-induced adhesion of B-lymphoma cells.', *Journal of*

virology, 78(9), pp. 4408–4420. doi: 10.1128/JVI.78.9.4408-4420.2004.

Higashi, Y. *et al.* (2009) 'Endothelial function and oxidative stress in cardiovascular diseases', *Circulation Journal*, 73(March), pp. 411–418. doi: JST.JSTAGE/circj/CJ-08-1102 [pii].

Hsieh, H. J. *et al.* (2014) 'Shear-induced endothelial mechanotransduction: The interplay between reactive oxygen species (ROS) and nitric oxide (NO) and the pathophysiological implications', *Journal of Biomedical Science*, 21(1), pp. 1–15. doi: 10.1186/1423-0127-21-3.

Hsue, P. Y. and Waters, D. D. (2018) 'Time to recognize HIV infection as a major cardiovascular risk factor', *Circulation*, 138, pp. 1113–1115. doi: 10.1161/CIRCULATIONAHA.118.036211.

Hubert HB, Feinleib M, McNamara PM, C. W. (1983) 'Obesity as an independent risk factor for cardiovascular disease: a 26-year follow-up of participants in the Framingham Heart Study.', *Circulation*, 67, pp. 968–77. doi: 10.1161/01.CIR.67.5.968.

Hunt, P. W. (2012) 'HIV and inflammation: Mechanisms and consequences', *Current HIV/AIDS Reports*, 9(2), pp. 139–147. doi: 10.1007/s11904-012-0118-8.

Hyle, E. P. *et al.* (2017) 'The association between HIV and atherosclerotic cardiovascular disease in sub-Saharan Africa: A systematic review', *BMC Public Health*. BMC Public Health, 17(1), pp. 1–15. doi: 10.1186/s12889-017-4940-1.

Iantorno, M. *et al.* (2017) 'Coronary artery endothelial dysfunction is present in HIV-positive individuals without significant coronary artery disease', *AIDS*, 31(9), pp. 1281–1289. doi: 10.1097/QAD.0000000000001469.

Insull, W. (2009) 'The pathology of atherosclerosis: Plaque development and plaque responses to medical treatment', *American Journal of Medicine*. Elsevier Inc. Elsevier Inc., 122(1 SUPPL.), pp. S3–S14. doi: 10.1016/j.amjmed.2008.10.013.

Islam, F. M. *et al.* (2012) 'Relative risk of cardiovascular disease among people living with HIV : a systematic review and meta-analysis', *HIV Medicine*, 13, pp. 453–468. doi: 10.1111/j.1468-1293.2012.00996.x.

Jamaluddin, M. S. *et al.* (2010) 'Non-nucleoside reverse transcriptase inhibitor efavirenz increases monolayer permeability of human coronary artery endothelial cells', *Atherosclerosis*, 208(1), pp. 104–111. doi: 10.1016/j.atherosclerosis.2009.07.029.

Jiang, J. *et al.* (2010) 'HIV gp120 induces endothelial dysfunction in tumour necrosis factor-α-activated porcine and human endothelial cells', *Cardiovascular Research*, 87(2), pp. 366–374. doi: 10.1093/cvr/cvq013.

Joseph, P. *et al.* (2017) 'Short-term changes in arterial inflammation predict long-term changes in atherosclerosis progression', *European Journal of Nuclear Medicine and Molecular Imaging*. European Journal of Nuclear Medicine and Molecular Imaging, 44(1), pp. 141–150. doi: 10.1007/s00259-016-3524-0.

Kanmogne, G. D. *et al.* (2007) 'HIV-1 gp120 compromises blood-brain barrier integrity and enhance monocyte migration across blood-brain barrier: Implication for viral neuropathogenesis', *Journal of Cerebral Blood Flow and Metabolism*, 27(1), pp. 123–134. doi: 10.1038/sj.jcbfm.9600330.

Kim, C. *et al.* (2011) 'Abacavir, didanosine and tenofovir do not induce inflammatory, apoptotic or oxidative stress genes in coronary endothelial cells', *Antiviral Therapy*, 16(8), pp. 1335–1339. doi: 10.3851/IMP1891.

Kline, E. R. and Sutliff, R. L. (2008) 'The roles of HIV-1 proteins and antiretroviral drug therapy in HIV-1-associated endothelial dysfunction', *Journal of Investigative Medicine*, 56(5), pp. 752–769. doi: 10.1097/JIM.0b013e3181788d15.

Knowles, R. G. and Moncada, S. (1994) 'Nitric oxide synthases in mammals', *Biochemical Journal*, 258, pp. 249–258.

Kojima, H. *et al.* (1998) 'Detection and imaging of nitric oxide with novel fluorescent indicators: diaminofluoresceins', *Analytical Chemistry*, 70(13), pp. 2446–2453. doi: 10.1021/ac9801723.

Kranzer, K. and Ford, N. (2011) 'Unstructured treatment interruption of antiretroviral therapy in clinical practice: A systematic review', *Tropical Medicine and International Health*, 16(10), pp. 1297–1313. doi: 10.1111/j.1365-3156.2011.02828.x.

Laemmli, U. K. (1970) 'Cleavage of structural proteins during the assembly of the head of bacteriophage T4', *Nature*, 227(5259), pp. 680–685. doi: 10.1038/227680a0.

Lambert, C. T. *et al.* (2016) 'HIV , highly active antiretroviral therapy and the heart : a cellular to epidemiological review', *HIV*, 17, pp. 411–424. doi: 10.1111/hiv.12346.

Lee, J. J. *et al.* (2016) 'Association of changes in abdominal fat quantity and quality with incident cardiovascular disease risk factors', *Journal of the American College of Cardiology*, 68(14), pp. 1509–1521. doi: 10.1016/j.jacc.2016.06.067.

Lee, K. *et al.* (2014) 'Functional role of NF-kB in expression of human endothelial nitric oxide synthase', *Biochemical and Biophysical Research Communications*. Elsevier Inc., 448, pp. 101–107. doi: 10.1016/j.bbrc.2014.04.079.

Li, H., Horke, S. and Förstermann, U. (2013) 'Oxidative stress in vascular disease and its

pharmacological prevention', *Trends in Pharmacological Sciences*. Elsevier Current Trends, pp. 313–319. doi: 10.1016/j.tips.2013.03.007.

Li, L. *et al.* (2005) 'Roles of HIV-1 auxiliary proteins in viral pathogenesis and host-pathogen interactions', *Cell Research*, pp. 923–934. doi: 10.1038/sj.cr.7290370.

Liao, J. K. (2013) 'Linking endothelial dysfunction with endothelial cell activation', *Journal of Clinical Investigation*, 123(2), pp. 540–541. doi: 10.1172/JCI66843.540.

Liu, K. *et al.* (2005) 'HIV-1 Tat protein-induced VCAM-1 expression in human pulmonary artery endothelial cells and its signaling', *American Journal of Physiology - Lung Cellular and Molecular Physiology*, 289(2), pp. L252–L260. doi: 10.1152/ajplung.00200.2004.

Liu, V. W. T. and Huang, P. L. (2008) 'Cardiovascular roles of nitric oxide: A review of insights from nitric oxide synthase gene disrupted mice', *Cardiovascular Research*, 77, pp. 19–29. doi: 10.1016/j.cardiores.2007.06.024.

Luiking, Y. C., Engelen, M. P. K. J. and Deutz, N. E. P. (2010) 'Regulation of nitric oxide production in health and disease', *Current Opinion in Clinical Nutrition & Metabolic Care*, 13(1), pp. 97–104. doi: 10.1097/MCO.0b013e328332f99d.

Ma, Q. *et al.* (2016) 'Long-term efavirenz use is associated with worse neurocognitive functioning in HIV-infected patients', *Journal of NeuroVirology*. Journal of NeuroVirology, 22(2), pp. 170–178. doi: 10.1007/s13365-015-0382-7.

Maartens, G., Celum, C. and Lewin, S. R. (2014) 'HIV infection: Epidemiology, pathogenesis, treatment, and prevention', *The Lancet*. Elsevier Ltd, 384(9939), pp. 258–271. doi: 10.1016/S0140-6736(14)60164-1.

MacDonald, K. *et al.*, (2008) 'In-gel protein quantitation using the criterion stain-free gel imaging system', *Bio-Rad Laboratories*, tech note 5782B.

Marin, M. *et al.* (2003) 'HIV-1 Vif protein binds the editing enzyme APOBEC3G and induces its degradation', *Nature Medicine*, 9(11), pp. 1398–1403. doi: 10.1038/nm946.

Marincowitz, C. *et al.* (2018) 'Vascular endothelial dysfunction in the wake of HIV and ART', *FEBS Journal.* doi: 10.1111/febs.14675

Maron, B. A. and Michel, T. (2012) 'Subcellular localization of oxidants and redox modulation of endothelial nitric oxide synthase', *Circulation Journal*, 76(11), pp. 2497–2512. doi: 10.1253/circj.CJ-12-1207.

Mazzone, T., Chait, A. and Plutzky, J. (2008) 'Cardiovascular disease risk in type 2 diabetes mellitus: insights from mechanistic studies', *The Lancet*, 371(9626), pp. 1800–1809. doi: http://dx.doi.org/10.1016/S0140-6736%2808%2960768-0.

McCutchan, F. E. (2006) 'Global epidemiology of HIV', *Journal of Medical Virology*, 78, pp. S7–S12. doi: 10.1002/jmv.

Mestas, J. and Ley, K. (2008) 'Monocyte-endothelial cell interactions in the development of atherosclerosis', *Trends in Cardiovascular Medicine*. Elsevier Inc., 18(6), pp. 228–232. doi: 10.1016/j.tcm.2008.11.004.

Mons, U. *et al.* (2015) 'Impact of smoking and smoking cessation on cardiovascular events and mortality among older adults: meta-analysis of individual participant data from prospective cohort studies of the CHANCES consortium', *BMJ*, 350(apr20 2), pp. h1551–h1551. doi: 10.1136/bmj.h1551.

Montezano, A. C. *et al.* (2015) 'Oxidative stress and human hypertension: Vascular mechanisms, biomarkers, and novel therapies', *Canadian Journal of Cardiology*, 31(5), pp. 631–641. doi: 10.1016/j.cjca.2015.02.008.

Moore, K. J. and Tabas, I. (2011) 'Macrophages in the pathogenesis of atherosclerosis', *Cell*. Elsevier, 145(3), pp. 341–355. doi: 10.1016/j.cell.2011.04.005.

Morris, P. B. *et al.* (2015) 'Cardiovascular effects of exposure to cigarette smoke and electronic cigarettes: Clinical perspectives from the prevention of cardiovascular disease section leadership council and early career councils of the American college of cardiology', *Journal of the American College of Cardiology*, 66(12), pp. 1378–1391. doi: 10.1016/j.jacc.2015.07.037.

Mu, H. *et al.* (2007) 'Current update on HIV-associated vascular disease and endothelial dysfunction', *World Journal of Surgery*, 31(4), pp. 632–643. doi: 10.1007/s00268-006-0730-0.

Mudau, M. *et al.* (2012) 'Endothelial dysfunction : the early predictor of atherosclerosis', *Cardiovascular Journal of Africa*, 23(4), pp. 222–231. doi: 10.5830/CVJA-2011-068.

Nabel, E. G. and Braunwald, E. (2012) 'A tale of coronary artery disease and myocardial infarction', *New England Journal of Medicine*, 366(1), pp. 54–63. doi: 10.1056/NEJMra1112570.

National Department of Health of South Africa (2015) 'National consolidated guidelines for the prevention of mother-to-child transmission of HIV (PMTCT) and the management of HIV in children, adolescents and adults'. Pretoria: Department of Health.

Nisole, S. and Saïb, A. (2004) 'Early steps of retrovirus replicative cycle', *Retrovirology*. doi: 10.1186/1742-4690-1-9.

Nojilana, B. *et al.* (2016) 'Emerging trends in non-communicable disease mortality in South Africa, 1997 - 2010', *South African Medical Journal*, 106(5), p. 477. doi: 10.7196/SAMJ.2016.v106i5.10674.

Noor, M. A. *et al.* (2006) 'Effects of atazanavir / ritonavir and lopinavir / ritonavir on glucose uptake and insulin sensitivity : demonstrable differences in vitro and clinically', *AIDS (London, England)*, 20(14), pp. 1813–1821.

Nordestgaard, B. G. and Varbo, A. (2014) 'Triglycerides and cardiovascular disease', *The Lancet*, 384(9943), pp. 626–635. doi: 10.1016/S0140-6736(14)61177-6.

Odegaard, A. O. *et al.* (2016) 'Oxidative stress, inflammation, endothelial dysfunction and incidence of type 2 diabetes', *Cardiovascular Diabetology*. BioMed Central, 15(1), pp. 1–12. doi: 10.1186/s12933-016-0369-6.

De Pablo, C. *et al.* (2012) 'Differential effects of tenofovir/emtricitabine and abacavir/lamivudine on human leukocyte recruitment', *Antiviral Therapy*, 17(8), pp. 1615–1619. doi: 10.3851/IMP2357.

Palmer, R. M. J., Ferrige, A. G. and Moncada, S. (1987) 'Nitric oxide release accounts for the biological activity of endothelium-derived relaxing factor', *Nature*. Nature Publishing Group, 327, p. 524. Available at: http://dx.doi.org/10.1038/327524a0.

Park, I.-W. *et al.* (2001) 'HIV-1 Tat Induces microvascular endothelial apoptosis through caspase activation', *The Journal of Immunology*, 167(5), pp. 2766–2771. doi: 10.4049/jimmunol.167.5.2766.

Parker, I. K. *et al.* (2014) 'Pro-atherogenic shear stress and hiv proteins synergistically upregulate cathepsin K in endothelial cells', *Annals of Biomedical Engineering*, 42(6), pp. 1185–1194. doi: 10.1007/s10439-014-1005-9.

Phillips, A. N. *et al.* (2008) 'Interruption of antiretroviral therapy and risk of cardiovascular disease in persons with HIV-1 infection: exploratory analyses from the SMART trial', *Antiviral Therapy*, 13(January), pp. 177–187.

Pirro, M. *et al.* (2016) 'Urinary albumin-to-creatinine ratio is associated with endothelial dysfunction in HIV-infected patients receiving antiretroviral therapy', *Scientific Reports*. Nature Publishing Group, 6(June), pp. 1–8. doi: 10.1038/srep28741.

Price, T. O. *et al.* (2005) 'HIV-1 viral proteins gp120 and Tat induce oxidative stress in brain endothelial cells', *Brain Research*, 1045(1–2), pp. 57–63. doi: 10.1016/j.brainres.2005.03.031.

Qi, Y. *et al.* (2011) 'PDGF-BB and TGF-β1 on cross-talk between endothelial and smooth muscle cells in vascular remodeling induced by low shear stress', *PNAS*, 108, pp. 1908–1913. doi: 10.1073/pnas.1019219108/-/DCSupplemental.www.pnas.org/cgi/doi/10.1073/pnas.1019219108.

Rabkin, M. *et al.* (2015) 'Missed opportunities to address cardiovascular disease risk factors amongst adults attending an urban HIV clinic in South Africa', *PLoS ONE*, 10(10), pp. 1–9. doi: 10.1371/journal.pone.0140298.

Rader, D. J. and Hovingh, G. K. (2014) 'HDL and cardiovascular disease', *The Lancet*. Elsevier Ltd, 384(9943), pp. 618–625. doi: 10.1016/S0140-6736(14)61217-4.

Ray, P. D., Huang, B. W. and Tsuji, Y. (2012) 'Reactive oxygen species (ROS) homeostasis and redox regulation in cellular signaling', *Cellular Signalling*. Elsevier Inc., 24(5), pp. 981–990. doi: 10.1016/j.cellsig.2012.01.008.

Reiss, P. *et al.* (2007) 'Class of antiretroviral drugs and the risk of myocardial infarction', *New England Journal of Medicine*, 356(17), pp. 1723–1735. doi: 10.1056/NEJMoa062744.

Riccardi, C. and Nicoletti, I. (2006) 'Analysis of apoptosis by propidium iodide staining and flow cytometry', *Nature Protocols*, 1(3), pp. 1458–1461. doi: 10.1038/nprot.2006.238.

Ridker, P. M. (2014) 'LDL cholesterol: Controversies and future therapeutic directions', *The Lancet*. Elsevier Ltd, 384(9943), pp. 607–617. doi: 10.1016/S0140-6736(14)61009-6.

Rosenson, R. S. *et al.* (2016) 'Dysfunctional HDL and atherosclerotic disease', *Nature Reviews Cardiology*, 13(January), pp. 48–60. doi: 10.1038/nrcardio.2015.124.

Ross, A. C. *et al.* (2009) 'Relationship between inflammatory markers, endothelial activation markers, and carotid intima-media thickness in HIV-infected patients receiving antiretroviral therapy', *Clinical Infectious Diseases*, 49(7), pp. 1119–1127. doi: 10.1086/605578.

Russell, F. D. and Hamilton, K. D. (2014) 'Nutrient deprivation increases vulnerability of endothelial cells to proinflammatory insults', *Free Radical Biology and Medicine*. Elsevier, 67, pp. 408–415. doi: 10.1016/j.freeradbiomed.2013.12.007.

Sanson, M. *et al.* (2009) 'Oxidized low-density lipoproteins trigger endoplasmic reticulum stress in vascular cells: Prevention by oxygen-regulated protein 150 expression', *Circulation Research*, 104(3), pp. 328–336. doi: 10.1161/CIRCRESAHA.108.183749.

Sasaki, C. Y. *et al.* (2005) 'Phosphorylation of RelA/p65 on serine 536 defines an IkappaBalpha-independent NF-kappaB pathway', *Journal of Biological Chemistry*, 280(14), pp. 34538–34547.

Schuler, G., Adams, V. and Goto, Y. (2013) 'Role of exercise in the prevention of cardiovascular disease: Results, mechanisms, and new perspectives', *European Heart Journal*, 34(24), pp. 1790–1799. doi: 10.1093/eurheartj/eht111.

Shafran, S., Mashinter, L. and Roberts, S. (2005) 'The effect of low-dose ritonavir monotherapy on fasting serum lipid concentrations', *HIV Medication*, 6(6), pp. 421–425. doi: 10.1111/j.1468-1293.2005.00328.x.

Shah, A. S. V. *et al.* (2018) 'Global burden of atherosclerotic cardiovascular disease in people living with HIV', *Circulation*, 138, pp. 1100–1112. doi: 10.1161/CIRCULATIONAHA.117.033369.

Shannon, K. *et al.* (2015) 'Global epidemiology of HIV among female sex workers: Influence of structural determinants', *The Lancet*, 385(9962), pp. 55–71. doi: 10.1016/S0140-6736(14)60931-4.

Sharp, P. M. and Hahn, B. H. (2011) 'Origins of HIV and the AIDS pandemic', *Additional Perspectives on HIV*, pp. 1–22. doi: 10.1101/cshperspect.a006841.

Shaw, G. M. and Hunter, E. (2012) 'HIV transmission', *Cold Spring Harbor Perspectives in Medicine*. Cold Spring Harbor Laboratory Press, 2(11), p. a006965. doi: 10.1101/cshperspect.a006965.

Sorin, M. and Kalpana, G. V (2006) 'HIV-1 dynamics in the host cell : A review of viral- and host- protein interactions and potential therapeutic targets for HIV-1 infection', *The Einstein Journal of Biology and Medicine*, 22, pp. 10–24.

de Souza, R. J. *et al.* (2015) 'Intake of saturated and trans unsaturated fatty acids and risk of all cause mortality, cardiovascular disease, and type 2 diabetes: systematic review and meta-analysis of observational studies', *BMJ*, p. h3978. doi: 10.1136/bmj.h3978.

Statistics South Africa (2015) 'Mortality and causes of death in South Africa, 2014: Findings from death notification', *Stats SA*. Pretoria. doi: Statistical release P0309.3.

Stepp, D. W. *et al.* (2002) 'Native LDL and minimally oxidized LDL differentially regulate superoxide anion in vascular endothelium in situ.', *American Journal of Physiology - Heart and Circulatory Physiology*, 283, pp. H750–H759. doi: 10.1152/ajpheart.00029.2002.

Sugden, S. M., Pham, T. N. Q. and Cohen, E. A. (2017) 'HIV-1 Vpu downmodulates ICAM-1 expression, resulting in decreased killing of infected CD4+ T cells by NK cells', *Journal of Virology*, 91(8), pp. e02442-16.

Talukder, M. A. H. *et al.* (2011) 'Chronic cigarette smoking causes hypertension, increased oxidative stress, impaired NO bioavailability, endothelial dysfunction, and cardiac remodeling in mice', *American Journal of Physiology - Heart and Circulatory Physiology*, 300(1), pp. H388–H396. doi: 10.1152/ajpheart.00868.2010.

Tarpey, M. M. and Fridovich, I. (2001) 'Methods of detection of vascular reactive species', *Circulation research*, 89(Vitamin C), pp. 224–237. doi: 10.1161/hh1501.094365.

Turner, B. G. and Summers, M. F. (1999) 'Structural biology of HIV', *Journal of Molecular Biology*, pp. 1–32. doi: 10.1006/jmbi.1998.2354.

UNAIDS (2016) *Global AIDS Update 2016*, *Joint United Nations Programme on HIV/AIDS*. Available at: http://www.unaids.org/en/resources/documents/2016/Global-AIDS-update-2016.

Vermund, S. H. (2014) 'Global HIV epidemiology: A guide for strategies in prevention and care', *Current HIV/AIDS Reports*, 11(2), pp. 93–98. doi: 10.1007/s11904-014-0208-x.

Villarroya, F., Domingo, P. and Giralt, M. (2010) 'Drug-induced lipotoxicity: Lipodystrophy associated with HIV-1 infection and antiretroviral treatment', *Biochimica et Biophysica Acta - Molecular and Cell Biology of Lipids*. Elsevier B.V., 1801(3), pp. 392–399. doi: 10.1016/j.bbalip.2009.09.018.

Wang, H. *et al.* (2016) 'Global, regional, and national life expectancy, all-cause mortality, and cause-specific mortality for 249 causes of death, 1980–2015: a systematic analysis for the Global Burden of Disease Study 2015', *The Lancet*, 388(10053), pp. 1459–1544. doi: 10.1016/S0140-6736(16)31012-1.

Wang, T. *et al.* (2014) 'Transfer of intracellular HIV Nef to endothelium causes endothelial dysfunction', *PLoS ONE*, 9(3), p. e91063. doi: 10.1371/journal.pone.0091063.

Wang, T. *et al.* (2015) 'Increased cardiovascular disease risk in the HIV-positive population on ART: potential role of HIV-Nef and Tat', *Cardiovascular Pathology*, 24(5), pp. 279–282. doi: 10.1016/j.carpath.2015.07.001.

Wang, X. *et al.* (2009) 'Roles and mechanisms of human immunodeficiency virus protease inhibitor ritonavir and other anti-human immunodeficiency virus drugs in endothelial dysfunction of porcine pulmonary arteries and human pulmonary artery endothelial cells', *American Journal of Pathology*. American Society for Investigative Pathology, 174(3), pp. 771–781. doi: 10.2353/ajpath.2009.080157.

Warren, T. Y. *et al.* (2010) 'Sedentary behaviors increase risk of cardiovascular disease mortality in men', *Medicine & Science in Sports & Exercise*, 42(5), pp. 879–885. doi: 10.1249/MSS.0b013e3181c3aa7e.Sedentary.

Wawer, M. J. *et al.* (2005) 'Rates of HIV-1 transmission per coital act, by stage of HIV-1 infection, in Rakai, Uganda', *The Journal of Infectious Diseases*. Oxford University Press, 191(9), pp. 1403–1409. doi: 10.1086/429411.

Weiß, M. *et al.* (2016) 'Efavirenz causes oxidative stress, endoplasmic reticulum stress, and autophagy in endothelial cells', *Cardiovascular Toxicology*, 16(1), pp. 90–99. doi: 10.1007/s12012-015-9314-2.

Weiss, R. A. (1993) 'How does HIV cause AIDS?', *Science*, 260(5112), pp. 1273–1279. doi: 10.1126/science.8493571.

Weller, S. C. and Davis-Beaty, K. (2002) 'Condom effectiveness in reducing heterosexual HIV transmission', in *Cochrane Database of Systematic Reviews*. doi: 10.1002/14651858.CD003255.

Wentzel, J. J. *et al.* (2012) 'Endothelial shear stress in the evolution of coronary atherosclerotic plaque and vascular remodelling: Current understanding and remaining questions', *Cardiovascular Research*, 96(2), pp. 234–243. doi: 10.1093/cvr/cvs217.

WHO (2017) *Cardiovascular diseases (CVDs) fact sheet*, *World Health Organisation Media Centre*. Available at: http://www.who.int/mediacentre/factsheets/fs317/en/ (Accessed: 31 January 2018).

WHO (2018) *HIV/AIDS fact sheet*, *fact sheets*. Available at: http://www.who.int/news-room/fact-sheets/detail/hiv-aids (Accessed: 24 May 2018).

Willig, J. H. *et al.* (2008) 'Increased regimen durability in the era of once daily fixed-dose combination antiretroviral therapy', *AIDS*, 22(15), pp. 1951–1960. doi: 10.1097/QAD.0b013e32830efd79.

World Health Organization (2016) *Consolidated guidelines on the use of antiretroviral drugs for treating and preventing HIV infection: recommendations for a public health approach*, *World Health Organization*. doi: 10.1016/j.jped.2014.04.007.

Xu, R. *et al.* (2012) 'HIV-1 Tat protein increases the permeability of brain endothelial cells by both inhibiting occludin expression and cleaving occludin via matrix metalloproteinase-9', *Brain Research*. Elsevier B.V., 1436, pp. 13–19. doi: 10.1016/j.brainres.2011.11.052.

Yang, B. *et al.* (2009) 'HIV-1 gp120 induces cytokine expression, leukocyte adhesion, and transmigration across the blood-brain barrier: modulatory effects of STAT1 signaling', *Microvascular Research*. Elsevier Inc., 77(2), pp. 212–219. doi: 10.1016/j.mvr.2008.11.003.

Yang, Z. and Klionsky, D. J. (2010) 'Eaten alive: A history of macroautophagy', *Nature Cell Biology,* 12(9), pp. 814–822. doi: 10.1038/ncb0910-814.

Younas, M. *et al.* (2016) 'Immune activation in the course of HIV-1 infection: Causes, phenotypes and persistence under therapy', *HIV Medicine*, 17(2), pp. 89–105. doi: 10.1111/hiv.12310.

Yusuf, S. *et al.* (2004) 'Effect of potentially modifiable risk factors associated with myocardial infarction in 52 countries in a case-control study based on the INTERHEART study', *Lancet*. Elsevier, 364(9438), pp. 937–952. doi: 10.1016/S0140-6736(04)17018-9.

Yusuf, S. *et al.* (2016) 'Cholesterol lowering in intermediate-risk persons without cardiovascular disease', *New England Journal of Medicine*, 374(21), pp. 2021–2031. doi: 10.1056/NEJMoa1600176.

Zuma, K. *et al.* (2016) 'New insights into HIV epidemic in South Africa: Key findings from the National HIV

Prevalence, Incidence and Behaviour Survey, 2012', *African Journal of AIDS Research*, 15(1), pp. 67–75. doi: 10.2989/16085906.2016.1153491.

APPENDIX A

The FEBS Journal

FEBS PRESS science publishing by scientists

REVIEW ARTICLE

Vascular endothelial dysfunction in the wake of HIV and ART

Clara Marincowitz[1], Amanda Genis[1], Nandu Goswami[2], Patrick De Boever[3,4], Tim S. Nawrot[4,5] and Hans Strijdom[1]

1 Division of Medical Physiology, Stellenbosch University, Cape Town, South Africa
2 Department of Physiology and Otto Loewi Research Centre, Medical University of Graz, Austria
3 Health Unit, Flemish Institute for Technological Research (VITO), Mol, Belgium
4 Centre for Environmental Sciences, Hasselt University, Diepenbeek, Belgium
5 Centre for Environment and Health, Department for Public Health and Primary Care, KU Leuven, Belgium

Keywords
antiretroviral therapy; endothelial dysfunction; endothelial nitric oxide synthase; HIV-induced proinflammatory cytokines; HIV-proteins; human immunodeficiency virus; nitric oxide; oxidative stress; reactive oxygen species; vascular endothelium

Correspondence
C. Marincowitz, Division of Medical Physiology, Faculty of Medicine and Health Sciences, University of Stellenbosch, Francie van Zijl Drive, Tygerberg, 7505, Cape Town, South Africa
Fax: +27 21 938 9476
Tel: +27 21 938 9387 or +27 21 938 9072
E-mails: 15016420@sun.ac.za or claramarincowitz@gmail.com
Website: www.sun.ac.za/english/faculty/healthsciences/medical_physiology

(Received 8 June 2018, revised 30 August 2018, accepted 12 September 2018)

doi:10.1111/febs.14657

Mounting evidence points to increased rates of cardiovascular disease (CVD) among people living with HIV/AIDS (PLWHA). Endothelial dysfunction (loss of endothelium-dependent vascular relaxation in response to provasodilatory stimuli) constitutes an early pathophysiological event in atherogenesis and CVD. Both HIV-1 infection and antiretroviral therapy (ART) are implicated in the development of endothelial dysfunction; however, conclusions are frequently drawn from associations shown in epidemiological studies. In this narrative review of mainly *in vitro* and animal studies, we report on the current understanding of how various HIV-1 proteins, HIV-1-induced proinflammatory cytokines and common antiretroviral drugs directly impact vascular endothelial cells. Proposed cellular mechanisms underlying the switch to a dysfunctional state are discussed, including oxidative stress, impaired expression and regulation of endothelial nitric oxide (NO) synthase (eNOS) and increased expression of vascular adhesion molecules. From the literature, it appears that increased reactive oxygen species (ROS) production, linked to decreased NO bioavailability and ensuing endothelial dysfunction, may be proposed as a putative final common pathway afflicting the vascular endothelium in PLWHA. The HIV-1-proteins Tat, Gp120 and Nef in particular, the proinflammatory cytokine, TNF-α, and the antiretroviral drugs Efavirenz and Lopinavir, most commonly postulated to be primary causal agents of endothelial dysfunction, are also discussed. We conclude that, despite existing evidence from basic research papers, a significant gap remains in terms of the exact

Abbreviations
3TC, lamivudine; ADMA, asymmetric dimethylarginine; AIDS, acquired immunodeficiency syndrome; ART, antiretroviral therapy; CCR5, monocyte C-C chemokine receptor type 5; CRP, C-reactive protein; CVD, cardiovascular disease; EFV, Efavirenz; eNOS, endothelial nitric oxide synthase; ER, endoplasmic reticulum; FDC, fixed-dose combination; FMD, flow-mediated dilation; FTC, Emtricitabine; HAART, highly active antiretroviral therapy; HDL, high density lipoprotein; HIV, human immunodeficiency virus; HPAEC, human pulmonary artery endothelial cell; ICAM-1, intercellular adhesion molecule 1; IL-1β, interleukin-1β; IL-6, interleukin-6; IL-8, interleukin-8; IMT, intima media thickness; JAM-1, junctional adhesion molecule-1; JNK, c-Jun N-terminal Kinase; LDL, low-density lipoprotein; LPV/r, ritonavir-boosted Lopinavir; MCP-1, monocyte chemoattractant protein-1; NADPH, nicotinamide-adenine-dinucleotide phosphate; NFκB, nuclear factor kappa-light-chain-enhancer of activated B cells; NNRTI, non-nucleoside reverse transcriptase inhibitor; NO, nitric oxide; NRTI, nucleoside-analogue reverse transcriptase inhibitor; PI, protease inhibitor; PLWHA, people living with HIV/AIDS; ROS, reactive oxygen species; TDF, Tenofovir; TNF-α, tumour necrosis factor-alpha; VCAM-1, vascular cell adhesion molecule 1; VLDL, very low-density lipoprotein; ZO-1, zonula occludens-1; ZO-2, zonula occludens-2.

underlying cellular mechanisms involved in HIV-1 and ART induced endothelial dysfunction. Bridging this gap could help pave the way for future strategies to prevent and treat early cardiovascular changes in PLWHA.

Introduction

Mounting evidence is pointing to an association between the infective human immunodeficiency virus-1 (HIV-1) and noncommunicable cardiovascular disease (CVD). A meta-analysis by Islam *et al.* [1] found the relative risk of developing CVD in people living with HIV/AIDS (PLWHA) to be 61% higher than that of the HIV uninfected population. Furthermore, the same study showed that the cardiovascular risk in PLWHA receiving highly active antiretroviral therapy (HAART) was twice that of HIV-positive individuals who were treatment-naïve. The United Nations AIDS update indicates that in 2015, 17.0 million people worldwide were living with HIV and receiving antiretroviral therapy [2]. Therefore, considering the sheer prodigiousness of this global pandemic and the troubling data on its comorbidity with CVD, zooming in on HIV's intersection with antiretroviral therapy and cardiovascular health is consequently imperative, as we have previously emphasised [3].

Endothelial dysfunction is regarded as one of the first pathophysiological events in the development of atherosclerosis and subsequent CVD [4], with HIV-1-induced proinflammatory cytokines, HIV-1 proteins and antiretroviral drugs all implicated in its development [5]. A better understanding of the link between HIV-infection and endothelial dysfunction, is therefore invaluable for researchers and clinicians alike and we are currently conducting a prospective cohort study investigating whether HIV-infection with and without antiretroviral therapy (ART) exerts changes to vascular endothelial function as measured by flow-mediated dilation (FMD) of the brachial artery [6]. Given the vastness and complexity of this topic, and the fact that multiple, interacting cellular mechanisms and pathways are involved, integrating the literature available becomes a mammoth task. Although a number of review papers have been published on the interaction between HIV infection and endothelial dysfunction [5,7–11], few have integrated findings from *in vitro,* endothelial cell-based studies that account for both viral and treatment factors. In the present narrative review, we endeavour to address this paucity and elucidate the current understanding of how HIV-1-induced proinflammatory cytokines, various HIV-1 proteins and common antiretroviral drugs directly impact vascular endothelial cells, focusing in particular on *in vitro* and animal studies.

In our search, standard scientific search engines such as PubMed and Google Scholar were utilised entering keywords including: 'vascular endothelium', 'vascular endothelial cells', 'HIV' and 'endothelial dysfunction' in combination with the names of the individual HIV proteins, common antiretroviral drugs and proinflammatory cytokines that have previously been shown to be upregulated during HIV-1 infection [12]. Relevant studies focussing on *in vitro* investigations were included, and although a comprehensive review of epidemiological studies falls outside the scope of the present paper, findings from selected human/clinical studies were included with the aim to provide context.

The vascular endothelium and endothelial dysfunction

The vascular endothelium plays an important part in regulating vascular homoeostasis. It achieves this by responding to various physical and chemical signals via the production of a wide variety of factors that regulate vascular tone, cell adhesion, coagulation, smooth muscle cell proliferation and inflammation. One of the key agents in this regard is the gaseous free-radical, nitric oxide (NO), functioning to maintain the vascular wall in a homoeostatic state by opposing, among others, inflammation, cellular proliferation and thrombosis [13]. In endothelial cells, NO is constitutively synthesised by the dimeric enzyme endothelial nitric oxide synthase (eNOS) from the amino acid L-arginine, utilising oxygen and reduced nicotinamide-adenine-dinucleotide phosphate (NADPH) as cosubstrates [14]. When vascular homoeostasis is disturbed beyond the regulating capabilities of the endothelium, the scale is consequently tipped from endothelial function to dysfunction, a scenario in which the modification of both NO and eNOS is pivotally implicated.

Endothelial dysfunction is defined as the loss of the endothelium's ability to induce vascular relaxation in response to provasodilatory stimuli such as shear stress [4]. Essentially, it represents a state where a reduction in NO bioavailability leads to a switch in cellular

signalling, propelling the endothelium into an activated, proinflammatory state. A reduction in NO bioavailability, the consequence of a decrease in NO production and/or increased NO inactivation, is ascribed by most authors to oxidative stress. An increase in reactive oxygen species (ROS) contributes to the reduction in NO bioavailability in two ways: first, by reacting with NO and transforming it into a damaging reactive nitrogen species, peroxynitrite, and second, by uncoupling eNOS, and hence modifying it into a ROS producing enzyme [4,13–15]. Circulating leucocytes are generally not adhesive to endothelial cells in a nonactivated state. The inflammatory response, characterised by the migration of leucocytes across endothelial cells, is dependent on adhesion molecules which facilitate this movement [16] and, under homoeostatic conditions, this is a normal process. However, in the case of endothelial dysfunction (which can perhaps be alternately termed nonhomoeostatic endothelial cell activation), this process becomes a maladaptive response. Endothelial dysfunction occurs at susceptible sites in the arterial vasculature where pro-atherogenic, low endothelial shear stress occurs. Endothelial shear stress is the frictional force exerted on the endothelial cells of the arterial wall by the flowing blood. Blood flow may be either smooth and laminar, tending to result in moderate/physiological to high shear stress which is considered atheroprotective, or it can be disturbed, characterised by areas of flow reversal, resulting in low endothelial shear stress and this is where the atherosclerotic plaques tend to develop [17]. NO provides a critical link between endothelial shear stress and endothelial dysfunction as increased fluid shear stress is one of the triggers resulting in the activation of eNOS and, as outlined above, subsequent NO synthesis [14]. A reduction in NO bioavailability due to oxidative stress is thus catastrophic for these susceptible sites in the vasculature, already characterised by lower NO production, and the consequent endothelial dysfunction constitutes the initial step of atherosclerotic plaque formation. This is followed by the infiltration and trapping of circulating lipoprotein particles in the subendothelial space, leucocyte recruitment into the intima and subsequent differentiation into macrophages and finally lipid-filled foam cells – the hallmark of the atherosclerotic plaque [18].

Known cardiovascular risk factors all seem to contribute to the development of endothelial dysfunction, with oxidative stress emerging as a common underlying mechanism [4]. Similarly, both HIV-1 infection and its treatment have been linked to endothelial dysfunction, with oxidative stress branded the apparent culprit [19]. Dirajlal-Fargo *et al.*[20] found perinatally infected HIV-positive youth to have higher levels of endothelial dysfunction and immune activation when compared to their behaviourally infected counterparts, possibly due to a longer cumulative duration of HIV infection. These researchers indicate that multiple factors, including metabolic factors, inflammation and ART regimen, contribute to the progression of vascular disease in HIV-infected youth. In addition, although beyond the scope of this review, dyslipidaemia and impaired cholesterol metabolism, which are both possibly fuelled by HIV and HAART, enhance the pathogenesis of atherosclerosis as well [9,21]. In the following sections, the association of HIV with endothelial dysfunction will be explored, both as a consequence of the virus itself and as a side-effect of ART.

HIV-1 and endothelial dysfunction

Whether or not HIV-1 actively infects vascular endothelial cells *in vivo* has been described as controversial [5]. Some reviewers argue that cells are indeed directly infected [19], whereas others are more cautious in this regard [22]. What is certain, however, is that the vascular endothelium of an HIV-1-infected individual is constantly exposed to a variety of stimuli – of viral origin and consequent to HAART – some of which have damaging downstream effects [5,19]. Central to these downstream consequences seems to be a decrease in NO bioavailability, possibly due to increased ROS generation, which, via multiple mechanisms, steers the vascular endothelium into a dysfunctional state (Fig. 1).

HIV-1 proteins and endothelial dysfunction

The HIV-1 genome contains nine main genes: *Gag* encodes for three structural proteins, *pol* encodes for three enzymes, *env* encodes for two envelope proteins, *tat* and *rev* encode for the regulatory proteins and *vpu, vpr, vif* and *nef* encode for accessory proteins (Fig. 2) [5,23]. The three structural proteins include matrix proteins, capsid proteins and nucleocapsid proteins. The matrix is located between the virus envelope and the capsid, a cone-shaped structure at the centre of the mature virion, that encapsidates the viral RNA, enzymes and the nucleocapsid proteins [23]. The three enzymes, encoded by *pol,* are essential for the synthesis of the viral proteins and they include reverse transcriptase, which enables the transcription of single-stranded viral RNA into double-stranded provisional DNA that

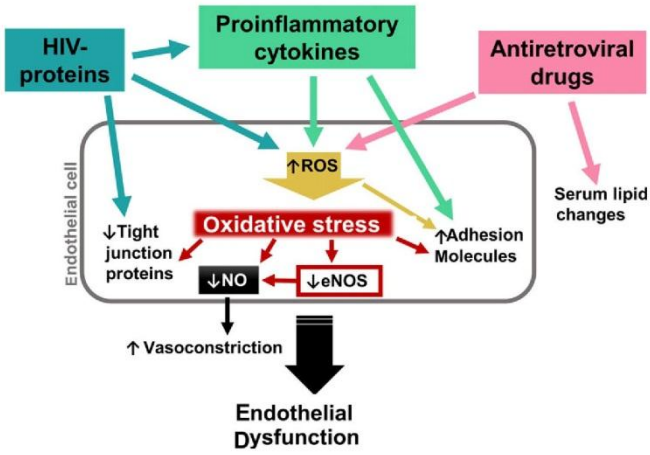

Fig. 1. Schematic overview of the effects of HIV-1 infection and its treatment on vascular endothelial cells. HIV-proteins, pro-inflammatory cytokines and antiretroviral drugs all result in increased ROS. Oxidative stress ensues, which in turn induces eNOS uncoupling and decreased NO bioavailability. These mechanisms culminate in endothelial dysfunction, a state characterised by decreased endothelial tight junction proteins, increased vascular adhesion molecules and vasoconstriction. ROS, reactive oxygen species, eNOS, endothelial nitric oxide synthase, NO, nitric oxide.

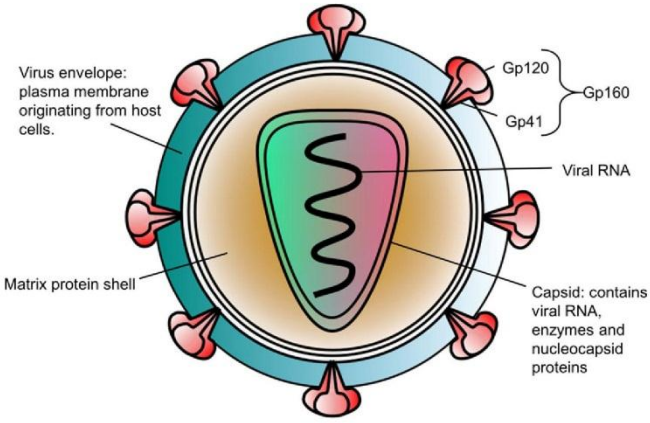

Fig. 2. A representation of the HIV-1 virus. The HIV virion is enclosed by a virus envelope studded with Gp160 proteins. Gp160 comprises two associated envelope proteins, Gp120, a surface glycoprotein, and Gp41, a transmembrane component. The matrix is located between the virus envelope and the capsid, which contains the viral RNA, enzymes and nucleocapsid proteins (Illustration: Neeske Alexander).

Tat

Human immunodeficiency virus-1 Tat, trans-activator of viral replication, enhances viral transcription and replication, which means that it is able to enter the host cell's nucleus. It can also be secreted by infected cells in the absence of cell lysis and imported by various target cells, including endothelial cells [27]. Tat has been linked to many of the characteristics of endothelial dysfunction, such as enhanced ROS production, increased endothelial cell permeability and adhesion molecule expression.

In rat brain endothelial cells, exposure to Tat caused a significant increase in oxidative stress [28]. Tat's ability to induce ROS production was found to be associated with the activation of the transcription factor, nuclear factor kappa-light-chain-enhancer of activated B cells (NFκB), in human pulmonary artery endothelial cells. In these cells, Tat exposure induced the expression of vascular cell adhesion molecule 1 (VCAM-1), which the researchers speculated might be mediated by ROS production, p38 mitogen-activated protein kinase (MAPK) activation and the nuclear translocation of NFκB [29]. Treatment of human umbilical vein endothelial cells with Tat caused monocyte adhesion via increased intercellular adhesion molecule 1 (ICAM-1) expression, where activation of the MAPK pathways also resulted in NFκB nuclear translocation which ultimately led to the increased ICAM-1 [30].

HPAECs [42]. In two mouse models of atherosclerosis, injected recombinant Nef resulted in dyslipidaemia and the accumulation of cholesterol within macrophages in the animals' vessel walls [43]. In the light of the above, Nef clearly contributes to the development of endothelial dysfunction, which can ultimately culminate in atherosclerosis.

Vpu and Vpr

Viral Protein U is a membrane protein that, similar to Nef, induces the degradation of the CD4 receptor in HIV-infected lymphocytes and, additionally, it is able to form ion channels in cell membranes. Via these mechanisms, Vpu counteracts host cell factors that hamper the release of progeny virions from infected cells. In this way, Vpu acts as an antagonist to the host's innate immune response in HIV infection [40,44]. For instance, in lymphocytic cell lines, it has been shown that an increase in the mRNA expression of ICAM-1 observed in these cells when infected with HIV-1 is counteracted by Vpu through the downregulation of ICAM-1 from the cell surface. This results in a decrease in the formation of conjugates between infected CD4-positive T cells and NK cells and consequently a reduction in the NK cell-mediated killing of HIV-infected T cells [45]. Viral Protein R is involved in the nuclear import of proviral DNA, where it is known to interfere with host cell cycle progression and can induce apoptosis [40]. Very little is known about the endothelial effects of Vpu and Vpr. In an *in vitro* setting where cultured human umbilical vein endothelial cells were infected with recombinant adenoviruses that expressed individual HIV-proteins, cultured B-lymphocyte cells adhered exclusively to Vpu-expressing endothelial cells. This was attributed to the ability of Vpu to upregulate endothelial CD40, which in turn resulted in the efficient expression of VCAM-1 [46]. Vpr treatment induced apoptosis in primary human brain microvascular endothelial cells, an effect that was synergistically enhanced by cotreatment with ethanol [47].

HIV-1-induced proinflammatory cytokines and endothelial dysfunction

Most nucleated cells are able to synthesise and respond to cytokines and, proinflammatory variants such as interleukin-1β (IL-1β), interleukin-6 (IL-6) and tumour necrosis factor-alpha (TNF-α), promote inflammation [48,49]. Cytokines are, however, primarily produced by lymphocytes and macrophages in response to toxins, injury or inflammatory mediators [50]. HIV infection is characterised by a sustained state of immune activation, which persists even in the presence of HAART [51]. Compared to HIV-negative men, HIV-positive men were shown to have significantly higher blood levels of biomarkers of inflammation, including IL-6, ICAM-1 and soluble TNFα receptor I and II [52]. The sustained inflammation present in HIV infection has been ascribed to ongoing viral replication; coinfections (most notably other chronic viral infections); the translocation of microbial by-products across a dysfunctional gut mucosa; the loss of immunoregulatory cells and damage to immune structures [53,54]. Furthermore, the viral proteins themselves have been shown to prompt the production of inflammatory cytokines in host cells [36,37] Inflammation has emerged as a key mechanism responsible for the high prevalence of CVD in the HIV-infected population [51]. Proinflammatory cytokines promote the inflammation-dependent activation of endothelial cells causing an increase in adhesion molecule expression with subsequent monocyte adherence, increased vascular permeability, and elevated ROS production contributing to the development of endothelial dysfunction (Fig. 1)[50,55].

The effects of HIV-1 infection on cytokine production are extensive. The virus decreases the production of some cytokines, while increasing the production of others, thus, dysregulating cytokine homoeostasis [12]. Due to the large amount of data available on this topic, it was decided, for the purposes of this review, to limit our search to cytokines that have traditionally been described as proinflammatory [48,56,57] and most commonly thought to be up-regulated in the context of HIV infection [12,56,58]. Therefore, the focus will be on TNF-α, IL-1β and IL-6.

Tumour necrosis factor-alpha

Vascular endothelial cells are regarded as the primary targets of TNF-α [59] and this proinflammatory cytokine has been implicated in their dysfunction. Previous studies conducted in our laboratory showed that short term *in vitro* TNF-α treatment resulted in rat cardiac endothelial cell dysfunction as demonstrated by the attenuation of the eNOS-NO biosynthesis pathway and increased oxidative stress [60]. Other *in vitro* and animal-based studies have also pointed to TNF-α in a reduction in NO bioavailability, and thus subsequent endothelial dysfunction [61,62]. Upon binding to its receptor, TNF-α prompts the translocation of NFκB form the cytosol to the nucleus, where it elicits the transcription of a number of proinflammatory genes including TNF-α itself, perpetuating the inflammatory

state, and the adhesion molecules VCAM-1 and ICAM-1, promoting leucocyte adhesion. While TNF-α and IL-1β both resulted in an increase in VCAM-1 and ICAM-1 in human cerebral microvascular endothelial cells, TNF-α induced a considerably higher level of expression [63]. Besides TNF-α, NFκB can also be activated by several agonists such as oxidised low-density lipoprotein (LDL), very low-density lipoprotein (VLDL), glucose and viral infection [16]. NFκB activation thus emerges as a common pathway induced by many of the known contributors to CVD.

Several human studies have demonstrated that HIV infection is associated with increased TNF-α. From the early stages of HIV-1 infection, serum levels of TNF-α seem to be elevated [64]. In HIV-infected women, augmented TNF-α levels persisted even after antiretroviral treatment was initiated and circulating HIV RNA was below the detectable limit [65]. TNF-α was also independently associated with increased internal carotid artery intima-media thickness (IMT), a subclinical marker of atherosclerosis, in HIV-positive subjects [66]. Since findings from *in vitro* studies have demonstrated a direct contribution of TNF-α to decreased NO levels in endothelial cells, TNF-α may also be a candidate causal agent in HIV-associated endothelial dysfunction. Indeed, an *in vitro* investigation by Jiang *et al.* (2010) identified synergistic effects of TNF-α with HIV-1 proteins. They showed that pretreatment of porcine coronary arteries and human coronary artery endothelial cells with TNF-α resulted in substantially increased endothelial ICAM-1 expression and a significant downregulation of eNOS when these cells were subsequently treated with the HIV-related protein, Gp120. However, overall there is a paucity of *in vitro* studies on the direct endothelial cellular effects of TNF-α in the context of HIV, warranting further investigations into the mechanisms linking this co-occurrence with endothelial dysfunction.

Interleukin-1β and Interleukin-6

Interleukin-1β can be regarded as the apical proinflammatory cytokine. It is a multifunctional protein with downstream effects that include the translocation of NFκB to the nucleus and, as with TNF-α, elicits the transcription of a host of proinflammatory genes [67]. Activation of the NOD-like receptor family pyrin domain containing 3 (NLRP3) inflammasome results in the cleavage of pro-interleukin (IL)-1β into active IL-1β, which exerts further downstream effects on IL-6 and c-reactive protein (CRP) production. Both IL-1β and IL-6 have been linked to increased vascular inflammation, endothelial dysfunction and atherosclerosis [68].

Human immunodeficiency virus-1 infection was found to induce IL-1β production in human monocytes [69] and although there is limited data available on IL-1β and its direct effects on endothelial function in the context of HIV, this inflammatory cytokine has been linked to increased adhesion molecule expression. In human cerebral microvascular endothelial cells IL-1β resulted in an increase in ICAM-1 and VCAM-1 [63] and in human umbilical vein endothelial cells IL-1β activated ICAM-1 and E-selectin as well as the inflammatory mediators MCP-1 and NFκB [70]. From the available knowledge, it could thus be speculated that the increase in IL-1β production associated with HIV plays a part in the endothelial dysfunction related to this virus. However, more basic research, especially in the context of HIV, is needed to add substance to this supposition.

Interleukin-1β levels chiefly drive IL-6 signalling and IL-6 predominantly functions as a secondary signalling cytokine, exacting its effects on CRP [68]. CRP, together with most acute-phase proteins, is present during both acute and chronic inflammation and it contributes to many of the pathophysiologic effects in the inflammatory process, including the recognition of foreign pathogens and damaged cells, activating the complement system and inducing inflammatory cytokines' release from monocytes, to name a few [71]. In humans, IL-6 is strongly associated with an increase in all-cause mortality in HIV-positive individuals [72,73] and both IL-6 and CRP have been linked to an increase in cardiovascular risk in this population independent of other cardiovascular risk factors [74]. Moreover, a meta-analysis by Howren *et al.* [75] noted that depression was linked to IL-6 and CRP in patients with CVD. Most human studies report CRP levels when investigating systemic inflammation as it is the more commonly used inflammatory marker. CRP has been associated with atherosclerosis in both HIV-positive and control group subjects, with a positive correlation noted between serum CRP levels and common carotid and internal carotid artery IMT [66]. In an international study of almost 10 000 HIV-infected persons, higher HIV RNA levels correlated with higher IL-6 levels, and higher nadir CD4 positive cell counts were associated with lower IL-6 levels [76]. In 149 HIV-infected individuals receiving ART with undetectable viral loads, higher monocyte C-C chemokine receptor type 5 (CCR5) expression and plasma IL-6 levels were associated with atherosclerosis independent of traditional cardiovascular risk factors. Furthermore, increased plasma IL-6 and carotid IMT were

individually associated with all-cause mortality [77]. In patients with ST-elevation acute myocardial infarction treated by successful percutaneous coronary intervention (PCI), local IL-6 levels positively predicted for microvascular dysfunction [78].

With regard to *in vitro* studies investigating their direct endothelial cell effects, both IL-6 and CRP have been shown to exact consequences associated with endothelial dysfunction. CRP has been linked to increased adhesion molecule expression [79] in endothelial cells as well as reduced NO bioavailability via a mechanism that involves decreased eNOS expression [80,81]. In human umbilical vein endothelial cells, IL-6 resulted in increased endothelial permeability in a dose- and time-dependent manner. These changes were linked to a rearrangement of the tight junction protein, zonula occludens-1 (ZO-1) and cytoskeletal actin [82]. Alsaffar *et al.*[83] demonstrated that IL-6 promotes an increase in endothelial monolayer permeability which lasts over 24 hours. However, they speculated that the changes observed in the localisation of the tight junction molecules VE-cadherin and ZO-1 were not the cause of the increased permeability, since these changes were only evident several hours after the maximal IL-6 response (which occurred at 6 hours post treatment). This suggests that while the events were a consequence of the IL-6 signalling pathway, they were not the cause of the initial increase in permeability.

The above results provide a possible explanation for the associations between IL-6/CRP as well as IL-1β and CVD in HIV, with endothelial dysfunction appearing as the point of convergence. However, there is paucity in the data available on the direct endothelial cellular effects of these proinflammatory cytokines, especially in the context of HIV, and more basic research is needed to elucidate the mechanisms involved.

Antiretroviral therapy and endothelial dysfunction

Antiretroviral drugs block HIV replication at various stages in the virus life-cycle and are accordingly divided into five classes (for an overview of the drugs and drug classes see Maartens *et al.* [22]). Highly active antiretroviral therapy (HAART), where a cocktail of these drugs, most often combining Nucleoside-analogue Reverse Transcriptase Inhibitors (NRTIs) and/or Non-Nucleoside Reverse Transcriptase Inhibitors (NNRTIs) with Protease Inhibitors (PIs), are given to patients, has been linked to lipodystrophy, dyslipidaemia, direct mitochondrial DNA damage as well as insulin resistance – all risk factors for atherosclerotic cardiovascular disease [19]. In the 'Data Collection on Adverse Events of Anti-HIV Drugs (DAD)' study, a large, ongoing cohort study of HIV-positive participants on treatment, a significant association was noted between the duration of exposure to ART and the risk of myocardial infarction. The findings furthermore suggest that the risk varies according to the ART drug class, with especially PIs contributing to a significant increase in myocardial infarction risk. However, the researchers speculated that this might partly be a consequence of the adverse effects of the drugs on serum lipids [84]. PIs have also been linked to higher IL-6 levels, compared to efavirenz [76]. The extent of the observed cardiovascular risk associated with ART has burgeoned to a point where there is now controversy regarding whether living with HIV or being on ART presents a greater cardiovascular threat [85].

In the light of the many cardiovascular and other adverse effects of ART, a CD4-positive T-cell count-guided use of these drugs, as opposed to lifelong continuous use, has been proposed. This was investigated by the 'Strategies for Management of AntiRetroviral Therapy (SMART)' trial, yet, contrary to expectations, they noted an increase in the rate of adverse cardiovascular events associated with the interruption of antiretroviral therapy, albeit with borderline statistical significance. Changes in serum lipids were less favourable in participants using CD4-positive T-cell count-guided ART, which might have, in part, accounted for the observed increase in cardiovascular risk in this treatment group [86].

Since endothelial dysfunction is widely regarded as an early hallmark of atherogenesis and subsequent CVD, it comes as little surprise that it is also implicated as a putative link between ART and cardiovascular risk (Fig. 1). Yet, there have been some discrepancies in this regard. In HIV-positive human participants who were either treatment naïve or had not used ART for at least 6 months, ART seemed to lower asymmetric dimethylarginine (ADMA) levels – a novel marker of endothelial dysfunction [87]; in addition, Francisci *et al.*[88] showed that the levels of several biomarkers of vascular inflammation (sVCAM-1, MCP-1 and von Willebrand factor) were lowered by short-term HAART. In our laboratory, treatment with a fixed-dose combination of Emtricitabine–Tenofovir–Efavirenz improved vascular function in the aortas of rats, which was associated with increased eNOS expression [89]. In 2013, the WHO published new recommendations on first-line ART regimens [90]. According to these guidelines, it is strongly recommended that first-line ART be initiated as a fixed-dose combination (FDC) consisting of two NRTIs,

Tenofovir (TDF) plus Lamivudine (3TC) or Emtricitabine (FTC), and one NNRTI, Efavirenz (EFV). Subsequently, the use of FDC regimens has gained popularity in many countries, including South Africa, which manages the world's largest Government ART roll-out programme. Once-daily FDC, due to smaller pill burdens and less frequent dosing, imparts a considerable decrease in regimen complexity, which, together with the enhanced drug tolerability of contemporary regimens, has been shown to allow for improved initial ART regimen durability [91]. According to the WHO recommendations, second-line ART should comprise two NRTIs as well as a ritonavir-boosted protease inhibitor such as Lopinavir (LPV/r). Components of both first- and second-line FDC treatments have been associated with endothelial dysfunction. Given the contrasting findings on the endothelial effects of ART from previous studies, a closer examination of the mechanisms involved is warranted considering the sheer scope of FDC roll-out programmes globally. For the purposes of this review, the following commonly used ART drugs, will be discussed: TDF, FTC and EFV, as well as Lopinavir and Ritonavir.

Tenofovir, Emtricitabine and Efavirenz

With regards to endothelial effects, the NNRTI, EFV, is the most widely researched drug in the reverse transcriptase class and an association with impaired endothelial function has been shown in humans [92] and rats [93]. In an *in vitro* study of human coronary artery endothelial cells, EFV significantly increased monolayer permeability, which researchers ascribed to decreased expression of the tight junction proteins ZO-1, claudin-1, occludin and JAM-1 – effects mediated by increased ROS generation and the activation of JNK and NFκB [94]. In mice and in human cerebral microvascular endothelial cells, EFV was shown to affect endothelial integrity, where exposure to the drug led to decreased levels of the tight junction protein, claudin-5, and increased endothelial permeability [95]. In human umbilical vein endothelial cells, treatment with EFV resulted in an increase in ROS, which was additionally associated with the induction of heat-shock proteins, endoplasmic reticulum stress as well as autophagy [96]. In brain microvessels of HIV transgenic mice receiving continuous EFV treatment, endothelial cells displayed endoplasmic reticulum (ER) stress associated with a reduction in autophagy; these phenomena were also detected in human blood brain barrier cells, including cultured cerebral microvascular endothelial cells. These findings were somewhat unexpected as the induction of ER stress is generally associated with an increase in autophagic activity [97]. Bearing the aforementioned effects on blood brain barrier cells in mind, it may not be surprising that long-term EFV use was associated with poorer neurocognitive outcomes compared to LPV/r in a retrospective cohort study of 445 HIV-positive patients [98]. In a study researching the effects of Atripla®, a FDC antiretroviral drug consisting of TDF, FTC and EFV, the EFV component and not TDF or FTC, was found to be associated with increased oxidative stress and PARP, a DNA repair enzyme, activity in cultured endothelial cells as well as increased apoptosis and necrosis. In the same study, EFV also promoted impaired endothelium-derived function in rat aortic rings [93].

The antiviral activity of acyclic nucleoside phosphonates, which includes TDF, was discovered in the 1980s by Antonín Holý and Erik De Clercq [99] and although not as well researched as EFV, current evidence suggests that TDF is not associated with endothelial dysfunction. FTC has also not been linked to notable vascular consequences. When human umbilical vein endothelial cells and leucocytes were treated with TDF and FTC *in vitro*, both in combination and separately, no changes were observed in leucocyte-endothelial cell interactions [100]. Kim *et al.*[101] found no evidence of any direct *in vitro* effects by TDF on the gene transcription and expression of proinflammatory, pro-oxidative stress or pro-apoptotic genes in human coronary artery endothelial cells.

Lopinavir and Ritonavir

Of the protease inhibitors recommended for second-line ART by the WHO, Ritonavir has been most directly associated with endothelial dysfunction, and our search was unable to identify studies investigating the endothelial effects of Lopinavir in isolation. When the effects of several HIV protease inhibitors on porcine coronary arteries were investigated, significant vasomotor dysfunction, decreased eNOS expression and increased superoxide anion production were observed, with Ritonavir exhibiting the more potent effects [102]. Ritonavir has been found to cause impaired endothelial function through a reduction in eNOS expression and enhancement of oxidative stress levels in porcine pulmonary arteries and human pulmonary artery endothelial cells. In the porcine pulmonary artery rings, Ritonavir significantly reduced contraction and endothelium-dependent relaxation in a concentration-dependent manner. A significant reduction in eNOS mRNA and protein levels was observed in cultured human pulmonary artery endothelial cells subsequent to Ritonavir treatment [103]. Ritonavir-boosted protease

inhibitors have been shown to induce vascular endothelial cell dysfunction, ROS production, inflammation and senescence to varying degrees in human coronary artery endothelial cells, with the strongest effects detected in cells treated with Lopinavir boosted with Ritonavir (LPV/r). Both eNOS expression and NO production were decreased by LPV/r, while endothelin-1 (an endothelium-derived vasoconstrictor) expression was increased. Furthermore, the secretion of soluble ICAM or soluble VCAM (indicative of altered cell integrity) was increased ~ 2-3 fold by LPV/r [104]. However, contrary to the above *in vitro* studies, a study investigating the effects of LPV/r in healthy, nonobese human subjects, failed to show evidence of endothelial dysfunction [105].

Apart from the direct effects of Ritonavir on endothelial cells, the drug can potentially also contribute to endothelial dysfunction in a more indirect manner as it has additionally been associated with serum lipid changes, a known risk factor for the development of endothelial dysfunction. In a cohort of HIV-negative human subjects, 100 mg of Ritonavir taken twice daily significantly increased total cholesterol, LDL cholesterol, total cholesterol/high-density lipoprotein (HDL) cholesterol ratio and triglycerides and reduced HDL cholesterol in the participants [106]. In a human study conducted in Ethiopia, Gleason *et al.*[107] suggested that current EFV and Lopinavir-Ritonavir treatment regimens may play a role in the development of HIV-associated preclinical atherosclerosis as these subjects exhibited elevated cholesterol, total cholesterol/HDL cholesterol ratio and triglycerides as well as elevated markers of inflammation.

Conclusion

Attributing the disproportionately high incidence of CVD in the HIV-positive population to a single cause is not possible. This is clearly a multifaceted phenomenon encompassing a complex interplay of direct and indirect factors. Yet, endothelial dysfunction appears to be a common underlying factor, emphasising the overwhelming importance of the role played by this homoeostasis-regulating organ in health and disease. In this paper, we reviewed the extant *in vitro* evidence on the direct endothelial effects of the human immunodeficiency virus and its treatment, focussing on HIV-1 proteins, HIV-induced proinflammatory cytokines and common ART drugs (Table 1). Increased ROS production and oxidative stress, linked to decreased NO bioavailability and ensuing endothelial dysfunction, have emerged as the common underlying mechanisms afflicting the vascular endothelium in the wake of HIV and ART. It is clear from the literature, however, that a significant gap still exists in terms of basic research papers providing data on the exact underlying cellular mechanisms involved in HIV-1 infection and ART. Bridging this gap could pave the way for the development of future strategies aimed at the prevention and treatment of early cardiovascular changes in PLWHA.

Acknowledgements

This work was supported by the National Research Foundation of South Africa; the Department of Science and Technology, South Africa; Early Research Career Funding (Stellenbosch University) and the Harry Crossley Foundation (Stellenbosch University).

Conflict of interest

None.

Author contributions

The review was conceptualised by CM, AG and HS. CM developed the manuscript draft and outline, and it was refined and edited by all the authors. The final manuscript was reviewed and approved by all the authors.

References

1 Islam FM, Wu J, Jansson J & Wilson DP (2012) Relative risk of cardiovascular disease among people living with HIV: a systematic review and meta-analysis. *HIV Med* **13**, 453–468.
2 UNAIDS (2016) *Global AIDS Update 2016*.
3 Strijdom H, De Boever P, Nawrot TS & Goswami N (2016) HIV/AIDS: Emerging threat to cardiovascular health in sub-Saharan Africa. *South African Med J* **106**, 537.
4 Mudau M, Genis A, Lochner A & Strijdom H (2012) Endothelial dysfunction: the early predictor of atherosclerosis. *Cardiovasc J Afr* **23**, 222–231.
5 Kline ER & Sutliff RL (2008) The roles of HIV-1 proteins and antiretroviral drug therapy in HIV-1-associated endothelial dysfunction. *J Investig Med* **56**, 752–769.
6 Strijdom H, De Boever P, Walzl G, Essop MF, Nawrot TS, Webster I, Westcott C, Mashele N, Everson F, Malherbe ST *et al.* (2017) Cardiovascular risk and endothelial function in people living with HIV/AIDS: design of the multi-site, longitudinal EndoAfrica study in the Western Cape Province of South Africa. *BMC Infect Dis* **17**, 1–9.

7 Andrade ACO & Cotter BR (2006) Endothelial function and cardiovascular diseases in HIV infected patient. *Braz J Infect Dis* **10**, 139–145.
8 Skowyra A, Zdziechowicz I, Mikuła T & Wiercińska-Drapało A (2012) Endothelial dysfunction – an important factor in the progression of atherosclerosis in HIV-infected persons. *HIV AIDS Rev* **11**, 57–60.
9 Mu H, Chai H, Lin PH, Yao Q & Chen C (2007) Current update on HIV-associated vascular disease and endothelial dysfunction. *World J Surg* **31**, 632–643.
10 Graham SM, Mwilu R & Liles WC (2013) Clinical utility of biomarkers of endothelial activation and coagulation for prognosis in HIV infection: a systematic review. *Spec Sect Spec Focus Endothel Act* **4**, 564–571.
11 Mazzuca P, Caruso A & Caccuri F (2016) HIV-1 infection, microenvironment and endothelial cell dysfunction. *New Microbiol* **39**, 163–173.
12 Kedzierska K & Crowe SM (2001) Cytokines and HIV-1: interactions and clinical implications. *Antivir Chem Chemother* **12**, 133–150.
13 Deanfield JE, Halcox JP & Rabelink TJ (2007) Endothelial function and dysfunction: testing and clinical relevance. *Circulation* **115**, 1285–1295.
14 Förstermann U & Sessa WC (2012) Nitric oxide synthases: regulation and function. *Eur Heart J* **33**, 829–837.
15 Higashi Y, Noma K, Yoshizumi M & Kihara Y (2009) Endothelial function and oxidative stress in cardiovascular diseases. *Circ J* **73**, 411–418.
16 Xiao L, Liu Y & Wang N (2014) New paradigms in inflammatory signaling in vascular endothelial cells. *AJP Hear Circ Physiol* **306**, H317–H325.
17 Wentzel JJ, Chatzizisis YS, Gijsen FJH, Giannoglou GD, Feldman CL & Stone PH (2012) Endothelial shear stress in the evolution of coronary atherosclerotic plaque and vascular remodelling: current understanding and remaining questions. *Cardiovasc Res* **96**, 234–243.
18 Gimbrone MA & García-Cardeña G (2016) Endothelial cell dysfunction and the pathobiology of atherosclerosis. *Circ Res* **118**, 620–636.
19 Lambert CT, Sandesara PB, Hirsh B, Shaw LJ, Lewis W, Quyyumi AA, Schinazi RF, Post WS & Sperling L (2016) HIV, highly active antiretroviral therapy and the heart: a cellular to epidemiological review. *HIV* **17**, 411–424.
20 Dirajlal-Fargo S, Sattar A, Kulkarni M, Bowman E, Funderburg N & McComsey GA (2017) HIV-positive youth who are perinatally infected have impaired endothelial function. *Aids* **31**, 1917–1924.
21 Crowe SM, Westhorpe CLV, Mukhamedova N, Jaworowski A, Sviridov D & Bukrinsky M (2010) The macrophage: the intersection between HIV infection and atherosclerosis. *J Leukoc Biol* **87**, 589–598.
22 Maartens G, Celum C & Lewin SR (2014) HIV infection: Epidemiology, pathogenesis, treatment, and prevention. In *The Lancet*, Vol. 384, pp. 258–271. Elsevier Ltd., London.
23 Turner BG & Summers MF (1999) Structural biology of HIV. *J Mol Biol* **285**, 1–32.
24 Freed EO (2015) HIV-1 assembly, release and maturation. *Nat Rev Microbiol* **13**, 484–496.
25 Götte M, Li X & Wainberg MA (1999) HIV-1 reverse transcription: a brief overview focused on structure-function relationships among molecules involved in initiation of the reaction. *Arch Biochem Biophys* **365**, 199–210.
26 Hansen L, Parker I, Sutliff RL, Platt MO & Gleason RL (2013) Endothelial dysfunction, arterial stiffening, and intima-media thickening in large arteries from HIV-1 transgenic mice. *Ann Biomed Eng* **41**, 682–693.
27 Debaisieux S, Rayne F, Yezid H & Beaumelle B (2012) The Ins and Outs of HIV-1 Tat. *Traffic* **13**, 355–363.
28 Price TO, Ercal N, Nakaoke R & Banks WA (2005) HIV-1 viral proteins gp120 and Tat induce oxidative stress in brain endothelial cells. *Brain Res* **1045**, 57–63.
29 Liu K, Chi DS, Li C, Hall HK, Milhorn DM, Krishnaswamy G, Denise M & Tat GKH (2005) HIV-1 Tat protein-induced VCAM-1 expression in human pulmonary artery endothelial cells and its signaling. *Am J Physiol Lung Cell Mol Physiol* **289**, L252–L260.
30 Duan M, Yao H, Hu G, Chen XM, Lund AK & Buch S (2013) HIV Tat induces expression of ICAM-1 in HUVECs: implications for miR-221/-222 in HIV-associated cardiomyopathy. *PLoS ONE* **8**, 1–11.
31 Andras IE, Pu H, Deli MA, Nath A, Hennig B & Toborek M (2003) HIV-1 Tat protein alters tight junction protein expression and distribution in cultured brain endothelial cells. *J Neurosci Res* **74**, 255–265.
32 Xu R, Feng X, Xie X, Zhang J, Wu D & Xu L (2012) HIV-1 Tat protein increases the permeability of brain endothelial cells by both inhibiting occludin expression and cleaving occludin via matrix metalloproteinase-9. *Brain Res* **1436**, 13–19.
33 Cheng XW, Kikuchi R, Ishii H, Yoshikawa D, Hu L, Takahashi R, Shibata R, Ikeda N, Kuzuya M, Okumura K *et al.* (2013) Circulating cathepsin K as a potential novel biomarker of coronary artery disease. *Atherosclerosis* **228**, 211–216.
34 Parker IK, Roberts LM, Hansen L, Gleason RL, Sutliff RL & Platt MO (2014) Pro-atherogenic shear stress and hiv proteins synergistically upregulate cathepsin K in endothelial cells. *Ann Biomed Eng* **42**, 1185–1194.
35 Park I-W, Ullrich CK, Schoenberger E, Ganju RK & Groopman JE (2001) HIV-1 Tat induces microvascular endothelial apoptosis through caspase activation. *J Immunol* **167**, 2766–2771.

36 Planès R, Ben Haij N, Leghmari K, Serrero M, BenMohamed L & Bahraoui E (2016) HIV-1 Tat protein activates both the MyD88 and TRIF pathways to induce tumor necrosis factor alpha and interleukin-10 in human monocytes. *J Virol* **90**, 5886–5898.

37 Yang B, Akhter S, Chaudhuri A & Kanmogne GD (2009) HIV-1 gp120 induces cytokine expression, leukocyte adhesion, and transmigration across the blood-brain barrier: modulatory effects of STAT1 signaling. *Microvasc Res* **77**, 212–219.

38 Jiang J, Fu W, Wang X, Lin PH, Yao Q & Chen C (2010) HIV gp120 induces endothelial dysfunction in tumour necrosis factor-α-activated porcine and human endothelial cells. *Cardiovasc Res* **87**, 366–374.

39 Kanmogne GD, Schall K, Leibhart J, Knipe B, Gendelman HE & Persidsky Y (2007) HIV-1 gp120 compromises blood-brain barrier integrity and enhance monocyte migration across blood-brain barrier: implication for viral neuropathogenesis. *J Cereb Blood Flow Metab* **27**, 123–134.

40 Li L, Li HS, Pauza CD, Bukrinsky M & Zhao RY (2005) Roles of HIV-1 auxiliary proteins in viral pathogenesis and host-pathogen interactions. *Cell Res* **15**, 923–934.

41 Wang T, Green LA, Gupta SK, Kim C, Wang L, Almodovar S, Flores SC, Prudovsky IA, Jolicoeur P, Liu Z *et al.* (2014) Transfer of intracellular HIV Nef to endothelium causes endothelial dysfunction. *PLoS ONE* **9**, e91063.

42 Duffy P, Wang X, Lin PH, Yao Q & Chen C (2009) HIV Nef protein causes endothelial dysfunction in porcine pulmonary arteries and human pulmonary artery endothelial cells. *J Surg Res* **156**, 257–264.

43 Cui HL, Ditiatkovski M, Kesani R, Bobryshev YV, Liu Y, Geyer M, Mukhamedova N, Bukrinsky M & Sviridov D (2014) HIV protein Nef causes dyslipidemia and formation of foam cells in mouse models of atherosclerosis. *FASEB J* **28**, 2828–2839.

44 Guatelli JC (2009) Interactions of viral protein U (Vpu) with cellular factors. In Current Topics in Microbiology and Immunology: HIV Interactions with Host Cell Proteins (Spearman P & Freed EO, eds), pp. 27–45. Springer-Verlag, Berlin Heidelberg.

45 Sugden SM, Pham TNQ & Cohen EA (2017) HIV-1 Vpu downmodulates ICAM-1 expression, resulting in decreased killing of infected CD4+ T cells by NK cells. *J Virol* **91**, e02442–16.

46 Henderson WW, Ruhl R, Lewis P, Bentley M, Nelson JA & Moses AV (2004) Human immunodeficiency virus (HIV) type 1 Vpu induces the expression of CD40 in endothelial cells and regulates HIV-induced adhesion of B-lymphoma cells. *J Virol* **78**, 4408–4420.

47 Acheampong E, Mukhtar M, Parveen Z, Ngoubilly N, Ahmad N, Patel C & Pomerantz RJ (2002) Ethanol strongly potentiates apoptosis induced by HIV-1 proteins in primary human brain microvascular endothelial cells. *Virology* **304**, 222–234.

48 Dinarello CA (2000) Proinflammatory cytokines. *CHEST J* **118**, 503–508.

49 Kofler S, Nickel T & Weis M (2005) Role of cytokines in cardiovascular diseases: a focus on endothelial responses to inflammation. *Clin Sci* **108**, 205–213.

50 Zhang C (2008) The role of inflammatory cytokines in endothelial dysfunction. *Basic Res Cardiol* **103**, 398–406.

51 Hunt PW (2012) HIV and inflammation: mechanisms and consequences. *Curr HIV/AIDS Rep* **9**, 139–147.

52 Bahrami H, Budoff M, Haberlen SA, Rezaeian P, Ketlogetswe K, Tracy R, Palella F, Witt MD, McConnell MV, Kingsley L *et al.* (2016) Inflammatory markers associated with subclinical coronary artery disease: the multicenter AIDS cohort study. *J Am Heart Assoc* **5**, 1–13.

53 Younas M, Psomas C, Reynes J & Corbeau P (2016) Immune activation in the course of HIV-1 infection: causes, phenotypes and persistence under therapy. *HIV Med* **17**, 89–105.

54 Deeks SG (2011) HIV infection, inflammation, immunosenescence, and aging. *Annu Rev Med* **62**, 141–155.

55 Steyers CM & Miller FJ (2014) Endothelial dysfunction in chronic inflammatory diseases. *Int J Mol Sci* **15**, 11324–11349.

56 Freeman ML, Shive CL, Nguyen TP, Younes SA, Panigrahi S & Lederman MM (2016) Cytokines and T-Cell homeostasis in HIV infection. *J Infect Dis* **214**, S51–S57.

57 Cavaillon JM (2001) Pro- versus anti-inflammatory cytokines: myth or reality. *Cell Mol Biol (Noisy-le-grand)*. **47**, 695–702.

58 Appay V & Sauce D (2008) Immune activation and inflammation in HIV-1 infection: causes and consequences. *J Pathol* **214**, 231–241.

59 Madge LA & Pober JS (2001) TNF signaling in vascular endothelial cells. *Exp Mol Pathol* **70**, 317–325.

60 Genis A, Smit S, Westcott C, Mthethwa M & Strijdom H (2014) Attenuation of eNOS-NO biosynthesis, up-regulation of antioxidant proteins and differential protein regulation in TNF-Alpha treated cardiac endothelial cells: Early signs of endothelial dysfunction. In *Endothelial Dysfunction: Risk Factors, Role in Cardiovascular Diseases and Therapeutic Approaches*. Nova Scientific Publishers, Hauppauge, NY.

61 Corda S, Laplace C, Vicaut E & Duranteau J (2001) Rapid reactive oxygen species production by mitochondria in endothelial cells exposed to tumor necrosis factor-alpha is mediated by ceramide. *Am J Respir Cell Mol Biol* **24**, 762–768.

62 Gao X, Belmadani S, Picchi A, Xu X, Potter BJ, Tewari-Singh N, Capobianco S, Chilian WM & Zhang

C (2007) Tumor necrosis factor- induces endothelial dysfunction in Leprdb mice. *Circulation* **115**, 245–254.
63 O'Carroll SJ, Kho DT, Wiltshire R, Nelson V, Rotimi O, Johnson R, Angel CE & Graham ES (2015) Pro-inflammatory TNFα and IL-1β differentially regulate the inflammatory phenotype of brain microvascular endothelial cells. *J Neuroinflammation* **12**, 1–18.
64 Norris PJ, Pappalardo BL, Custer B, Spotts G, Hecht FM & Busch MP (2006) Elevations in IL-10, TNF-α, and IFN-γ from the earliest point of HIV type 1 infection. *AIDS Res Hum Retroviruses* **22**, 757–762.
65 Kaplan RC, Landay AL, Hodis HN, Gange SJ, Norris PJ, Young M, Anastos K, Tien PC, Xue X, Lazar J *et al.* (2012) Potential cardiovascular disease risk markers among HIV-infected women initiating antiretroviral treatment. *J Acquir Immune Defic Syndr* **60**, 359–368.
66 Ross AC, Rizk N, O'Riordan MA, Dogra V, El-Bejjani D, Storer N, Harrill D, Tungsiripat M, Adell J & McComsey GA (2009) Relationship between Inflammatory Markers, Endothelial Activation Markers, and Carotid Intima-Media Thickness in HIV-Infected Patients Receiving Antiretroviral Therapy. *Clin Infect Dis* **49**, 1119–1127.
67 Bujak M & Frangogiannis NG (2009) The role of IL-1 in the pathogenesis of heart disease. *Arch Immunol Ther Exp (Warsz)* **57**, 165–176.
68 Ridker PM (2016) From C-Reactive protein to interleukin-6 to interleukin-1: moving upstream to identify novel targets for atheroprotection. *Circ Res* **118**, 145–156.
69 Guo H, Gao J, Taxman DJ, Ting JPY & Su L (2014) HIV-1 infection induces interleukin-1β production via TLR8 protein-dependent and NLRP3 inflammasome mechanisms in human monocytes. *J Biol Chem* **289**, 21716–21726.
70 Makó V, Czúcz J, Weiszhár Z, Herczenik E, Matkó J, Prohászka Z & Cervenak L (2010) Proinflammatory activation pattern of human umbilical vein endothelial cells induced by IL-1β, TNF-α, and LPS. *Cytom Part A* **77**, 962–970.
71 Gabay C & Kushner I (1999) Acute-phase proteins and other systemic responses to inflammation. *N Engl J Med* **340**, 448–454.
72 Kuller LH, Tracy R, Belloso W, De Wit S, Drummond F, Lane HC, Ledergerber B, Lundgren J, Neuhaus J, Nixon D *et al.* (2008) Inflammatory and coagulation biomarkers and mortality in patients with HIV infection. *PLoS Med* **5**, 1496–1508.
73 French MA, Cozzi-Lepri A, Arduino RC, Johnson M, Achhra AC, Landay A & Group TISS (2015) Plasma levels of cytokines and chemokines and the risk of mortality in HIV-infected individuals: a case-control analysis nested in a large clinical trial. *AIDS* **29**, 847–851.
74 Duprez DA, Neuhaus J, Kuller LH, Tracy R, Belloso W, De Wit S, Drummond F, Lane HC, Ledergerber B, Lundgren J *et al.* (2012) Inflammation, coagulation and cardiovascular disease in HIV-infected individuals. *PLoS ONE* **7**, e44454.
75 Howren MB, Lamkin DM & Suls J (2009) Associations of depression with c-reactive protein, IL-1, and IL-6: A meta-analysis. *Psychosom Med* **71**, 171–186.
76 Borges ÁH, O'Connor JL, Phillips AN, Rönsholt FF, Pett S, Vjecha MJ, French MA & Lundgren JD (2015) Factors associated with plasma IL-6 levels during HIV infection. *J Infect Dis* **212**, 585–595.
77 Hsu DC, Ma YF, Hur S, Li D, Rupert A, Scherzer R, Kalapus SC, Deeks S, Sereti I & Hsue PY (2016) Plasma IL-6 levels are independently associated with atherosclerosis and mortality in HIV-infected individuals on suppressive antiretroviral therapy. *Aids* **30**, 2065–2074.
78 Guo F, Dong M, Ren F, Zhang C, Li J, Tao Z, Yang J & Li G (2014) Association between local interleukin-6 levels and slow flow/microvascular dysfunction. *J Thromb Thrombolysis* **37**, 475–482.
79 Pasceri V, Willerson JT & Yeh ETH (2000) Direct proinflammatory effect of C-reactive protein on human endothelial cells. *Circulation* **102**, 2165–2168.
80 Verma S, Wang CH, Li SH, Dumont AS, Fedak PWM, Badiwala MV, Dhillon B, Weisel RD, Li RK, Mickle DAG *et al.* (2002) A self-fulfilling prophecy: C-reactive protein attenuates nitric oxide production and inhibits angiogenesis. *Circulation* **106**, 913–919.
81 Venugopal SK, Devaraj S, Yuhanna I, Shaul P & Jialal I (2002) Demonstration that C-reactive protein decreases eNOS expression and bioactivity in human aortic endothelial cells. *Circulation* **106**, 1439–1441.
82 Desai TR, Leeper NJ, Hynes KL & Gewertz BL (2002) Interleukin-6 causes endothelial barrier dysfunction via the protein kinase C pathway. *J Surg Res* **104**, 118–123.
83 Alsaffar H, Martino N, Garrett JP & Adam AP (2018) Interleukin-6 promotes a sustained loss of endothelial barrier function via Janus kinase-mediated STAT3 phosphorylation and de novo protein synthesis. *Am J Physiol – Cell Physiol* **314**, C589–C602.
84 Reiss P, Sabin CA, Weber R, El-sadr W, De Wit S, Universi- CH, Kirk O, Fontas E, Hos- C, Law MG *et al.* (2007) Class of antiretroviral drugs and the risk of myocardial infarction. *N Engl J Med* **356**, 1723–1735.
85 Wang T, Yi R, Green LA, Chelvanambi S, Seimetz M & Clauss M (2015) Increased cardiovascular disease risk in the HIV-positive population on ART: potential role of HIV-Nef and Tat. *Cardiovasc Pathol* **24**, 279–282.
86 Phillips AN, Carr A, Neuhaus J, Visnegarwala F, Prineas R, Burman WJ, Williams I, Drummond F, Duprez D, Belloso WH *et al.* (2008) Interruption of

antiretroviral therapy and risk of cardiovascular disease in persons with HIV-1 infection: exploratory analyses from the SMART trial. *Antivir Ther* **13**, 177–187.
87 Baker JV, Neuhaus J, Duprez D, Freiberg MS, Bernardino JI, Badley AD, DaE Nixon, Lundgren JD, Tracy RP & Neaton JD (2012) HIV replication, inflammation, and the effect of starting antiretroviral therapy on plasma asymmetric dimethylarginine, a novel marker of endothelial dysfunction. *J Acquir Immune Defic Syndr* **60**, 128–134.
88 Francisci D, Giannini S, Baldelli F, Leone M, Belfiori B, Guglielmini G, Malincarne L & Gresele P (2009) HIV type 1 infection, and not short-term HAART, induces endothelial dysfunction. *Aids* **23**, 589–596.
89 Strijdom H, Goswami N, De Boever P, Westcott C, Ogundipe T, Everson F & Genis A (2016) Cardiometabolic and vascular effects of treatment with a fixed-dose combination anti-retroviral drug containing nucleoside and non-nucleoside reverse transcriptase inhibitors (NRTIs and NNRTIs) in adult rats. *Atherosclerosis* **252**, e166.
90 WHO (2013) HIV/AIDS Summary of new recommendations. Consol. ARV Guidel. June 2013.
91 Willig JH, Abroms S, Westfall AO, Routman J, Adusumilli S, Varshney M, Allison J, Chatham A, Raper JL, Kaslow RA *et al.* (2008) Increased regimen durability in the era of once daily fixed-dose combination antiretroviral therapy. *AIDS* **22**, 1951–1960.
92 Gupta SK, Shen C, Moe SM, Kamendulis LM, Goldman M & Dubé MP (2012) Worsening endothelial function with Efavirenz compared to protease inhibitors: a 12-month prospective study. *PLoS ONE* **7**, 5–10.
93 Faltz M, Bergin H, Pilavachi E, Grimwade G & Mabley JG (2017) Effect of the anti-retroviral drugs Efavirenz, Tenofovir and Emtricitabine on endothelial cell function: role of PARP. *Cardiovasc Toxicol* **17**, 393–404.
94 Jamaluddin MS, Lin PH, Yao Q & Chen C (2010) Non-nucleoside reverse transcriptase inhibitor efavirenz increases monolayer permeability of human coronary artery endothelial cells. *Atherosclerosis* **208**, 104–111.
95 Bertrand L, Dygert L & Toborek M (2016) Antiretroviral treatment with Efavirenz disrupts the blood-brain barrier integrity and increases stroke severity. *Sci Rep* **6**, 39738.
96 Weiß M, Kost B, Renner-Müller I, Wolf E, Mylonas I & Brüning A (2016) Efavirenz causes oxidative stress, endoplasmic reticulum stress, and autophagy in endothelial cells. *Cardiovasc Toxicol* **16**, 90–99.
97 Bertrand L & Toborek M (2015) Dysregulation of endoplasmic reticulum stress and autophagic responses by the antiretroviral drug Efavirenz. *Mol Pharmacol* **88**, 304–315.
98 Ma Q, Vaida F, Wong J, Sanders CA, Kao Y ting, Croteau D, Clifford DB, Collier AC, Gelman BB, Marra CM *et al.* (2016) Long-term efavirenz use is associated with worse neurocognitive functioning in HIV-infected patients. *J Neurovirol* **22**, 170–178.
99 De Clercq E & Holý A (2005) Case history: Acyclic nucleoside phosphonates: A key class of antiviral drugs. *Nat Rev Drug Discov* **4**, 928–940.
100 De Pablo C, Orden S, Calatayud S, Martí-Cabrera M, Esplugues JV & Álvarez Á (2012) Differential effects of tenofovir/emtricitabine and abacavir/lamivudine on human leukocyte recruitment. *Antivir Ther* **17**, 1615–1619.
101 Kim C, Gupta SK, Green L, Taylor BM, Deuter-Reinhard M, Desta Z & Clauss M (2011) Abacavir, didanosine and tenofovir do not induce inflammatory, apoptotic or oxidative stress genes in coronary endothelial cells. *Antivir Ther* **16**, 1335–1339.
102 Chai H, Yang H, Yan S, Li M, Lin PH, Lumsden AB, Yao Q & Chen C (2005) Effects of 5 HIV protease inhibitors on vasomotor function and superoxide anion production in porcine coronary arteries. *J Acquir Immune Defic Syndr* **40**, 12–19.
103 Wang X, Chai H, Lin PH, Yao Q & Chen C (2009) Roles and mechanisms of human immunodeficiency virus protease inhibitor ritonavir and other anti-human immunodeficiency virus drugs in endothelial dysfunction of porcine pulmonary arteries and human pulmonary artery endothelial cells. *Am J Pathol* **174**, 771–781.
104 Auclair M, Afonso P, Capel E, Caron-Debarle M & Capeau J (2014) Impact of darunavir, atazanavir and lopinavir boosted with ritonavir on cultured human endothelial cells: Beneficial effect of pravastatin. *Antivir Ther* **19**, 773–782.
105 Dubé MP, Shen C, Greenwald M & Mather KJ (2008) No Impairment of endothelial function or insulin sensitivity with 4 weeks of the HIV protease inhibitors Atazanavir or Lopinavir-Ritonavir in healthy subjects without HIV infection: a placebo-controlled trial. *Clin Infect Dis* **47**, 567–574.
106 Shafran S, Mashinter L & Roberts S (2005) The effect of low-dose ritonavir monotherapy on fasting serum lipid concentrations. *HIV Medicat* **6**, 421–425.
107 Gleason RL, Caulk AW, Seifu D, Parker I, Vidakovic B, Getenet H, Assefa G & Amogne W (2015) Current efavirenz (EFV) or ritonavir-boosted lopinavir (LPV/r) use correlates with elevate markers of atherosclerosis in HIV-infected subjects in Addis Ababa, Ethiopia. *PLoS ONE* **10**, e0117125.

APPENDIX B

HIV-1-protein Medium and Vehicle Control Cocktail Dilutions

For HIV-Medium 1:

Gp160 – 25ng/ml

Calculation for dosage of Gp160:

For a final concentration of 25ng/ml of Gp160 in 1ml of medium:

We make use of the formula: C1V1 = C2V2

Where:

C1 = 1mg/ml (this is the concentration at which we received the protein)

C2 = 25ng/ml (this is the final, working concentration that we want)

V1 = X (this is the volume of the protein in stock that we need to add to 1ml of medium to get the final, working concentration)

V2 = 1ml (this is the amount of medium per plate in an experimental setup)

Convert all to micro-units

1000ug/ml x X = 0.025ug/ml x 1000ul

X = 0.025*1000/1000

X = 0.025ul

You have to add 0.025ul to 1ml of medium to get the final concentration, but it is a very small amount, so we prepare a stock that is x1000 concentrated

Original conc.:

25ng/ml = 0.025ug/ml

X1000:

25ug/ml

The protein is received in 1mg/ml

0.025mg / 1mg x 1ml = 0.025ml = 25µl

*Thus take 25µl of original stock received (1mg/ml) and add to 975ul of PBS to get 1ml of an x1000 concentrated stock of 25µg/ml.

This step is to calculate how much of the concentrated stock we need to add to 1ml medium

To get the final correct concentration of 25ng/ml:

C1V1 = C2V2

25ug/mlx X = 25ng/mlx 1ml

Change all to micro-units:

25 x X = 0.025 x 1000

X = 0.025*1000/25

= 1

Thus, add 1ul of x1000 stock in 1ml of medium to get 25ng/ml.

Nef – 25ng/ml

Calculation for dosage of Nef:

For a final concentration of 25ng/ml of Nef in 1ml of medium:

We make use of the formula: C1V1 = C2V2

Where:

C1 = 1mg/ml (this is the concentration at which we received the protein)

C2 = 25ng/ml (this is the final, working concentration that we want)

V1 = X (this is the volume of the protein in stock that we need to add to 1ml of medium to get the final, working concentration)

V2 = 1ml (this is the amount of medium per plate in an experimental setup)

Convert all to micro-units

1000ug/ml x X = 0.025ug/ml x 1000ul

X = 0.025*1000/1000

X = 0.025ul

You have to add 0.025ul to 1ml of medium to get the final concentration, but it is a very small amount, so we prepare a stock that is x1000 concentrated

Original conc.:

25ng/ml= 0.025ug/ml

X1000:

25ug/ml

The protein is received in 1mg/ml

0.025mg / 1mg x 1ml = 0.025ml = 25µl

*Thus take 25µl of original stock received (1mg/ml) and add to 975ul of PBS to get 1ml of an x1000 concentrated stock of 25ug/ml.

This step is to calculate how much of the concentrated stock we need to add to 1ml medium

To get the final correct concentration of 25ng/ml:

C1V1 = C2V2

25ug/mlx X = 25ng/mlx 1ml

Change all to micro-units:

25 x X = 0.025 x 1000

X = 0.025*1000/25

= 1

Thus, add 1ul of x1000 stock in 1ml of medium to get 25ng/ml.

Tat – 25ng/ml

Calculation for dosage of Tat:

For a final concentration of 25ng/ml of Tat in 1ml of medium:

We Make use of the formula: C1V1 = C2V2

Where:

C1 = 50ug/ml (this is the concentration that we will reconstitute the protein in)

C2 = 25ng/ml (this is the final, working concentration that we want)

V1 = X (this is the volume of the protein in stock that we need to add to 1ml of a medium to get the final, working concentration)

V2 = 1ml (this is the amount of medium per plate in an experimental setup)

Convert all to micro-units

50ug/mlx X = 0.025ug/ml x 1000ul

X = 0.025*1000/50

X = 0.5ul

You have to add 0.5ul to 1ml of medium to get the final concentration.

Thus, add 0.5ul of original stock in 1ml of medium to get 25ng/ml.

HIV-Medium 1: 1µl Gp160, 1µ Nef and 0.5µl Tat stocks in 1ml growth medium

Vehicle Control Cocktail 1: Thus 2.5µl of PBS in 1ml growth medium

For HIV-Medium 2:

Gp160 – 50ng/ml

Calculation for dosage of Gp160:

For a final concentration of 50ng/ml of Gp160 in 1ml of medium:

We Make use of the formula: C1V1 = C2V2

Where:

C1 = 1mg/ml (this is the concentration at which we received the protein)

C2 = 50ng/ml (this is the final, working concentration that we want)

V1 = X (this is the volume of the protein in stock that we need to add to 1ml of medium to get the final, working concentration)

V2 = 1ml (this is the amount of medium per plate in an experimental setup)

Convert all to micro-units

1000ug/ml x X = 0.050ug/ml x 1000ul

X = 0.050*1000/1000

X = 0.050ul

You have to add 0.050ul to 1ml of medium to get the final concentration, but it is a very small amount, so we prepare a stock that is x1000 concentrated

Original conc.:

50ng/ml= 0.050ug/ml

X1000:

50ug/ml= 50ug/ml

The protein is received in 1mg/ml

0.050mg / 1mg x 1ml = 0.050ml = 50µl

*Thus take 50µl of original stock received (1mg/ml) and add to 950ul of PBS to get 1ml of an x1000 concentrated stock of 50µg/ml.

This step is to calculate how much of the concentrated stock we need to add to 1ml medium

To get the final correct concentration of 50ng/ml:

C1V1 = C2V2

50ug/mlx X = 50ng/mlx 1ml

Change all to micro-units:

50 x X = 0.050 x 1000

X = 0.050*1000/50 = 1

Thus, add 1ul of x1000 stock in 1ml of medium to get 50ng/ml.

Nef – 50ng/ml

Calculation for dosage of Nef:

For a final concentration of 100ng/ml of Nef in 1ml of medium:

We Make use of the formula: C1V1 = C2V2

Where:

C1 = 1mg/ml (this is the concentration at which we received the protein)

C2 = 50ng/ml (this is the final, working concentration that we want)

V1 = X (this is the volume of the protein in stock that we need to add to 1ml of medium to get the final, working concentration)

V2 = 1ml (this is the amount of medium per plate in an experimental setup)

Convert all to micro-units

1000ug/ml x X = 0.050ug/ml x 1000ul

X = 0.050*1000/1000

X = 0.050ul

You have to add 0.050ul to 1ml of medium to get the final concentration, but it is a very small amount, so we prepare a stock that is x1000 concentrated

Original conc.:

50ng/ml= 0.050ug/ml

X1000:

50ug/ml= 50ug/ml

The protein is received in 1mg/ml

0.050mg / 1mg x 1ml = 0.050ml = 50µl

*Thus take 50µl of original stock received (1mg/ml) and add to 950ul of PBS to get 1ml of an x1000 concentrated stock of 50µg/ml.

This step is to calculate how much of the concentrated stock we need to add to 1ml medium

To get the final correct concentration of 50ng/ml:

C1V1 = C2V2

50ug/mlx X = 50ng/mlx 1ml

Change all to micro-units:

50 x X = 0.050 x 1000

X = 0.050*1000/50 = 1

Thus, add 1ul of x1000 stock in 1ml of medium to get 50ng/ml.

Tat – 50ng/ml

Calculation for dosage of Tat:

For a final concentration of 50ng/ml of Tat in 1ml of medium:

We Make use of the formula: C1V1 = C2V2

Where:

C1 = 50ug/ml (this is the concentration that we will reconstitute the protein in)

C2 = 50ng/ml (this is the final, working concentration that we want)

V1 = X (this is the volume of the protein in stock that we need to add to 1ml of medium to get the final, working concentration)

V2 = 1ml (this is the amount of medium per plate in an experimental setup)

Convert all to micro-units

50ug/mlx X = 0.050ug/ml x 1000ul

X = 0.050*1000/50

X = 1ul

You have to add 1ul to 1ml of medium to get the final concentration, so we can leave at this.

Thus, add 1ul of original stock in 1ml of medium to get 50ng/ml.

HIV-Medium 2: 1µl Gp160, 1µl Nef and 1µl Tat stocks in 1ml growth medium

Vehicle Control Cocktail 2: Thus 3µl of PBS in 1ml of medium

For HIV-Medium 3:

Gp160 – 100ng/ml

Calculation for dosage of Gp160:

For a final concentration of 100ng/ml of Gp160 in 1ml of medium:

We Make use of the formula: C1V1 = C2V2

Where:

C1 = 1mg/ml (this is the concentration at which we received the protein)

C2 = 100ng/ml (this is the final, working concentration that we want)

V1 = X (this is the volume of the protein in stock that we need to add to 1ml of medium to get the final, working concentration)

V2 = 1ml (this is the amount of medium per plate in an experimental setup)

Convert all to micro-units

1000ug/ml x X = 0.100ug/ml x 1000ul

X = 0.100*1000/1000

X = 0.1ul

You have to add 0.1ul to 1ml of medium to get the final concentration, but it is a very small amount, so we prepare a stock that is x1000 concentrated

Original conc.:

100ng/ml = 0.1ug/ml

X1000:

100ug/ml

The protein is received in 1mg/ml

100ug / 1000ug x 1000ul = 100µl

*Thus take 100µl of original stock received (1mg/ml) and add to 900ul of PBS to get 1ml of an x1000 concentrated stock of 100µg/ml.

This step is to calculate how much of the concentrated stock we need to add to 1ml medium

To get the final correct concentration of 50ng/ml:

C1V1 = C2V2

100ug/ml x X = 100ng/ml x 1ml

Change all to micro-units:

100 x X = 0.1 x 1000

X = 0.1*1000/100

= 1

Thus, add 1ul of x100 stock in 1ml of medium to get 100ng/ml

Nef – 100ng/ml ***(Note: Nef was recalculated when new stock arrived – see later)*

Calculation for dosage of Nef:

For a final concentration of 200ng/ml of Nef in 1ml of medium:

We Make use of the formula: C1V1 = C2V2

Where:

C1 = 1mg/ml (this is the concentration at which we received the protein)

C2 = 100ng/ml (this is the final, working concentration that we want)

V1 = (this is the volume of the protein in stock that we need to add to 1ml of medium to get the final, working concentration)

V2 = 1ml (this is the amount of medium per plate in an experimental setup)

Convert all to micro-units

1000ug/ml x X = 0.100ug/ml x 1000ul

X = 0.100*1000/1000

X = 0.1ul

You have to add 0.1ul to 1ml of medium to get the final concentration, but it is a very small amount, so we prepare a stock that is x1000 concentrated

Original conc.:

100ng/ml = 0.1ug/ml

X1000:

100ug/ml

The protein is received in 1mg/ml

100ug / 1000ug x 1000ul = 100µl

*Thus take 100µl of original stock received (1mg/ml) and add to 900ul of PBS to get 1ml of an x1000 concentrated stock of 100µg/ml.

This step is to calculate how much of the concentrated stock we need to add to 1ml medium

To get the final correct concentration of 50ng/ml:

C1V1 = C2V2

100ug/ml x X = 100ng/ml x 1ml

Change all to micro-units:

100 x X = 0.1 x 1000

X = 0.1*1000/100

= 1

Thus, add 1ul of x100 stock in 1ml of medium to get 100ng/ml.

Tat – 100ng/ml

Calculation for dosage of Tat:

For a final concentration of 100ng/ml of Ta in 1ml of medium:

We Make use of the formula: C1V1 = C2V2

Where:

C1 = 50ug/ml (this is the concentration that we will reconstitute the protein in)

C2 = 100ng/ml (this is the final, working concentration that we want)

V1 = X (this is the volume of the protein in stock that we need to add to 1ml of medium to get the final, working concentration)

V2 = 1ml (this is the amount of medium per plate in an experimental setup)

Convert all to micro-units

50ug/mlx X = 0.1ug/ml x 1000ul

X = 0.1*1000/50

X = 2ul

Thus, add 2ul of stock in 1ml of medium to get 100ng/ml.

HIV-Medium 3: 1ul of Gp160, 1ul of Nef and 2ul of Tat stocks in 1ml growth medium

Vehicle Control Cocktail 3: 4ul of PBS in 1ml growth medium

***New Nef – 100ng/ml**

Calculation for dosage of Nef:

For a final concentration of 100ng/ml of Nef in 1ml of medium:

We Make use of the formula: C1V1 = C2V2

Where:

C1 = 0.48mg/ml (this is the concentration at which we received the protein)

C2 = 100ng/ml (this is the final, working concentration that we want)

V1 = X (this is the volume of the protein in stock that we need to add to 1ml of medium to get the final, working concentration)

V2 = 1ml (this is the amount of medium per plate in an experimental setup)

Convert all to micro-units

480ug/ml x X = 0.1ug/ml x 1000ul

X = 0.1*1000/480

X = 0.208ul

You have to add 0.208ul to 1ml of medium to get the final concentration, but it is a very small amount, so we prepare a stock that is x1000 concentrated

Original conc.:

100ng/ml = 0.1ug/ml

X100:

10ug/ml

The protein is received in 20µg at concentration of 0.48mg/ml = 480µl/ml

We Make use of the formula: C1V1 = C2V2

Where:

C1 = 480µg/ml (this is the concentration at which we received the protein)

C2 = 10µg/ml (this is the final concentration that we want)

V1 = X (this is the volume of the stock that we need to add to 500µl of PBS to get the x100 concentration)

V2 = 500µl (this is the amount of PBS we will add the stock to)

480 x X = 10 x 500

X = 5000 / 480

= 10.416

*Thus take 10µl of original stock received (0.48mg/ml) and add to 490ul of PBS to get 500µl of an x100 concentrated stock of 10µg/ml.

This step is to calculate how much of the concentrated stock we need to add to 1ml medium

To get the final correct concentration of 100ng/ml:

C1V1 = C2V2

10ug/mlx	X	=	100ng/ml	x	1ml

Change all to micro-units:

100	x	X	=	0.1	x	1000
X			=	0.1*1000/10		
			=	10		

Thus, add 10ul of x100 stock in 1ml of medium to get 100ng/ml.

For New Nef Vehicle Control Cocktail: 10ul of PBS in 1ml of medium (instead of instead of 1ul)

Thus Vehicle Control Cocktail 3: 13µl of PBS in 1ml medium.

APPENDIX C

Antiretroviral Drug Medium and Vehicle Control Cocktail Dilutions

NRTI/NNRTI Medium

EFV: 5.6nM

The 10 mg EFV powder received was dissolved in 1.5 ml of Methanol (MeOH) to create an EFV stock solution (21mM). This stock was then divided into 40 µl aliquots and frozen away at -20°C until needed.

MW EFV = 315.67

For a concentration of 5.6nM EFV:

MW EFV = 315.67

1M = 315.67g/L

1mM = 315.67mg/L

1µM = 315.67µg/L

1nM = 0.31567µg/L

5.6nM = 1.767752µg/L

= 0.0017677µg/ml

21mM x 40µl = 5.6µM x X

21 x 0.040 = 0.0056 x X

X = 150ml

Dissolve Methanol stock of 21mM (volume of 40µl) in 150ml PBS to get stock of 5.6µM. From this take 1µl and add to 1ml growth medium to get final concentration.

FTC: 1.3µM

The 10 mg FTC powder received was dissolved in 4 ml of dH_2O to create an FTC stock solution (10mM). This stock was then divided into 65 ul aliquots and frozen away at - 20 °C until needed.

MW FTC = 247.25

For a concentration of 1.3µM FTC:

MW FTC = 247.25

1M = 247.25g/L

1mM = 247.25mg/L

1µM = 247.25µg/L

1.3µM = 321.425µg/L

= 0.321425µg/mL

10mM x 65µl = 1.3mM x X

10 x 0.065 = 1.3 x X

X = 0.5 ml

Dissolve dH_2O stock of 10mM (volume of 65µl) in 0.5ml PBS to get stock of 1.3mM. From this take 1µl and add to 1ml growth medium to get final concentration.

TDF: 500nM

The 10 mg TDF powder received was dissolved in 40 ml of dH_2O to create a TDF stock solution (393µM). This was then divided into 350 µl aliquots and frozen away at -20 °C until needed.

MW TDF = 635.51

For a concentration of 500nM FTC:

MW EFV = 635.51

1M = 635.51g/L

1mM = 635.51mg/L

1µM = 635.51µg/L

1nM = 0.63551µg/L

500nM = 317.755µg/L

= 0.317755µg/ml

393µM x 350µl = 0.5µM x X

X = 393 x 350 / 0.5

X = 275100µl

= 275ml

Dissolve the dH_2O stock of 393µM (volume of 350µl) in 275ml PBS to get stock of 500µM. From this take 1µl and add to 1ml medium to get final concentration.

NRTI/NNRTI Vehicle Control Cocktail:

To simplify calculations, we prepared a vehicle stock for each of the NRTI/NNRTI drugs:

EFV vehicle stock: *40µl* of *methanol to 150ml* of *PBS*

TDF vehicle stock: *350µl* of *dH_2O* to *275ml* of *PBS*

FTC vehicle stock: *65µl* of *dH_2O* to *0.5ml* of *PBS*

HIV Protein Vehicle: 8µl per 1ml of medium for all three proteins

Prepare Vehicle control cocktail 1 (VC1):

For 2ml: *add 16µl of PBS + 1µl EFV vehicle stock + 1µl TDF vehicle stock + 1µl FTC vehicle stock to 1.981ml medium*

Prepare Vehicle control cocktail 2 (VC2):

For 2ml: *add 16µl of PBS + 2µl EFV vehicle stock + 2µl TDF vehicle stock + 2µl FTC vehicle stock to 1.978ml medium*

Prepare Vehicle control cocktail 3 (VC3):

For 2ml: *add 16µl of PBS + 4µl EFV vehicle stock + 4µl TDF vehicle stock + 4µl FTC vehicle stock to 1.972ml medium*

PI Medium

LPV: 10µM

MW LPV = 628.80

For a concentration of 10µM LPV:

MW LPV = 628.80

1M = 628.80g/L

1mM = 628.80mg/L

1µM = 628.80µg/L

= 0.62880µg/mL

10µM = 6.2880µg/mL

Prepare Stock x1000 times concentrated:

10mM = 6288.0µg/ml

The powder is received in 10mg that will be dissolved in 1ml DMSO [6.288mµg / 10mg x 1ml = 0.62880ml = 628.80µl in 1 ml]. Take 200µl of DMSO stock and add to 118µl DMSO to get x1000 concentrated stock of 10mM. From this, take 1µl in 1ml medium for final concentration of 10µM (x1000 diluted)

RTV: 2µM

MW RTV = 720.94

For a concentration of 2µM RTV:

MW RTV = 720.94

1M = 720.94g/L

1mM = 720.94mg/L

1µM = 720.94µg/L

= 0.72094µg/mL

2µM = 1.4419µg/mL

Prepare Stock x1000 times concentrated:

2mM = 1441.88µg/ml

The powder is received in 10mg that will be dissolved in 1ml DMSO [1.44188mg / 10mg x 1ml = 0.144188ml = 144.188µl in 1 ml]. Take 144µl of DMSO stock and add to 856µl DMSO to get x1000 concentrated stock of 2mM. From this, take 1µl in 1ml medium for final concentration of 2µM (x1000 diluted)

PI Vehicle Control Cocktail:

To simplify calculations, we prepare a vehicle stock for each of the PI drugs:

LPV vehicle stock: Just DMSO

RTV vehicle stock: Just DMSO

HIV Protein Vehicle: 13µl PBS per 1ml of medium for all three proteins

Prepare Vehicle control cocktail 1 (VC1):

For 2ml: *add 26µl of PBS + 2µl DMSO to 1.972ml medium*

Prepare Vehicle control cocktail 2 (VC2):

For 2ml: *add 26µl of PBS + 4µl DMSO to 1.97ml medium*

Prepare Vehicle control cocktail 3 (VC3):

For 2ml: *add 26µl of PBS + 8µl DMSO to 1.966ml medium*

APPENDIX D

Passaging a P3 cell-line to 24-well plates.

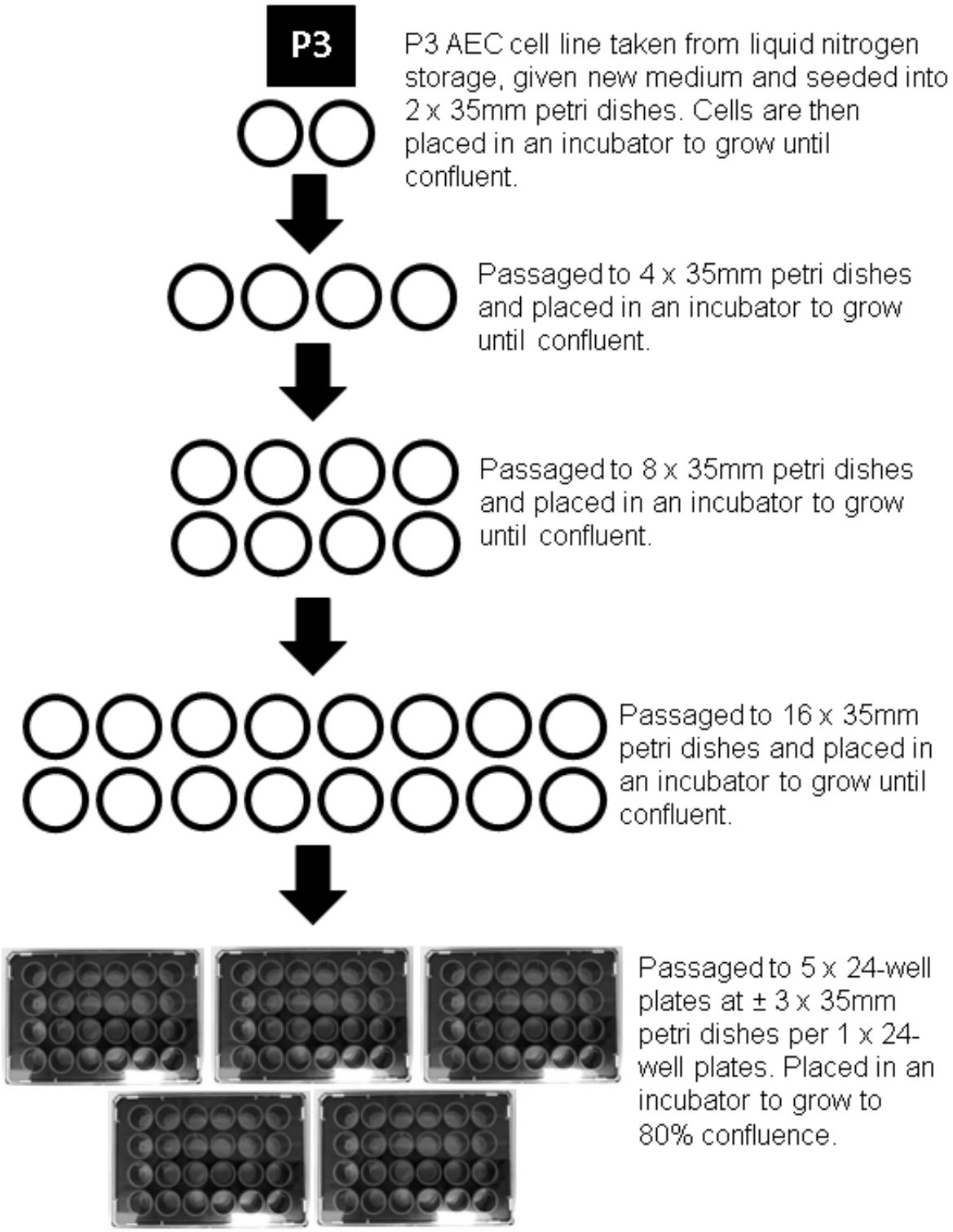

Passaging a P2 cell-line to 24-well plates

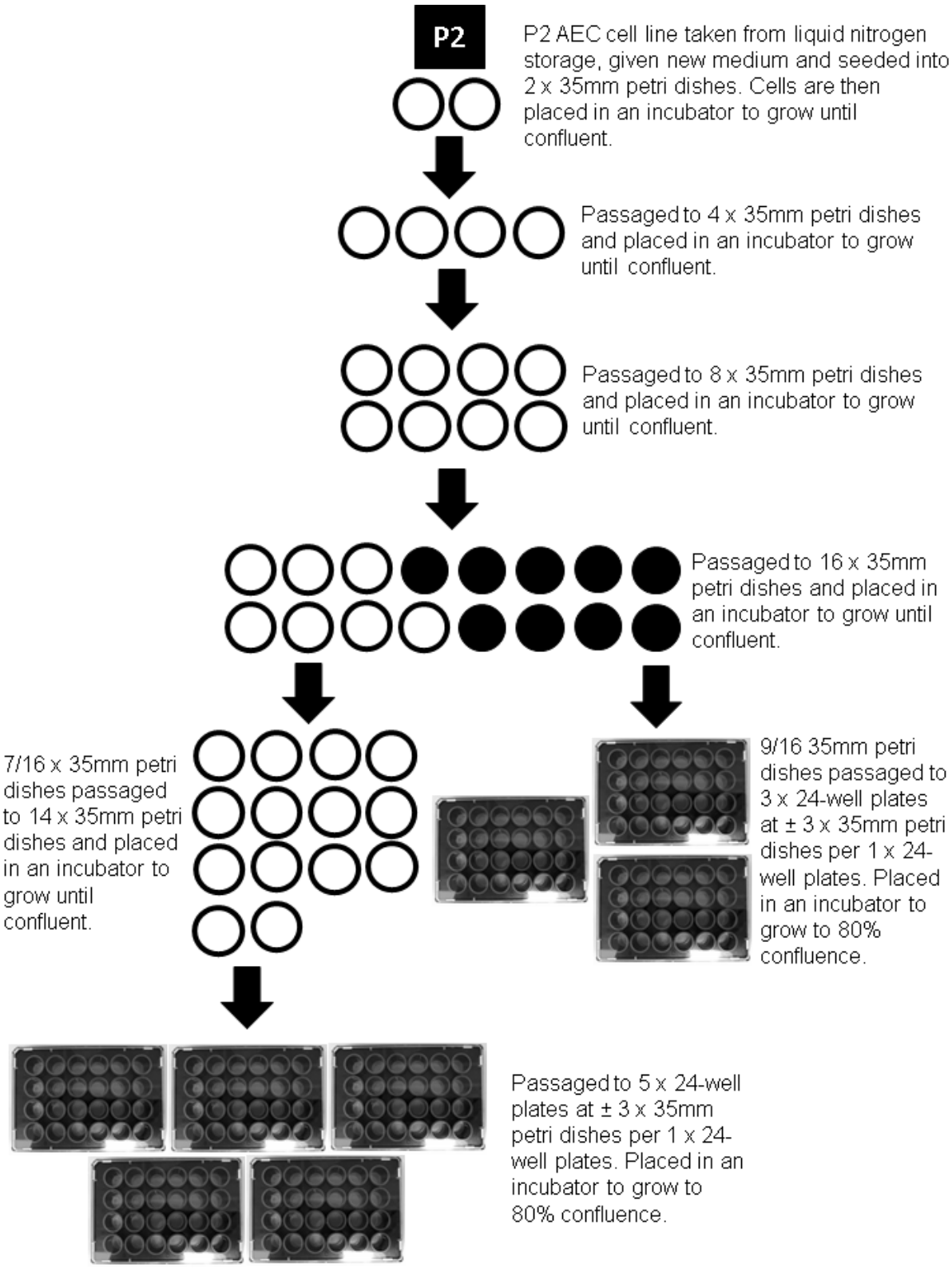

Passaging a P1 parent cell-line to 24-well plates

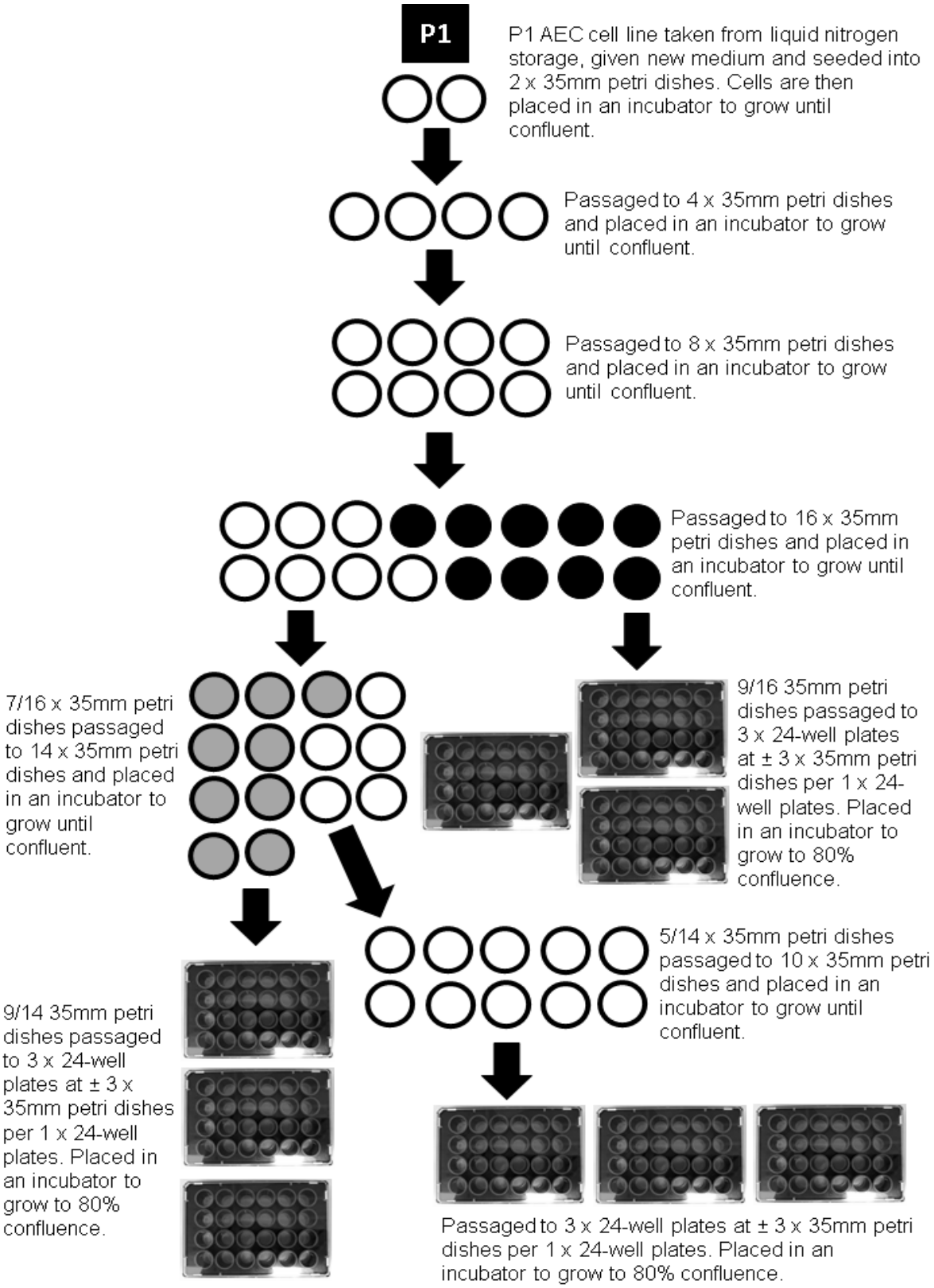

APPENDIX E

Plate Reader Protocols

Propidium Iodide (PI):

1. In an Eppendorf tube, add 200ul of dH_2O, and then turn off the fume-hood light.
2. Vortex the PI and then transfer 100ul PI into the Eppendorf tube containing 200ul dH_2O. [This will be enough to treat 29 wells]
3. Thoroughly vortex the tube and cover from the light.
4. Wash each well with 500ul warm PBS
5. Add 990ul PBS to each well, excluding the wells to be used for positive controls – these wells get 990ul dH_2O instead.
6. Re-vortex the PI mixture and add 10ul from the 300ul PI mixture to each well to have a total of 1ml per well.
7. Place all plates in the incubator for 15 minutes.
8. Leave the probe in & measure fluorescence using a plate-reader.

DAF-2/DA:

1. To prepare DAF, add 1ul of DAF from stock (Freezer draw) to 499ul of PBS per well (+ 1 extra). For 24 plates (+1) = 25, you will have:
    - 25 x 1ul DAF = 25ul of DAF
    - 25 x 499ul PBS = 12.475ml of PBS
2. Vortex this solution well.
3. Wash plates once with 500ul PBS and add 500ul of the above DAF solution per well, for 2 hours.
4. After 1h00, begin to prepare the positive control, DEA.
5. Weigh off 0.001g DEA, which is found in the -80C freezer, and place it in an Eppendorf tube.
6. After 1h20, add 50ul of PBS to the DEA Eppendorf tube and vortex well.
7. After 1h30, add 0.5ul of the DEA solution to each positive control well and put back in the incubator for the final 30 minutes of the total 2 hours.
8. After 2 hours, remove the probe, re-suspend in 500ul PBS per well and measure fluorescence using the plate-reader.

DHR-123:

1. To prepare DHR, add 2ul of DHR from stock (55ul aliquots can be found in the liquid nitrogen; note: vortex before use) to 998ul of PBS per well (+ 1 extra). For 24 wells (+1) = 25, you will have:
    - 25 x 2ul DHR = 50ul of DHR
    - 25 x 998ul PBS = 24.950ml of PBS
2. Vortex this solution well.
3. Wash plates once with 500ul PBS and add 1ml of the above DHR solution per well, for 3 hours.
4. After 45 minutes, remove the peroxynitrite from the -80 freezer and allow to thaw.
5. After 1h00, add 0.56ul of peroxynitrite to each positive control well and put back in the incubator for the final 2 hours of the total 3 hours.
6. Leave the probe in & measure fluorescence using the plate-reader.

APPENDIX F

Standard OD	Protein (ug)	Mean OD
0.077	1.2397	0.085
0.092		
0.178	2.4794	0.166
0.154		
0.3	4.9588	0.296
0.291		
0.503	9.9176	0.509
0.515		
0.679	14.8764	0.686
0.692		
0.877	19.8352	0.884
0.891		

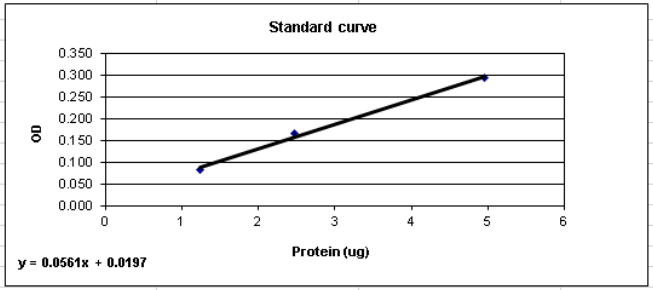

	Dilution row A		Dilution row B
Supernatant	20	From Row A	10
dH2O	80	dH2O	90
Total	100	Total	100.0
Dilution factor	5		10

y = bx + c

Samples:			Amount of protein	Amount of protein	Amount of protein	Amount of protein needed	Final lysate			
No.	Sample OD	Mean OD	in sample (µg)	in 1µl of sample	in whole sample (µg/µl)	per well (µg)	Amount of supernatant	ul LB	ul SB	ul Load
Example		=AVERAGE(B22:B23)	=(C23-c)/b	=D23/I9	=D23*K14	=25 (for example)	v = m / c	=8-G22	=J23/2	=10 (for example)
							=G22*20	**=H22*20**	**=I23*20**	
VC-1	0.146	0.140	2.14	0.11	1.07	8.00	7.5	1.51	9.00	18.0
	0.133						**150**	**30.15**	**180.00**	**360.00**
VC-2	0.134	0.137	2.09	0.10	1.05	8.00	7.7	1.35	9.00	18.0
	0.14						**153**	**26.96**	**180.00**	**360.00**
VC-3	0.161	0.167	2.62	0.13	1.31	8.00	6.1	2.89	9.00	18.0
	0.172						**122**	**57.71**	**180.00**	**360.00**
HIV-1	0.158	0.161	2.51	0.13	1.25	8.00	6.4	2.63	9.00	18.0
	0.163						**128**	**52.50**	**180.00**	**360.00**
HIV-2	0.152	0.146	2.24	0.11	1.12	8.00	7.1	1.86	9.00	18.0
	0.139						**143**	**37.30**	**180.00**	**360.00**
HIV-3	0.187	0.192	3.07	0.15	1.54	8.00	5.2	3.79	9.00	18.0
	0.197						**104**	**75.81**	**180.00**	**360.00**
NRTI/NNRTI-1	0.157	0.151	2.33	0.12	1.17	8.00	6.9	2.14	9.00	18.0
	0.144						**137**	**42.75**	**180.00**	**360.00**
NRTI/NNRTI-2	0.149	0.142	2.18	0.11	1.09	8.00	7.3	1.66	9.00	18.0
	0.135						**147**	**33.21**	**180.00**	**360.00**
NRTI/NNRTI-3	0.163	0.157	2.44	0.12	1.22	8.00	6.6	2.44	9.00	18.0
	0.15						**131**	**48.77**	**180.00**	**360.00**
PI-1	0.163	0.162	2.53	0.13	1.26	8.00	6.3	2.67	9.00	18.0
	0.16						**127**	**53.40**	**180.00**	**360.00**
PI-2	0.136	0.130	1.96	0.10	0.98	8.00	8.2	0.83	9.00	18.0
	0.123						**163**	**16.50**	**180.00**	**360.00**
PI-3	0.165	0.172	2.71	0.14	1.36	8.00	5.9	3.11	9.00	18.0
	0.179						**118**	**62.13**	**180.00**	**360.00**
NRTI/NNRTI+HIV-1	0.181	0.183	2.91	0.15	1.46	8.00	5.5	3.50	9.00	18.0
	0.185						**110**	**70.07**	**180.00**	**360.00**
NRTI/NNRTI+HIV-2	0.136	0.136	2.06	0.10	1.03	8.00	7.8	1.25	9.00	18.0
	0.135						**155**	**24.97**	**180.00**	**360.00**
NRTI/NNRTI+HIV-3	0.199	0.192	3.06	0.15	1.53	8.00	5.2	3.78	9.00	18.0
	0.184						**104**	**75.51**	**180.00**	**360.00**
PI+HIV-1	0.152	0.147	2.27	0.11	1.13	8.00	7.1	1.95	9.00	18.0
	0.142						**141**	**38.98**	**180.00**	**360.00**
PI+HIV-2	0.125	0.122	1.81	0.09	0.91	8.00	8.8	0.18	9.00	18.0
	0.118						**176**	**3.65**	**180.00**	**360.00**
PI+HIV-3	0.168	0.175	2.77	0.14	1.38	8.00	5.8	3.22	9.00	18.0
	0.182						**116**	**64.40**	**180.00**	**360.00**
		#DIV/0!	#DIV/0!	#DIV/0!	#DIV/0!		#DIV/0!	#DIV/0!	0.00	
							#DIV/0!	**#DIV/0!**	**0.00**	**#DIV/0!**

APPENDIX G

Table 3.2: Cell viability after 24 hours of HIV-1-protein exposure.

	VC 1	25 ng/ml	VC 2	50 ng/ml	VC 3	100 ng/ml
Mean %	100	104.5	100	98.01	100	100.5
SEM %	0.66	11.41	0.63	1.41	0.41	3.06

Data expressed as percentage propidium iodide fluorescence of vehicle control (vehicle control adjusted to 100%). VC 1: vehicle control for 25 ng/ml HIV-protein cocktail; VC 2: vehicle control for 50 ng/ml HIV-protein cocktail; VC 3: vehicle control for 100 ng/ml HIV-protein cocktail.

Table 3.3: NO production after 24 hours of HIV-1-protein exposure.

	VC 1	25 ng/ml	VC 2	50 ng/ml	VC 3	100 ng/ml
Mean %	100	100.8	100	86.72	100	72.05*
SEM %	1	5.25	0.92	9.26	1.55	8.37

Data expressed as percentage DAF-2/DA fluorescence of vehicle control (vehicle control adjusted to 100%). VC 1: vehicle control for 25 ng/ml HIV-protein cocktail; VC 2: vehicle control for 50 ng/ml HIV-protein cocktail; VC 3: vehicle control for 100 ng/ml HIV-protein cocktail. *: $p<0.05$ vs. VC 3 and 25 ng/ml.

Table 3.4: Nitrosative stress after 24 hours of HIV-1-protein exposure.

	VC 1	25 ng/ml	VC 2	50 ng/ml	VC 3	100 ng/ml
Mean %	100	103.4	100	94.47	100	86.81
SEM %	0.8	5.67	1.05	6.78	1.7	13.53

Data expressed as percentage DHR-123 fluorescence of vehicle control (vehicle control adjusted to 100%). VC 1: vehicle control for 25 ng/ml HIV-protein cocktail; VC 2: vehicle control for 50 ng/ml HIV-protein cocktail; VC 3: vehicle control for 100 ng/ml HIV-protein cocktail.

Table 3.5: Cell viability after 48 hours of HIV-1-protien exposure.

	VC 1	25 ng/ml	VC 2	50 ng/ml	VC 3	100 ng/ml
Mean %	100	98.37	100	108.8	100	118.2*
SEM %	1.15	4.61	0.82	5.31	0.49	7.69

Data expressed as percentage propidium iodide fluorescence of vehicle control (vehicle control adjusted to 100%). VC 1: vehicle control for 25 ng/ml HIV-protein cocktail; VC 2: vehicle control for 50 ng/ml HIV-protein cocktail; VC 3: vehicle control for 100 ng/ml HIV-protein cocktail. *: $p<0.05$ vs. 25 ng/ml.

Table 3.6: NO production after 48 hours of HIV-1-protein exposure.

	VC 1	25 ng/ml	VC 2	50 ng/ml	VC 3	100 ng/ml
Mean %	100	94.72	100	100.9	100	91.62
SEM %	0.26	3.03	0.31	5.49	0.32	5.28

Data expressed as percentage DAF-2/DA fluorescence of vehicle control (vehicle control adjusted to 100%). VC 1: vehicle control for 25 ng/ml HIV-protein cocktail; VC 2: vehicle control for 50 ng/ml HIV-protein cocktail; VC 3: vehicle control for 100 ng/ml HIV-protein cocktail.

Table 3.7: Nitrosative stress after 48 hours of HIV-1-protein exposure.

	VC 1	25 ng/ml	VC 2	50 ng/ml	VC 3	100 ng/ml
Mean %	100	92.59	100	104.2	100	104.2
SEM %	0.72	4.02	1.39	3.74	1.43	4.84

Data expressed as percentage DHR-123 fluorescence of vehicle control (vehicle control adjusted to 100%). VC 1: vehicle control for 25 ng/ml HIV-protein cocktail; VC 2: vehicle control for 50 ng/ml HIV-protein cocktail; VC 3: vehicle control for 100 ng/ml HIV-protein cocktail.

Table 3.8: Cell viability after 24 hours of NRTI/NNRTI treatment within an HIV-1 environment.

	VC 1	Half Dose	VC 2	Single Dose	VC 3	Double Dose
Mean %	100	95.56	100	96.17	100	104.7*
SEM %	0.17	0.63	0.46	3.4	0.3	2.7

Data expressed as percentage propidium iodide fluorescence of vehicle control (vehicle control adjusted to 100%). VC 1: vehicle control for half dose treatment; VC 2: vehicle control for single dose treatment; VC 3: vehicle control for double dose treatment. *: $p<0.05$ vs. Half Dose and Single Dose.

Table 3.9: NO levels after 24 hours of NRTI/NNRTI treatment within an HIV-1 environment.

	VC 1	Half Dose	VC 2	Single Dose	VC 3	Double Dose
Mean %	100	100.6	100	99.78	100	100.3
SEM %	0.43	0.56	0.44	1.88	0.18	2.65

Data expressed as percentage DAF-2/DA fluorescence of vehicle control (vehicle control adjusted to 100%). VC 1: vehicle control for half dose treatment; VC 2: vehicle control for single dose treatment; VC 3: vehicle control for double dose treatment.

Table 3.10: Nitrosative stress after 24 hours of NRTI/NNRTI treatment within an HIV-1 environment.

	VC 1	Half Dose	VC 2	Single Dose	VC 3	Double Dose
Mean %	100	86.57*	100	83.19**	100	86.14**
SEM %	0.28	3.52	0.22	3.5	0.48	3.29

Data expressed as percentage DHR-123 fluorescence of vehicle control (vehicle control adjusted to 100%). VC 1: vehicle control for half dose treatment; VC 2: vehicle control for single dose treatment; VC 3: vehicle control for double dose treatment. *: $p<0.05$ vs. VC 1; **: $p<0.01$ for Single Dose vs. VC 2 and for Double Dose vs. VC 3.

Table 3.11: Cell viability after 24 hours of PI treatment within an HIV-1 environment.

	VC 1	Half Dose	VC 2	Single Dose	VC 3	Double Dose
Mean %	100	94.26	100	94.33	100	106.7*
SEM %	0.41	0.89	0.37	0.79	0.28	6.14

Data expressed as percentage propidium iodide fluorescence of vehicle control (vehicle control adjusted to 100%). VC 1: vehicle control for half dose treatment; VC 2: vehicle control for single dose treatment; VC 3: vehicle control for double dose treatment. *: $p<0.05$ vs. Half Dose and Single Dose.

Table 3.12 NO levels after 24 hours of PI treatment within an HIV-1 environment.

	VC 1	Half Dose	VC 2	Single Dose	VC 3	Double Dose
Mean %	100	100.2	100	92.74**	100	85** ***
SEM %	0.09	1.85	0.67	1.40	0.56	1.81

Data expressed as percentage DAF-2/DA fluorescence of vehicle control (vehicle control adjusted to 100%). VC 1: vehicle control for half dose treatment; VC 2: vehicle control for single dose treatment; VC 3: vehicle control for double dose treatment. **: $p<0.01$ for Single Dose vs. VC 2 and Half Dose and for Double Dose vs. Single Dose; ***: $p<0.001$ for Double Dose vs. VC 3 and Half Dose.

Table 3.13: Nitrosative stress after 24 hours of PI treatment within an HIV-1 environment.

	VC 1	Half Dose	VC 2	Single Dose	VC 3	Double Dose
Mean %	100	98.66	100	93.37	100	77.12
SEM %	0.37	10.98	0.27	9.6	0.22	7.15

Data expressed as percentage DHR-123 fluorescence of vehicle control (vehicle control adjusted to 100%). VC 1: vehicle control for half dose treatment; VC 2: vehicle control for single dose treatment; VC 3: vehicle control for double dose treatment.

Table 3.14: Cell viability after 24 hours of CVC exposure.

	Control	CVC
Mean	100	96.89
SEM	5.54	1.81

Data expressed as percentage propidium iodide fluorescence of vehicle control (vehicle control adjusted to 100%). For Control n=3 and for CVC n=6. CVC: Combined Vehicle Control

.

Table 3.15: NO levels after 24 hours of CVC exposure.

	Control	CVC
Mean%	100	98.3
SEM%	0.77	0.77

Data expressed as percentage propidium iodide fluorescence of vehicle control (vehicle control adjusted to 100%). For Control n=3 and for CVC n=6. CVC: Combined Vehicle Control.

Table 3.16: eNOS expression after 24 hours.

	CVC	HIV	NRTI/NNRTI	PI	HIV+NRTI/NNRTI	HIV+PI
Mean	1	1.17	1	0.93	0.66	0.28* **
SEM	0.21	0.16	0.09	0.1	0.01	0.04

Converted values. Original normalised pixel-counts expressed in relation to the CVC. CVC: Combined Vehicle Control. HIV: HIV-protein cocktail; NRTI/NNRTI: nucleoside analogue reverse transcriptase inhibitors/non-nucleoside reverse transcriptase inhibitors; PI: protease inhibitors. *: $p<0.05$ vs. CVC and PI; **: $p<0.01$ vs. HIV.

Table 3.17: Phosphorylated eNOS after 24 hours.

	CVC	HIV	NRTI/NNRTI	PI	HIV+NRTI/NNRTI	HIV+PI
Mean	1	0.89	0.86	0.91	0.86	0.41
SEM	0.22	0.14	0.13	0.08	0.04	0.17

Converted values. Original normalised pixel-counts expressed in relation to the CVC. CVC: Combined Vehicle Control. HIV: HIV-protein cocktail; NRTI/NNRTI: nucleoside analogue reverse transcriptase inhibitors/non-nucleoside reverse transcriptase inhibitors; PI: protease inhibitors.

Table 3.18: Phosphorylated / total eNOS ratio after 24 hours.

	CVC	HIV	NRTI/NNRTI	PI	HIV+NRTI/NNRTI	HIV+PI
Mean	1	0.76	0.85	0.99	1.31	1.34
SEM	0.04	0.05	0.06	0.07	0.05	0.49

Converted values. Original normalised pixel-counts expressed in relation to the CVC. CVC: Combined Vehicle Control. HIV: HIV-protein cocktail; NRTI/NNRTI: nucleoside analogue reverse transcriptase inhibitors/non-nucleoside reverse transcriptase inhibitors; PI: protease inhibitors.

Table 3.19: PKB/Akt expression after 24 hours.

	CVC	HIV*	NRTI/NNRTI	PI	HIV+NRTI/NNRTI	HIV+PI
Mean	1	0.84	0.79**	0.79**	0.83*	0.68* ***
SEM	0.03	0.03	0.04	0.01	0.05	0.02

Converted values. Original normalised pixel-counts expressed in relation to the CVC. CVC: Combined Vehicle Control. HIV: HIV-protein cocktail; NRTI/NNRTI: nucleoside analogue reverse transcriptase inhibitors/non-nucleoside reverse transcriptase inhibitors; PI: protease inhibitors. *: $p<0.05$ for HIV vs. CVC, HIV+NRTI/NNRTI vs. CVC and HIV+PI vs. HIV; **: $p<0.01$ for NRTI/NNRTI vs. CVC and PI vs. CVC; ***: $p<0.001$ for HIV+PI vs. CVC.

Table 3.20: Phosphorylated PKB/Akt after 24 hours.

	CVC	HIV	NRTI/NNRTI	PI	HIV+NRTI/NNRTI	HIV+PI
Mean	1	0.85	0.91	0.79	0.9	0.62
SEM	0.06	0.07	0.1	0.13	0.05	0.05

Converted values. Original normalised pixel-counts expressed in relation to the CVC. CVC: Combined Vehicle Control. HIV: HIV-protein cocktail; NRTI/NNRTI: nucleoside analogue reverse transcriptase inhibitors/non-nucleoside reverse transcriptase inhibitors; PI: protease inhibitors.

Table 3.21: Phosphorylated / total PKB/Akt ratio after 24 hours.

	CVC	HIV	NRTI/NNRTI	PI	HIV+NRTI/NNRTI	HIV+PI
Mean	1	1.01	1.14	1	1.09	0.91
SEM	0.08	0.06	0.09	0.16	0.07	0.04

Converted values. Original normalised pixel-counts expressed in relation to the CVC. CVC: Combined Vehicle Control. HIV: HIV-protein cocktail; NRTI/NNRTI: nucleoside analogue reverse transcriptase inhibitors/non-nucleoside reverse transcriptase inhibitors; PI: protease inhibitors.

Table 3.22: IκBα expression after 24 hours.

	CVC	HIV	NRTI/NNRTI	PI	HIV+NRTI/NNRTI	HIV+PI
Mean	1	0.93	0.86	0.69	0.79	0.37* ** ***
SEM	0.15	0.019	0.03	0.08	0.05	0.03

Converted values. Original normalised pixel-counts expressed in relation to the CVC. CVC: Combined Vehicle Control. HIV: HIV-protein cocktail; NRTI/NNRTI: nucleoside analogue reverse transcriptase inhibitors/non-nucleoside reverse transcriptase inhibitors; PI: protease inhibitors. *: $p<0.05$ vs. HIV+NRTI/NNRTI; **: $p<0.01$ vs. HIV; ***: $p<0.001$ vs. CVC.

Table 3.23: Cleaved PARP after 24 hours.

	CVC	HIV	NRTI/NNRTI	PI	HIV+NRTI/NNRTI	HIV+PI
Mean	1	0.81	0.74*	0.79	0.81	0.64**
SEM	0.03	0.07	0.05	0.02	0.06	0.05

Converted values. Original normalised pixel-counts expressed in relation to the CVC. CVC: Combined Vehicle Control. HIV: HIV-protein cocktail; NRTI/NNRTI: nucleoside analogue reverse transcriptase inhibitors/non-nucleoside reverse transcriptase inhibitors; PI: protease inhibitors. *: $p<0.05$ vs. CVC; **: $p<0.01$ vs. CVC.

Table 3.24: Cleaved Caspase-3 after 24 hours.

	CVC	HIV	NRTI/NNRTI	PI	HIV+NRTI/NNRTI	HIV+PI
Mean	1	0.82	0.76	0.58	0.9	0.63
SEM	0.05	0.11	0.16	0.12	0.23	0.46

Converted values. Original normalised pixel-counts expressed in relation to the CVC. CVC: Combined Vehicle Control. HIV: HIV-protein cocktail; NRTI/NNRTI: nucleoside analogue reverse transcriptase inhibitors/non-nucleoside reverse transcriptase inhibitors; PI: protease inhibitors.

Table 3.25: Nitrotyrosine levels after 24 hours.

	CVC	HIV	NRTI/NNRTI	PI	HIV+NRTI/NNRTI	HIV+PI
Mean	1	2.39	2.74	2.95	2.54	0.54
SEM	0.18	0.34	0.97	0.34	1.21	0.06

Converted values. Original normalised pixel-counts expressed in relation to the CVC. CVC: Combined Vehicle Control. HIV: HIV-protein cocktail; NRTI/NNRTI: nucleoside analogue reverse transcriptase inhibitors/non-nucleoside reverse transcriptase inhibitors; PI: protease inhibitors.

Table 3.26 p22phox levels after 24 hours.

	CVC	HIV	NRTI/NNRTI	PI	HIV+NRTI/NNRTI	HIV+PI
Mean	1	0.89	0.7	0.58	0.96	0.51
SEM	0.05	0.1	0.08	0.23	0.1	0.11

Converted values. Original normalised pixel-counts expressed in relation to the CVC. CVC: Combined Vehicle Control. HIV: HIV-protein cocktail; NRTI/NNRTI: nucleoside analogue reverse transcriptase inhibitors/non-nucleoside reverse transcriptase inhibitors; PI: protease inhibitors.

APPENDIX H

Fluorescent Probe Functionality

- For the propidium iodide assay, dH_2O was used as the positive control
- For the DAF/2-DA assay, DEA/NO was used as the positive control
- For the DHR-123 assay, peroxynitrite was used as the positive control

HIV-Protein Model Time- and Concentration-Response Investigations

24-hours

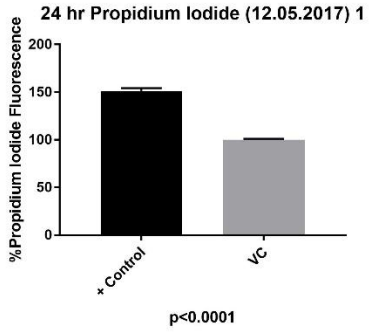

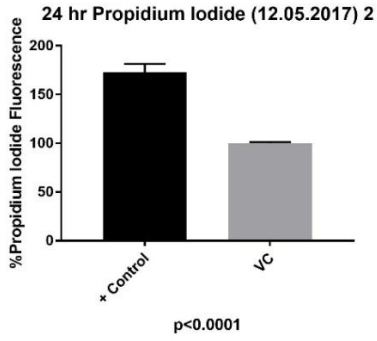

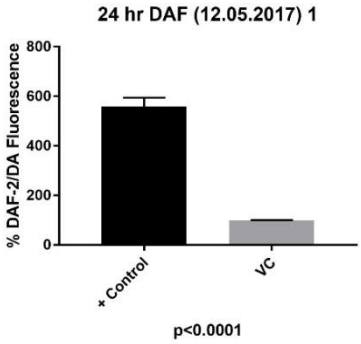

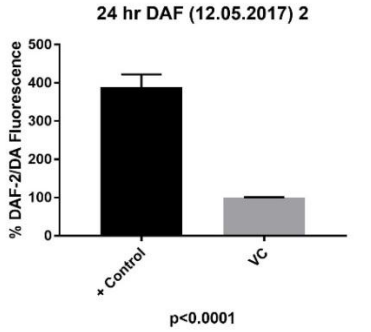

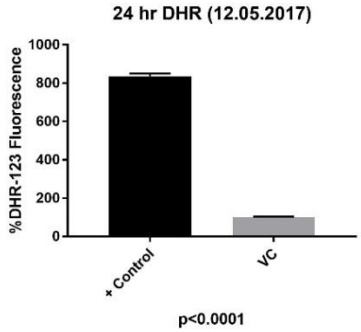

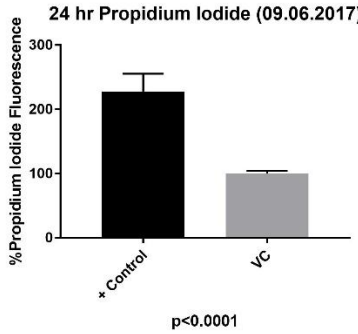

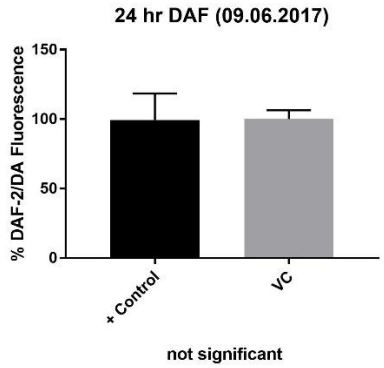

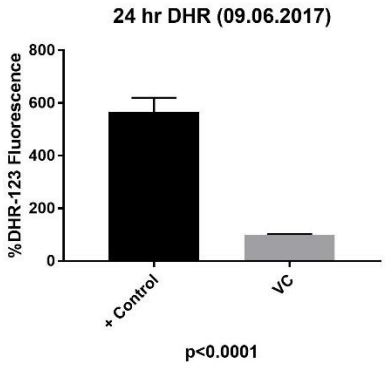

*Upon investigation, it was ascertained that it was the positive control, DEA/NO, that did not function.

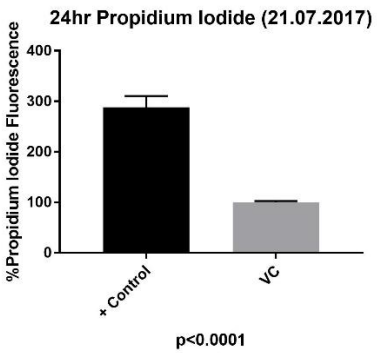

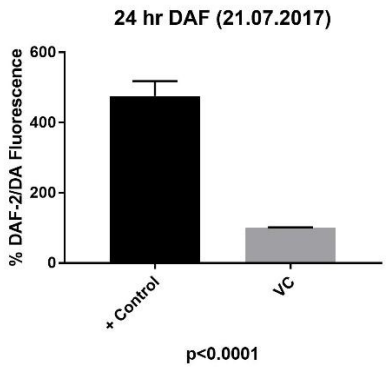

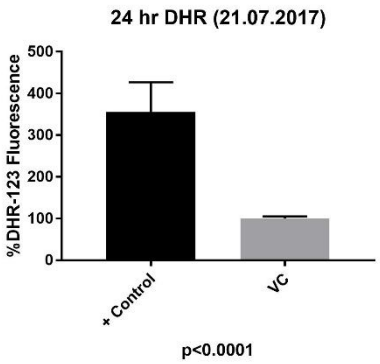

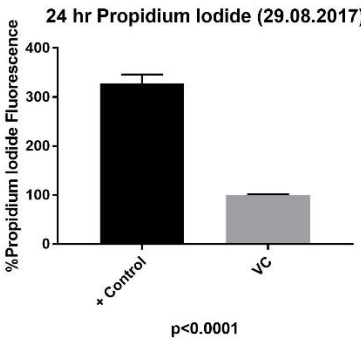

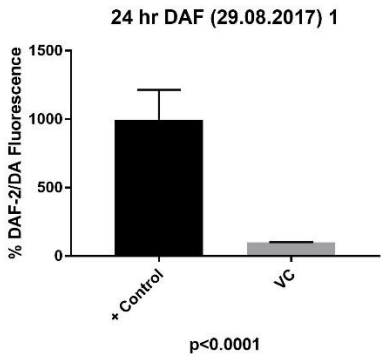

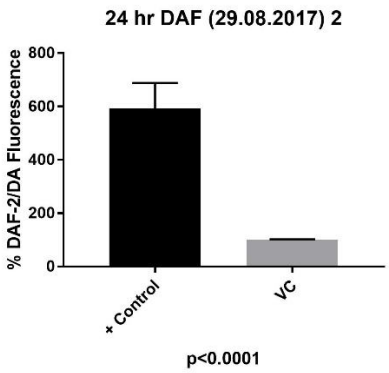

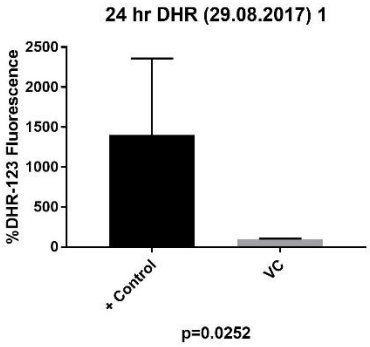

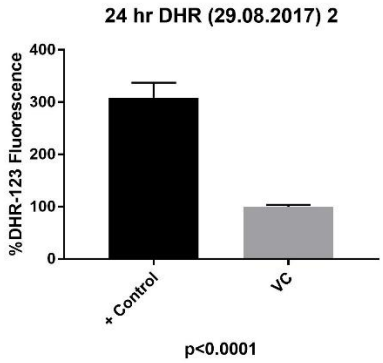

48-hours

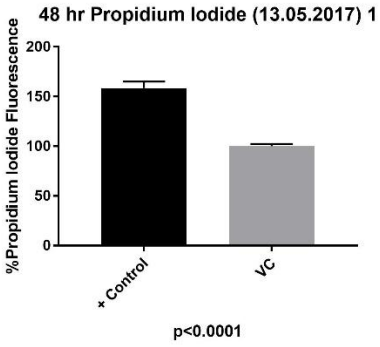

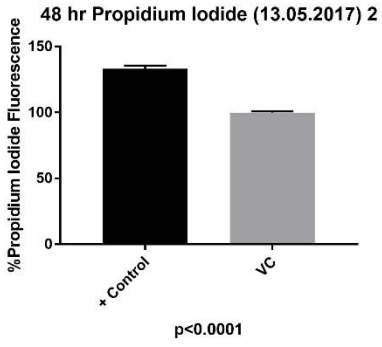

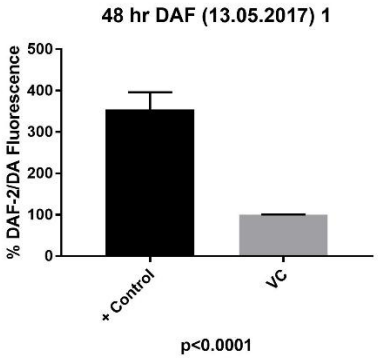

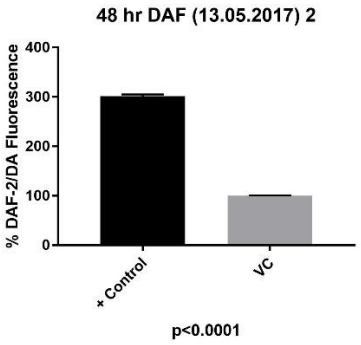

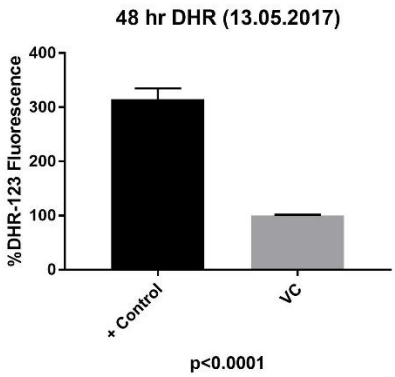

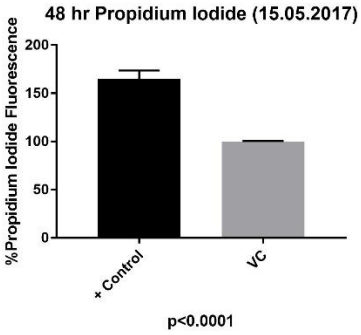

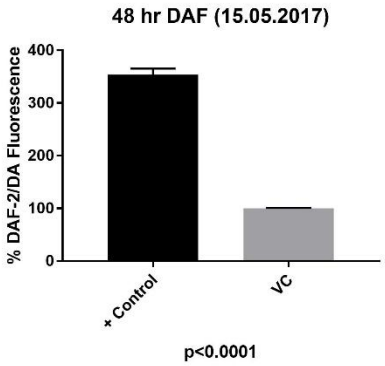

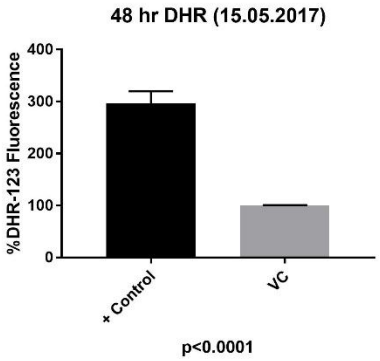

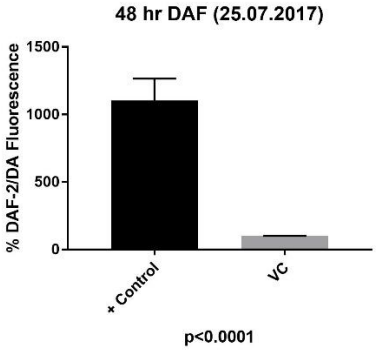

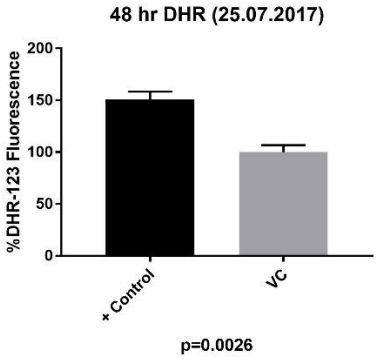

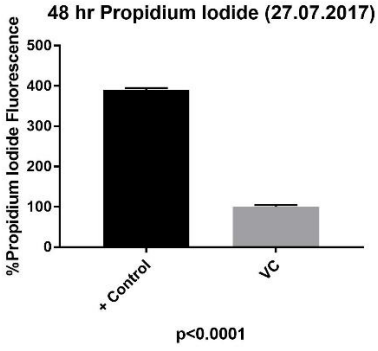

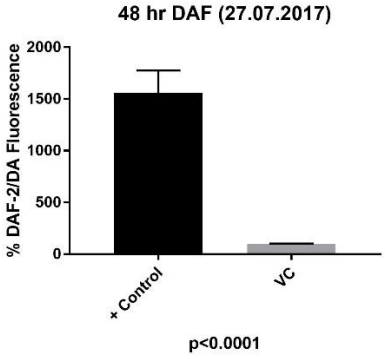

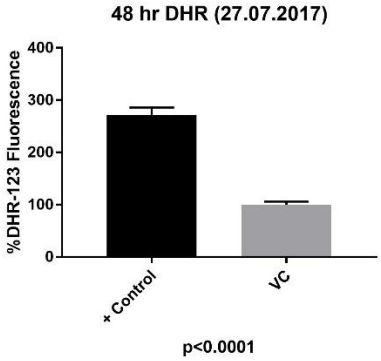

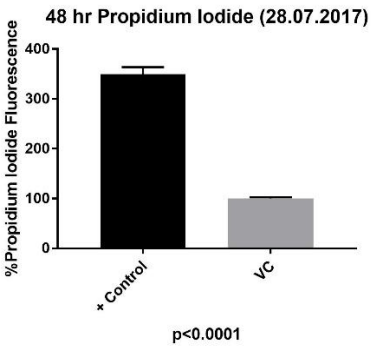

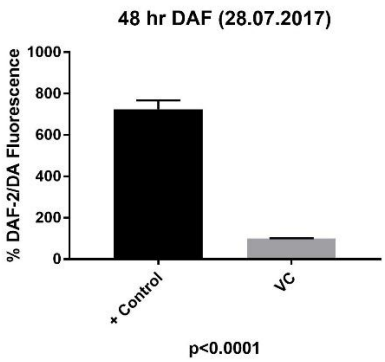

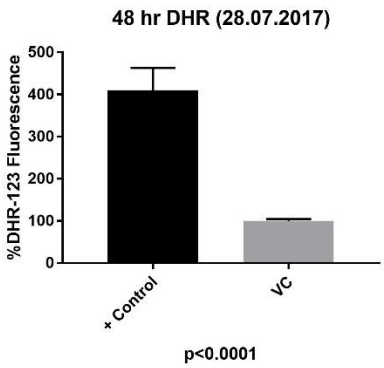

ART Concentration-Response Investigations

NRTI/NNRTI Treatment

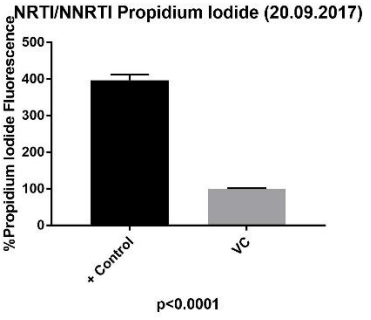

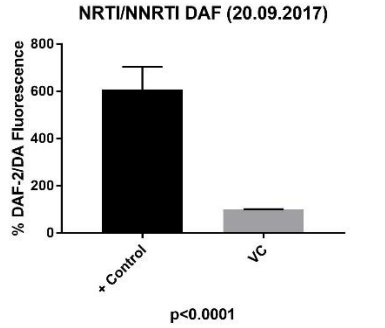

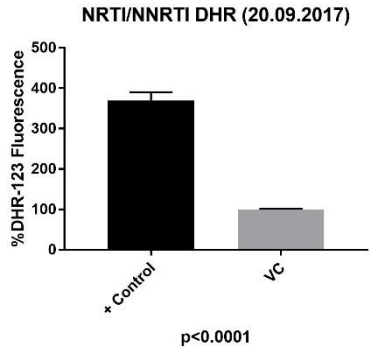

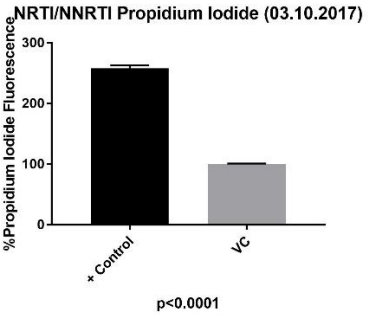

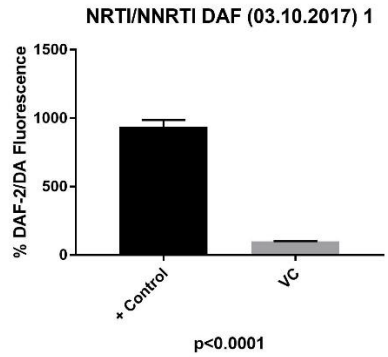

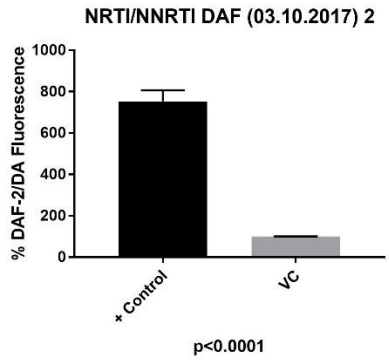

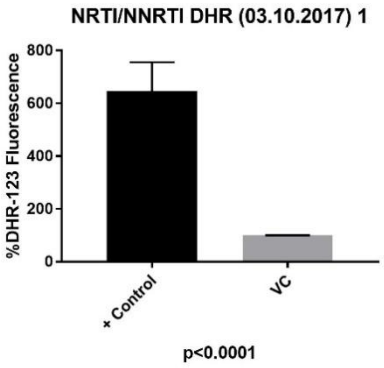

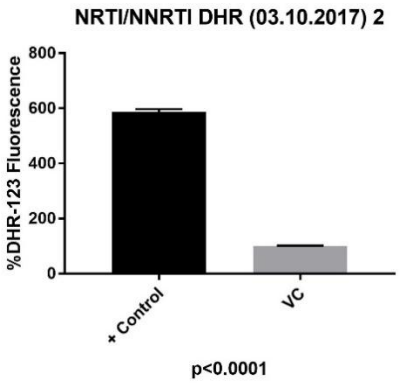

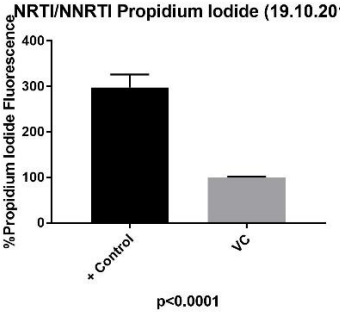

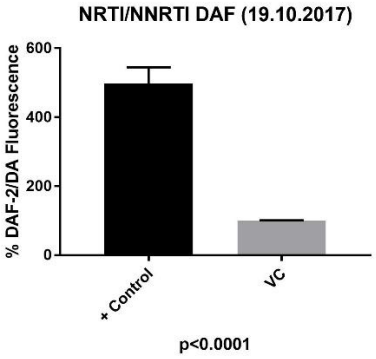

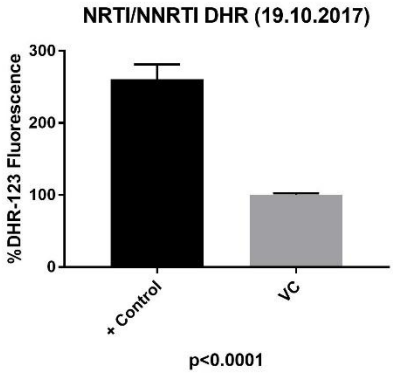

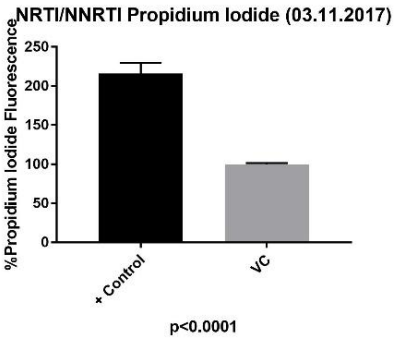

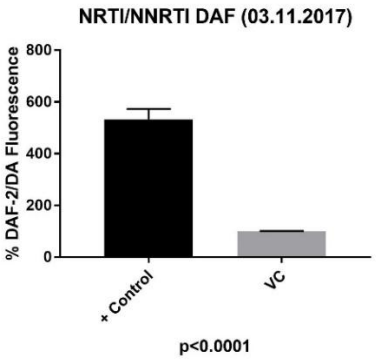

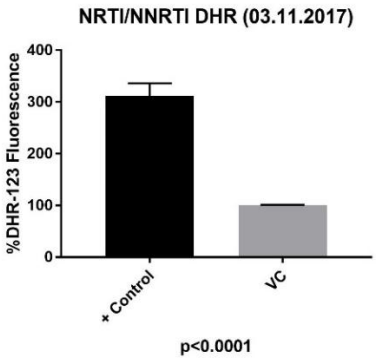

PI Treatment

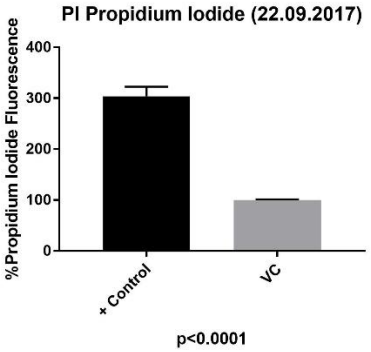

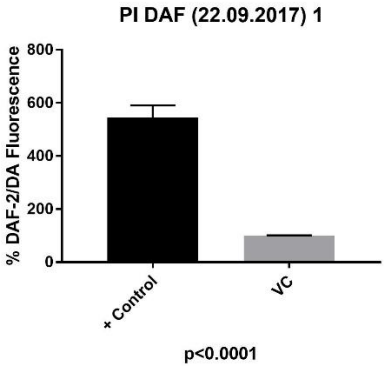

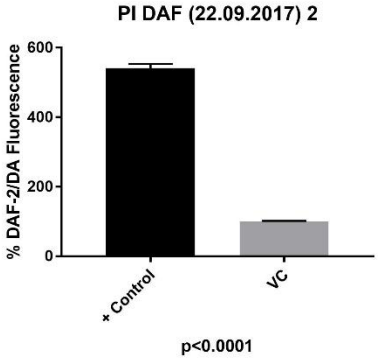

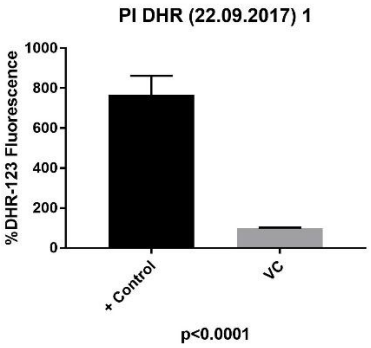

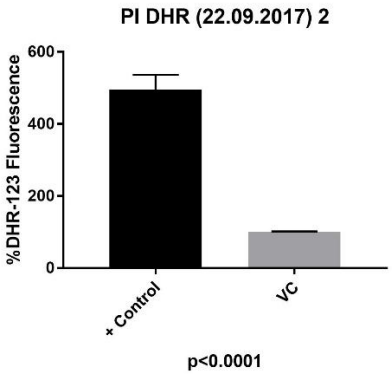

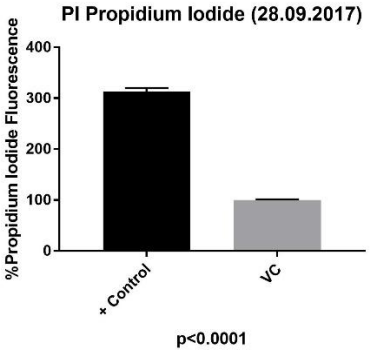

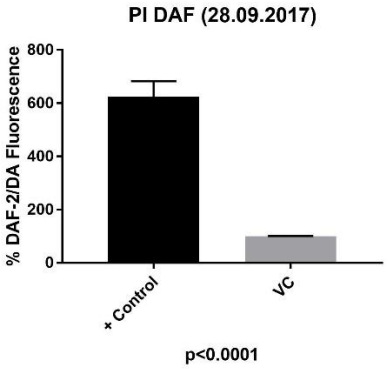

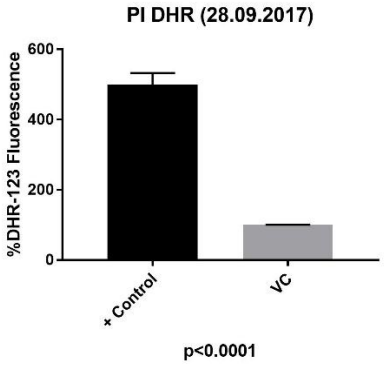

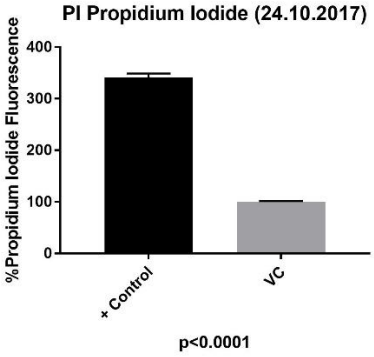

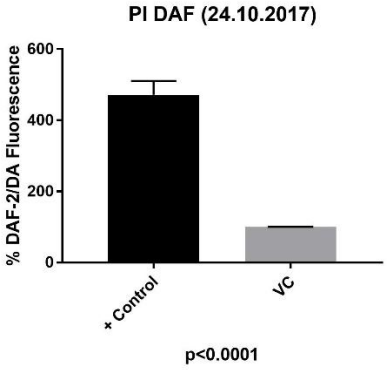

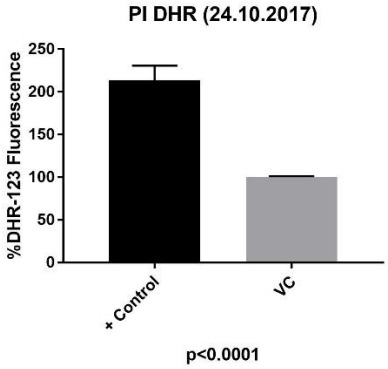

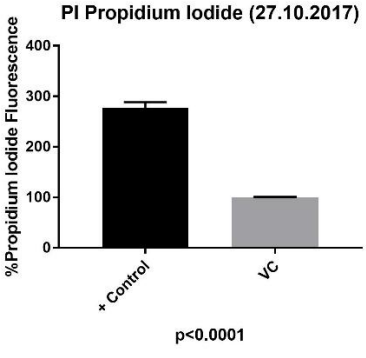

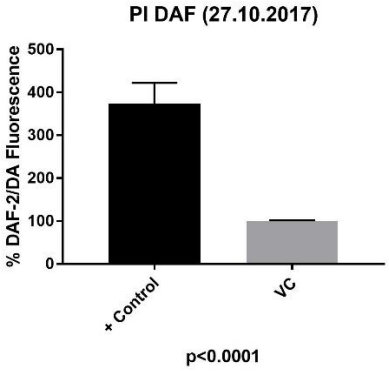

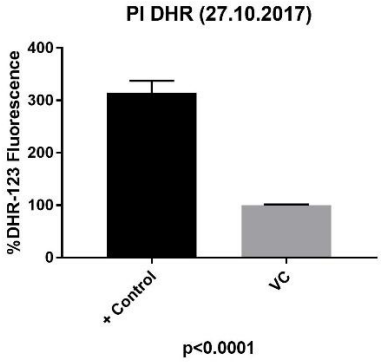

Combined Vehicle Control Test

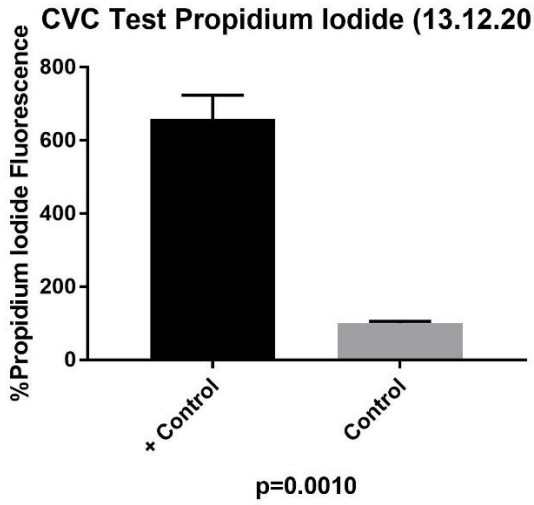

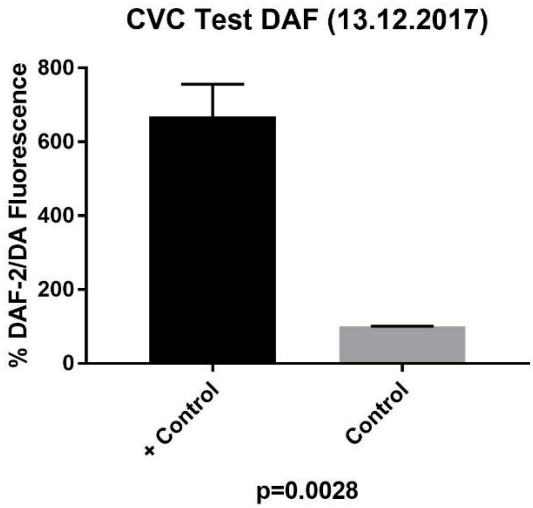

APPENDIX I

Below are images of the membranes (of transferred proteins from the 26-well Criterion™ TGX Stain-Free™ gels) that were used by the Lab™- 5 software (*Bio-Rad*, CA, USA) for the TPN of the western blot data.

Nitric Oxide Synthesis

Total eNOS

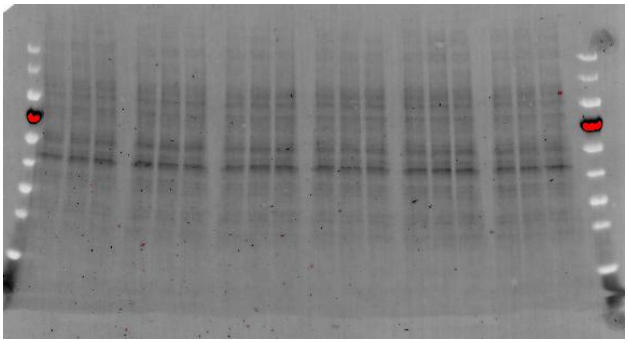

Total PKB/Akt

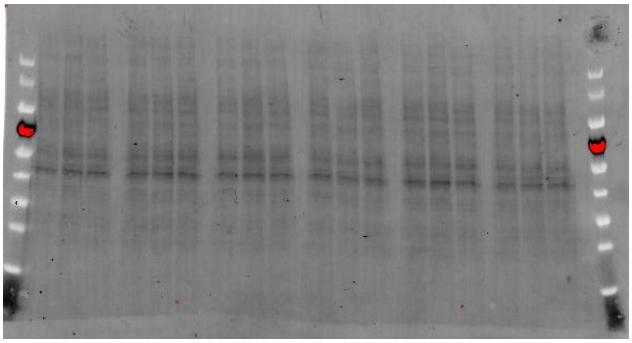

Phospho eNOS

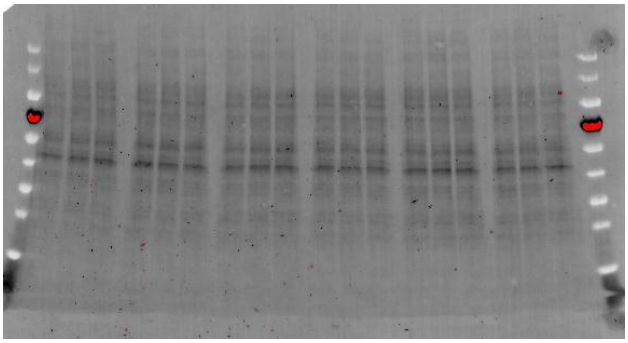

Phospho PKB/Akt

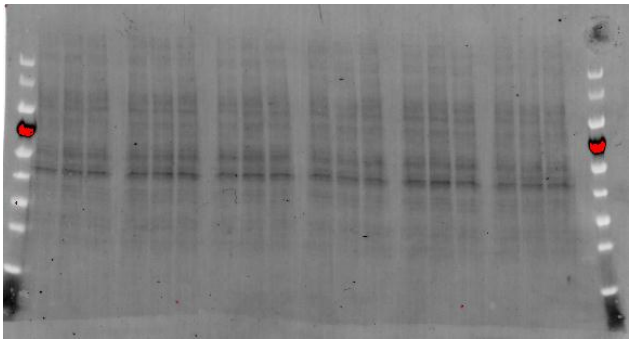

Inflammation

IκBα

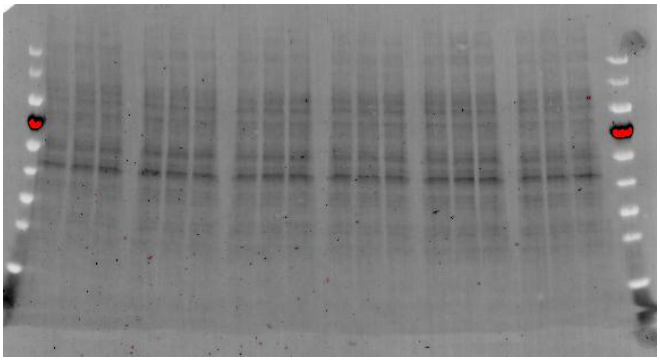

Apoptosis

Cleaved PARP

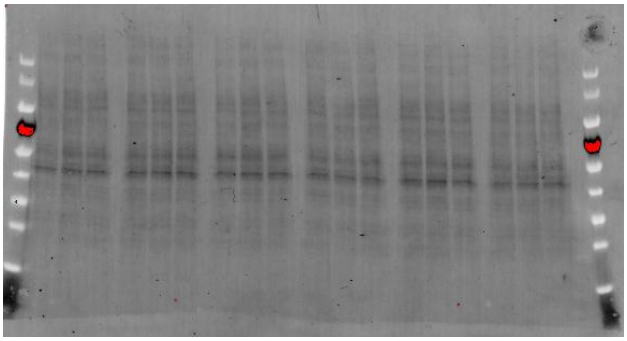

Cleaved Caspase-3

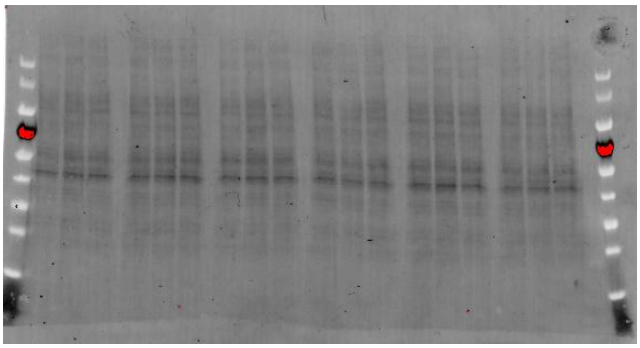

Nitrosative Stress

Nitrotyrosine

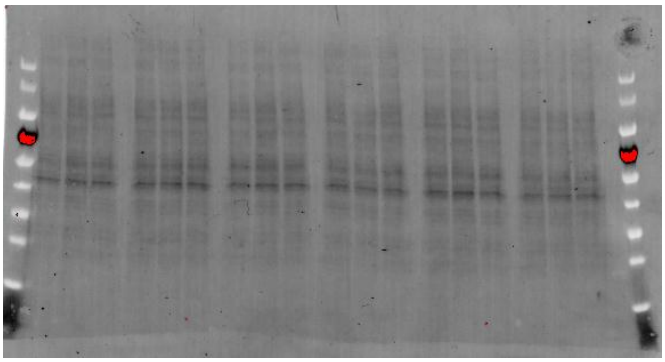

Oxidative stress

p22phox